


1-1-2013

# Progress Towards Understanding Of Mechanisms Of Action Of Potent Multifunctional Disease Modifying Therapeutics For Parkinson's Disease & Investigating The Methamphetamine-Induced Striatal Microglia Activation.

Mrudang M. Shah  
*Wayne State University,*

Follow this and additional works at: [http://digitalcommons.wayne.edu/oa\\_dissertations](http://digitalcommons.wayne.edu/oa_dissertations)

 Part of the [Medicinal Chemistry and Pharmaceutics Commons](#), [Neurosciences Commons](#), and the [Pharmacology Commons](#)

---

## Recommended Citation

Shah, Mrudang M., "Progress Towards Understanding Of Mechanisms Of Action Of Potent Multifunctional Disease Modifying Therapeutics For Parkinson's Disease & Investigating The Methamphetamine-Induced Striatal Microglia Activation." (2013). *Wayne State University Dissertations*. Paper 916.

This Open Access Dissertation is brought to you for free and open access by DigitalCommons@WayneState. It has been accepted for inclusion in Wayne State University Dissertations by an authorized administrator of DigitalCommons@WayneState.

**PROGRESS TOWARDS UNDERSTANDING OF MECHANISMS OF ACTION OF  
POTENT MULTIFUNCTIONAL DISEASE MODIFYING  
THERAPEUTICS FOR PARKINSON'S DISEASE  
&  
INVESTIGATING THE METHAMPHETAMINE-INDUCED  
STRIATAL MICROGLIA ACTIVATION**

by

**MRUDANG MANOJKUMAR SHAH**

**DISSERTATION**

Submitted to the Graduate School

Of Wayne State University,

Detroit, Michigan

in partial fulfillment of the requirements

for the degree of

**DOCTOR OF PHILOSOPHY**

2014

MAJOR: PHARMACEUTICAL SCIENCES

Approved by:

\_\_\_\_\_  
Advisor

\_\_\_\_\_  
Date

\_\_\_\_\_

\_\_\_\_\_

\_\_\_\_\_

\_\_\_\_\_

## **DEDICATION**

This dissertation is dedicated to two most important persons in my life, my wife, Nirali Shah and my sister, Shivani Shah. It would not have been possible to reach this milestone of my career without proper guidance, support and motivation from my parents,  
Manoj Shah and Dharini Shah.

## ACKNOWLEDGEMENTS

First of all, I would like to acknowledge my previous mentor Dr. David Thomas, who provided me an opportunity to delve into the field of neuroscience research. The independence provided by him was phenomenal and the most important factor that helped me develop broad knowledge of analytical skills during my tenure as a graduate student. I can't thank my current mentor Dr. Alope Dutta enough for all his support during critical stage of my graduate studies. Dr. Alope Dutta has been the most important person for providing me a meaningful insight to pursue research with maximum accuracy, efficiency and enthusiasm. Dr. Alope Dutta will always be my inspiration for approaching difficult problems with critical thinking and unique approach. I would also like to extend my appreciation for all the help and guidance provided by Dr. Donald Kuhn. He has been always very inspirational and encouraging throughout my journey as a graduate student.

I would like to thank all my committee members, Dr. Randall Commissaris, Dr. Anna Moszczynska, and Dr. Paul Stemmer for their continuous support and availability to discuss critical issues related to my research project.

I would especially like to thank my colleagues Ms. Liping Xu and Dr. Chandra Shekhar Voshavar for their unconditional support and guidance throughout my tenure in Dr. Alope Dutta's lab. The relationship established by them has made me believe them a part of my academic family. I would also like to thank my other colleagues Dr. Bhaskar Gopishetty, Dr. Mark Johnson, Mr. Gyan Prakash Modi, Dr. Horrick Sharma, Dr. Banibrata Das, Dr. Seenuvasan Vedachalam, Ms. Dan Liu, Ms. Asma Elmabruk, Mr. Fahd Dholkawala from Dr. Alope Dutta's

lab, Dr. Abiy Moussa Mohammad from Dr. David Thomas's lab, Dr. Mariana Angoa-Pérez and Ms. Dina Francescutti-Verbeem from Dr. Donald Kuhn's lab.

I am also grateful to all the collaborators who provided me broader perspective of neuroscience research. I would really like to thank Dr. Deepak Bhalla and Dr. Shane Perrine for providing me an additional angle to view neuroscience research.

I really appreciate the help and extra-ordinary efforts of Wayne State Proteomics Core and Wayne State Flow Cytometry Core, who helped me carry out many important experiments smoothly. I would particularly like to thank Ms. Namhee Shin, Dr. Paul Stemmer, Dr. Jessica Back, and Mr. Eric Van Buren for making my proteomics based and flow cytometry related experiments possible. I am really appreciative of Dr. Timothy Stemmler for providing us an ability to avail FPLC system for protein purification experiments. I would like to especially thank Ms. Lindsey Nico for her help with FPLC troubleshooting.

My journey would not have been enjoyable and exciting without the support, inspiration and encouragement from my friends and colleagues. I would really like to thank Dr. Rohan Uttarwar, Dr. Amit Wani, Mr. Hardik Doshi, Mr. Anand Gupta, Mr. Manit Shah, Dr. Venkat Nadithe, Dr. Roberta Traini, Dr. Bhavaani Jayaram, Ms. Sunitha Ravichandran, Ms. Anuja Vedapathak, Mrs. Sahana Nagaraja, Mrs. Kena Shah, and Ms. Heli Chauhan for all their support and love throughout my graduate studies.

Last but not the least; I would like to thank the department of Pharmaceutical Sciences for providing me an excellent opportunity to blossom into an experienced researcher from a novice student. I would like to extend special thanks to the departmental chair, Dr. George Corcoran for helping me out throughout my tenure as a graduate student. It would not have been

possible to develop into researcher without appropriate guidance from graduate student directors

Dr. David Oupický and Dr. Steven Firestine.

## TABLE OF CONTENTS

Dedication.....	ii
Acknowledgements.....	iii
List of Tables.....	viii
List of Figures.....	ix
List of Abbreviations.....	xiv
PROGRESS TOWARDS UNDERSTANDING OF MECHANISMS OF ACTION OF POTENT MULTIFUNCTIONAL DISEASE MODIFYING THERAPEUTICS FOR PARKINSON'S DISEASE	
Chapter 1: Introduction.....	1
Chapter 2: Hypotheses, rationale and study design.....	35
Chapter 3: Materials and Methods.....	47
Chapter 4: D-512 confers significant neuroprotection in PC12 and MN9D cell-lines.....	70
Chapter 5: D-240, D-436, and D-520 significantly modify aggregation kinetics of $\alpha$ -synuclein.....	95
INVESTIGATING THE METHAMPHETAMINE-INDUCED STRIATAL MICROGLIA ACTIVATION	
Chapter 6: Introduction.....	128
Chapter 7: Hypotheses, rationale and study design.....	157
Chapter 8: Materials and Methods.....	163

Chapter 9: Significant protein expression changes are induced by Methamphetamine in cell-culture and microglia isolated from animals.....	173
References.....	202
Abstract.....	230
Autobiographical Statement.....	234



## LIST OF TABLES

Table 1-1: Evidence of oxidative stress in Parkinson's disease.....	16
Table 1-2: Loci, genes and susceptibility factors involved in Parkinson's disease.....	25
Table 1-3: Current Parkinson's disease therapy.....	32
Table 3-1: Gradient elution protocol for purification of $\alpha$ -synuclein using Q-sepharose HP column.....	69

## LIST OF FIGURES

Figure 1-1: Neuropathology of Parkinson's disease.....	4
Figure 1-2: Immunostained Lewy bodies in SNPc dopaminergic neurons of Parkinson's disease.....	6
Figure 1-3: Substantia nigra from Parkinson's disease patient stained for $\alpha$ -synuclein.....	7
Figure 1-4: Spread of idiopathic Parkinson's disease pathology.....	8
Figure 1-5: Dopamine metabolism by enzymatic reaction and autooxidation.....	10
Figure 1-6: Iron(III) catalyzed reactions.....	11
Figure 1-7: Mitochondrial Electron Transport System (ETS).....	13
Figure 1-8: Lipid peroxidation process in presence of free radicals.....	15
Figure 1-9: Products of guanine oxidative damage via the intermediate C8-OH adduct radical .....	16
Figure 1-10: Carbonylation of protein amino acid side-chain.....	17
Figure 1-11: Glutathione synthesis and metabolism in the central nervous system.....	20
Figure 1-12: Representation of intracellular pathways of MPP <sup>+</sup> toxicity.....	22
Figure 1-13: Structural similarity between MPP <sup>+</sup> and Paraquat.....	23
Figure 1-14: Aggregation and functional domains of $\alpha$ -synuclein.....	27
Figure 1-15: Prion-like mechanism of $\alpha$ -synuclein transfer.....	28
Figure 1-16: Mode of action of current Parkinson's disease therapeutics.....	31
Figure 2-1: Design of potential multifunctional compounds for Parkinson's disease.....	36
Figure 2-2: Structures of known $\alpha$ -synuclein aggregation inhibitors and some lead compounds from our lab.....	38
Figure 2-3: Imbalance in reactive oxygen species generation and elimination.....	39
Figure 4-1: MTT assay 6-OHDA dose dependence.....	70

Figure 4-2: MTT assay D-512 dose dependence.....	71
Figure 4-3: Neuroprotective effect of D-512 pre-treatment and co-treatment on 6-OHDA induced cell death in PC12 cells.....	72
Figure 4-4: Neuroprotective effect of D-512 pre-treatment on 6-OHDA induced cell death in PC12 cells.....	72
Figure 4-5: Effect of 6-OHDA on total glutathione levels in PC12 cells (6 hours).....	73
Figure 4-6: Effect of 6-OHDA on total glutathione levels in PC12 cells (24 hours).....	74
Figure 4-7: Effect of D-512 on 6-OHDA induced changes in free glutathione levels (6 hours).....	75
Figure 4-8: Effect of D-512 on 6-OHDA induced changes in total glutathione levels (6 hours).....	76
Figure 4-9: Effect of D-512 on 6-OHDA induced changes in free glutathione levels (24 hours).....	76
Figure 4-10: Effect of D-512 on 6-OHDA induced changes in total glutathione levels (24 hours).....	77
Figure 4-11: Effect of BSO on total glutathione levels in PC12 cells (6 hours).....	78
Figure 4-12: Effect of BSO on total glutathione levels in PC12 cells (24 hours).....	78
Figure 4-13: Effect of D-512 pre-treatment and co-treatment on BSO-induced total glutathione depletion in PC12 cells (6 hours).....	79
Figure 4-14: Effect of D-512 pre-treatment and co-treatment on BSO-induced total glutathione depletion in PC12 cells (24 hours).....	80
Figure 4-15: Nuclear morphology characterization of PC12 cells by Hoescht staining.....	81
Figure 4-16: Determination of D-512's ability to alter DNA fragmentation induced by 6-hydroxydopamine.....	82
Figure 4-17: Evaluation of ability of D-512 to protect against lipid peroxidation induced by sodium nitroprusside.....	83
Figure 4-18: Effect of D-512 on 6-OHDA induced changes in phospho-ERK.....	84
Figure 4-19: Effect of D-512 on 6-OHDA induced changes in phospho-JNK.....	84

Figure 5-1: Silver staining of dopamine induced changes in $\alpha$ -synuclein.....	96
Figure 5-2: ThT assay for $\alpha$ -synuclein and dopamine experiment.....	97
Figure 5-3: TEM images of $\alpha$ -synuclein and $\alpha$ -synuclein with dopamine experiments.....	98
Figure 5-4: Silver staining of $\alpha$ -synuclein shaken at higher concentration.....	99
Figure 5-5: ThT assay of $\alpha$ -synuclein (50 $\mu$ M) experiment.....	99
Figure 5-6: TEM images of various $\alpha$ -synuclein experiments.....	100
Figure 5-7: Silver staining of $\alpha$ -synuclein and iron experiment.....	101
Figure 5-8: ThT assay of $\alpha$ -synuclein and iron experiment.....	101
Figure 5-9: Silver staining images of effect of various compounds on dopamine induced $\alpha$ -synuclein aggregation.....	102
Figure 5-10: TEM images of various experiments conducted to evaluate effect of various compounds on dopamine induced aggregation of $\alpha$ -synuclein.....	106
Figure 5-11: SEC profile of biorad globular protein standards.....	107
Figure 5-12: SEC profile of industrial grade $\alpha$ -synuclein monomer.....	107
Figure 5-13: SEC profile of $\alpha$ -synuclein after 10 days shaking with dopamine.....	109
Figure 5-14: SEC profile of $\alpha$ -synuclein after 10 days shaking with dopamine and ascorbic acid.....	110
Figure 5-15: SEC profile of $\alpha$ -synuclein after 10 days shaking with dopamine and rifampicin.....	110
Figure 5-16: SEC profile of $\alpha$ -synuclein after 10 days shaking with dopamine and D-436.....	111
Figure 5-17: SEC profile of $\alpha$ -synuclein after 10 days shaking with dopamine and D-520.....	111
Figure 5-18: SEC profiles of various experiments.....	112
Figure 5-19: MTT assay to evaluate effect of extracellular $\alpha$ -synuclein on PC12 cell viability.....	113

Figure 5-20: ThT assay results of $\alpha$ -synuclein (60 $\mu$ M) and $\alpha$ -synuclein (60 $\mu$ M) and dopamine (90 $\mu$ M) experiments.....	114
Figure 5-21: TEM images of various $\alpha$ -synuclein experiments.....	115
Figure 5-22: MTT assay to evaluate the effect of various compounds on cell death induced by extracellular $\alpha$ -synuclein.....	117
Figure 5-23: ThT assay of various experiments.....	118
Figure 5-24: TEM images of various experiments.....	119
Figure 6-1: Chemical structures of amphetamines.....	129
Figure 6-2: Chemical structures of synthetic amphetamines.....	130
Figure 6-3: Dopaminergic pathways in brain.....	140
Figure 6-4: Components of Dopaminergic neuronal system.....	142
Figure 6-5: Adverse consequences of METH administration.....	145
Figure 6-6: Microglia morphology as depicted by Rio-Hortega.....	147
Figure 6-7: Activity States of Microglia.....	149
Figure 6-8: Possible cues that can lead to “activated” state of microglia.....	151
Figure 6-9: Neuronal inhibitory influences on parenchymal microglia.....	154
Figure 6-10: Microglial PRRs identify neurotoxic and pro-inflammatory ligands.....	156
Figure 8-1: Experimental protocol to isolate murine microglia.....	172
Figure 9-1: MTT assay BV2 cells (6 hours post-treatment) .....	174
Figure 9-2: MTT assay BV2 cells (12 hours post-treatment) .....	175
Figure 9-3: MTT assay BV2 cells (24 hours post-treatment) .....	175
Figure 9-4: Dopamine levels of MN9D cells (12 hours post-treatment) .....	176
Figure 9-5: Effect of various treatments on dopamine levels of MN9D cells cultured in presence of BV2 cells.....	177
Figure 9-6: Protein expression changes between control and LPS-treated BV2 cells.....	178

Figure 9-7: Protein expression changes between control and 50 $\mu$ M METH-treated BV2 cells.....	179
Figure 9-8: Protein expression changes between control and 500 $\mu$ M METH-treated BV2 cells.....	180
Figure 9-9: Protein expression changes between control and LPS-treated co-cultured BV2 cells.....	182
Figure 9-10: Protein expression changes between control and 50 $\mu$ M METH-treated co-cultured BV2 cells.....	183
Figure 9-11: Protein expression changes between control and 500 $\mu$ M METH-treated co-cultured BV2 cells.....	184
Figure 9-12: Microglia isolation using fluorescence activated cell sorting.....	185
Figure 9-13: Evaluation of effectiveness of MACS as a technique to isolate microglia.....	186
Figure 9-14: FACS analysis of striatal microglia fraction isolated by density gradient centrifugation.....	187
Figure 9-15: FACS analysis of hippocampal and prefrontal cortical microglia fraction isolated by density gradient centrifugation.....	188
Figure 9-16: Fluorescence microscope images of eGFP expressing microglia.....	188
Figure 9-17: Evaluation of microglial fraction isolated from wild-type animals.....	189
Figure 9-18: Proteomic expression changes between microglia isolated from striata of METH-treated animals and untreated control animals.....	190

## LIST OF ABBREVIATIONS

3-MT: 3-methoxytyramine

4-HNE: 4-hydroxynonenal

6-OHDA: 6-hydroxydopamine

8-OHG: 8-hydroxy-2'-deoxyguanine

AD: Alzheimer's disease

ADHD: Attention deficit hyperactivity disorder

ADP: Adenosine diphosphate

ALS: Amyotrophic lateral sclerosis

AMPH: Amphetamine

ATP: adenosine triphosphate

BBB: Blood brain barrier

BCA: Bicinchoninic acid

BSA: Bovine serum albumin

BSO: L-buthionine sulfoximine

CD11b: Cluster of differentiation molecule 11b (Integrin alpha M)

CNS: Central nervous system

COMT: Catechol-O-methyl transferase

COX-2: Cyclooxygenase-2

DA: Dopamine

DAMP: Damage associated molecular patterns

DAT: Dopamine transporter

DDC: DOPA decarboxylase

DEA: Drug enforcement agency

DMSO: Dimethyl sulfoxide

DNA: Deoxyribonucleic acid

DOPAC: Dihydroxyphenyl acetic acid

DOPAL: 3, 4- dihydroxyphenylacetaldehyde

DPBS: Dulbecco's phosphate buffered saline

DTNB: Dithio-bis-nitro-benzoic acid

EDTA: Ethylene diamine tetra acetic acid

eGFP: enhanced green fluorescent protein

ERK1/2: Extracellular signal regulated kinase1/2

ETS: Electron transport system

FACS: Fluorescence activated cell sorting

FAPy-guanine: 2,6-diamino-4-hydroxy-5-formamidopyrimidine

GABA: Gamma amino butyric acid

GCL: Glutamate cysteine ligase

GFAP: Glial fibrillary acidic protein

GFP: Green fluorescent protein

GST: Glutathione-S-transferase

H<sub>2</sub>O<sub>2</sub>: hydrogen peroxide

HIV: Human immunodeficiency virus

HPLC: High performance liquid chromatography

HRP: horseradish peroxidase

HVA: Homovanillic acid

ICAM-5: Intracellular adhesion molecule-5



IFN: Interferon

IL-10: Interleukin-10

IL-1 $\beta$ : Interleukin-1 $\beta$

ILB: incidental Lewy bodies

iNOS: Inducible nitric oxide synthase

IPTG: Isopropyl thio galactoside

JNK: c-JUN N-terminal kinase

LB plates: Luria broth plates

L-DOPA: L-3, 4-dihydroxyphenylalanine

LFA-1: Lymphocyte function associated antigen-1

LPS: Lipopolysaccharide

LRRK2: Leucine rich repeat kinase-2

MAC-1: Macrophage antigen complex-1

MACS: Magnetic activated cell sorting

MAO: Monoamine oxidase

MAO-B: Mono amine oxidase-B

MAPKKK4: Mitogen activated protein kinase kinase kinase 4

MDA: Malondialdehyde

MDMA: 3,4-methylenedioxy-N-methylamphetamine

METH: Methamphetamine

MPDP+: 1-methyl-4-phenyl-2,3-dihydropyridinium

MPP+: 1-methyl-4-phenyl pyridinium

MPTP: 1-methyl-4-phenyl-1,2,3,6-tetrahydro pyridine

MRI: Magnetic resonance imaging

MS: Multiple sclerosis

mTOR: mammalian target of rapamycin

MTT: Dimethyl thiazolyl diphenyl tetrazolium

NADPH: Nicotinamide adenine dinucleotide phosphate

NFkB: Nuclear factor kappa-light chain enhancer of activated B cells

NMDA: N-methyl-D-aspartic acid

nNOS: Neuronal nitric oxide synthase

NSAID: Non steroidal anti-inflammatory drug

PBS: Phosphate buffered saline

PD: Parkinson's disease

PGS2: Prostaglandin G/H synthase 2

PI3K: Phosphatidylinositide 3-kinase

PPAR $\gamma$ : Peroxisome proliferator activated receptor- $\gamma$

PRR: Pattern recognition receptor

PUFA: Poly unsaturated fatty acids

PVDF: Polyvinyledene fluoride

ROS: reactive oxygen species

SDS: sodium dodecyl sulphate

SDS-PAGE: sodium dodecyl sulphate- polyacrylamide gel electrophoresis

SEC: Size-exclusion chromatography

SIP: Sterile isotonic percoll

SNP: Sodium nitroprusside

SNPc: Substantia nigra pars compacta

SNPr: Substantia nigra pars reticulata

SOC media: Super optimal broth with catabolite repression media

SRRM: Serine/arginine repetitive matrix

STAT: Signal transducer and activator of transcription

STDs: Sexually transmitted diseases

TBA: Thiobarbituric acid

TBARS: Thiobarbituric acid reactive species

TBS: Tris-buffered saline

TBST: Tris-buffered saline with Tween-20

TEM: Transmission electron microscopy

TGF- $\beta$ : Transforming growth factor- $\beta$

TH: Tyrosine hydroxylase

ThT: Thioflavin-T

TLR: Toll-like receptors

TNF: Tumor necrosis factor

t-SNARE: target associated Soluble NSF Attachment Protein Receptor

VMAT-1: Vesicular monoamine transporter-1

VMAT-2: Vesicular monoamine transporter-2

v-SNARE: Vesicle associated Soluble NSF Attachment Protein Receptor

VTA: Ventral tegmental area

$\gamma$ -GTP: Gamma-glutamyl transpeptidase

## CHAPTER 1

### INTRODUCTION

#### 1.1 Parkinson's disease

Parkinson's disease (PD) is a slowly progressing neurodegenerative disorder, which was initially described as "Paralysis agitans" by James Parkinson in 1817 in an essay on shaking palsy. He described tremors, postural instability, rigidity, festinating gait, sleep disturbances, and constipation as hallmark features of the disease in his essay (Parkinson 2002). Five out of six cases described by James Parkinson were subjects with age range from fifty to seventy two years. This implied aging as a common cause of the disease, which has been well established now (Shulman, De Jager et al. 2011). Afterwards, Jean-Martin Charcot described this disease in greater detail and named it after James Parkinson as Parkinson's disease. Surprisingly, all the symptoms of PD described by Parkinson and Charcot are still considered main clinical features for diagnosis purpose. Most of the patients with PD are diagnosed at a stage when their motor symptoms (tremors, postural instability, and rigidity) appear. However, it has been established now that non-motor symptoms of the disease such as sleep disturbances, constipation (dysautonomia), and loss of olfactory sense appear as early as 20 years before the appearance of cardinal motor symptoms (Hawkes 2008). After the discovery of dopamine (DA) as a neurotransmitter in 1957 (Carlsson, Lindqvist et al. 1957, Carlsson, Lindqvist et al. 1958), research in PD field has grown exponentially and wide variety of pathological targets have been identified. Significant therapeutic and surgical interventions have been developed after understanding the pathophysiology of PD. Also, various diagnostic tools have been developed to diagnose the progressive disorder in advance, which may help in disease intervention during its early phase.

## **1.2 Statistics, epidemiology and risk factors**

Currently, PD is the second most common neurodegenerative disease after Alzheimer's disease. Approximately 10 million people worldwide are living with the disease, 1 million of which are Americans. Every year around 60,000 Americans are diagnosed with PD. Total direct and indirect expenses in United States because of PD are estimated to be nearly \$25 billion per year.

1% people over age of 65 and 5% people over age of 85 suffer from PD. Aging is the most common risk factor associated with sporadic PD. Men are one and half times more likely to get PD than women (Van Den Eeden, Tanner et al. 2003, de Lau and Breteler 2006). Exposure to environmental toxins such as MPTP (meperidine analog), herbicide (paraquat) and pesticide (rotenone) has been shown to increase the risk of PD. Cigarette smoking and coffee consumption have been shown to reduce the risk of PD. Gene mutations are usually responsible for an early onset of PD and approximately 90% cases of PD are sporadic in nature. European ancestry increases the risk of PD because of genetic causes (Shulman, De Jager et al. 2011).

## **1.3 Pathophysiology of Parkinson's disease**

### **1.3.1 Dopamine and Parkinson's disease**

Interestingly, reserpine administration into animals and humans produce Parkinson's motor symptoms, and reserpine is a widely used toxin in Parkinson's animal models to induce immobility (Carlsson 1959). As reserpine was known to cause depletion of 5-hydroxytryptamine (serotonin), initial hypothesis for PD implicated depletion of brain serotonin as a culprit. However, restoration of serotonin levels in brains of reserpinized animals by administration of 5-hydroxytryptophan (a brain penetrable precursor of serotonin) did not change Parkinson's motor

symptoms, whereas, administration of 3,4-dihydroxyphenylalanine (L-DOPA), a precursor of catecholamines (dopamine, adrenaline and noradrenaline) caused almost complete reversal of reserpine's effects temporarily (Carlsson, Lindqvist et al. 1957).

Historically, DA was shown to be a neurotransmitter by Arvid Carlsson (Carlsson, Lindqvist et al. 1958, Carlsson 1959). Further investigations showed that high concentration of DA was localized to corpus striatum, an area of brain which is extrapyramidal motor center and controls motor functions (Carlsson 1959). Finally, studies by Hornykiewicz and workers showed that Parkinson's patients had depleted levels of DA in caudate nucleus and putamen (parts of striatum), the regions where nigrostriatal dopaminergic neurons from substantia nigra terminate (Birkmayer and Hornykiewicz 1961, Birkmayer and Hornykiewicz 1998). It was proposed that PD may result from imbalance between serotonin and catecholamines on one hand, and histamine and acetylcholine on the other (Barbeau 1962). Current hypothesis suggests the loss of dopaminergic neurons in substantia nigra pars compacta (SNPc) as a main pathological feature of PD (**figure 1-1**).

Various pathological assessments have clearly established that PD patients have significant dopaminergic neuronal degeneration in SNPc, which forms nigrostriatal tract. Nigrostriatal dopaminergic system is essential for motor co-ordination and its degeneration in PD results in cardinal motor symptoms which are tremors and postural instability. Unfortunately, Parkinson's motor symptoms do not appear until around ~60% of the dopaminergic neurons in SNPc have degenerated, which translates to around ~80% of dopamine depletion (Hornykiewicz and Kish 1987, Dauer and Przedborski 2003). Therefore, the disease is diagnosed at very advanced stage when significant neurodegeneration has already taken place.

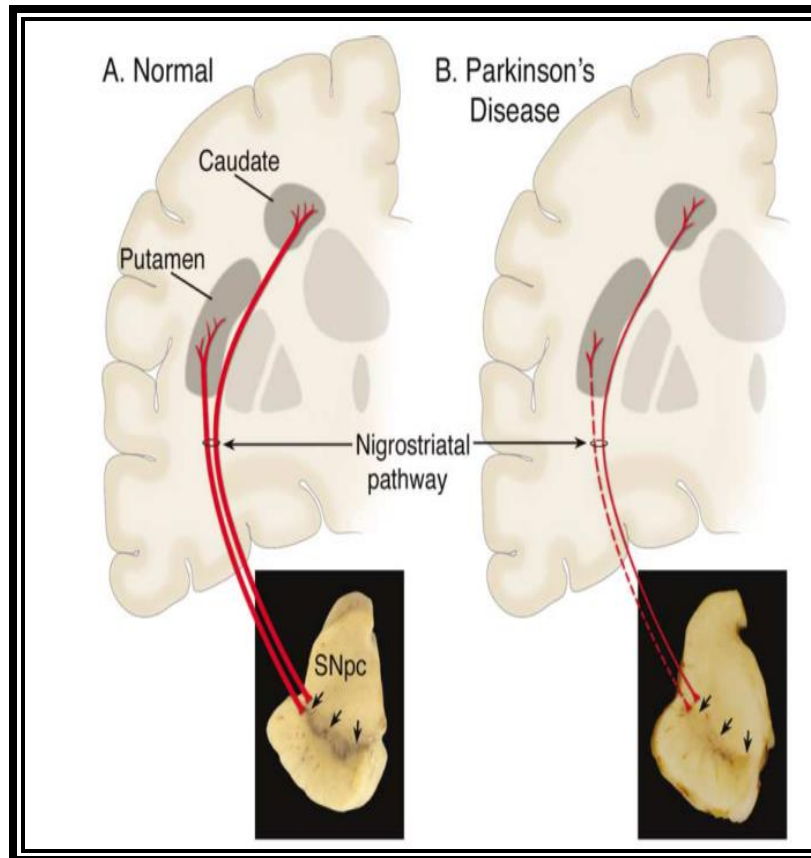


**Figure 1-1. Neuropathology of Parkinson's disease.**

**A. Normal nigrostriatal pathway, where dopaminergic neurons from SNpc project to caudate and putamen. (dopaminergic neurons are melanized and thus appear black colored); B. Nigrostriatal pathway in Parkinson's disease patient, where dopaminergic neurons projecting from SNpc to putamen have significantly degenerated and there is a moderate loss in projection from SNpc to caudate. Also, note the depigmentation of SNpc due to loss of dopaminergic neurons (Dauer and Przedborski 2003).**

### **1.3.2 Iron and Parkinson's disease**

PD patients show an increase in iron(III) accumulation and ferritin expression (iron(III) storage protein) in SNpc but not in substantia nigra pars reticulata (SNPr) (Jellinger, Paulus et al. 1990). Patients with advanced stage PD have significant accumulation of iron(III), whereas, cases with mild PD do not show increased accumulation in SNpc (Zecca, Youdim et al. 2004). Post-mortem analysis and non-invasive methods such as magnetic resonance imaging (MRI) have revealed age-related increase in iron concentration in various brain regions. Neuromelanin

in nigral dopaminergic neurons has a strong tendency to bind to iron(III) and it might be responsible for higher content of iron(III) in SNPc than any other brain regions (Bharath, Hsu et al. 2002). Highest amount of iron-melanin complex is observed in patients with Alzheimer's/Parkinson's disease (Jellinger, Kienzl et al. 1992). Iron(III) deposits have been shown to be present in microglia, astrocytes, and oligodendrocytes in the SNPc of patients with PD. Neuromelanin-iron complex has been shown to activate microglia (inflammatory mediators) in-vitro, which leads to release of various inflammatory mediators (Zecca, Youdim et al. 2004). Iron misregulation/accumulation can result in the demise of dopaminergic neurons only in case of genetic disorders. More than 90% cases of PD have very low amount of iron build-up. Thus, the neurotoxicity in PD may result from complex interactions between iron and other pathological factors involved in pathogenesis of PD.

There is an inverse relationship between DA concentration and iron(III) concentration in the putamen (dopaminergic neuron terminal site), but not in the substantia nigra (dopaminergic neuron origination site), which indicates that the neurodegeneration may be a retrograde process. This implies that the neurodegeneration may initiate at dopaminergic neuronal terminal site (striatum) and may proceed in retrograde path to permanently degenerate its origination site in the substantia nigra.

### **1.3.3 Lewy bodies and Lewy neurites in Parkinson's disease**

Post-mortem analysis of PD patient brain reveals accumulation of intra-cytoplasmic protein rich inclusions, which stain positive for ubiquitin (**figure 1-2**). In 1912, Fritz Jacob Heinrich Lewy described these cellular inclusions in various brain parts of patients with neurodegenerative disorders. Afterwards, in 1919 Tretiakoff et al. reported the presence of these inclusions (termed "Lewy bodies") in the substantia nigra of PD (Goedert, Spillantini et al.



2013). Lewy body pathology has been implicated as a cause of PD by promoting neurodegeneration. Surprisingly, Lewy body pathology in PD doesn't only restrain to central nervous system, but it also extends to peripheral nervous system and enteric nervous system.

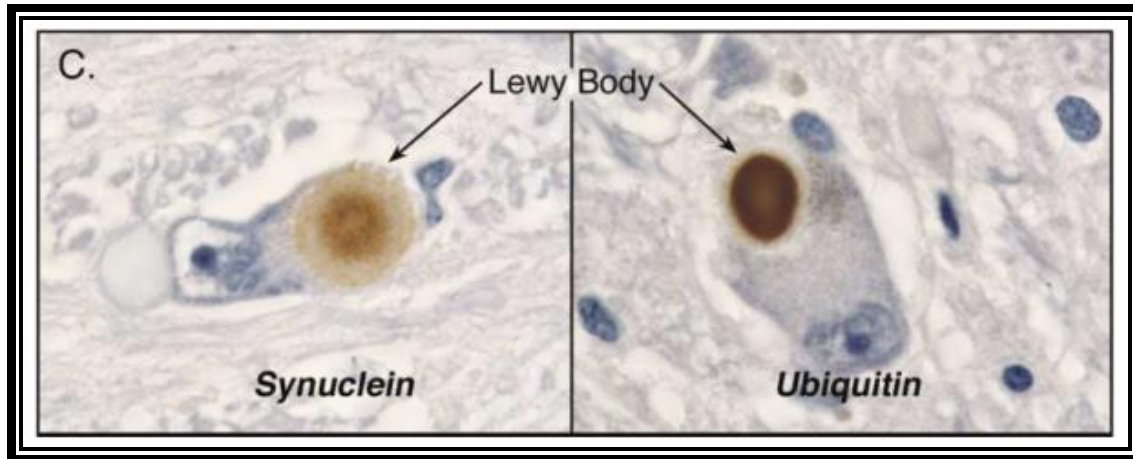


**Figure 1-2. Immunostained Lewy bodies in SNPc dopaminergic neurons of Parkinson's disease**

**Immunostaining with an antibody against  $\alpha$ -synuclein reveals intensely immunoreactive central core surrounded by faintly reactive peripheral zone. Whereas, staining with ubiquitin reveals diffused immunostaining throughout lewy body (Dauer and Przedborski 2003).**

In 1997, two research findings on  $\alpha$ -synuclein protein brought substantial change in the Lewy body research in PD field (Polymeropoulos, Lavedan et al. 1997, Spillantini, Schmidt et al. 1997). One of these studies identified  $\alpha$ -synuclein mutations in some familial cases of PD (Polymeropoulos, Lavedan et al. 1997). Immediately following this finding, Spillantini et al. showed that in idiopathic PD, Lewy bodies and Lewy neurites exhibited strong staining for  $\alpha$ -synuclein protein (**figures 1-2, 1-3**). Later, it was shown by electron microscopy that Lewy bodies and Lewy neurites are made of unbranched  $\alpha$ -synuclein filaments, with a length of 200-600nm and width of 5-10 nm and stain very strongly compared to traditional staining with

ubiquitin (Spillantini, Crowther et al. 1998). Now, it has been established that  $\alpha$ -synuclein forms the major filamentous portion of Lewy bodies and Lewy neurites in PD.

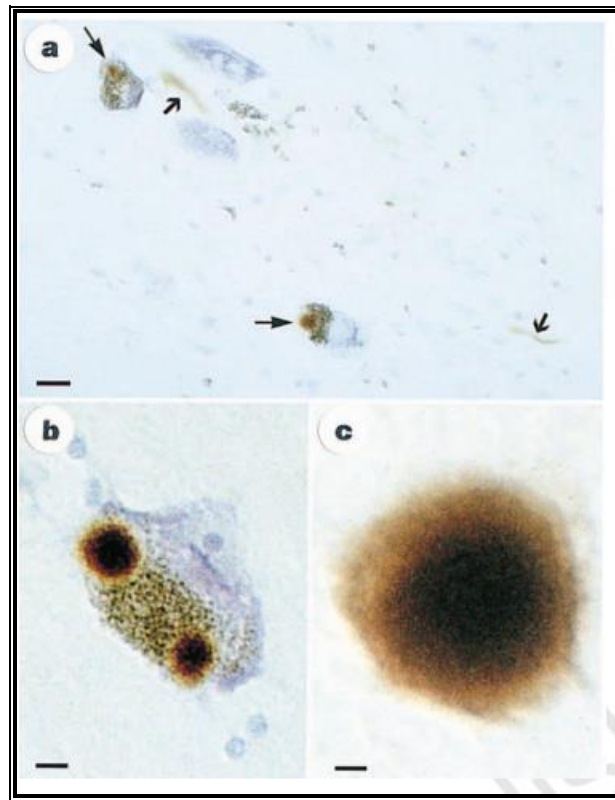


**Figure 1-3.** Substantia nigra from Parkinson's disease patient stained for  $\alpha$ -synuclein

(a) Shows two pigmented nerve cells, each containing an  $\alpha$ -synuclein positive Lewy bodies (thin line). Lewy neurites (thick line) are also immunopositive, (b) shows two  $\alpha$ -synuclein-positive Lewy bodies in single pigmented cell, and (c) shows  $\alpha$ -synuclein positive extracellular Lewy body (Spillantini, Schmidt et al. 1997).

Missense and gene dosage mutations in SNCA ( $\alpha$ -synuclein gene) are related to familial PD. However, 90% cases of PD are sporadic in nature.  $\alpha$ -synuclein pathology has been shown to spread in a prion-like manner, originating from small number of nerve cells (Goedert, Clavaguera et al. 2010).  $\alpha$ -synuclein positive Lewy bodies and Lewy neurites emerge in predictable order and Braak et al. have established a staging scheme for sporadic PD progression (Braak, Del Tredici et al. 2003) (figure 1-4).

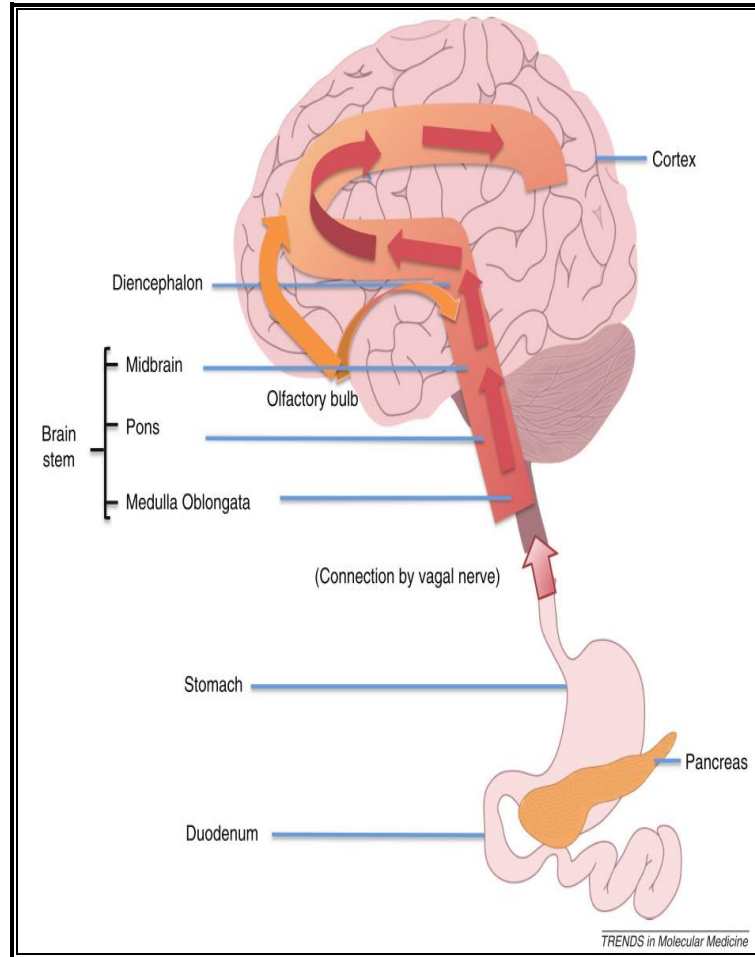


**Figure 1-4. Spread of idiopathic Parkinson's disease pathology**

**Lewy body pathology may arise from peripheral/enteric nervous system, possibly in gastrointestinal tract, and transfer to the brain stem via the glossopharyngeal and vagus nerves. Finally, it spreads to the cortex at a later stage of disease progression (red arrows). Alternatively, the pathology may start at the olfactory bulb and anterior olfactory nucleus and spread to the midbrain and cortex regions (orange arrows) (Hansen and Li 2012).**

According to the staging scheme, Lewy pathology spreads in PD patient in six distinguishable stages. Lewy pathology spreads to substantia nigra in 3<sup>rd</sup> stage. Staging scheme corroborates the findings that non-motor symptoms of PD appear before the motor symptoms. Schapira et al. have proposed that the detection of incidental Lewy bodies can be an early predictor of neurodegeneration and can help significantly in disease intervention in early stage of PD (Schapira and Tolosa 2010).

### **1.3.4 Oxidative stress and Parkinson's disease**

Human brain is highly susceptible to oxidative stress because of four reasons,

- i. High concentration of polyunsaturated fatty acids (PUFA), which are substrates for lipid peroxidation,
- ii. Brain utilizes the maximum amount of oxygen among all body parts and under chronic stress there is more probability of mitochondrial dysfunction,
- iii. Brain possess low concentrations of anti-oxidant protective mechanisms such as catalase, glutathione, glutathione peroxidase, tocopherol etc. than other body parts,
- iv. Iron is present at high concentration in specific brain regions which can catalyze various reactions that can cause generation of free radicals or hydroxyl ion (Olanow 1990).

Post-mortem analysis of PD brain show significant increase in oxidation of various biomolecules in substantia nigra, which implies involvement of free radicals and reactive oxygen species (ROS) in the pathology of PD. It has been suggested that exposure to environmental toxin or an endogenous toxic process might initiate generation of free radicals and promote vicious cycle of oxidative stress (Jenner, Dexter et al. 1992). However, the intimate relationship of oxidative stress with many other pathological factors involved in PD pathogenesis suggests that it is very difficult to conclude whether oxidative stress is responsible for initiation of PD or not, but it surely is responsible for the progression of PD (Jenner 2003). In PD, dopaminergic neuron milieu and increased iron accumulation can strongly promote excessive generation of free radicals, which can cause increased oxidative burden. In addition, mitochondrial dysfunction can result in increased generation of ROS. The extent of change in the oxidative stress in the substantia nigra suggests that the oxidative stress is not just limited to dopaminergic neurons but should also be taking place in other non-neuronal cells of substantia nigra. Early compensatory

changes in the turnover of DA because of nigral dopaminergic neuron degeneration may initiate an increase in oxidative stress and oxidative metabolites of DA.

Initially, the presence of neuromelanin (a product of DA oxidation) in nigral neurons attracted significant interest. Auto-oxidation of DA, formation of semiquinone, and polymerization of DA has been extensively studied as sources of oxidative stress (**figure 1-5**). DA auto-oxidation and its metabolism by monoamine oxidase-B (MAO-B) generate hydrogen peroxide. Under normal conditions, the generated hydrogen peroxide is neutralized by cellular anti-oxidant machinery (particularly glutathione system). However, in PD, overburden of oxidative species can compromise cellular anti-oxidant systems and result in excessive hydrogen peroxide accumulation.

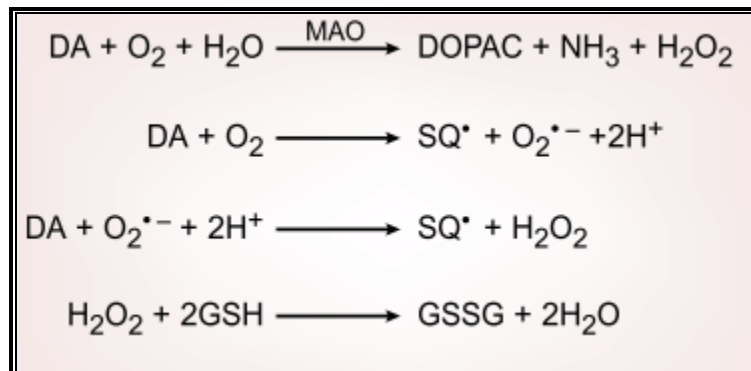


**Figure 1-5.** Dopamine metabolism by enzymatic reaction and autooxidation

**Enzymatic metabolism of dopamine by MAO-B liberates hydrogen peroxide. Auto-oxidation of dopamine results in formation of semi-quinones, free radicals which enter vicious cycle of oxidative stress by reacting with dopamine to liberate hydrogen peroxide and free radicals. Hydrogen peroxide generated by both reactions is neutralized by glutathione system in cells (Lotharius and Brundin 2002).**

Iron-melanin complexes have been shown to be elevated in PD substantia nigra (Jellinger, Kienzl et al. 1992). Iron(III) accumulation may selectively occur in melanized dopaminergic neurons because of melanin's high affinity to interact with iron(III). In PD substantia nigra, there is a shift in iron(II)/iron(III) ratio in favor of iron(III) and a subsequent

increase in iron(III)-binding protein ferritin (Riederer, Sofic et al. 1989). Iron can catalyze two different biochemical reactions which can cause generation of ROS and free radicals, increasing the oxidative burden in PD. Fenton reaction and Haber-Weiss reactions are known to be catalyzed by iron(II) in cells under physiological environment. Haber-Weiss reaction is very slow but can be catalyzed by iron(III) (**figure 1-6**). These reactions can convert the hydrogen peroxide generated by DA metabolism or by superoxide dismutase enzyme to highly toxic hydroxyl radical, which can result in increased oxidative stress in PD substantia nigra.

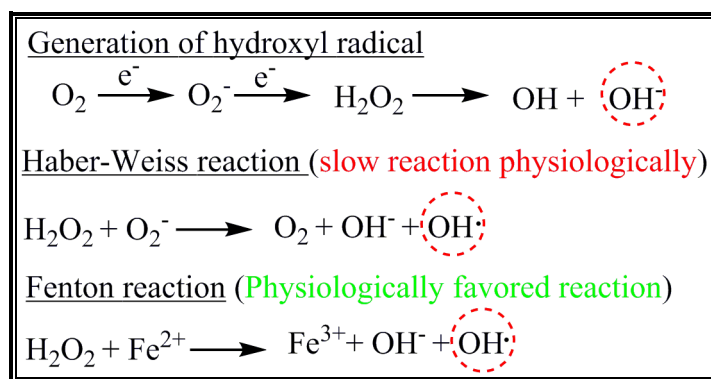


**Figure 1-6. Iron(III) catalyzed reactions**

Superoxide ions generated in cells are usually converted to hydrogen peroxide by superoxide dismutase enzyme (anti-oxidant enzyme) and the hydrogen peroxide is neutralized by glutathione system. However, higher oxidative burden can generate excessive superoxide ions which get converted into highly reactive hydroxyl radical by Haber Weiss reaction or Fenton reaction. Haber Weiss reaction is very slow at physiological conditions and superoxide dismutase is shown to neutralize superoxide before the reaction can take place. However, Fenton reaction is the mechanism which can generate hydroxyl radicals from hydrogen peroxide (Olanow 1990).

Energy for various cellular processes is provided by ATP, which are generated by mitochondria of cells. Aging, various environmental factors (toxins) and genetic risk factors associated with PD cause mitochondrial dysfunction by influencing the bioenergetics, dynamics, transport and quality control of mitochondria (Exner, Lutz et al. 2012). Mitochondrial oxidative phosphorylation generates ATP for various cellular processes and it depends on both

mitochondrial and nuclear DNA-encoded proteins for its function (**figure 1-7**). Systemic dysfunction of mitochondrial complex-I enzyme has been shown to be present in substantia nigra, platelets, skeletal muscles and frontal cortex of patients with PD (Exner, Lutz et al. 2012). Mitochondrial DNA has been also shown to undergo age dependent mutations and deletions, which can contribute to mitochondrial dysfunction in age related PD. Substantia nigra dopaminergic neurons are more susceptible to mitochondrial DNA mutations, as neurons from other regions of brain do not show high levels of mitochondrial DNA mutations.

Mitochondrial complex-I inhibition, which is widely used to model PD in various cell culture and animal models (discussed later) has been shown to cause decreased ATP production and increased formation of reactive oxygen species. This process can further damage mitochondrial DNA and trigger vicious cycle of mitochondrial impairment and oxidative stress (Lin and Beal 2006). Genes associated with PD have been also shown to be involved in inhibition of mitochondrial complex-I (discussed later).

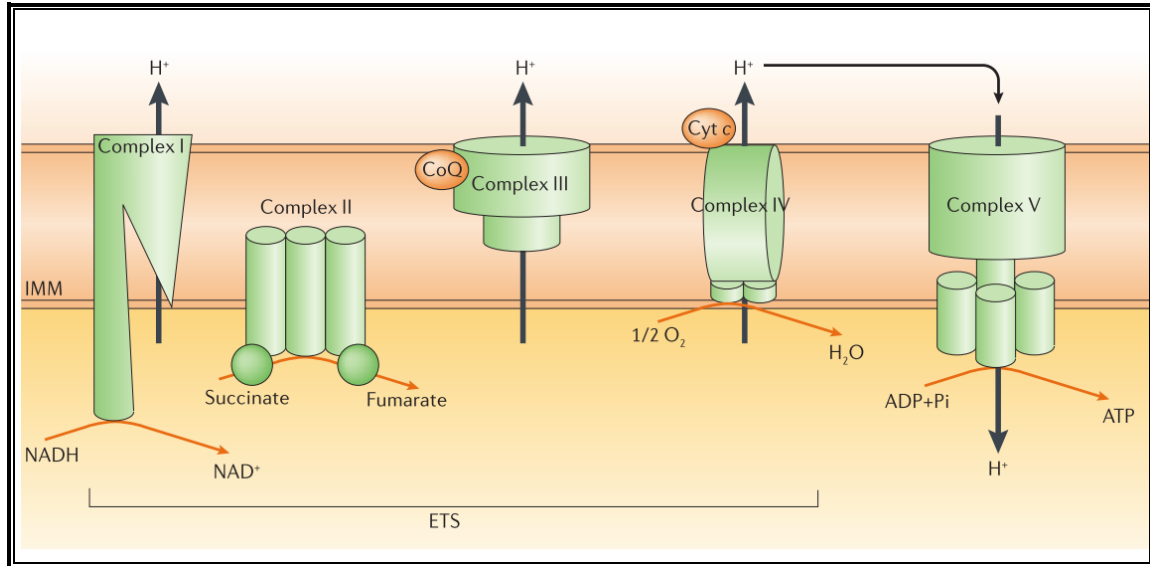


**Figure 1-7. Mitochondrial Electron Transport System (ETS)**

The ETS is located on inner mitochondrial membrane and has 4 membrane spanning enzyme complexes, which efflux protons out and generate protomotive force. These protons again enter mitochondrial inner membrane through Complex V and generate ATP from ADP. Parkinson's disease patients have significant decrease in their mitochondrial complex-I activity. Surprisingly, this decrease is not only limited to substantia nigra but it is widespread and shown to be present in platelets, skeletal muscles and frontal cortex (Abou-Sleiman, Muqit et al. 2006).

Excessive generation of reactive oxygen species or their inadequate clearance by anti-oxidant systems can lead to the oxidation of biomolecules in the substantia nigra. Because of unstable nature of superoxide, hydroxyl and other free radicals, they instantaneously react with surrounding lipids, proteins and DNA of substantia nigra cell population.

PUFA levels are significantly high in brain, which means there is high amount of lipids available as a substrate, which can undergo lipid peroxidation. Various studies have shown that the PUFA content in the PD substantia nigra is significantly reduced and simultaneously there is significant increase in Malondialdehyde (MDA) and 4-hydroxynonenal (4-HNE) levels which are late end-stage byproducts of lipid peroxidation (Dexter, Carter et al. 1989) (**figure 1-8**). Lipid hydroperoxides, which are early stage products of lipid peroxidation are shown to be present in



even higher concentration in PD substantia nigra (Jenner, Dexter et al. 1992). This implies that in PD substantia nigra, significant amount of PUFA undergo lipid peroxidation, which results in decrease in total PUFA available. One of the reasons for lipid peroxidation in PD substantia nigra may be excessive iron accumulation, which can catalyze chemical reactions to generate hydroxyl radical. The resulting 4-HNE is highly reactive and can form stable adducts with thiol and amine groups of proteins resulting in their damage.

Increase in the level of 8-hydroxy-2'-deoxyguanosine (8-OHG) (guanine oxidation product) and parallel decrease in the levels of FAPy-guanine (guanine reduction product) have been reported in PD, which indicates oxyradical-mediated damage to the nuclear DNA (Alam, Jenner et al. 1997). 8-OHG and FAPy-guanine have a common intermediate precursor, which when oxidized yields 8-OHG and when reduced gives FAPy-guanine. This suggests that the DNA damage may not be actually because of oxidative stress, but possibly because of change in redox status in the diseased tissue (Jenner 2003) (**figure 1-9**).

DNA damage is even more pronounced in mitochondria, as the DNA isolated from mitochondria showed 10 times high levels of 8-OHG (Mecocci, MacGarvey et al. 1993). It has been suggested that hydroxyl radical may not be involved in DNA damage as it can generate many diverse oxidation products of DNA, which are not observed in post-mortem PD substantia nigra. However, peroxy radicals from lipid peroxidation could selectively damage guanine and they could be potentially involved in DNA damage in PD (Shigenaga, Aboujaoude et al. 1994).

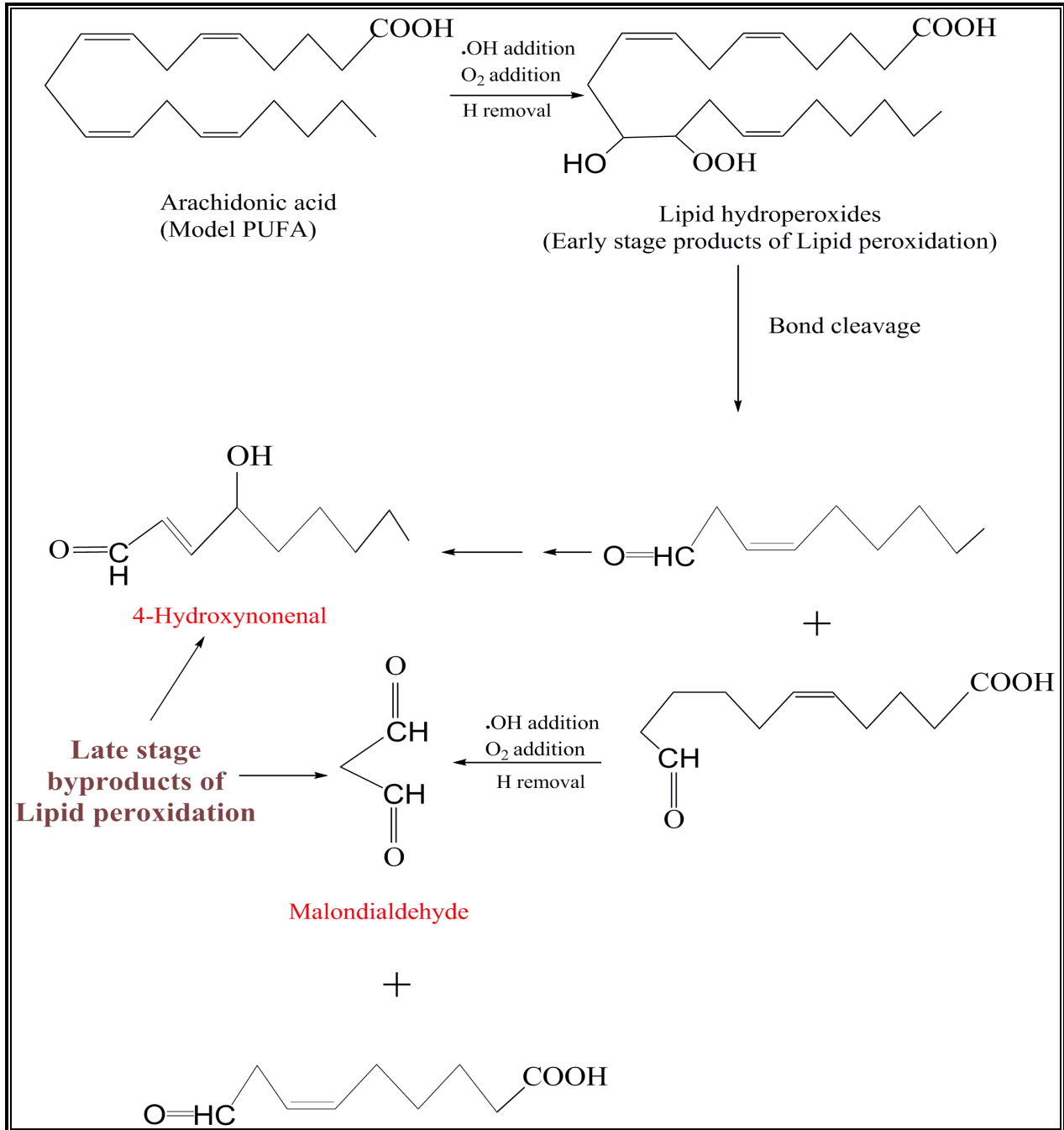


**Figure 1-8.** Lipid peroxidation process in presence of free radicals

Model of peroxidation of Arachidonic acid, where initial reaction with hydroxyl radical generates reactive intermediate which reacts with  $\text{O}_2$  to give lipid hydroperoxides. Lipid hydroperoxides react further to give MDA and 4-HNE (VanderJagt, Harrison et al. 2001).

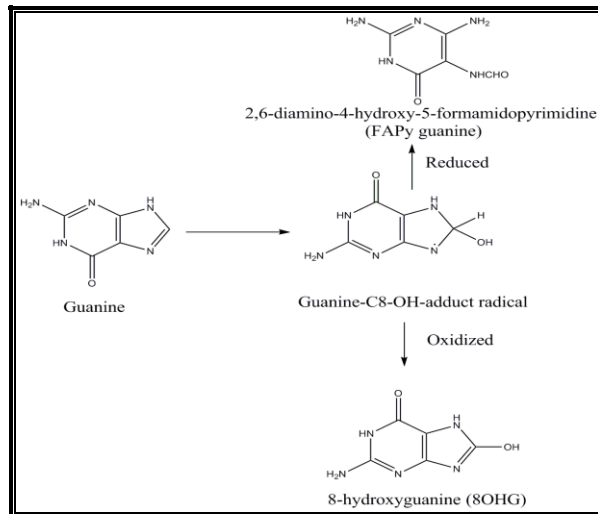


**Figure 1-9.** Products of guanine oxidative damage via the intermediate C8-OH adduct radical

Guanine under various oxidative conditions can form C8-OH-adduct radical, which can get converted to 8-OHG under oxidizing environment or can convert into FAPy guanine under reducing environment. It is postulated that the damage to DNA might be not due to radical attack but due to oxidizing environment in Parkinson's disease (Alam, Jenner et al. 1997).

Index	Brain region	Percentage of control
Total iron concentration	Substantia nigra	129%
	Cortex	100%
Superoxide dismutase	Substantia nigra	133%
	Cerebellum	95%
Lipid peroxidation	Substantia nigra	135%
	Cortex	94%
Protein oxidation	Substantia nigra	~200%
	Frontal cortex	~100%
DNA oxidation	Substantia nigra	238%
	Cerebellum	110%

**Table 1.1.** Evidence of oxidative stress in Parkinson's disease.

Oxidation of lipid, protein and DNA is dramatically elevated in the substantia nigra specifically. Iron accumulation in the substantia nigra of patients with Parkinson's disease results in Fenton reaction which causes ROS generation. Anti-oxidant enzyme levels reflect oxidative burden in substantia nigra compared to other brain regions (Lotharius and Brundin 2002).

Oxidative stress associated damage to proteins is also reported in patients with advanced stage PD (Floor and Wetzel 1998) (**figure 1-10**). Surprisingly, protein carbonyls have been shown to be elevated not only in the substantia nigra of advanced stage PD brain, but also in all other brain regions. Protein carbonyl levels in various brain areas of PD are independent of iron(III)/iron(II) level and thus iron might not play a primary role in generation of protein carbonyls. Also, protein carbonyl levels are not found to be changed in incidental Lewy body disease, which is considered presymptomatic PD. L-DOPA therapy (which can act as pro-oxidant) and/or more widespread effects of oxidative stress in advanced stage of the disease in PD patients could cause a generalized increase in protein carbonyl levels in brain (Fahn 1996, Alam, Daniel et al. 1997). Protein carbonylation is an irreversible and unreparable process. Additionally, PD patients have dysfunctional ubiquitin-proteasome system, which increases the possibility of protein carbonyls forming higher molecular weight aggregates that may be cytotoxic. Damage to proteins which are responsible for dopaminergic neurotransmission ( $\alpha$ -synuclein, DAT, VMAT2, v-SNARE, t-SNARE, and dopamine receptors) may cause direct damage in PD.

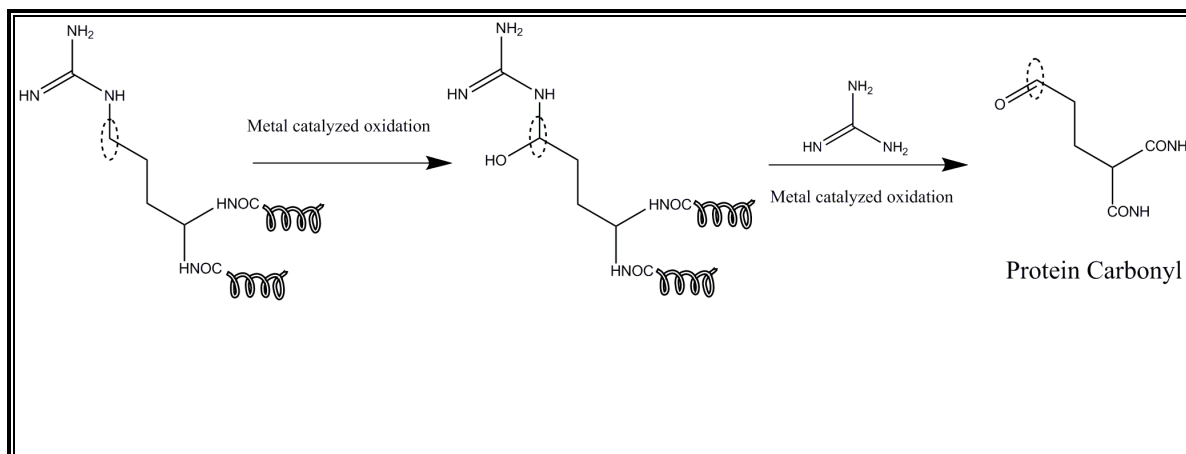


**Figure 1-10.** Carbonylation of protein amino acid side-chain

Increased oxidative stress in PD can overburden the anti-oxidant systems of cells. Unfortunately, as mentioned before, brain has less amount of catalase, tocopherol, glutathione, glutathione reductase, and glutathione peroxidase (key anti-oxidant defense systems in cells) compared to peripheral organs. Dysfunction of anti-oxidant systems in cells can result in decreased clearance of oxidative species and increased oxidative environment. Significant decrease in levels of reduced glutathione and total glutathione are reported in substantia nigra of patients with PD and there is no corresponding increase in oxidized glutathione (Perry, Godin et al. 1982, Sofic, Lange et al. 1992). Decrease in glutathione levels may reduce the clearance of  $H_2O_2$  (generated from dopamine auto-oxidation and metabolism) and promote the formation of hydroxyl radical in a reaction catalyzed by iron in substantia nigra.

Interestingly, the extent of glutathione depletion correlates well with the severity of PD (Jenner and Olanow 1996). Also, glutathione depletion has been shown to precede the loss of dopaminergic neurons as well as accumulation of “Lewy bodies” in PD patients. In patients with incidental Lewy body disease (ILB), glutathione is depleted to similar levels as PD patients. However, ILB patients do not show elevated levels of iron or impaired activity of mitochondrial complex-I. Thus, glutathione depletion may be an earliest biochemical marker for nigral neurodegeneration. Various studies have concluded that the glutathione depletion is not only limited to neuronal population, but glial cells of substantia nigra are also significantly depleted of glutathione because of huge amount of glutathione levels they possess. Corresponding increase in oxidized glutathione hasn't been observed because glutathione is shown to be effluxed by cells under persistent oxidative stress. No significant changes in glutathione system enzymes- glutathione reductase, glutathione peroxidase,  $\gamma$ -glutamylcysteine synthetase (rate-limiting enzyme in glutathione synthesis) and glutathione transferase have been reported. However, two

fold increase in an enzyme-  $\gamma$ -glutamyl transpeptidase ( $\gamma$ -GTP) has been reported (Sian, Dexter et al. 1994).  $\gamma$ -GTP is a cell membrane enzyme responsible for degradation and translocation of glutathione. Conjugation of glutathione and its amino acid (cysteine) with oxidized products of DA, L-DOPA, DOPAC (dopamine metabolite), and other catecholamines has been also suggested to result in decrease in reduced glutathione levels (Shen and Dryhurst 1996, Spencer, Jenner et al. 1998, Linert and Jameson 2000). **Figure 1-11** demonstrates the synthesis pathway of glutathione and its role in various detoxification processes in the cellular system.

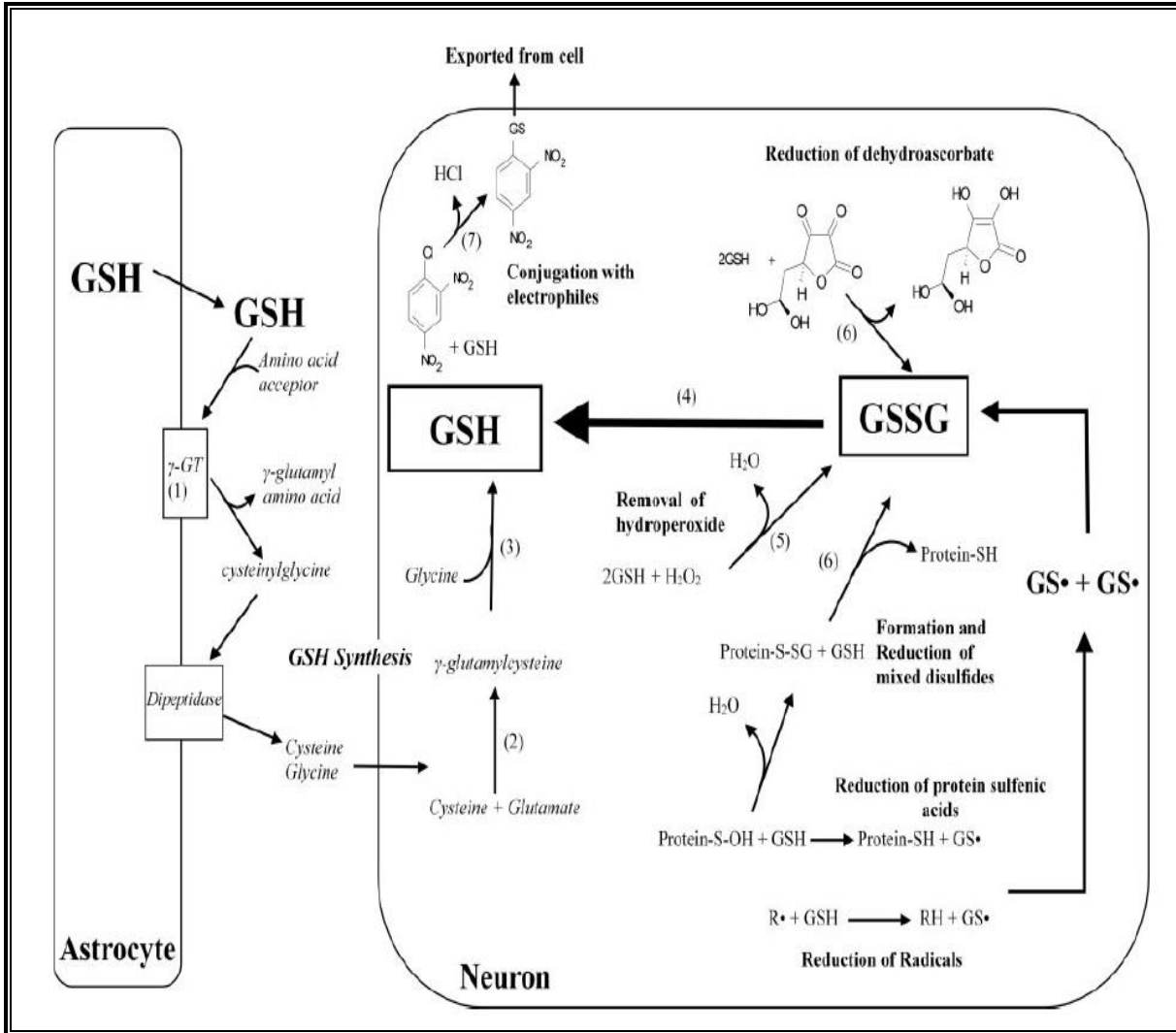


**Figure 1-11.** Glutathione synthesis and metabolism in the central nervous system

Both astrocytes and neurons can synthesize glutathione, but astrocytes also play important roles in substrate supply to neurons. Glutathione synthesized in astrocytes is exported in the extracellular space, where ectoenzyme  $\gamma$ -GTP (1) transfers the glutamyl group onto amino acid acceptor, creating cysteinylglycine, which is broken down into its constituents, cysteine and glycine. Glutathione is synthesized in two steps: first, glutamyl cysteine is formed from cysteine and glutamate, catalyzed by GCL (2), then glycine is added by glutathione synthase (3). Glutathione has many roles in detoxification and maintenance of redox equilibrium. The majority of these processes generate GSSG, which is reduced back to GSH by glutathione reductase and NADPH from pentose phosphate shunt (4). 1.  $\gamma$ -GTP, 2. GCL, 3. glutathione synthase, 4. glutathione reductase, 5. glutathione peroxidase, 6. glutaredoxin, 7. GST (Martin and Teismann 2009).

## 1.4 Etiology of Parkinson's disease

### 1.4.1 Environmental factors

Specific etiology of PD is not known. However, numbers of epidemiological studies and an accidental finding have concluded potential environmental factors that can significantly increase the risk of PD. The risk factors include exposure to pesticides, herbicides, well water, industrial chemicals, wood pulp mills, farming and living in rural environment.

Current hypothesis implicates exposure to dopaminergic and mitochondrial toxins as a risk factor for PD. MPTP (meperidine analog), rotenone (insecticide) (Betarbet, Sherer et al. 2000) and paraquat (herbicide) (Liou, Tsai et al. 1997) are known to induce PD. In fact, accidental exposure to MPTP induced chronic parkinsonism in human subjects (Langston, Ballard et al. 1983), which led to its use as in-vitro and in-vivo model of PD. Surprisingly, all the toxins mentioned above cause mitochondrial dysfunction in cells, particularly they damage mitochondrial complex-I, whose activity has been shown to be decreased in PD patients.

Generation of pyridinium metabolite has been shown to cause PD symptoms in MPTP-induced Parkinsonism (Markey, Johannessen et al. 1984). MPTP is highly lipophilic and crosses the blood-brain barrier within minutes of administration. Afterwards, MPTP is oxidized by MAO-B (located in glial cells and serotonergic neurons only) to 1-methyl-4-phenyl-2,3-dihydropyridine (MPDP<sup>+</sup>). It is then converted to MPP<sup>+</sup> (probably by spontaneous oxidation), the toxic metabolite, which is substrate for DAT. MPP<sup>+</sup> enters dopaminergic neurons and can cause damage by three possible mechanisms,

- i) Bind to VMAT-2 which can translocate MPP<sup>+</sup> to synaptosomal vesicles,
- ii) Concentrate in mitochondria and block electron transport chain by inhibiting complex-I activity,



- iii) Can remain in cytosol to interact with cytosolic enzymes, especially the one carrying negative charge (**figure 1-12**).

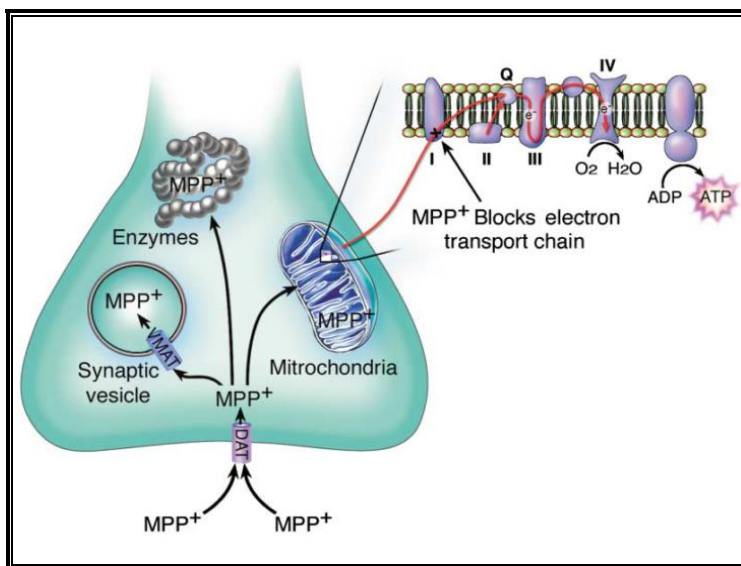


**Figure 1-12. Representation of intracellular pathways of MPP<sup>+</sup> toxicity (Dauer and Przedborski 2003)**

Paraquat is a herbicide structurally similar to MPP<sup>+</sup> and found to be present in environment (**figure 1-13**). It doesn't penetrate blood-brain barrier easily (Shimizu, Ohtaki et al. 2001). Paraquat has been shown to produce toxicity by inhibition of mitochondrial complex-I and by generation of superoxide radicals. Systemic administration of Paraquat in mice leads to selective degeneration of SNpc dopaminergic neurons with appearance of "Lewy bodies" containing  $\alpha$ -synuclein aggregates (McCormack, Thiruchelvam et al. 2002). Surprisingly, Paraquat induced dopaminergic neurodegeneration doesn't reflect similar loss of DA levels in animal models. It has been suggested that paraquat might selectively damage dopaminergic neuronal cell bodies, sparing the neuronal terminals. Tyrosine hydroxylase activity in paraquat treated animals is also shown to be increased, which suggests some compensatory changes taking place after paraquat induced neurodegeneration (McCormack, Thiruchelvam et al. 2002).

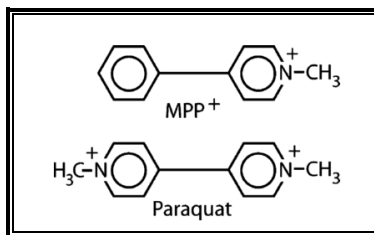


**Figure 1-13. Structural similarity between MPP<sup>+</sup> and Paraquat**

Rotenone is a naturally occurring compound found in roots of Leguminosa plant species. It is used as an insecticide and to kill unwanted fish. It has been shown to selectively inhibit mitochondrial complex-I activity, without affecting complex-II and complex-IV activity. Rotenone is highly hydrophobic and can easily cross biological membranes. It doesn't require dopamine transporter to be taken up into dopaminergic neurons. MPTP induces dopaminergic neuronal complex-I inhibition, whereas in PD, complex-I inhibition is observed systemically. Rotenone has been shown to induce systemic partial defect in complex-I, which is enough to produce behavioral, neurochemical and neuropathological symptoms of PD (Betarbet, Sherer et al. 2000). Selective damage of dopaminergic neurons by rotenone suggests that the dopaminergic neurons may be more vulnerable than other cell population to mitochondrial complex-I inhibition.

#### **1.4.2 Genetic factors**

PD was earlier thought as sporadic disorder in nature and not related to genetic inheritance. However, numerous findings in last two decades have implicated various genes that may increase the susceptibility to PD. Genetic inheritance has been shown to be significantly involved in the cases of young-onset PD. 10-30% PD patients report a positive family history. Additionally, first-degree relatives of subjects with PD were shown to have two to seven-fold increase in relative risk of PD (Shulman, De Jager et al. 2011). Initially, linkage analysis which

analyzed multiple family members affected by Mendelian PD revealed rare genetic variant which have high penetrance effect. On the other side, Genome wide association analysis compared control and case subjects and identified statistically significant genetic variants with incomplete penetrance responsible for sporadic PD. Surprisingly, both approaches yielded some genes which overlap. Thus, now PD is considered to be a complex disease resulting from interaction of environment/gene and/or gene/gene.

More than 13 loci and 9 genes are associated with autosomal dominant or autosomal recessive form of PD (Lesage and Brice 2009) (**table 1-2**). Identified genes can be divided into two types: causal genes and associated genes. Causal gene alone without the influence of other genes or environmental factors causes PD in person who inherits it, whereas, associated gene does not cause PD but increases the possibility of developing it. Associated gene's interaction with other genes or environmental factors can trigger PD in the person who inherits it. SNCA, PARK2, and PARK7 are causal genes, whereas, LRRK2 is an associated gene.

SNCA ( $\alpha$ -synuclein) has been clearly shown to be involved in pathophysiology of familial and sporadic PD. It is the major component of Lewy bodies and Lewy neurites found in PD patients. Three missense mutation in SNCA: A30P (Kruger et al. 1998), E46K (Zarranz, Alegre et al. 2004), and A53T (Polymeropoulos, Lavedan et al. 1997, Spira, Sharpe et al. 2001) are extremely rare. However, all the patients with missense mutations have early onset of disease and dementia with Lewy bodies. Duplication (Chartier-Harlin, Kachergus et al. 2004) and triplication (Singleton, Farrer et al. 2003) of the locus containing SNCA support the hypothesis that the increase in  $\alpha$ -synuclein concentration is toxic. Early stage patients with SNCA duplication resemble patients with "idiopathic" PD. Interestingly, patients with SNCA triplication have earlier onset, faster disease progression, marked dementia, and frequent

dysautonomia (Ross, Braithwaite et al. 2008). This further corroborates the dosing effect of SNCA gene.

PARK Loci	Gene	Forms of PD	Mutations
PD- associated loci and genes with conclusive evidence			
PARK1/PARK4	SNCA	EOPD AD and sporadic	A30P, E46K, A53T Genomic duplications/triplications
PARK8	LRRK2	LOPD AD and sporadic	40 missense variants, >7 of them pathogenic, including the common G2019S
PARK2	Parkin	Juvenile and EOPD AR and sporadic	>100 mutations (point mutations, exonic rearrangements)
PARK6	PINK1	ARPD	>40 point mutations, rare large deletions
PARK7	DJ-1	EOPD AR	>10 point mutations and large deletions
PARK9	ATP13A2	Juvenile AR Kufor-rakeb syndrome and EOPD	>5 point mutations

**Table 1-2. Loci, genes and susceptibility factors involved in Parkinson's disease**

**EO, Early onset; LO, Late onset; AD, Autosomal dominant; AR, Autosomal recessive; PD, Parkinson's disease; SNCA,  $\alpha$ -synuclein; LRRK2, Leucine-Rich Repeat Kinase-2; PINK1, PTEN-induced kinase 1 (Lesage and Brice 2009).**

$\alpha$ -synuclein is a small, 140 amino acid protein that contains an amphipathic amino terminal, a hydrophobic central core [termed "non-amyloid component" (NAC region)] and negatively charged c-terminus (**figure 1-14**). It is expressed homogeneously throughout the nervous system. It is enriched at presynaptic nerve terminals, where it is found in association

with synaptic vesicular membranes. The physiological role of  $\alpha$ -synuclein is not well understood. Some studies suggest that it may be playing a critical role in neurotransmitter release and synaptic vesicle recycling (Lotharius and Brundin 2002). Brundin et al. have proposed that the mutant forms of  $\alpha$ -synuclein (A30P, E46K, A53T) might have a loss of normal function. Effect of toxic function of mutant protein may prevent the sequestration of DA into synaptic vesicles. Therefore, it may cause increased cytoplasmic concentration of DA, which may result in increased oxidative stress because of excessive DA metabolism and DA auto-oxidation in PD (Lotharius and Brundin 2002). Full length  $\alpha$ -synuclein normally occurs as a natively unfolded monomer. However, at higher concentrations, it can form oligomers (SDS-sensitive, non-covalently bound, soluble), which are termed “protofibrils”. Protofibrils can seed in a nucleation dependent manner to form fibrils (SDS-sensitive, non-covalently bound, insoluble) present in Lewy bodies (**figure 1-14**). A30P and A53T mutations of  $\alpha$ -synuclein increase the tendency of the protein to form protofibrils (Conway, Harper et al. 2000). Initial study by Lansbury et al. established that the protofibrils (oligomers) may be responsible for neuronal toxicity (Goldberg and Lansbury 2000). It may be possible that the fibrillar inclusions (Lewy bodies) may sequester the toxic species and/or divert  $\alpha$ -synuclein from toxic assembly pathways and protect neurons. It is further supported by the fact that the neuronal cells of post-mortem PD patients showing Lewy bodies appear healthy.

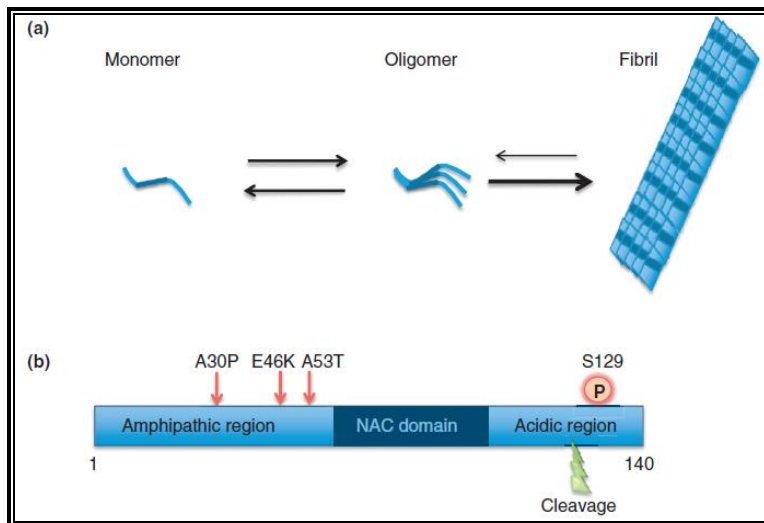


**Figure 1-14. Aggregation and functional domains of  $\alpha$ -synuclein**

$\alpha$ -synuclein natively occurs as an unfolded monomer, which at higher concentration or in presence of point mutations or by interaction of dopamine can aggregate to form oligomers (“protofibrils”), oligomers can seed in a nucleation-dependent manner to produce fibril structure ( $\beta$ -sheet rich structure) found in Lewy bodies [except for dopamine-induced oligomers] (a). Two point mutations A53T and E46K are genetically linked to Parkinson’s disease and speed up the process of oligomerization. Whereas, third point mutation A30P causes fragmentation of fibrils, which then accelerates the seeding process forming new fibrils. The amphipathic N-terminal region of  $\alpha$ -synuclein forms  $\alpha$ -helices when it associates with lipid membranes. This region and the hydrophobic NAC domain of protein are important for oligomerization. Synuclein can be phosphorylated at Ser129 by several different polo-like and casein kinases, however fibril form is usually found in phosphorylated form than the monomer form (Hansen and Li 2012).

Surprisingly, dopamine-quinone generated by auto-oxidation of DA can form covalent adduct with  $\alpha$ -synuclein and prevent the conversion of oligomers (SDS-resistant, covalently bound, soluble) to  $\beta$ -sheet bearing fibrillar structure (Conway, Rochet et al. 2001). Specifically 3 DA molecules under oxidizing condition have been shown to bind per  $\alpha$ -synuclein monomer, which yields its highly extended state (Illes-Toth, Dalton et al. 2013). It has been established that the “protofibrils” involved in the process of fibrillization are more toxic than the mature fibrils themselves (Goldberg and Lansbury 2000, Bucciantini, Giannoni et al. 2002, Li, Lin et al. 2005). It has been suggested that because of strong oxidizing environment in dopaminergic neurons

(easy ability of dopamine to convert into dopamine quinone),  $\alpha$ -synuclein “protofibrils” do not convert into fibrils rapidly when compared to environment in other neurons. The slower conversion may cause selective toxicity of protofibrils in dopaminergic neurons. Covalently modified oligomeric form of  $\alpha$ -synuclein has been shown to be able to attack and disrupt the biological membranes easily (Rochet, Outeiro et al. 2004). These oligomeric forms can further damage DA containing vesicles and increase the cytoplasmic levels of dopamine, which in turn can lead to vicious cycle of oxidative stress and dopamine- $\alpha$ -synuclein adduct formation. In addition, protofibrillar form of  $\alpha$ -synuclein has also been shown to transfer to other neighbouring neurons in prion-like manner (Prusiner 2012). This has been shown by presence of  $\alpha$ -synuclein containing Lewy bodies in patients grafted with fetal human mesencephalic dopaminergic neurons (Li, Englund et al. 2008) (**figure 1-15**).

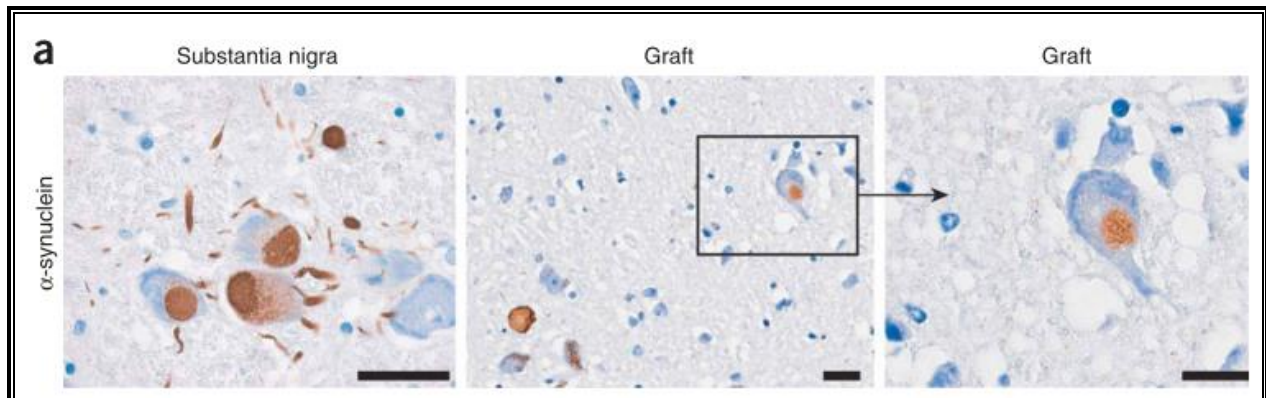


**Figure 1-15. Aggregation and functional domains of  $\alpha$ -synuclein**

**$\alpha$ -synuclein positive Lewy bodies in host substantia nigra and grafted dopaminergic neurons in Parkinson’s disease patient (Li, Englund et al. 2008).**

Mutations in PARK8 have been shown to be involved in sporadic as well as autosomal dominant familial Parkinson’s disease. PARK8 codes for leucine rich repeat kinase-2 (LRRK2) protein. The most common and best studied LRRK2 variant is G2019S, which is found in 1% to 4% in PD patients with European descent. However, populations with LRRK2 mutation has been

found to be developing PD symptoms after the age of 60 or in some cases found to be normal. Thus, additional genetic and environmental factors must be interacting to cause the disease onset.

Mutations in PARK2 have been shown to be involved in development of autosomal recessive juvenile PD. Patients with PARK2 mutations show degeneration of dopaminergic neurons without the presence of Lewy bodies. PARK2 encodes for Parkin, which is a E3-ubiquitin-protein ligase. Mutant Parkin from autosomal recessive PD patient doesn't have the E3-ubiquitin-protein ligase activity. Thus, it might result in accumulation of proteins which may cause dopaminergic neuronal demise. The onset of PD in population with PARK2 mutations is around 30 years of age.

Mutations in PINK-1 is the second most common cause of autosomal recessive juvenile PD. PINK-1 encodes a serine-threonine kinase that is widely expressed in mitochondria. Some data from animal models suggest that PINK-1 and Parkin may function coordinately (Exner, Lutz et al. 2012). Mutations in PARK7, which encodes DJ-1 is a rare cause of autosomal recessive juvenile PD. DJ-1 is a ubiquitously expressed protein with unknown function. However, it has been known to translocate to mitochondria in response to oxidative stress and may have protective role. Mutations in ATP13A2 have been shown to cause loss of function of ATP13A2 protein (lysosomal type 5 P-type ATPase). It has been suggested that there may be a link between aggregation of mutant protein in endoplasmic reticulum and proteasomal or lysosomal function (Ramirez, Heimbach et al. 2006).



### 1.5 Therapeutic interventions for Parkinson's disease

As discussed above, PD is a multi-factorial disorder for which the exact etiology is not known. Variety of interactions between aging, environmental factors, and genetic components may be potentially involved in dysfunction of the dopaminergic system of brain by increasing the oxidative burden and mitochondrial dysfunction selectively in the dopaminergic neurons. Unfortunately, PD motor symptoms, which are the cardinal features for diagnosis of PD, appear after significant dopaminergic neurodegeneration has already taken place and are currently used for diagnosis purpose. Most clinically used PD therapeutics are targeted towards restoring the normal dopaminergic function in the brain. Currently available therapeutics are either precursor of DA, DA receptor agonists or inhibitors of enzymes responsible for DA metabolism.

Surprisingly, L-DOPA which was discovered immediately following the discovery of DA still remains the gold standard to relieve motor deficits of PD (Birkmayer and Hornykiewicz 1961). L-DOPA is a prodrug of DA, which converts to DA through decarboxylation process by aromatic amino acid decarboxylase (AADC) enzyme. L-DOPA is combined with other drugs such as peripheral dopa decarboxylase inhibitors (DDC) or catechol-O-methyl-transferase (COMT) inhibitors or monoamine oxidase-B (MAO-B) inhibitors to either avoid its peripheral conversion to dopamine or to prevent its breakdown into dopamine metabolite in CNS (**figure 1-16**). Combination therapy helps in increasing the duration of action of L-DOPA. However, L-DOPA use results in production of dyskinesia and its long-term use results in sudden “on-off” effects (Marsden and Parkes 1976). DA receptor agonists such as pramipexole and ropinirole are also widely used. DA receptor agonists bind post-synaptic dopaminergic receptors to mimic response(s) similar to that produced by DA.

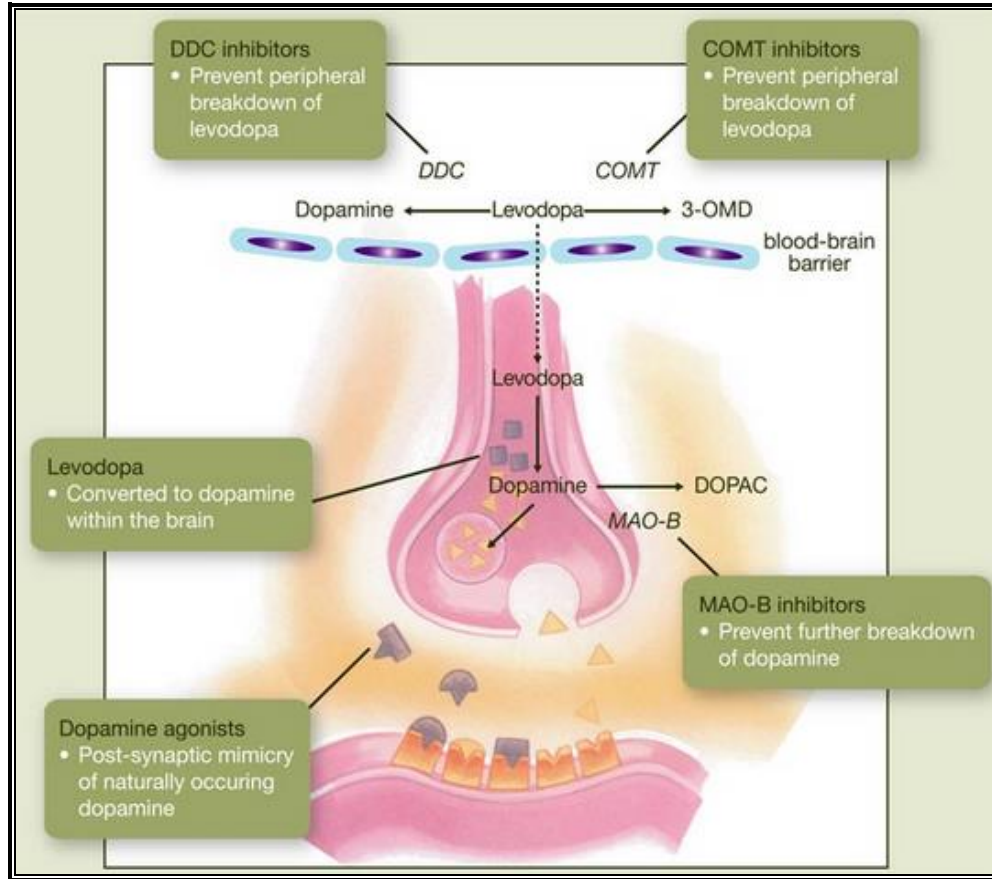


**Figure 1-16. Mode of action of current Parkinson's disease therapeutics**

**Levodopa is a gold-standard drug to relieve motor symptoms of Parkinson's disease. It is usually combined with other drugs such as peripheral dopa decarboxylase inhibitors or COMT inhibitors to prevent its peripheral breakdown. Levodopa is also combined with MAO-B inhibitors, which inhibit the breakdown of dopamine generated by levodopa. Dopamine agonists are also widely used to mimic effects of dopamine at post-synaptic dopaminergic receptors.**

Present PD therapeutics only provide symptomatic relief and are very useful in early stage of the disease. The critical issue that needs be addressed is that none of the clinically used drugs prevent the progression of neurodegeneration or resolve the underlying cause of the disease. Thus, over the course of disease, drug's effect diminishes and disease pathology leads to more complications. In addition, there is some evidence that L-DOPA increases oxidative burden and enhances PD progression (Basma, Morris et al. 1995, Fahn 1996). Table 1-3 mentions clinically used PD therapeutics with their mechanisms of action.

Drug Class (Generic name)	Brand Name	Mechanism of Action
<p><b>Dopamine replacement therapy</b></p> <p>(Carbidopa/Levodopa Carbidopa/Levodopa controlled release Carbidopa/Levodopa/Entecapone Carbidopa/Levodopa Orally disintegrating tablet)</p>	<p>Sinemet Sinemet CR Stalevo Parcopa</p>	<p>Levodopa is a precursor of dopamine, which is usually combined with Carbidopa (peripheral aromatic amino acid decarboxylase inhibitor) or Entecapone (COMT-inhibitor) to increase its CNS bioavailability and prevent its peripheral breakdown and resulting side-effects.</p>
<p><b>Dopamine Agonist</b></p> <p>(Pramipexole Ropinirole Rotigotine Pergolide Bromocriptine)</p>	<p>Mirapex Requip Neupro Permax Parlodel</p>	<p>Simulates the effect(s) of dopamine at post-synaptic dopamine receptors site.</p> <p>Table 1-3 continued on next page</p>

Drug Class (Generic name)	Brand Name	Mechanism of Action
<b>COMT inhibitors</b> (Tolcapone Entecapone)	Tasmar Comtan	COMT inhibition increases levodopa bioavailability in CNS by decreasing peripheral levodopa metabolism
<b>MAO-B inhibitors</b> (Selegeline Selegeline ODT Rasagiline)	Eldepryl Zelapar Azilect	Irreversible inhibitor of MAO-B which is responsible for breakdown of dopamine in CNS

**Table 1-3. Current Parkinson's disease therapy**

Ideal PD therapeutic should have the ability to halt or slow the progression of neurodegeneration in the disease process. Currently available PD therapeutics suffer a major drawback that they were designed to act on one of the many pathological targets responsible for PD. As PD is a multi-factorial disease involving complex sequence of events in its pathogenesis/progression, PD treatment can either include combination of drugs that act on different pathological targets (polypharmacy), or a single drug should be designed to possess the ability to act on multiple pathological targets involved in disease pathology (multifunctional drug) (Youdim 2010). Drug's ability to act on multiple targets associated with disease

progression/pathogenesis can potentially provide disease-modifying effect, which is highly desired to prevent or slow down the progression of PD.

Currently, there isn't any drug in market that was designed to aim at multiple pathological targets in PD. However, some clinically used drugs have been serendipitously found to possess ability to act on multiple pathological targets. Pramipexole and Rasagiline have been shown to possess some neuroprotective property in addition to their DA receptor agonist and MAO-B inhibition property respectively (Hall, Andrus et al. 1996, Dooley and Markham 1998). Rasagiline has been shown to have not only neuroprotective, but also neurorestorative property in MPTP and lactacystin-induced degeneration of nigrostriatal dopaminergic neurons (Sagi, Mandel et al. 2007, Zhu, Xie et al. 2008). In addition, Rasagiline is the only drug that may possess disease-modifying activity as shown by clinical trials (Olanow, Rascol et al. 2009). Thus, it seems more appealing to design drugs that can aim at multiple pathological targets involved in PD to yield disease-modifying therapeutics. In fact, Youdim et al., who contributed significantly in development of Rasagiline as a PD therapeutic, have designed some structurally modified moieties based on Rasagiline (MAO-B inhibitor), which possess multifunctional activity (Zhu, Xie et al. 2007, Youdim 2013). Youdim et al. targeted iron and MAO-B to design multifunctional therapeutics and one of their compounds M30 has been shown to possess significant disease-modifying activities in animal models of PD (Youdim 2013). As iron accumulation has been shown to be critical in pathogenesis of PD, it is ideal to have drugs with iron-chelator property. Other pathological targets that can be aimed at include dopamine receptors, COMT,  $\alpha$ -synuclein aggregation modifiers, and anti-oxidants.

## CHAPTER 2

### HYPOTHESES

#### Global Hypotheses

We hypothesized that as PD is a complex disorder resulting from interaction of multiple pathological factors, the ideal way to target the disease process is to design and develop a potential therapeutic that can act on various pathological factors responsible for PD. In fact, there is vast literature evidence that some of the clinically used drugs for PD have broad mechanisms of action rather than selectivity for one particular pathological target of PD (Shoulson 1998, Ramirez, Wong et al. 2003, Olanow, Rascol et al. 2009). Hence, we aimed to design therapeutics which can target more than one pathogenesis factors involved in PD progression. Initially, we developed some hybrid ligands that can preferentially target dopamine D<sub>2</sub> and/or D<sub>3</sub> receptors (Biswas, Hazeldine et al. 2008, Li, Biswas et al. 2010, Johnson, Antonio et al. 2012). Afterwards, we further optimized their structures to incorporate iron-chelation, anti-oxidant or  $\alpha$ -synuclein aggregation inhibition property (Ghosh, Antonio et al. 2010, Gogoi, Antonio et al. 2011, Johnson, Antonio et al. 2012). Our quest to develop multifunctional PD therapeutic yielded some versatile compounds, which exhibited quite promising results as multi-functional compounds in animal models and cell-culture models (Ghosh, Antonio et al. 2010, Gogoi, Antonio et al. 2011, Santra, Xu et al. 2013). As shown in **figure 2-1**, we designed our compounds based on Pramipexole pharmacophore to retain DA receptor activity and incorporated additional moieties to generate multifunctional properties.

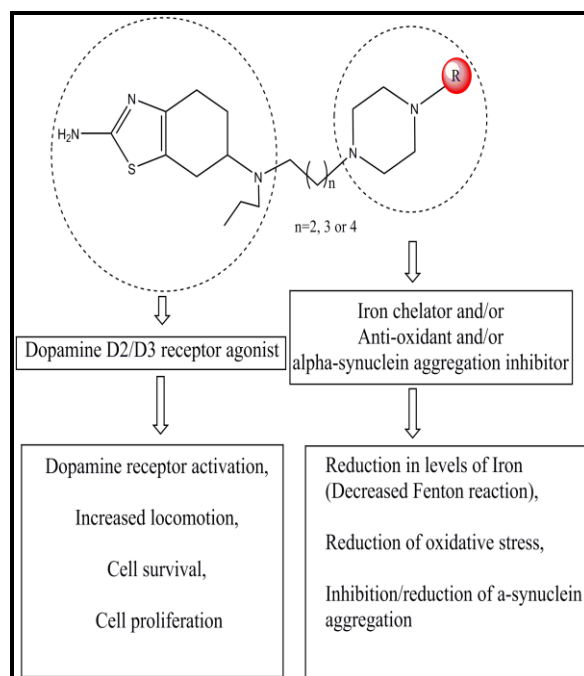


**Figure 2-1. Design of potential multifunctional compounds for Parkinson's disease**

Our efforts to generate multifunctional PD therapeutics yielded an interesting compound D-512 ((-)-19), which showed potent agonist activity at  $D_2$  and  $D_3$  receptors (non-preferential agonist) (Johnson, Antonio et al. 2012). D-512 showed exceptional anti-oxidant activity. D-512 also showed ability to reverse hypolocomotion in long-lasting manner induced by reserpine in rat model of PD.

### **Project hypotheses**

First hypothesis of my dissertation study was that as D-512 exhibited neuroprotective effects in a cell-line devoid of dopaminergic receptors (Santra, Xu et al. 2013), D-512 is a non-prefering DA  $D_2/D_3$  receptor agonist, and D-512 also possess a potent anti-oxidant property as shown by DPPH assay (Johnson, Antonio et al. 2012), it should exhibit robust neuroprotection activity if evaluated in a cell-culture model which simulates dopaminergic neurons. In addition, I also hypothesized that as D-512 has been shown to be an antioxidant, it must act on oxidative

stress producing machinery and its related pathways in the cell culture system. Thus, D-512 should be able to prevent cell-death and provide neuroprotection in a cell-culture model by DA receptor dependent and independent mechanisms.

Second hypothesis of my dissertation study was that as some polyphenolic compounds have been shown to inhibit the aggregation of  $\alpha$ -synuclein (Li, Zhu et al. 2004, Zhu, Rajamani et al. 2004, Li, Lin et al. 2005), the compounds inspired from similar structural features (D-240, D-436, and D-520) should also be able to inhibit  $\alpha$ -synuclein aggregation (**figure 2-2**). In addition, if such compounds inhibit the aggregation of  $\alpha$ -synuclein, they should also be able to prevent cytotoxicity in dopaminergic cell line because of modulation of  $\alpha$ -synuclein aggregation. Thus, our compounds should possess  $\alpha$ -synuclein aggregation inhibition property in addition to their dopaminergic receptor agonist potency.



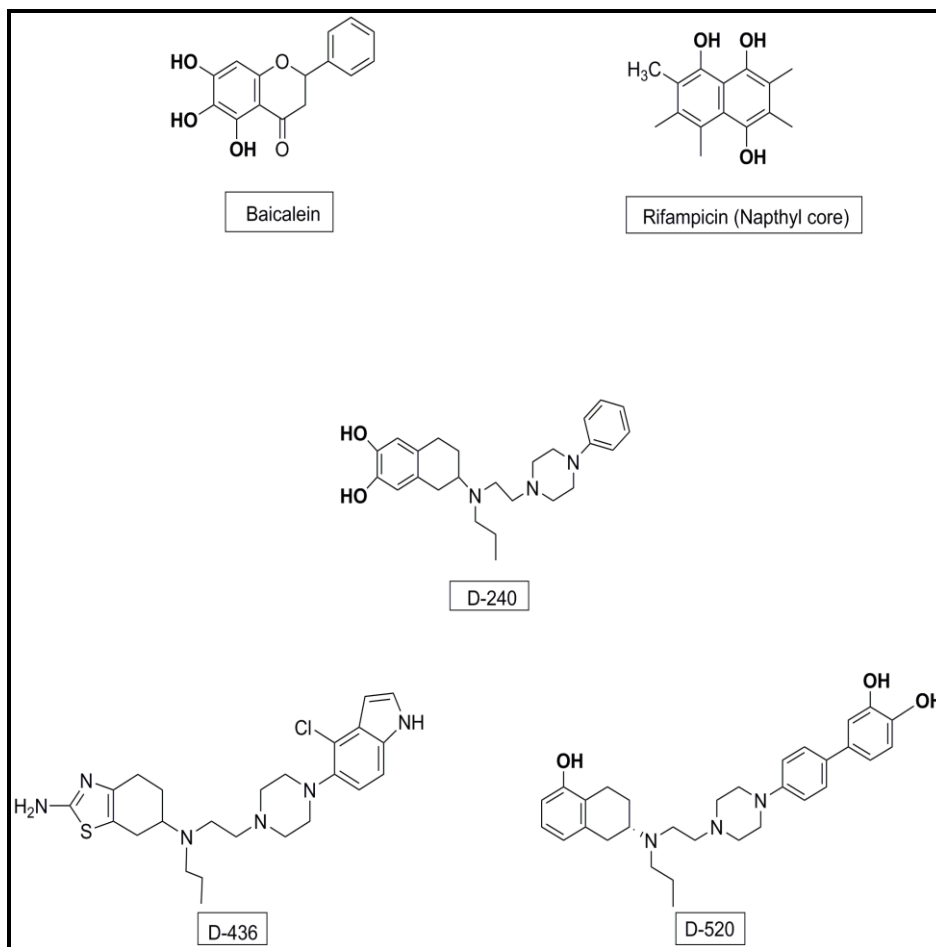


**Figure 2-2. Structures of known  $\alpha$ -synuclein aggregation inhibitors and some lead compounds from our lab**

### **STUDY DESIGN AND RATIONALE**

The main objective for first part of my project was to use various biochemical assays for evaluating neuroprotective and anti-oxidant activities of D-512 against PD cell-culture model. Main focus of my project was to evaluate the ability of D-512 to rescue PC12 cells from oxidative stress generated by 6-hydroxydopamine (6-OHDA). We determined to use 6-OHDA as a toxin, as it has been shown to be elevated in PD patients and also various animal models have been developed based on intra-striatal injections of 6-OHDA, which causes selective

degeneration of dopaminergic neurons. In addition, it has been demonstrated by various independent studies that 6-OHDA exerts its toxic effects by generation of various reactive oxygen species, which are also known to be major reason for progression of PD. As our main objective was to determine D-512's effectiveness as an anti-oxidant, 6-OHDA was appropriate toxin to be used. As we were previously able to verify D-512's neuroprotective as well as anti-oxidant activities in dopaminergic cell-line devoid of dopaminergic receptors, it was ideal to choose PC12 cell-line, which expresses various dopaminergic neuronal markers (dopamine D<sub>2</sub> receptor, dopamine transporter, tyrosine hydroxylase and dopamine) and hence should be able to mimic dopaminergic neurons.

As discussed in the introduction, PD patients show significant dopaminergic neuronal degeneration and changes in various oxidative stress markers. An ideal PD therapeutic should be able to provide protection from dopaminergic neuronal degeneration and also alter oxidative stress induced changes in cells. As shown in **figure 2-3**, excessive oxidative stress can damage critical cellular biomolecules such as DNA, proteins and lipids. In addition, oxidative stress can also alter anti-oxidant machinery present in cells making them more vulnerable to cell death.

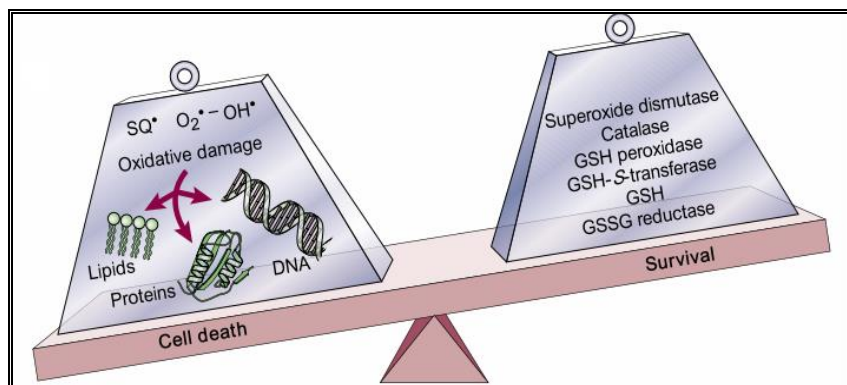


**Figure 2-3. Imbalance in reactive oxygen species generation and elimination**

(Lotharius and Brundin 2002)

To achieve the specific aims of this project, I evaluated D-512's ability to protect PC12 cells against cytotoxicity induced by 6-OHDA. Furthermore, I performed various biochemical assays to evaluate oxidation status of biomolecules following exposure of PC12 cells to 6-OHDA and ability of D-512 to reverse or prevent such oxidative stress induced changes. To accomplish the objectives, I proposed to:

- ❖ Test the hypothesis that D-512 has an ability to protect/reverse the cell-death induced by oxidative stress produced by 6-OHDA in PC12 cell-line.

This analysis was crucial to carry out further experiments, as D-512's ability to protect PC12 cells against cell-death would establish that it is neuroprotective in nature. As D-512 also possesses dopamine receptor agonist activity, the neuroprotective ability would ensure that it may be a potential disease-modifying PD therapeutic.

- ❖ Test the hypothesis that D-512 has an ability to prevent free radical and ROS induced damage to various biomolecules in cell culture system and/or capability to act on anti-oxidant system in PC12 cells. I proposed to perform analysis of changes in oxidized and reduced glutathione levels to determine effect of D-512 on anti-oxidant system in PC12 cells using buthionine sulfoximine (BSO) and 6-OHDA. For determining D-512's anti-oxidant activity against free radicals, I proposed to perform lipid peroxidation assay, DNA fragmentation assay, and nuclear condensation assay using 6-OHDA (or similar oxidizing agents) in PC12 cells.

The rationale behind performing glutathione assays was that if D-512 shows neuroprotective ability against 6-OHDA, it should have an ability to alter oxidative changes induced by 6-OHDA in PC12 cells. Interestingly, glutathione levels have been shown to be

significantly depleted in patients with PD. 6-OHDA has been shown to alter level of glutathione in cells including PC12 cells. Therefore, we wanted to evaluate whether D-512 is able to alter 6-OHDA induced changes in PC12 cells in order to provide anti-oxidant effect. We planned to carry out analysis of free glutathione levels, because free glutathione is responsible for neutralizing various ROS and toxins generated by abnormal cellular metabolism. We also analyzed levels of total glutathione as they would provide us the redox status of cells. As the mechanism by which glutathione is depleted in PC12 cells by 6-OHDA hasn't been fully elucidated, we determined to use BSO, which has been known to inhibit  $\gamma$ -glutamylcysteine synthetase and deplete cellular glutathione levels. Thus, we tested D-512's ability to restore changes in glutathione levels induced by 2 different toxins, in order to assure its capability to act on anti-oxidant system of cells.

The rationale behind performing DNA fragmentation and nuclear condensation assays was to understand the mechanism by which D-512 and 6-OHDA act on PC12 cells. Cells can undergo cell death by two different mechanisms, necrosis or apoptosis. It has been shown that 6-OHDA induces cell death in dopaminergic neurons by apoptosis (Ochu, Rothwell et al. 1998). The cells undergoing apoptosis display some characteristic features such as membrane blebbing, cell shrinkage, nuclear condensation, fragmentation of DNA, phosphatidyl serine externalization. Therefore, it was important to evaluate the effect of 6-OHDA on PC12 cells by performing nuclear condensation and DNA fragmentation assays. Furthermore, it was crucial to understand the ability of D-512 to rescue PC12 cells from 6-OHDA induced apoptotic cell death. Therefore, we tested anti-apoptotic effects of D-512 against 6-OHDA induced apoptotic cell death.

- ❖ Test the hypothesis that D-512 should alter some critical cell signaling pathways at earlier time-point following exposure to oxidative stress (6-OHDA) which may be potent molecular mechanism(s) by which D-512 has an ability to confer neuroprotection.

The rationale behind performing analysis of cellular signaling molecules was based on the fact that cell fate is determined by balance between various signaling molecules. Imbalance in various signaling cascades of cells following exposure to variety of stimuli can influence cellular decisions such as cell survival, cell proliferation, cell differentiation, cell migration, cell death, etc. Sustained activation of mitogen activated protein kinase signaling molecule, extracellular signal regulated kinases (ERK1/2), has been shown in PC12 following exposure to 6-OHDA. ERK1/2 activation has been shown to be a key event responsible for cell death in PC12 cells. In addition, another type of mitogen activated protein kinase signaling molecule, c-Jun N-terminal kinases (JNKs) respond to various stress-related stimuli, such as cytokines, inflammatory signals and increase in oxidative stress. JNK has also been shown to be activated following exposure of PC12 cells to 6-OHDA. Therefore, we evaluated the ability of D-512 to alter the changes in ERK1/2 and JNK following exposure of PC-12 cells to 6-OHDA. As signaling molecules are the early determinants of cellular fate, understanding their modulation by D-512 would help understand the mechanism of D-512 at molecular level.

The main objective of the second part of my project was to assess the ability of some of our lead compounds to inhibit  $\alpha$ -synuclein aggregation. As discussed in the introduction,  $\alpha$ -synuclein has been shown to be responsible for PD pathology. Duplication or triplication of SNCA locus, several point mutations of  $\alpha$ -synuclein, and interaction with dopamine and/or iron can result in generation of aggregates of  $\alpha$ -synuclein. Lewy bodies have been shown to be a

characteristic feature of PD pathology. Lewy bodies contain significant amounts of aggregated forms of  $\alpha$ -synuclein. Hence, it is critical to address the issue of  $\alpha$ -synuclein aggregation, as it may be a significant pathological factor involved in PD progression and/or initiation. My project focused on generating variety of  $\alpha$ -synuclein aggregates using chemicals which have been known to be responsible for PD pathology and  $\alpha$ -synuclein aggregation. For generating  $\alpha$ -synuclein aggregates, I employed cell-free system approach to understand direct interactions between known factors responsible for  $\alpha$ -synuclein aggregation. I used DA, iron, or higher concentration of  $\alpha$ -synuclein to generate various types of  $\alpha$ -synuclein aggregates. I also evaluated the extracellular toxicity of  $\alpha$ -synuclein aggregates (formed in a cell-free system) in PC12 cells, as it has been shown that such aggregates can transfer from one neuron to another in a prion-like manner to cause damage. I used PC12 cells to simulate dopaminergic neuronal system. To establish a standard to evaluate the effect of our lead compounds, I used a known  $\alpha$ -synuclein aggregation inhibitor rifampicin. I carried out various experiments in cell-free system with lead compounds and rifampicin to compare their relative ability to prevent the aggregation of  $\alpha$ -synuclein. Several studies have shown that co-valent modification of  $\alpha$ -synuclein by DA generates  $\alpha$ -synuclein oligomers, which are potentially toxic species for dopaminergic neurons. Oxidation of DA into dopamine quinone is shown to be responsible for formation of oligomers. Therefore, in experiments involving dopamine, I included a potent anti-oxidant ascorbic acid. To achieve the objective of my project, I proposed to:

- ❖ Test the hypothesis that different chemicals interact with  $\alpha$ -synuclein to generate aggregates of  $\alpha$ -synuclein which have distinct structural features. I proposed to perform the cell-free system based aggregation assays using  $\alpha$ -synuclein alone,  $\alpha$ -synuclein in presence of DA, and  $\alpha$ -synuclein in presence of iron. I proposed to

analyze the formed aggregates using SDS-PAGE followed by silver-staining method, Thioflavin-T assay (ThT) and transmission electron microscopy.

The rationale behind these experiments was to simulate PD conditions. Abnormal accumulation of iron takes place in PD. In addition, some studies also show presence of products of abnormal dopamine metabolism. Hence, it was necessary to understand the contribution of iron or DA in the process of  $\alpha$ -synuclein aggregation. The formed aggregates can be co-valently modified or non-covalently modified by chemicals. Polyacrylamide gel electrophoresis of samples in presence of SDS can help differentiate co-valently modified forms of protein from non-covalently modified form, as non-covalent forms break apart in presence of SDS. Silver-staining of the fractionated samples can help visualize various forms of aggregates which are resistant to SDS. I planned to evaluate the aggregates by thioflavin-T, as the dye has an ability to bind to  $\beta$ -sheet structure of protein, which can form by modification of  $\alpha$ -synuclein by chemicals used in this experiment. It is crucial to know the structure of  $\alpha$ -synuclein as fibrillar forms of protein show strong ThT activity, whereas, oligomeric forms (co-valently modified by dopamine) do not exhibit strong ThT activity. In addition, transmission electron microscopy was employed to physically visualize the protein aggregates, as there wasn't comparable robust assay method that would have helped us understand the aggregate morphology more clearly.

- ❖ Test the hypothesis that potent anti-oxidant (ascorbic acid) and our lead compounds (potent anti-oxidants) should be able to alter DA induced aggregation of  $\alpha$ -synuclein. I proposed to carry out cell-free system experiments with  $\alpha$ -synuclein and DA,  $\alpha$ -synuclein and DA with ascorbic acid,  $\alpha$ -synuclein and DA with rifampicin,  $\alpha$ -synuclein and DA with D-436,  $\alpha$ -synuclein and DA with D-520. I proposed to

analyze the formed aggregates using SDS-PAGE followed by silver-staining method, transmission electron microscopy, and size-exclusion chromatography.

The rationale behind this experiment was that as dopamine quinones (which are oxidized species of DA) generate toxic oligomers of  $\alpha$ -synuclein, anti-oxidant such as ascorbic acid should be able to prevent/slow down the generation of dopamine quinones. Therefore, ascorbic acid should decrease/inhibit the generation of oligomeric species of  $\alpha$ -synuclein. As our lead compounds also possess anti-oxidant activity, they should also be able to exhibit similar activity towards DA induced  $\alpha$ -synuclein aggregation. It was critical to evaluate the formed aggregates using SDS-PAGE followed by silver-staining, as it was critical to understand the modulation of different compounds on dopamine-quinone induced co-valent modification of  $\alpha$ -synuclein. Transmission electron microscopy helped us physically visualize the aggregates to understand the structural alterations of  $\alpha$ -synuclein upon incubation with various compounds. Furthermore, size-exclusion chromatography helped us understand the differences in various dimensions of aggregates from different experiments.

- ❖ Test the hypothesis that our lead compounds should be able to alter the aggregation of  $\alpha$ -synuclein such that they would prevent or reduce the extracellular toxicity of  $\alpha$ -synuclein aggregates in cell culture system. Initially, I proposed to evaluate the extracellular toxicity of aggregates formed using cell-free system assay with  $\alpha$ -synuclein alone (at high concentration) or  $\alpha$ -synuclein and dopamine in PC12 cells in a time dependent manner. After determining the maximum toxicity of aggregates, I proposed to carry out cell-free system experiments with our lead compounds to determine their ability to prevent or alter  $\alpha$ -synuclein aggregation. The extracellular



toxicity of various types of aggregates formed was evaluated using PC12 cells. The structure of the formed aggregates was confirmed by ThT assay. We also carried out transmission electron microscopy to evaluate the physical characteristics of aggregates.

The rationale behind the cell-free system experiments was to understand the influence of known compounds on the aggregation of  $\alpha$ -synuclein. Our initial experiments using aggregates formed by  $\alpha$ -synuclein alone or  $\alpha$ -synuclein and DA would help us understand which type of aggregates can cause more toxicity when incubated extracellularly with PC12 cells. These experiments could probably reflect upon a fact that which  $\alpha$ -synuclein aggregates might be involved in dopaminergic cell death induced in PD. Once it would be determined that which types of aggregates are more toxic when incubated with PC12 cells extracellularly, we would carry out assays to assess the ability of our lead compounds to prevent the toxicity and aggregation of  $\alpha$ -synuclein. The rationale behind these assays was that if our lead compounds could prevent/alter the process of  $\alpha$ -synuclein aggregation, they can potentially prevent the extracellular toxicity of  $\alpha$ -synuclein aggregates in PC12 cells. Thus, we would simulate the extracellular toxicity of  $\alpha$ -synuclein aggregates on dopaminergic neurons and the influence of our lead compounds to alter the toxicity. We conducted ThT assay to understand the structural characteristics of the aggregates formed under various conditions. Our transmission electron microscopy results helped us understand the influence of our lead compounds and standards on process of  $\alpha$ -synuclein aggregation.

## CHAPTER 3

### MATERIALS AND METHODS: ANTI-OXIDANT EFFECTS OF LEAD MOLECULE

#### 3.1 Materials

**Chemicals:** Poly-L-lysine, 6-hydroxydopamine hydrochloride, dimethyl sulfoxide (DMSO), methanol, methyl thiazolyl blue tetrazolium bromide (MTT), reduced L-glutathione, buthionine sulfoximine (BSO), sulfosalicylic acid, dithio-bis-nitrobenzoic acid (DTNB), glutathione reductase, NADPH, thiobarbituric acid, dulbecco's phosphate-buffered saline (1X PBS), ribonuclease A, proteinase K, and triton-X-100 were purchased from Sigma-Aldrich (St. Louis, MO, USA). Ethanol, Hoechst 33342, ethidium bromide, tris, EDTA, BCA protein assay kit and bovine serum albumin were purchased from Fisher scientific (New Jersey, USA). 10X tris-glycine solution, 10X tris-glycine-SDS solution, 10X TBS solution (tris-buffered saline), tween-20, 20% SDS solution, 10% TGX-mini protean gels, 12% TGX- mini protean gels, and PVDF membranes were purchased from Biorad (Hercules, CA, USA). Sodium nitroprusside and isopropanol were purchased from Acros organics (New Jersey, USA). Agarose was purchased from invitrogen (Grand Island, NY, USA). Ammonium acetate was purchased from G biosciences (St.Louis, MO, USA). 4% paraformaldehyde solution was purchased from Electron Microscopy Sciences (Hatfield, PA, USA). ECL-Plus reagent was obtained from Perkin-Elmer (Waltham, MA, USA). Glutathione fluorescence detection kit was purchased from arbor assays (Ann arbor, MI, USA). D-512 mesylate was synthesized in our lab as described in a recent publication by Johnson et al. (Johnson, Antonio et al. 2012).

**Antibodies:** Antisera directed against phospho-ERK1/2, phospho-JNK, total ERK1/2, total JNK, and GAPDH were from Cell signaling technology (Danvers, MA, USA). Anti-mouse

and anti-rabbit IgG-horseradish peroxidase conjugates were from MP biomedical (Santa Ana, CA, USA).

**Cell-culture and treatments:** PC12 Adh (ATCC® CRL1721.1™) cells, a rat adrenal pheochromocytoma cell line, were purchased from ATCC. Stock solutions of D-512 (100 mM) and 6-OHDA (0.5M) were prepared in DMSO and aliquots were stored at -20°C and -80°C respectively. Stock solution of reduced glutathione standard (10 mM) and BSO (10 mM) were prepared in distilled water and aliquots were stored at -20°C. Stock solution of sodium nitroprusside was prepared fresh in distilled water before treatment.

PC12 cells were cultured in T-75 flask (Sarstedt Inc, Newtown, NC, USA) and maintained in RPMI 1640 medium supplemented with 10% heat-inactivated horse serum, 5% fetal bovine serum, penicillin (100 units/mL), and streptomycin (100 µg/mL) at 37°C in 5% CO<sub>2</sub> atmosphere.

### 3.2 Measurement of cell viability

To determine the neuroprotective effect of D-512 on 6-OHDA induced cell death, quantitative and colorimetric MTT assay was used. PC12 cells were plated at 17000 cells/well density in 100µL media in 96 well plates for 24 hours to allow their attachment. Adhered PC12 cells were treated with different concentrations of 6-OHDA or different doses of D-512 to determine their direct effect on cell viability and to determine the optimum concentration of 6-OHDA to use in neuroprotection experiments. Neuroprotection experiments were conducted by treating adhered PC12 cells for 24 hours with different concentrations of D-512 followed by their treatment with 75 µM 6-OHDA alone (pre-treatment only) or with 75 µM 6-OHDA and different concentrations of D-512 for another 24 hours (pre-treatment and co-treatment). After incubation,

10  $\mu$ L 5 mg/mL MTT was added to the cells and the plate was further incubated at 37°C in 95% air/5% CO<sub>2</sub> atmosphere for 3 hours to produce dark blue formazan crystals. Afterwards, the plate was centrifuged at 1500 rpm for 10 minutes and the supernatants were carefully removed. The formazan crystals were dissolved by adding 100  $\mu$ L of DMSO/methanol (50:50) mixture to each well and shaking the plate gently at room temperature at 400rpm for 30 minutes at room temperature using a Thermomix R shaker (Eppendorf, Hamburg, Germany). The absorbance values were measured using Epoch microplate reader (Biotek, Winooski, VT, USA) at 570 nm with background correction done at 690nm. Data from at least 3 experiments were analyzed using Graphpad software (Version 4, San Diego, USA). Cell viability was defined as a percentage reduction in absorbance compared to untreated controls.

### **3.3 Measurement of total glutathione levels**

To determine the potential effect of D-512 on cellular antioxidant mechanisms, total glutathione levels were evaluated using quantitative and colorimetric assay (Tietze 1969). For all experiments, PC12 cells were seeded at  $2 \times 10^5$  cells/well density in 2 mL media in 12 well plates for 24 hours to allow their attachment. Adhered PC12 cells were treated with different concentrations of buthionine sulfoximine (BSO) or 6-hydroxydopamine (6-OHDA) for 6 hours or 24 hours to determine their optimum concentration for neuroprotection experiments. Neuroprotection experiments were performed by pre-treating adhered PC12 cells for 24 hours with different concentrations of D-512 followed by their co-treatment with 1.56  $\mu$ M BSO or 25  $\mu$ M 6-OHDA and various concentrations of D-512 for 6 hours or 24 hours. After incubation, cells were scraped with rubber policeman, centrifuged, and washed with 1X PBS. Cells were resuspended in 25  $\mu$ L 5% sulfosalicylic acid. Resuspended cells were subjected to 2 freeze-thaw cycles. Cell lysate was incubated on ice for 10 minutes. Cell debris were removed by

centrifugation at 14000 rpm for 10 minutes at 4°C. 10 µL of supernatant was added to 96 well plate. Total glutathione levels were measured by adding 150 µL mixture of dithionitrobenzoic acid (1.5 mg/mL) and glutathione reductase (~ 6 units/mL) and starting the color formation by addition of 50 µL NADPH (0.16 mg/mL) after 5 minute incubation at room temperature. Color formation because of formation of nitrobenzoic acid was measured after 5 minutes at 412 nm by Synergy microplate reader (Biotek, Winooski, VT, USA). Total glutathione levels for samples were calculated by generating standard curve with known glutathione standards prepared using reduced glutathione. Total glutathione levels were expressed as percentage of control cells.

### **3.4 Measurement of free glutathione levels**

To delineate the influence of D-512 and 6-OHDA on free and oxidized glutathione levels, free glutathione levels were measured using glutathione fluorescent detection kit. For all experiments, PC12 cells were seeded at  $5 \times 10^5$  cells/well density in 2 mL media in 6 well plate for 24 hours to allow their attachment. Adhered PC12 cells were treated with different concentrations of D-512 for 24 hours followed by their co-treatment with 25 µM 6-OHDA and various concentrations of D-512 for 6 hours or 24 hours. After incubation, cells were scraped with rubber policeman, centrifuged, and washed with 1X PBS. Cell pellets were resuspended in 50 µL 5% sulfosalicylic acid. Resuspended cells were subjected to 2 freeze-thaw cycles. Cell lysate was incubated on ice for 10 minutes. Cell debris were removed by centrifugation at 14000 rpm for 10 minutes at 4°C. Supernatant was diluted 1:5 with assay buffer to make the final concentration of sulfosalicylic acid 1%. 50 µL of diluted sample was incubated with 25 µL of thiostar reagent for 15 minutes. Free glutathione levels of samples were obtained by reading fluorescence at 370 nm excitation and 510 nm emission wavelengths using synergy microplate reader (Biotek, Winooski, VT, USA). Afterwards, total glutathione levels of same samples were

determined by incubating samples for 15 minutes with 25  $\mu\text{L}$  reaction mixture (containing glutathione reductase and NADPH) and obtaining the fluorescence signal at 370 nm excitation and 510 nm emission wavelength. Both free and total glutathione levels of samples were calculated by generating standard curve with known glutathione standards. Free and total glutathione levels were expressed as percentage of control cells.

### **3.5 Hoechst staining**

To qualitatively evaluate the ability of D-512 to protect against nuclear condensation, a feature of apoptotic cell death induced by 6-OHDA, Hoechst 33342 staining was done. PC12 cells were seeded at  $2 \times 10^5$  cells/well density in 12 well plate. Cells were allowed to adhere for 24 hours, old medium was taken out from each well, and 1.5 ml of fresh medium containing  $10 \mu\text{M}$  D-512 was added. Following 24 hours of pretreatment with the drug,  $75 \mu\text{M}$  6-OHDA was added to treatment wells and co-treatment was continued for 16 hours. The medium was removed and the cells were washed twice with 1X PBS. The cells were fixed with 1 ml 4% paraformaldehyde solution (EM sciences) for 15 min at room temperature followed by washing twice with 1X PBS. The cells were stained with 0.5 mM Hoechst 33342 (Thermo)/ 0.15% triton-X-100 (Sigma) solution 1 ml for 15 min at room temperature followed by washing twice with 1X PBS. Cell imaging was performed using fluorescence microscopy at 40X magnification (EVOS FL digital Inverted microscope, AMG) at 357 nm excitation and 447 nm emission wavelength.

### **3.6 DNA fragmentation assay**

To semiquantitatively evaluate the ability of D-512 to protect against nuclear damage, a feature of apoptotic cell death induced by 6-OHDA, DNA ladder assay was performed.  $4 \times 10^6$  cells were plated in 100 mm petri-dish in 10mL media and they were allowed to adhere to the surface for 24 hours. Adhered cells were pre-treated with different concentrations of D-512 for

24 hours. The pre-treated cells were co-treated with 75  $\mu\text{M}$  6-OHDA and different concentrations of D-512 for another 24 hours. Upon completion of the treatment, media was collected and 1 ml trypsin was added to 100 mm dishes to dissociate the cells. Cells were scraped and media was added back to stop the trypsin activity. Cells were centrifuged (2000 rpm, 5 min), and washed with 1X PBS (2000 rpm, 5 min). The cell pellets were lysed using 100  $\mu\text{L}$  lysis buffer (0.1% Triton-X-100 in 20 mM EDTA, 50 mM Tris-HCl, pH 7.5) for 5 minutes with intermittent pipetting. Cell debris were removed by centrifugation (3,000 rpm, 5 min) and supernatant was treated with 10  $\mu\text{L}$  of 10% SDS solution. The lysate was treated with 10  $\mu\text{L}$  of 50 mg/mL RNaseA for 2 hours at 56°C. Afterwards, lysate was treated with 12.5  $\mu\text{L}$  of 20 mg/ml proteinase K for 2 hours at 37°C. The resulting lysate was treated with 65  $\mu\text{L}$  10M ammonium acetate and 250  $\mu\text{L}$  ice-cold isopropanol. After vigorous shaking, isopropanol precipitation was performed by incubating lysate at -20°C for 3 days. Precipitated DNA was collected by centrifugation at 12000 rpm for 20 minutes. DNA was washed with 200  $\mu\text{L}$  80% ice-cold ethanol and air-dried for 10 min at room temperature. DNA was dissolved in 50  $\mu\text{L}$  tris-EDTA buffer. 4  $\mu\text{g}$  of DNA from each sample was separated using 1.2% agarose gel (containing 0.5  $\mu\text{g}/\text{mL}$  ethidium bromide) at 5V/cm for 4 hours using horizontal agarose gel electrophoresis cell (BIORAD). Agarose gel image was taken using Biorad Gel Doc XR+ imaging system.

### **3.7 Lipid peroxidation**

To determine the free radical quenching ability of D-512, lipid peroxidation assay was performed on PC12 cells and MN9D cells using sodium nitroprusside. For all experiments, PC12 cells were plated at  $2 \times 10^5$  cells/well density in 2 mL media in 12 well plates. PC12 cells were allowed to adhere to the surface for 24 hour. For optimization experiments, adhered PC12 or MN9D cells were treated with different concentrations of sodium nitroprusside for 8 hours to determine the concentration to use for inducing appropriate lipid peroxidation. For other

experiments, adhered PC12 cells were pre-treated with different concentrations of D-512 for 24 hours followed by their co-treatment with 200  $\mu$ M sodium nitroprusside and D-512 for 8 hours. Cells were harvested using rubber policeman, centrifuged, and washed with 1X PBS. Cell pellet was resuspended in 120  $\mu$ L 1X PBS. Suspended cells were sonicated 3 times for 5 seconds using ultrasonicator (Branson Inc, Danbury, CT) at 30% amplitude. Whole cell lysate was used to determine thiobarbituric acid (TBA) reactive species (TBARS). 100  $\mu$ L 1% SDS and 100  $\mu$ L whole cell lysate were mixed with 4mL color reagent (The color reagent was prepared by mixing 320 mg TBA dissolved in 30 mL 0.1M sodium hydroxide and 30 mL diluted acetic acid). Mixture was boiled for 1 hour at 100°C in dark and the fluorescence was read at 520 nm excitation and 550 nm emission wavelength using synergy microplate reader (Biotek, Winooski, VT, USA). Fluorescence was plotted after subtracting blank (which was prepared using 100  $\mu$ L 1X PBS, 100  $\mu$ L 1% SDS, and 4 mL color reagent) and considering control (which consisted of 100  $\mu$ L cell lysate without any treatment, 100  $\mu$ L 1% SDS, and 4mL color reagent) fluorescence as 100%.

### **3.8 Western Blot Analysis**

To understand the molecular mechanisms associated with neuroprotection conferred by D-512 against 6-OHDA induced cell death, expression levels of various phosphoprotein signaling molecules were evaluated at earlier time point. PC12 cells were plated at  $5 \times 10^5$  cells/well density in 6 well plate and they were allowed to adhere for 24 hours. Adhered PC12 cells were pre-treated with 10  $\mu$ M D-512 for 24 hours. Afterwards, PC12 cells were co-treated with 75  $\mu$ M 6-OHDA for 30 minutes, 2 hours and 4 hours. 40  $\mu$ g of proteins were separated on 10% tris-glycine gel by SDS-PAGE. Afterwards, proteins were transferred to PVDF membrane (BIORAD). Membrane was blocked with 5% Bovine Serum Albumin (BSA) in TBST (Tris-



buffered saline with Tween-20) for 2 hours. Blocked membrane was incubated overnight with primary antibody against phospho-ERK1/2, phospho-JNK, total ERK1/2, total JNK, and GAPDH (1:1000 dilution) in 5% BSA in TBST. Afterwards, membrane was incubated with appropriate HRP-conjugated secondary antibody (anti-mouse or anti-rabbit) (1:4000 dilution) in 1% BSA in TBST. The image was visualized using ECL-Plus reagent (PerkinElmer, Waltham, MA, USA) and ImageQuant LAS 4000 imager (GE Healthcare Biosciences, Pittsburgh, PA, USA). Densitometric analysis was performed using ImageJ software.

## MATERIALS AND METHODS

### $\alpha$ -SYNUCLEIN AGGREGATION MODIFICATION PROPERTIES

#### OF LEAD MOLECULES

#### 3.9 Materials

**Chemicals:**  $\alpha$ -synuclein was purchased from rpeptide (Bogart, GA, USA). Dopamine hydrochloride, ammonium iron(II) sulphate hexahydrate, ascorbic acid, rifampicin, sodium thiosulphate, silver nitrate, sodium hydroxide, formalin (36.5-38% formaldehyde in water), and thioflavin-T (ThT) were purchased from Sigma-Aldrich (St. Louis, MO, USA). Sodium carbonate, methanol, HPLC grade acetonitrile, and HPLC grade water were purchased from EMD Millipore (Billerica, MA, USA). Glacial acetic acid, sodium phosphate, LB broth (Miller), glycerol, ethanol, and sodium chloride were purchased from Fisher scientific (New Jersey, USA). 400 mesh copper grids with carbon/formvar coating, uranyl acetate and 4% paraformaldehyde solution were purchased from Electron Microscopy Sciences (Hatfield, PA, USA). Ammonium acetate was purchased from G-biosciences (St. Louis, MO, USA). Trifluoroacetic acid was purchased from Oakwood chemicals (West Columbia, SC, USA). Streptomycin sulphate was purchased from Calbiochem (Billerica, MA, USA). Ammonium sulphate was purchased from Research organics (St. Louis, MO, USA). Ampicillin and isopropyl thiogalactoside (IPTG) were purchased from Gold Biotechnology (St. Louis, MO, USA). ECL-plus reagent was purchased from Perkin-Elmer (Waltham, MA, USA).

**Analytical columns and standards:** Size-exclusion chromatography was performed using BIOSEP-SEC-S2000 column from Phenomenex (Torrance, CA, USA). Reverse phase chromatography was performed using C4-Jupiter 300A column from Phenomenex (Torrance, CA, USA). Gel-filtration standard containing mixture of known globular proteins from Biorad

(Hercules, CA, USA) was used for size-exclusion chromatography.  $\alpha$ -synuclein purification was performed using 5mL pre-packed Q-sepharose HP column purchased from GE lifesciences (Pittsburgh, PA, USA).

**Antibodies:** Antisera directed against wild-type  $\alpha$ -synuclein was purchased from BD biosciences (San Jose, CA, USA). Anti-mouse IgG-horseradish peroxidase conjugate was from MP biomedical (Santa Ana, CA, USA).

**Cell-culture and treatments:** PC12 Adh (ATCC<sup>®</sup> CRL1721.1<sup>™</sup>) cells, a rat adrenal pheochromocytoma cell line, were purchased from ATCC. RPMI 1640, heat-inactivated horse serum, fetal bovine serum, penicillin-streptomycin, and trypsin were purchased from GIBCO (Grand Island, NY, USA).

PC12 cells were cultured in T-75 flask (Sarstedt Inc, Newtown, NC, USA) and maintained in RPMI 1640 medium supplemented with 10% heat-inactivated horse serum, 5% fetal bovine serum, penicillin (100 units/mL), and streptomycin (100  $\mu$ g/mL) at 37°C in 5% CO<sub>2</sub> atmosphere.

**Plasmid and bacteria:** E.coli BL21(DE3) strain was purchased from Invitrogen (Grand Island, NY, USA). pET-3a plasmid containing amino acid sequence for wild-type  $\alpha$ -synuclein was kindly provided by Dr. Suzanne Scarlatta (Stony Brooke University).

### **3.10 Generation of $\alpha$ -synuclein aggregates using cell-free system**

For cell-free system experiments, all solutions were prepared in 1X PBS. Shaking experiments were conducted on Thermomix R shaker (Eppendorf, Hamburg, Germany) at 1400 rpm and 37°C. 1mg  $\alpha$ -synuclein was dissolved in 576.3  $\mu$ L 1X PBS to generate 120  $\mu$ M stock

solution of protein (protein concentration was also verified by BCA protein assay). 400  $\mu\text{M}$  dopamine hydrochloride was made by dissolving 2mg dopamine hydrochloride in 26.36 mL 1X PBS. 35  $\mu\text{M}$  ammonium iron(II) sulfate hexahydrate was prepared by diluting 350  $\mu\text{M}$  ammonium iron(II) sulfate hexahydrate, which was prepared by dissolving 2.05mg ammonium iron(II) sulfate hexahydrate in 15mL 1X PBS.

**Protocol A:** Generation of dopamine-induced, SDS-resistant  $\alpha$ -synuclein oligomers

$\alpha$ -synuclein oligomers were generated by shaking  $\alpha$ -synuclein (17.5  $\mu\text{M}$ ) and dopamine (200  $\mu\text{M}$ ) solution for 10 days. 115  $\mu\text{L}$  (35  $\mu\text{M}$ )  $\alpha$ -synuclein and 115  $\mu\text{L}$  (400  $\mu\text{M}$ ) dopamine hydrochloride were mixed and 30  $\mu\text{L}$  aliquot was removed for day 0. 30  $\mu\text{L}$  aliquots were removed for day 2, day 4, day 6, day 8 and day 10 after starting the shaking. The aliquots were used for silver-staining (10  $\mu\text{L}$ ), ThT assay (10  $\mu\text{L}$ ), and in some cases for transmission electron microscopy (10  $\mu\text{L}$ ).

**Protocol B:** Generation of  $\alpha$ -synuclein fibrils using high concentration of  $\alpha$ -synuclein

$\alpha$ -synuclein fibrils were generated by shaking  $\alpha$ -synuclein (70 $\mu\text{M}$ ) solution for 10 days. 230  $\mu\text{L}$  (70  $\mu\text{M}$ )  $\alpha$ -synuclein was prepared and 30  $\mu\text{L}$  aliquot was removed for day 0. 30  $\mu\text{L}$  aliquots were removed for day 2, day 4, day 6, day 8 and day 10 after starting the shaking. The aliquots were used for silver-staining (10  $\mu\text{L}$ ), ThT assay (10  $\mu\text{L}$ ), and in some cases for transmission electron microscopy (10  $\mu\text{L}$ ).

**Protocol C:** Generation of iron-induced, SDS-sensitive  $\alpha$ -synuclein fibrils

$\alpha$ -synuclein fibrils were generated by shaking  $\alpha$ -synuclein (17.5  $\mu\text{M}$ ) and iron(II) (17.5  $\mu\text{M}$ ) for 6 days. 110  $\mu\text{L}$  of 35  $\mu\text{M}$   $\alpha$ -synuclein and 110  $\mu\text{L}$  of 35  $\mu\text{M}$  ammonium ferric citrate were mixed and 30  $\mu\text{L}$  aliquot was removed for day 0. 30  $\mu\text{L}$  aliquots were removed for day 1, day 2, day 3, day 4, day 5, and day 6 after starting the shaking. The aliquots were used for silver-

staining (10  $\mu\text{L}$ ), ThT assay (10  $\mu\text{L}$ ), and in some cases for transmission electron microscopy (10  $\mu\text{L}$ ).

### **3.11 Assessment of potential lead compounds', standards' and anti-oxidant's ability to modify $\alpha$ -synuclein aggregation kinetics in cell-free system**

We evaluated the effects of ascorbic acid (anti-oxidant), rifampicin (known  $\alpha$ -synuclein aggregation inhibitor), and 2 of our lead compounds (D-436 and D-520) on dopamine-induced  $\alpha$ -synuclein oligomerization employing cell-free system. All solutions were prepared in 1X PBS. Shaking experiments were conducted on Thermomix R shaker (Eppendorf, Hamburg, Germany) at 1400 rpm and 37°C. 1 mg  $\alpha$ -synuclein was dissolved in 266  $\mu\text{L}$  1X PBS to generate 260  $\mu\text{M}$  stock solution of protein (protein concentration was also verified by BCA protein assay). 260  $\mu\text{M}$   $\alpha$ -synuclein was diluted to 70  $\mu\text{M}$  protein solution. 800  $\mu\text{M}$  dopamine hydrochloride was prepared by dissolving 2 mg dopamine hydrochloride in 13.18 mL 1X PBS. 800  $\mu\text{M}$  ascorbic acid was made by dissolving 1.4 mg ascorbic acid in 10 mL 1X PBS. 800  $\mu\text{M}$  rifampicin was prepared by dissolving 1mg rifampicin in 1.52 mL 1X PBS. 800 $\mu\text{M}$  D-436 was prepared by dissolving 2.6 mg D-436 trifluoroacetate in 4 mL 0.1X PBS. 800  $\mu\text{M}$  D-520 was prepared by dissolving 4.2 mg D-520 hydrobromide in 7 mL 1X PBS (containing 1% DMSO).

#### **Protocol for ascorbic acid experiment**

62.5  $\mu\text{L}$   $\alpha$ -synuclein (70  $\mu\text{M}$ ) was mixed with 62.5  $\mu\text{L}$  dopamine hydrochloride (800  $\mu\text{M}$ ). To this mixture, 125  $\mu\text{L}$  ascorbic acid (800  $\mu\text{M}$ ) was added to get total volume of 250  $\mu\text{L}$ . This resulted in final concentration of 17.5  $\mu\text{M}$   $\alpha$ -synuclein, 200  $\mu\text{M}$  dopamine and 400  $\mu\text{M}$  ascorbic acid. 30  $\mu\text{L}$  of day 0 aliquot was removed and the mixture was shaken for 10 days. 30 $\mu\text{L}$  aliquots were collected at day 2, day 4, day 6, day 8, and day 10. The aliquots were used

for silver staining (10  $\mu\text{L}$ ), size-exclusion chromatography (10  $\mu\text{L}$ ), and in some cases for transmission electron microscopy (10  $\mu\text{L}$ ).

#### **Protocol for rifampicin experiment**

62.5  $\mu\text{L}$   $\alpha$ -synuclein (70  $\mu\text{M}$ ) was mixed with 62.5  $\mu\text{L}$  dopamine hydrochloride (800  $\mu\text{M}$ ). To this mixture, 125  $\mu\text{L}$  rifampicin (800  $\mu\text{M}$ ) was added to get total volume of 250  $\mu\text{L}$ . This resulted in final concentration of 17.5  $\mu\text{M}$   $\alpha$ -synuclein, 200  $\mu\text{M}$  dopamine and 400  $\mu\text{M}$  rifampicin. 30  $\mu\text{L}$  of day 0 aliquot was removed and the mixture was shaken for 10 days. 30  $\mu\text{L}$  aliquots were collected at day 2, day 4, day 6, day 8, and day 10. The aliquots were used for silver staining (10  $\mu\text{L}$ ), size-exclusion chromatography (10  $\mu\text{L}$ ), and in some cases for transmission electron microscopy (10  $\mu\text{L}$ ).

#### **Protocol for D-436 experiment**

62.5  $\mu\text{L}$   $\alpha$ -synuclein (70  $\mu\text{M}$ ) was mixed with 62.5  $\mu\text{L}$  dopamine hydrochloride (800  $\mu\text{M}$ ). To this mixture, 125  $\mu\text{L}$  D-436 (800  $\mu\text{M}$ ) was added to get total volume of 250  $\mu\text{L}$ . This resulted in final concentration of 17.5  $\mu\text{M}$   $\alpha$ -synuclein, 200  $\mu\text{M}$  dopamine and 400  $\mu\text{M}$  D-436. 30  $\mu\text{L}$  of day 0 aliquot was removed and the mixture was shaken for 10 days. 30  $\mu\text{L}$  aliquots were collected at day 2, day 4, day 6, day 8, and day 10. The aliquots were used for silver staining (10  $\mu\text{L}$ ), size-exclusion chromatography (10  $\mu\text{L}$ ), and in some cases for transmission electron microscopy (10  $\mu\text{L}$ ).

#### **Protocol for D-520 experiment**

62.5  $\mu\text{L}$   $\alpha$ -synuclein (70  $\mu\text{M}$ ) was mixed with 62.5  $\mu\text{L}$  dopamine hydrochloride (800  $\mu\text{M}$ ). To this mixture, 125  $\mu\text{L}$  D-520 (800  $\mu\text{M}$ ) was added to get total volume of 250  $\mu\text{L}$ . This resulted in final concentration of 17.5  $\mu\text{M}$   $\alpha$ -synuclein, 200  $\mu\text{M}$  dopamine and 400  $\mu\text{M}$  D-520. 30  $\mu\text{L}$  of day 0 aliquot was removed and the mixture was for 10 days. 30  $\mu\text{L}$  aliquots were

collected at day 2, day 4, day 6, day 8, and day 10. The aliquots were used for silver staining (10  $\mu$ L), size-exclusion chromatography (10  $\mu$ L), and in some cases for transmission electron microscopy (10  $\mu$ L).

### **3.12 Visualization of $\alpha$ -synuclein aggregates by silver-staining**

Aliquots collected on different days from cell-free system experiments were fractionated on 12% tris-glycine-SDS gel to separate protein aggregates according to their molecular weight. After fractionation, the gel was fixed using fixation solution (50% methanol, 12% glacial acetic acid, 0.05% formalin) for 2 hours. Fixed gel was washed thrice for 30 minutes with washing solution (35% ethanol). Gel was sensitized using 0.02% sodium thiosulphate for 2 minutes. Afterwards, the gel was washed thrice with distilled water for 5 minutes. The gel was stained using silver staining solution (0.2% silver nitrate and 0.076% formalin) for 20 minutes. Stained gel was washed twice with distilled water for 1 minute. The gel was developed using silver-staining developer solution (6% sodium carbonate, 0.05% formalin, and 0.0004% sodium thiosulphate). The developer reaction was stopped by adding stop solution (50% methanol, 12% acetic acid) for 5 minutes. Gel image was taken using Biorad Gel Doc XR+ imaging system.

### **3.13 Confirmation of $\beta$ -sheet positive protein structure by Thioflavin-T assay**

ThT assay was performed to evaluate the impact of chemicals or protein concentration on protein's structure. 40  $\mu$ M ThT was prepared by diluting 500  $\mu$ M ThT, which was prepared by dissolving 1.1 mg Thioflavin-T in 7 mL 1X PBS. Afterwards, 10  $\mu$ L of protein aliquot and 10  $\mu$ L ThT (40  $\mu$ M) were mixed together and transferred to 384 plate. Fluorescence generated was read using Synergy microplate reader (Biotek, Winooski, VT, USA) at 440 nm excitation and 485 nm emission wavelengths. Control consisted of 10  $\mu$ L 1X PBS mixed with 10  $\mu$ L ThT (40  $\mu$ M).

### **3.14 Evaluating the size-distribution of protein aggregates using size-exclusion chromatography**

Aliquots collected from different time points were analyzed for residual protein monomer left and higher molecular weight aggregates of protein formed using size-exclusion chromatography. Samples (10  $\mu$ L) were loaded into Biosep-SEC-S2000 column attached to Waters HPLC system to measure hydrodynamic dimensions of eluted species (Stokes radius,  $R_s$ ) (Li et al. 2004). The mobile phase consisted of 20 mM sodium phosphate buffer, pH 7. Flow rate was set to 1 mL/minute. Eluted species of protein were detected using UV detector set at 215 nm wavelength (ideal for monomer detection) and 275 nm wavelength (ideal for oligomer detection). Single chromatographic run was set to 15 minutes. 10  $\mu$ L mixture of globular protein standards (Biorad laboratories) with known  $R_s$  values was also injected using same protocol to estimate the apparent molecular weight of protein species eluted from experimental samples.

### **3.15 Detection of monomeric and higher molecular weight structures of protein using reverse-phase chromatography**

Aliquots collected from different time points were analyzed for monomer and higher molecular weight aggregates of protein formed using reverse-phase chromatography. 10  $\mu$ L sample was loaded into reverse phase chromatography column (C4, Phenomenex Jupiter, 300A, 5  $\mu$ M) attached to Waters HPLC system. Gradient elution was carried out using acetonitrile (containing 0.085% trifluoroacetic acid) versus water (containing 0.1% trifluoroacetic acid): from 5% to 35% over 5 minutes, from 35% to 55% over 20 minutes, from 55% to 95% over 2 minutes. 0.6 mL/minute flow rate was used during elution. Single chromatographic run was set to 30 minutes. The eluting species were monitored using UV detector set at 226 nm wavelength.  $\alpha$ -synuclein from industrial source was used as a control to compare elution pattern of other



samples.

### **3.16 Visualization of $\alpha$ -synuclein using transmission electron microscopy**

Transmission electron microscopy (TEM) was used to physically image  $\alpha$ -synuclein monomer and modified species generated under different experimental conditions. TEM samples were prepared on 400 mesh copper grids with carbon/formvar coating. 4  $\mu$ L sample was loaded on the grid for 4 minutes. Afterwards, it was wicked-off using whatman filter paper. Grid was loaded with 4  $\mu$ L distilled water 2 times and wicked off quickly to wash-off excess sample. Before imaging, grid was loaded with 4  $\mu$ L 2% Uranyl acetate (prepared in distilled water) for 30 seconds to negatively stain grid surface. The solution was wicked-off using whatman filter paper. Grid was allowed to dry for 5-10 minutes before starting TEM imaging. JEOL (JEM-2010) transmission electron microscope was used for imaging protein samples. All TEM images were taken at 80000X magnification.

### **3.17 Generation of $\alpha$ -synuclein aggregates to assess extracellular toxicity in cell-culture models**

$\alpha$ -synuclein aggregates were generated with primary goal to evaluate the effect of various extracellular  $\alpha$ -synuclein species on cellular viability in PC12 cells. In this experiment,  $\alpha$ -synuclein aggregates were formed by two different methods, either to yield  $\beta$ -sheet positive fibrillar structure or to yield  $\beta$ -sheet negative dopamine-induced and co-valently modified oligomeric structure of  $\alpha$ -synuclein. All samples were prepared in 1X PBS. Shaking experiments were conducted on Thermomix R shaker (Eppendorf, Hamburg, Germany) at 1400 rpm and 37°C. 1 mg  $\alpha$ -synuclein was dissolved in 576.3  $\mu$ L 1X PBS to yield 120  $\mu$ M stock solution. 180  $\mu$ M dopamine was prepared by dissolving 1mg dopamine hydrochloride in 29.24 mL 1X PBS.

**Protocol A:** Generation of  $\alpha$ -synuclein fibrils

250  $\mu$ L  $\alpha$ -synuclein (120  $\mu$ M) was mixed with 250  $\mu$ L 1X PBS to yield 60  $\mu$ M  $\alpha$ -synuclein. 70  $\mu$ L aliquot was taken from the mixture and then the solution was shaken for 10 days. 70  $\mu$ L aliquots were collected at day 2, day 4, day 6, day 8, and day 10. Aliquots were used to assess cytotoxicity (40  $\mu$ L), ThT assay (10  $\mu$ L), and in some cases transmission electron microscopy (10  $\mu$ L).

**Protocol B:** Generation of  $\alpha$ -synuclein oligomers co-valently modified with dopamine

250  $\mu$ L  $\alpha$ -synuclein (120  $\mu$ M) was mixed with 250  $\mu$ L 180  $\mu$ M dopamine to yield the mixture of 60  $\mu$ M  $\alpha$ -synuclein and 90  $\mu$ M dopamine. 70  $\mu$ L aliquot was taken from the mixture and then solution was shaken for 10 days. 70  $\mu$ L aliquots were collected at day 2, day 4, day 6, day 8, and day 10. Aliquots were used to assess cytotoxicity (40  $\mu$ L), ThT assay (10  $\mu$ L), and in some cases transmission electron microscopy (10  $\mu$ L).

### **3.18 Evaluation of cytotoxicity of extracellular $\alpha$ -synuclein aggregates (pre-formed) in cell-culture system**

Aliquots obtained from experiments mentioned above were used to evaluate the effect of (pre-formed) various species generated from  $\alpha$ -synuclein aggregation experiments on PC12 cell viability (extracellular toxicity). The main objective of this experiment was to optimize the time-point and the aggregation environment that would induce desired cytotoxicity (in ideal conditions, ~50% cell death). For cell-culture experiments, 40  $\mu$ L aliquots (60  $\mu$ M  $\alpha$ -synuclein) from various time-points were diluted with 200  $\mu$ L PC12 cell media to make the final concentration of  $\alpha$ -synuclein 10  $\mu$ M for cell culture experiments.

**Experimental protocol:** Cell viability assay to assess extracellular toxicity of various  $\alpha$ -synuclein aggregation species

Quantitative and colorimetric MTT assay was used to evaluate cytotoxic effects of  $\alpha$ -synuclein. PC12 cells were seeded at 17000 cells/well density in 100  $\mu$ L media in 96 well plate. Cells were allowed to adhere to the surface for 24 hours. Media was removed and the adhered PC12 cells were treated with 55  $\mu$ L  $\alpha$ -synuclein (10  $\mu$ M) containing media. Control cells were treated with appropriately diluted PC12 media. Treatment with extracellular  $\alpha$ -synuclein was conducted for 24 hours. After incubation, 6  $\mu$ L 5 mg/mL MTT was added to the cells and the plate was further incubated at 37°C in 95% air/5% CO<sub>2</sub> atmosphere for 3 hours to produce dark blue formazan crystals. Afterwards, the plate was centrifuged at 1500 rpm for 10 minutes and the supernatants were carefully removed. The formazan crystals were dissolved by adding 100  $\mu$ L of DMSO/methanol (50:50) mixture to each well and shaking the plate gently at room temperature at 400 rpm for 30 minutes at room temperature using a Thermomix R shaker (Eppendorf, Hamburg, Germany). The absorbance values were measured using Epoch microplate reader (Biotek, Winooski, VT, USA) at 570 nm with background correction done at 690 nm. Data from at least 3 experiments were analyzed using Graphpad software (Version 4, San Diego, USA). Cell viability was defined as a percentage reduction in absorbance compared to untreated controls.

### **3.19 Assessment of some lead compounds and standard drug's ability to alter cytotoxicity induced by extracellular $\alpha$ -synuclein**

$\alpha$ -synuclein alone (60  $\mu$ M) was able to induce around ~ 40% cell death after shaking for 6 days. Therefore, we assessed the ability of some of our lead compounds (D-240, D-436, D-

520) and a standard drug (rifampicin) to alter cytotoxicity induced by  $\alpha$ -synuclein (60  $\mu$ M) after shaking for 6 days. All solutions were prepared in 1X PBS. Shaking experiments were conducted on Thermomix R shaker (Eppendorf, Hamburg, Germany) at 1400 rpm and 37°C. 120  $\mu$ M  $\alpha$ -synuclein was prepared by dissolving 1 mg  $\alpha$ -synuclein in 576.3  $\mu$ L 1X PBS. 240  $\mu$ M rifampicin was prepared by dissolving 1mg rifampicin in 4.84 mL 1X PBS. 240  $\mu$ M D-240 was prepared by dissolving 1 mg D-240 in 6.25 mL 1X PBS. 240  $\mu$ M D-436 was prepared by dissolving 1 mg D-436 in 5.1 mL 1X PBS. 240  $\mu$ M D-520 was prepared by dissolving 1 mg D-520 in 5.6 mL 1X PBS.

#### **Protocol for $\alpha$ -synuclein alone experiment**

70  $\mu$ L  $\alpha$ -synuclein (120 $\mu$ M) was mixed with 70  $\mu$ L 1X PBS to yield 60  $\mu$ M  $\alpha$ -synuclein. 50  $\mu$ L aliquot was taken from the mixture and the remaining mixture was shaken for 6 days. After 6 days, the mixture was frozen at -20°C until further use. From day 0 aliquot, 40  $\mu$ L was used for cell viability assay and 10  $\mu$ L was used for ThT assay, whereas, from day 6 aliquot, 40  $\mu$ L was used for cell viability assay, 10  $\mu$ L was used for ThT assay, and remaining volume was used for electron microscopy.

#### **Protocols for rifampicin, D-240, D436, and D520 experiments**

70  $\mu$ L  $\alpha$ -synuclein (120  $\mu$ M) was mixed with 70  $\mu$ L rifampicin (240  $\mu$ M)/70  $\mu$ L D-240 (240  $\mu$ M)/70  $\mu$ L D-436 (240  $\mu$ M) or 70  $\mu$ L D-520 (240  $\mu$ M) to yield 60  $\mu$ M  $\alpha$ -synuclein and 120  $\mu$ M rifampicin/D-240/D-436/D-520. 50  $\mu$ L aliquot was taken from the mixture and the remaining mixture was shaken for 6 days. After 6 days, the mixture was frozen at -20°C until further use. From day 0 aliquot, 40  $\mu$ L was used for cell viability assay and 10  $\mu$ L was used for

ThT assay, whereas, from day 6 aliquot, 40  $\mu\text{L}$  was used for cell viability assay, 10  $\mu\text{L}$  was used for ThT assay, and remaining volume was used for electron microscopy.

### **Evaluation of ability of potential lead compounds' and standard's ability to alter cytotoxicity induced by extracellular $\alpha$ -synuclein**

The aliquots were diluted with PC12 media to get final concentration of  $\alpha$ -synuclein to 10  $\mu\text{M}$  in PC12 media. MTT assay was carried out as described in 3.18 with aliquots obtained from experiments mentioned above.

#### **3.20 Expression, isolation and purification of recombinant $\alpha$ -synuclein**

We developed a method to purify recombinant  $\alpha$ -synuclein in our lab to avoid the use of  $\alpha$ -synuclein from industrial source. Our protocol included expression of  $\alpha$ -synuclein using transformation of E.coli with a plasmid containing the amino acid sequence necessary to generate wild-type  $\alpha$ -synuclein, bacterial culturing protocol to yield maximum amount of  $\alpha$ -synuclein that can be isolated, isolation of proteins from grown bacterial culture, and processing of protein lysate to yield high purity  $\alpha$ -synuclein protein.

#### **Expression of $\alpha$ -synuclein and preparation of glycerol stocks**

pET-3a plasmid (containing amino acid sequence to express wild-type  $\alpha$ -synuclein) was used to transform E.coli strain BL21(DE3). Heat-shock transformation protocol was used to induce transformation. One vial of one-shot cells was thawed on ice. 10 ng pET-3a DNA (in around  $\sim 2$   $\mu\text{L}$ ) was added to the cells and the vial was mixed gently. Vial was incubated on ice for 30 seconds. Heat shock was induced by incubating the vial for 30 seconds in  $42^\circ\text{C}$  water bath. Afterwards, vial was quickly placed on ice. 250  $\mu\text{L}$  SOC medium (supplied with bacteria)

was added to vial. The vial was shaken in an incubator at 37°C for 1 hour at 225 rpm. 12.5 µL or 25 µL volumes from transformation reaction were streaked on LB plates containing ampicillin. The plates were inverted and incubated overnight at 37°C.

Next morning, 2-3 transformants were collected (individual colonies were preferentially selected) and added separately to 2.5 mL LB medium containing ampicillin in 14 mL vials. The vials were shaken in an incubator at 37°C overnight. Next morning, 250 mL fresh LB medium containing ampicillin was inoculated with overnight culture such that the optical density  $OD_{600}=0.05-1.0$ . The medium was shaken in an incubator at 37°C and 225 rpm to reach an  $OD_{600}=0.8-1.0$ . 0.8 mL bacterial culture was mixed with 0.2 mL glycerol to generate glycerol stock of bacteria expressing  $\alpha$ -synuclein. Several vials generated by such method were stored at -80°C to use them for bacterial culturing experiments. Expression of  $\alpha$ -synuclein from bacterial cultures was verified by western blotting.

### **Bacterial culturing protocol**

Transformed BL21(DE3) bacteria were scraped from glycerol stock and expelled into 3 mL LB media containing ampicillin in 14 mL vial. The bacteria were grown in an incubator shaker at 37°C and 250 rpm for 6 hours. Afterwards, 400 µL of bacterial culture was added to 50 mL fresh LB medium containing ampicillin and bacterial culturing was continued overnight in incubator shaker at 37°C and 250 rpm. Next morning, 50 mL bacterial culture was added to 700 mL fresh LB media containing ampicillin. Culturing was continued in an incubator shaker at 37°C and 250 rpm for 3 hours to reach  $OD_{600}\sim 0.8-1.0$ . Bacterial culture was induced with 0.1M IPTG for 3 hours. The resulting bacterial culture was centrifuged at 6000 rpm for 10 minutes. The supernatant medium was decanted and the pellet containing bacteria was resuspended in 7.5

mL buffer (50 mM tris pH 8, 10 mM EDTA, 150 mM sodium chloride). The resuspended bacteria were stored at -80°C.

### **Purification of $\alpha$ -synuclein from bacterial pellet**

Resuspended bacterial cells were directly placed on boiling water-bath for 7 minutes. Afterwards, the tubes were centrifuged at 14000 rpm for 10 minutes. Resulting supernatant was transferred to new tube and streptomycin sulphate (136  $\mu$ L of 10% solution/mL of supernatant) and glacial acetic acid (228  $\mu$ L/mL of supernatant) were added. The mixture was centrifuged for 10 minutes at 14000 rpm. Resulting supernatant was transferred to new tube and precipitated with ammonium sulphate (saturated ammonium sulphate at 4°C was used 1:1 v/v) on shaker for 1 hour at 4°C. Precipitated protein was collected by centrifugation for 10 minutes at 14000 rpm. The protein pellet was washed once with 1mL ammonium sulphate solution (4°C, 1:1 v/v saturated ammonium sulphate (4°C) and water). The washed pellet was resuspended in (900  $\mu$ L) 100 mM ammonium acetate (to form cloudy solution) and precipitated by adding an equal volume of ethanol at room temperature. Precipitation in ethanol was repeated twice, followed by a final resuspension in 100 mM ammonium acetate. The resulting solution was dialyzed against water overnight and frozen in liquid nitrogen before undergoing further purification.

Further purification of  $\alpha$ -synuclein was carried out by anion exchange chromatography. The whole protocol was carried out using a 10 mL syringe attached to the Q-sepharose HP column (5 mL pre-packed column). Frozen protein solution was thawed slowly on ice and pH was adjusted to pH 8. Q-sepharose HP column (5mL) was equilibrated with 25 mL buffer A (tris 50 mM, EDTA 10 mM, sodium chloride 0 mM, pH 8.0). Protein solution was loaded into the column slowly (< 1 mL/minute flow rate). Afterwards, the column was washed with 25 mL

buffer A. Gradient elution was carried out using buffer A with sodium chloride concentrations varying from 50 mM to 600 mM (pH 8.0) using total volume of 100 mL (20 column volumes) as described in the table below. 5mL aliquots were collected for entire run and kept on ice. All aliquots, the solution loaded into the column and the solution eluted from the column were fractionated on 12% tris-glycine-SDS gel. Silver-staining was performed to visualize proteins separated by gel electrophoresis.  $\alpha$ -synuclein was found to be eluted in the fractions corresponding to the sodium chloride concentrations of 250 mM-350 mM. The fractions were combined and concentrated using Chemicon centrifuge filters. Concentrated samples were dialyzed against 20 mM tris (pH 8.0) overnight. Next morning, dialyzed samples were divided into several tubes and frozen at  $-80^{\circ}\text{C}$ . Small aliquots were taken to determine final concentration of protein and its purity.

mM NaCl	Total mL	mL (Tris-EDTA)	mL (Tris-EDTA, 1M NaCl)
50	10	9.5	0.5
100	10	9	1
150	8	6.8	1.2
200	8	6.4	1.6
250	8	6	2
300	8	5.6	2.4
350	8	5.2	2.8
400	8	4.8	3.2
450	8	4.4	3.6
500	8	4	4
550	8	3.6	4.4
600	8	3.2	4.8

**Table 3-1. Gradient elution protocol for purification of  $\alpha$ -synuclein using Q-sepharose HP column**



## CHAPTER 4

### RESULTS

#### 4.1 D-512 prevents cytotoxicity induced by 6-OHDA in PC12 cells

6-OHDA dose dependently induced toxicity on PC12 cells following exposure for 24 hours (**figure 4-1**). Cell viability was significantly decreased (~50%) when PC12 cells were exposed to 75  $\mu\text{M}$  6-OHDA for 24 hours. Cells treated with D-512 alone (0.001  $\mu\text{M}$ , 0.01  $\mu\text{M}$ , 0.1  $\mu\text{M}$ , 1  $\mu\text{M}$ , 5  $\mu\text{M}$ , and 10  $\mu\text{M}$  concentrations) showed no significant toxicity when compared to untreated control cells, whereas, D-512 at concentrations of 20  $\mu\text{M}$  and 30  $\mu\text{M}$  showed some toxicity (~20-30%) to PC12 cells (**figure 4-2**).

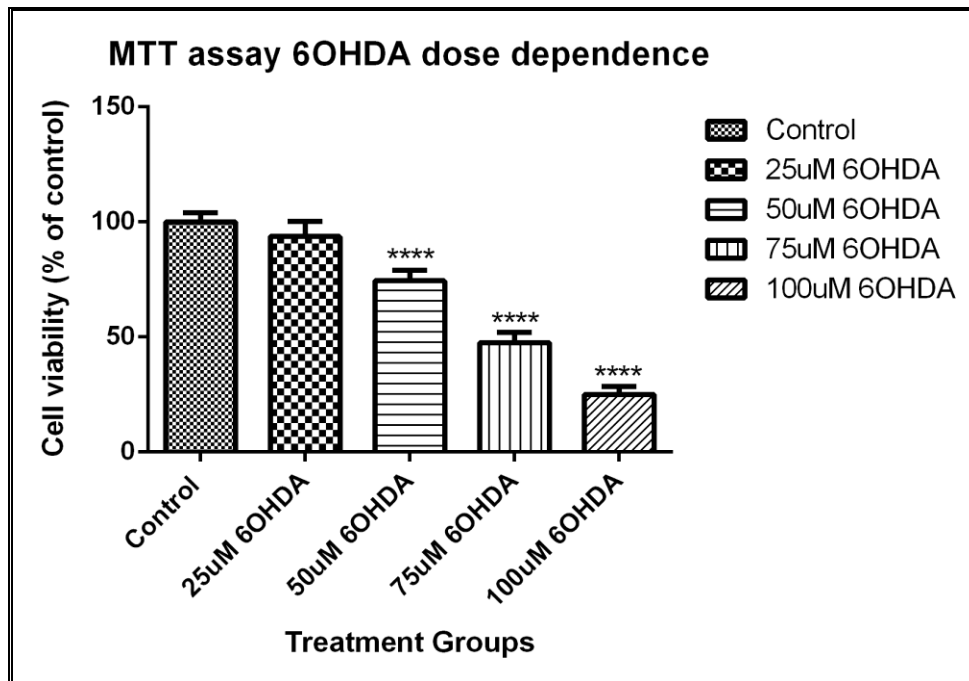


**Figure 4-1.** MTT assay 6-OHDA dose dependence

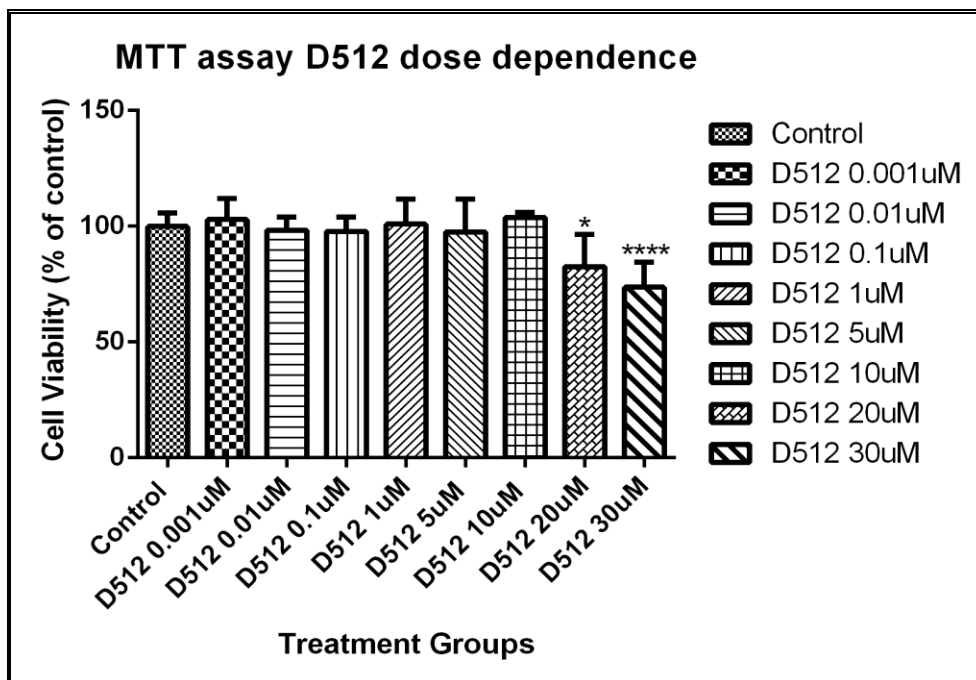


**Figure 4-2. MTT assay D-512 dose dependence**

Then, we evaluated the neuroprotective effect of D-512 on 6-OHDA induced toxicity using two different treatment methods. In the first protocol, D-512 pre-treatment (various concentrations) for 24 hours was followed by exposure to 6-OHDA (75  $\mu$ M) and varied concentration of D-512 for 24 hours. We observed that D-512 was able to significantly restore the cell viability of PC12 cells at 1  $\mu$ M, 5  $\mu$ M, 10  $\mu$ M and 20  $\mu$ M concentrations (**figure 4-3**). Our other protocol consisted of pre-treatment of PC12 cells with D-512 for 24 hours followed by treatment with 6-OHDA (75  $\mu$ M) for another 24 hours. Here, we observed that in either of the protocols D-512 was able to significantly protect the PC12 cells against 6-OHDA-induced toxicity to an extent of 20-40% at 5  $\mu$ M, 10  $\mu$ M, 20  $\mu$ M and 30  $\mu$ M concentrations (**figure 4-4**). This suggests that D-512 has a neuroprotective effect on cell death induced by 6-OHDA in PC12 cells.

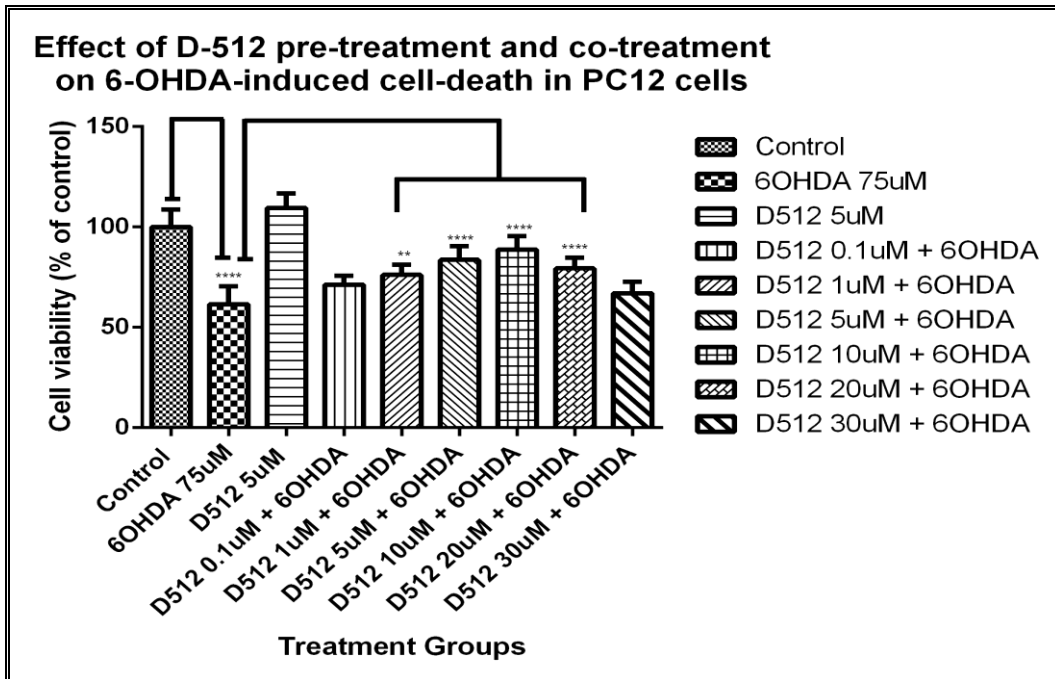


**Figure 4-3. Neuroprotective effect of D-512 pre-treatment and co-treatment on 6-OHDA induced cell death in PC12 cells**

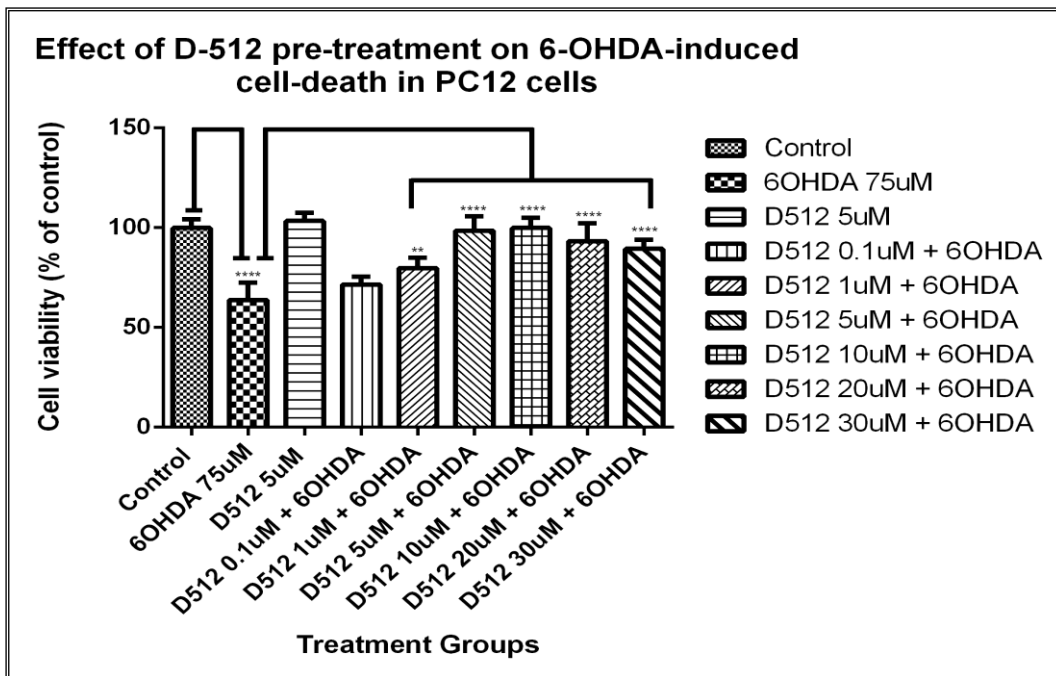


**Figure 4-4. Neuroprotective effect of D-512 pre-treatment on 6-OHDA induced cell death in PC12 cells**

#### 4.2 D-512 partially restores free and total glutathione levels in 6-OHDA treated PC12 cells

Initially, we evaluated the effect of 6-OHDA alone in dose and time-dependent manner on total glutathione levels in PC12 cells (**figure 4-5 and figure 4-6**). From our experiments shown in **figure 4-5 and figure 4-6**, we observed an interesting trend in the level of total glutathione in 6 hours and 24 hours treatment. 6 hours treatment with 25  $\mu\text{M}$  6-OHDA caused around ~20% total GSH depletion, whereas, 24 hours treatment with 25  $\mu\text{M}$  6-OHDA caused around ~65% increase in total GSH levels compared to untreated control cells. In case of 24 hours experiment, we observed an increasing trend for 12.5  $\mu\text{M}$ , 25  $\mu\text{M}$ , and 25  $\mu\text{M}$  6-OHDA treatments, whereas, 6-OHDA concentrations of 75  $\mu\text{M}$  and 100  $\mu\text{M}$  showed decrease in total glutathione levels compared to untreated control cells.

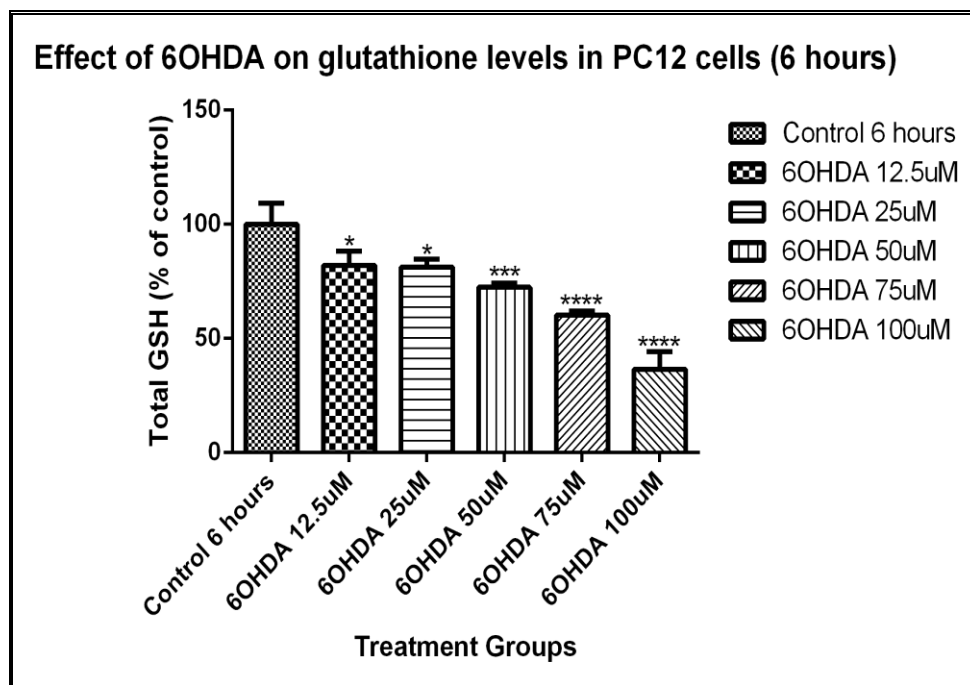


**Figure 4-5.** Effect of 6-OHDA on total glutathione levels in PC12 cells (6 hours)

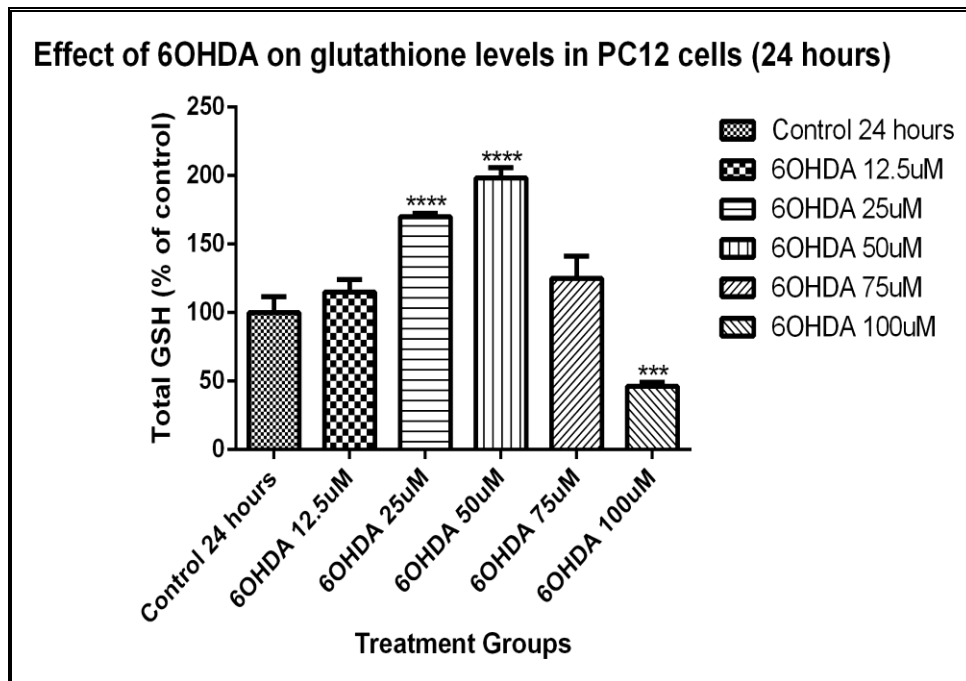


**Figure 4-6.** Effect of 6-OHDA on total glutathione levels in PC12 cells (24 hours)

**NOTE:** Higher dose of 6OHDA (75  $\mu$ M and 100  $\mu$ M causes significant amount of cell death and this might be the reason that the apparent levels of glutathione seem to be decreasing.) No normalization was performed for this experiment as it was done to select optimal dose of 6OHDA for further studies.

To assess the effect of D-512 on free glutathione and total glutathione levels, we employed 25  $\mu$ M 6-OHDA as a toxin and 3 different concentrations of D-512 (10  $\mu$ M, 5  $\mu$ M and 1  $\mu$ M) to assess its neuroprotective ability at 2 different time points, 6 hours and 24 hours. In the 6 hours treatment with 6-OHDA and D-512, we observed that D-512 at 10  $\mu$ M concentration was able to restore the free glutathione levels as well as total glutathione levels depleted by 25  $\mu$ M 6-OHDA in PC12 cells (**figure 4-7 and figure 4-8**). However, 24 hour treatment with 6-OHDA and D-512 showed that none of the doses of D-512 restored the increase in free glutathione levels or total glutathione levels by 25  $\mu$ M 6-OHDA alone in PC12 cells to control level (**figure 4.9 and figure 4.10**). This suggests that D-512 may induce changes in free and total

glutathione levels during earlier time-point of exposure to 6-OHDA in PC12 cells (6 hours). However, D-512 doesn't have ability to alter free or total glutathione level in PC12 cells treated with 6-OHDA at higher time-point (24 hours).

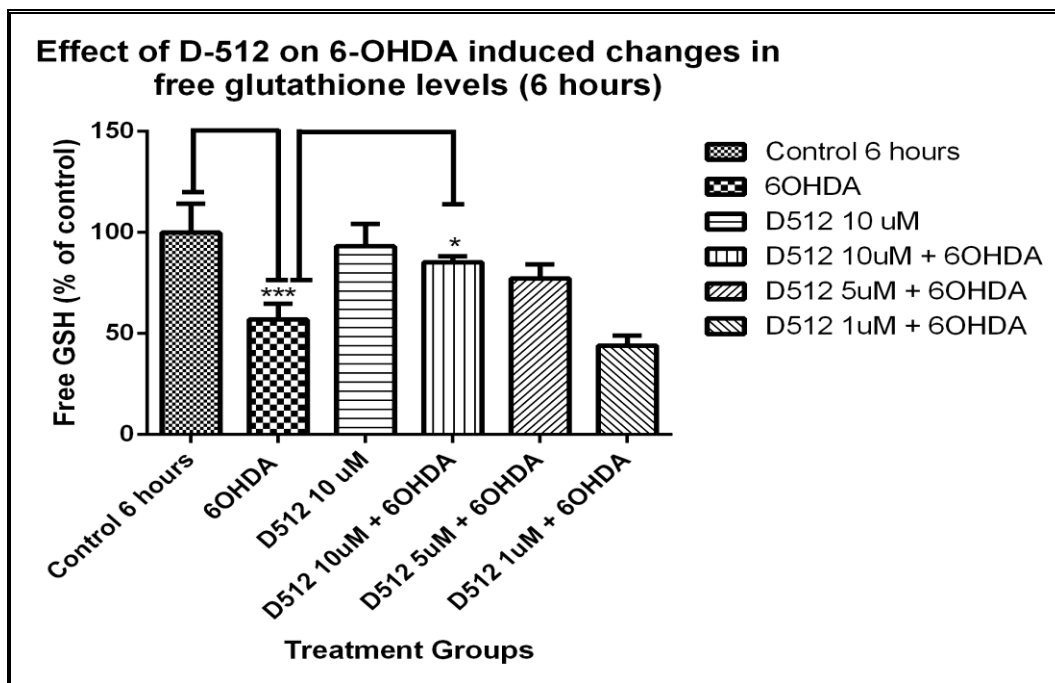


**Figure 4-7.** Effect of D-512 on 6-OHDA induced changes in free glutathione levels (6 hours)

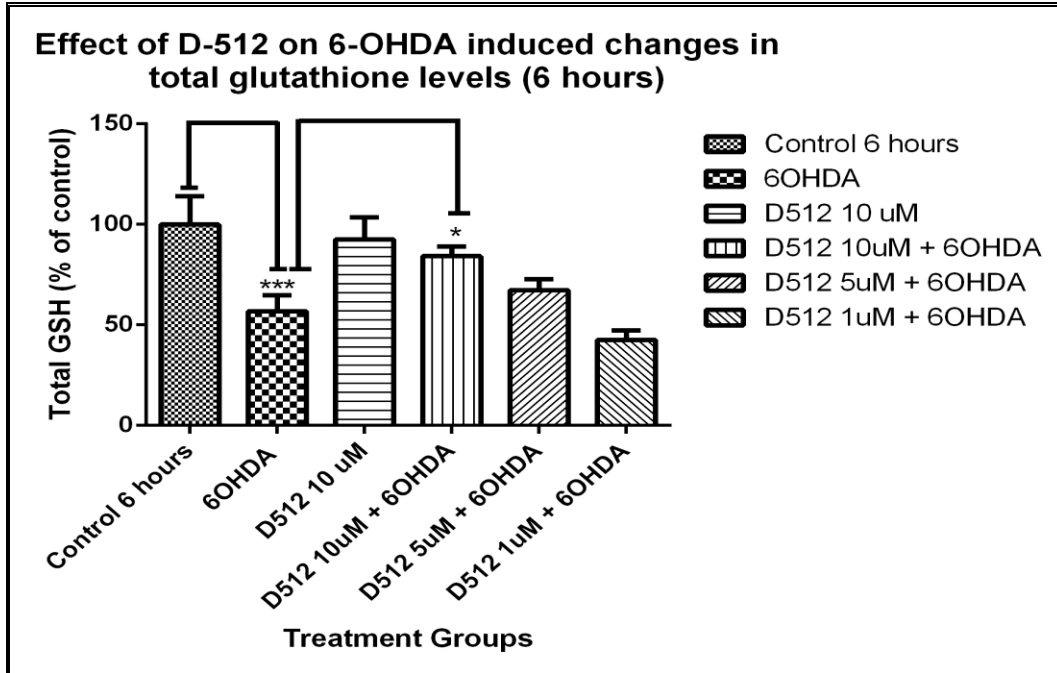


**Figure 4-8. Effect of D-512 on 6-OHDA induced changes in total glutathione levels (6 hours)**

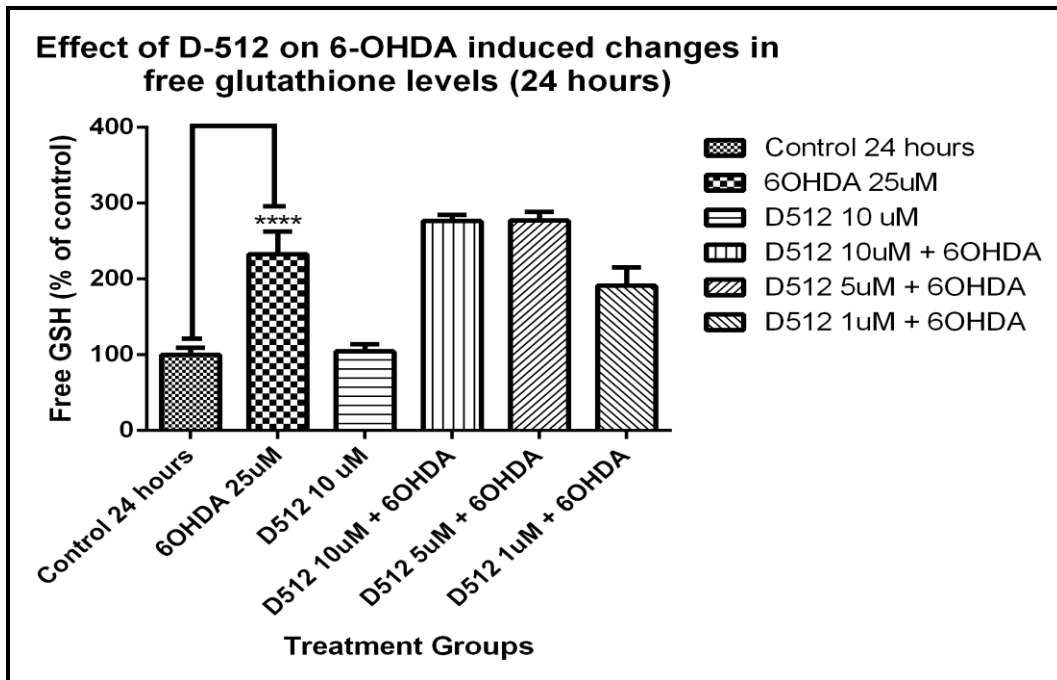


**Figure 4-9. Effect of D-512 on 6-OHDA induced changes in free glutathione levels (24 hours)**

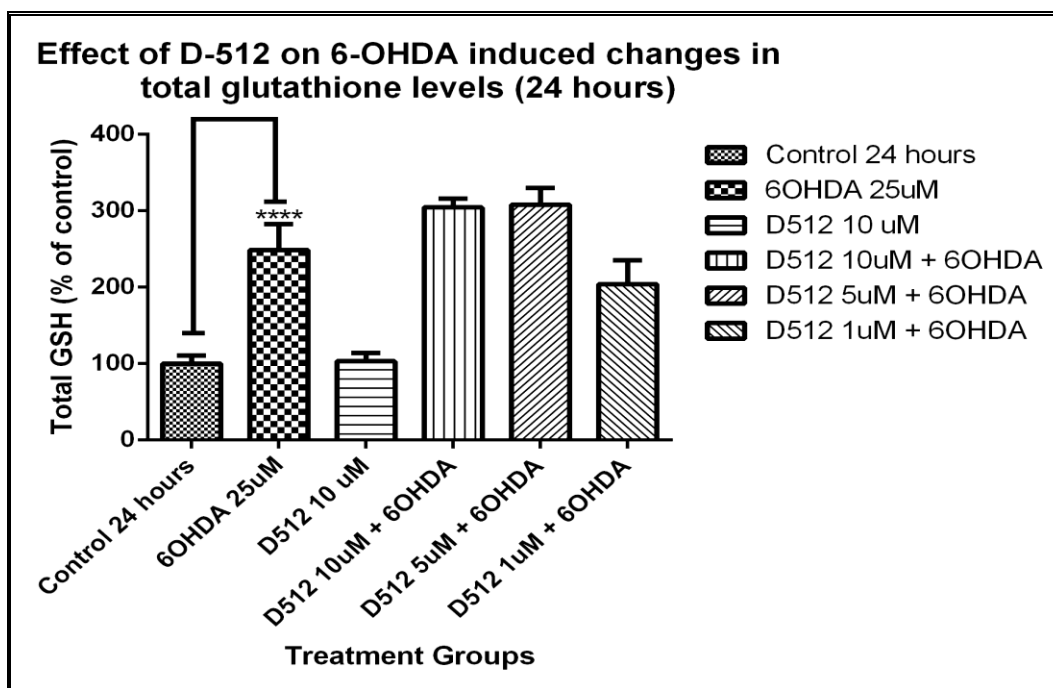


**Figure 4-10. Effect of D-512 on 6-OHDA induced changes in total glutathione levels (24 hours)**

#### 4.3 D-512 has an ability to restore total glutathione levels in BSO treated PC12 cells

Buthionine sulfoximine (BSO) is a well-known compound for the inhibition of enzyme  $\gamma$ -glutamylcysteine synthetase, which has a key role in glutathione synthesis. Initially, we evaluated the effect of BSO on total glutathione levels in PC12 cells in dose and time-dependent manner (**figures 4-11 and figure 4-12**). Total GSH was depleted dose dependently at both 6 and 24 hours by BSO. It was observed that at 6 hours, 1.56  $\mu$ M BSO causes ~20% total GSH depletion (**figure 4-11**), while the same dose causes ~55% depletion at 24 hours compared to untreated control cells (**figure 4-12**).



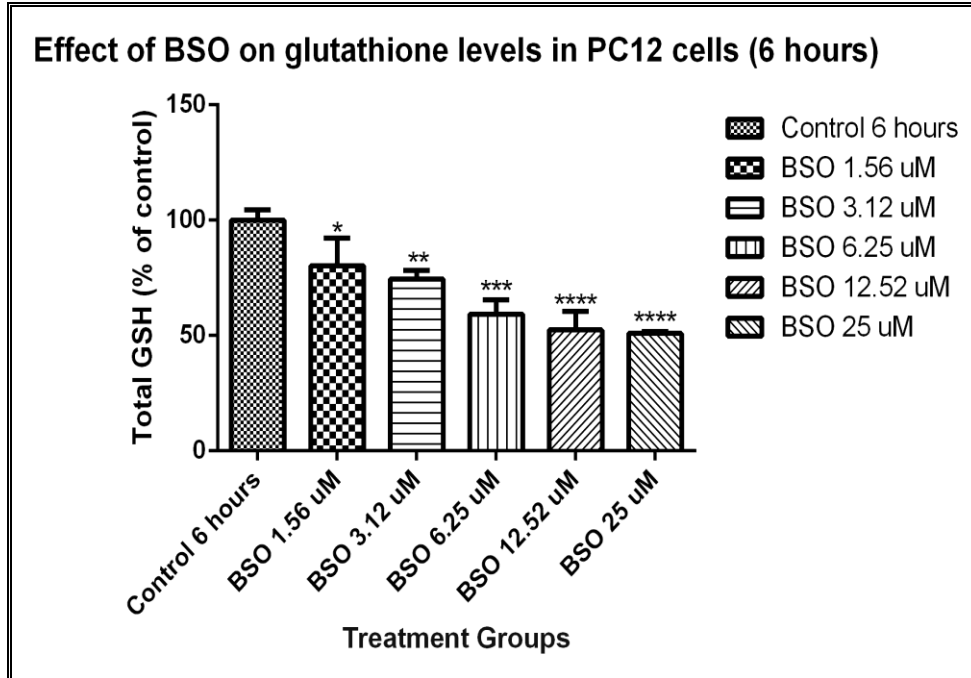


**Figure 4-11.** Effect of BSO on total glutathione levels in PC12 cells (6 hours)

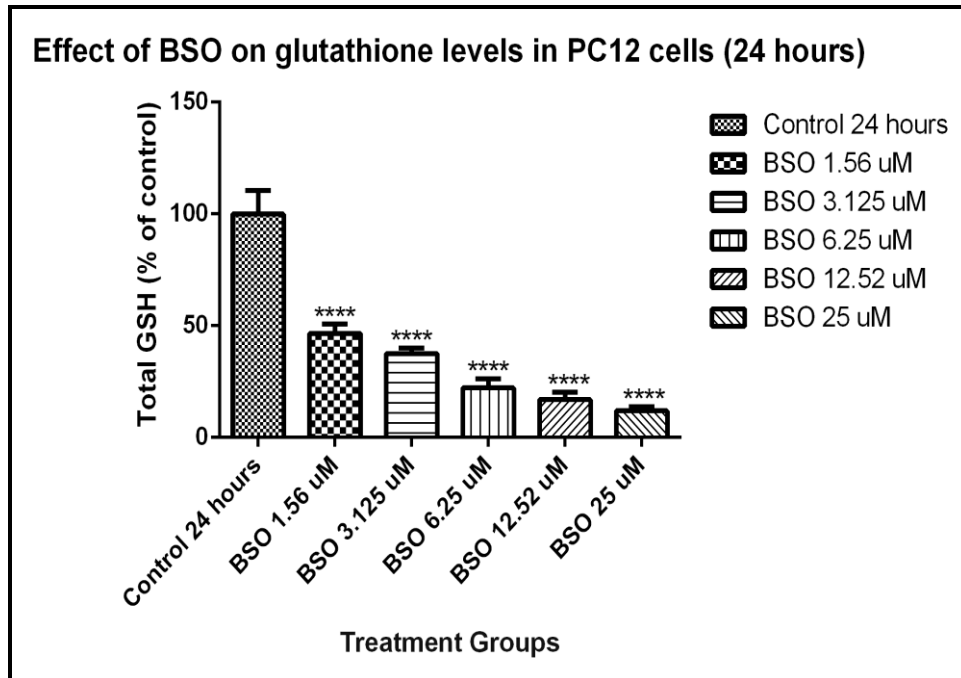


**Figure 4-12.** Effect of BSO on total glutathione levels in PC12 cells (24 hours)

To evaluate the effect of D-512 against BSO induced glutathione depletion, PC12 cells were pre-treated with 4 different concentrations of D-512 (20  $\mu$ M, 10  $\mu$ M, 5  $\mu$ M and 1  $\mu$ M) for 24 hours followed by co-treatment with 1.56  $\mu$ M BSO and 4 different concentrations of D-512 for either 6 hours or 24 hours. In case of BSO and D-512 treatment for 6 hours (**figure 4-13**), D-512 at 20  $\mu$ M, 10  $\mu$ M, and 5  $\mu$ M concentrations partially restored total glutathione levels, which were depleted by 1.56  $\mu$ M BSO. In another experiment, which involved treatment of 1.56  $\mu$ M BSO and various D-512 concentrations for 24 hours (**figure 4-14**), D-512 concentrations of 20  $\mu$ M and 10  $\mu$ M provided statistically significant restoration of total glutathione levels in PC12 cells.

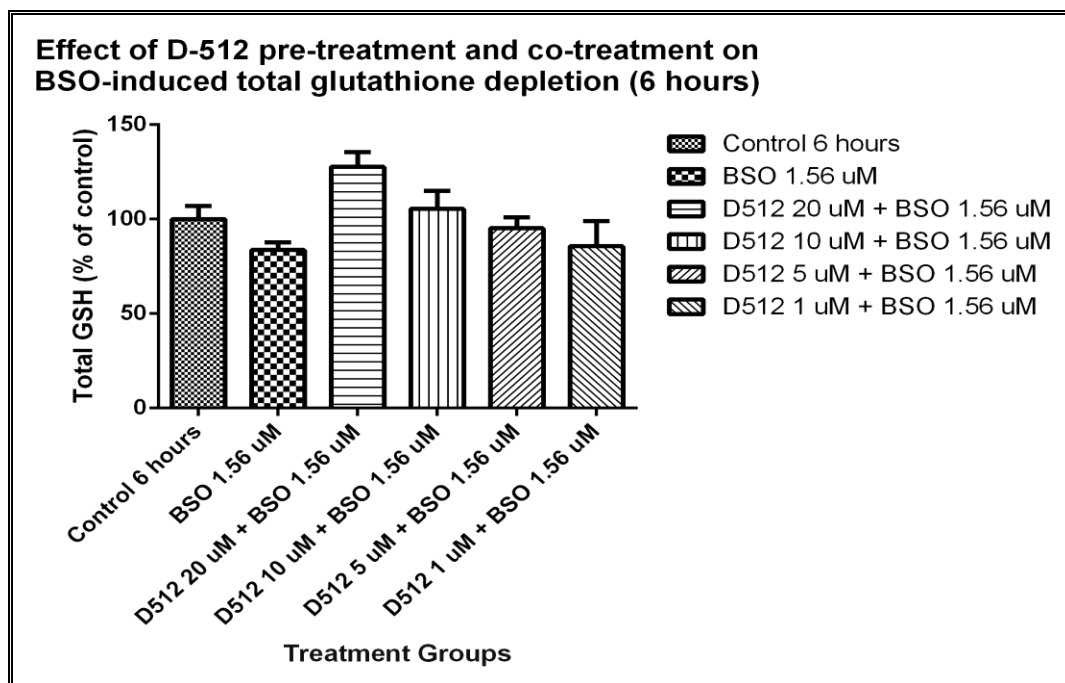


**Figure 4-13.** Effect of D-512 pre-treatment and co-treatment on BSO-induced total glutathione depletion in PC12 cells (6 hours)

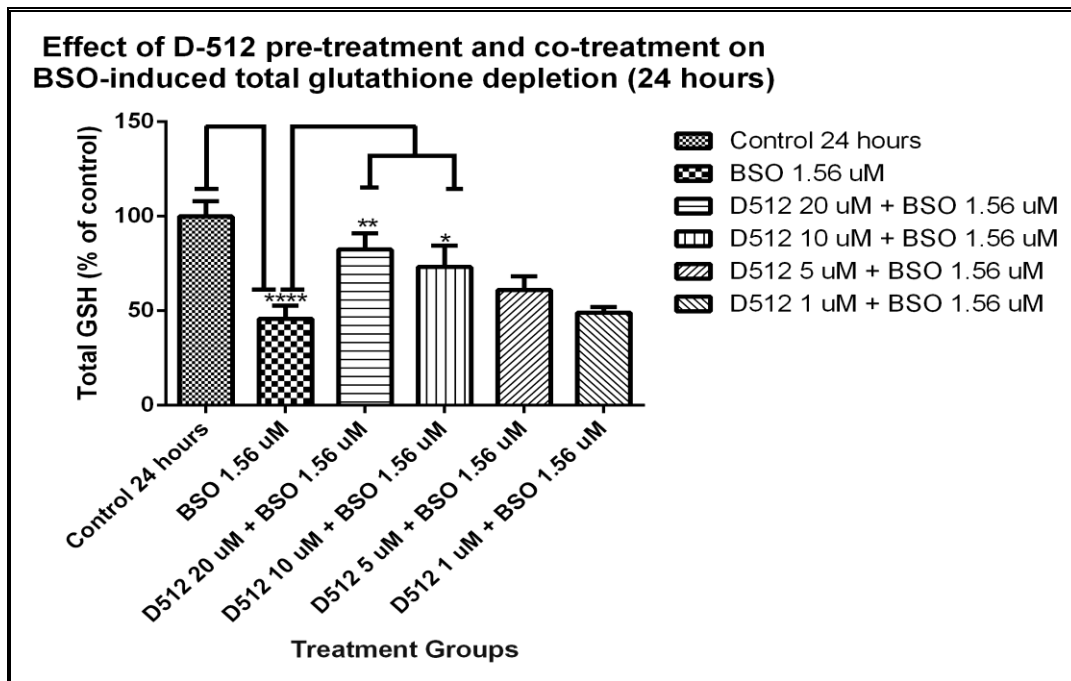


**Figure 4-14. Effect of D-512 pre-treatment and co-treatment on BSO-induced total glutathione depletion in PC12 cells (24 hours)**

#### 4.4 D-512 is able to partially restore nuclear morphology changes in 6-OHDA treated PC12 cells

Nuclear morphology is one of the characteristic features of assessing the cell integrity. Changes in nuclear morphology of PC12 cells treated with D-512 followed by exposure to 6-OHDA were assessed by Hoescht 33342 staining. Control cells showed homogeneous staining of their nuclei without any abnormalities, whereas, PC12 cells treated with 75  $\mu$ M 6-OHDA showed nuclear condensation. 10  $\mu$ M D-512 alone didn't cause any change in nuclear morphology compared to control cells. However, when 10  $\mu$ M D-512 treated PC12 cells were exposed to 75  $\mu$ M 6-OHDA, it reduced nuclear condensation significantly when compared to 6-OHDA alone treated cells (**figure 4-15**).

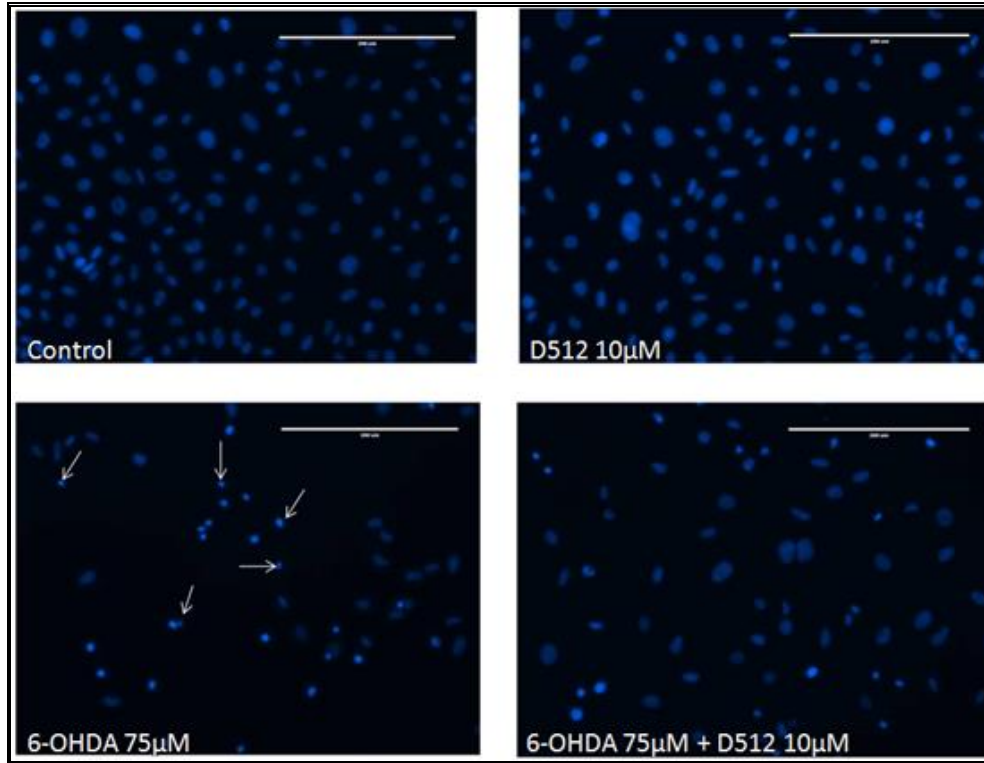


**Figure 4-15. Nuclear morphology characterization of PC12 cells by Hoescht staining**

#### 4.5 D-512 partially prevents DNA fragmentation induced by 6-OHDA in PC12 cells

DNA fragmentation is a hallmark feature of apoptosis. We assessed the effect of D-512 treatment on 6-OHDA induced DNA fragmentation. Control cells and D-512 alone 10  $\mu\text{M}$  treated cells did not yield any fragmented DNA. However, PC12 cells treated with 75  $\mu\text{M}$  6-OHDA yielded highly fragmented DNA. D-512 rescued the fragmentation of DNA in a dose-dependent manner in PC12 cells treated with 75  $\mu\text{M}$  6-OHDA. D-512 10  $\mu\text{M}$  was found to be most effective concentration when compared with D-512 5  $\mu\text{M}$  and 1  $\mu\text{M}$  in preventing DNA fragmentation upon exposure to 6-OHDA (**figure 4-16**).

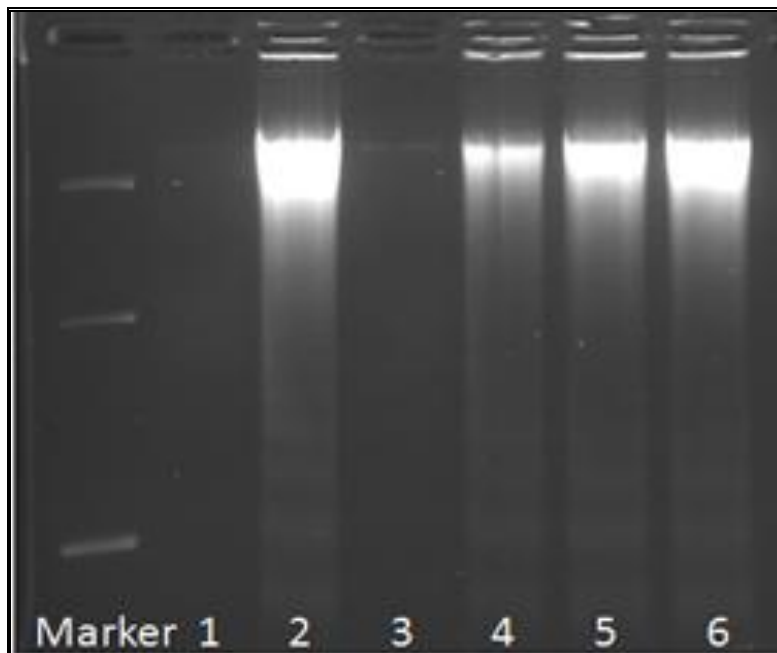


**Figure 4-16.** Determination of D-512's ability to alter DNA fragmentation induced by 6-hydroxydopamine.

**1. Control cells; 2. Cells treated with 6-OHDA (75  $\mu$ M); 3. Cells treated with D-512 alone (10  $\mu$ M); 4, 5, 6. Cells treated with 6-OHDA and D-512 10  $\mu$ M/D-512 5  $\mu$ M or D-512 1  $\mu$ M, respectively.**

#### 4.6 D-512 prevents sodium nitroprusside induced lipid peroxidation in PC12 cells

We utilized sodium nitroprusside (SNP) to generate lipid peroxidation as 6-OHDA did not induce lipid peroxidation in PC12 cells (data not shown). We observed that SNP 200  $\mu$ M was able to induce ~90% increase in lipid peroxidation compared to untreated control cells. D-512 showed dose-dependent effect in preventing the lipid peroxidation induced by SNP. As shown in **figure 4-17**, 1  $\mu$ M of D-512 significantly prevented lipid peroxidation (~65%), whereas, 0.5  $\mu$ M D-512 showed ~42% decrease in lipid peroxidation induced by 200  $\mu$ M sodium nitroprusside. However, D-512 at 0.25  $\mu$ M concentration wasn't able to prevent lipid peroxidation in PC12 cells.

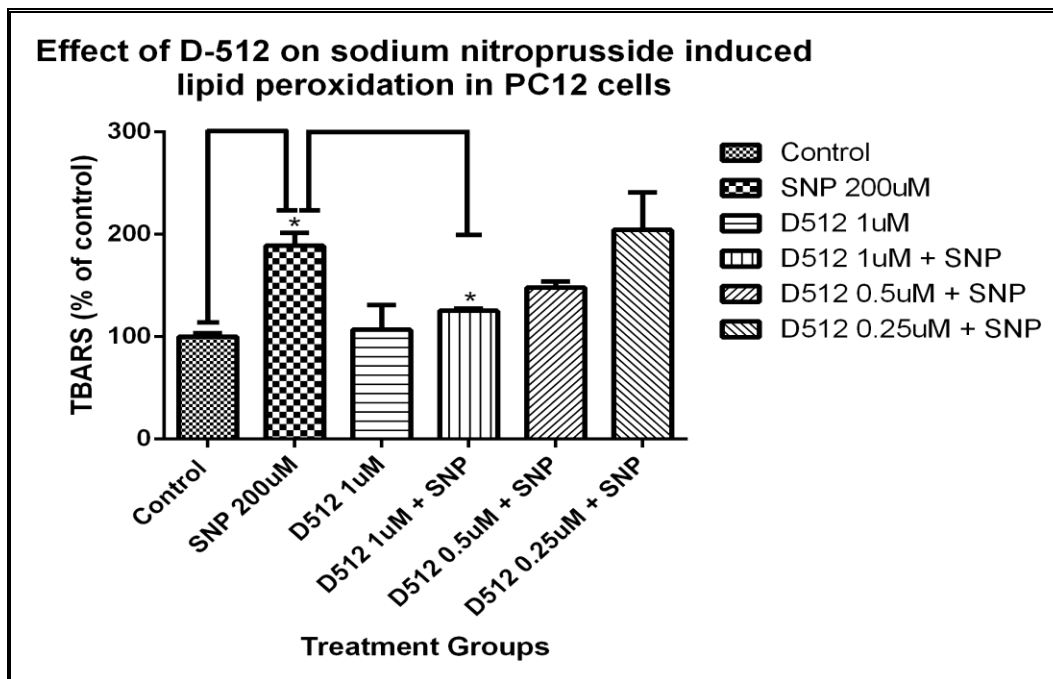


**Figure 4-17.** Evaluation of ability of D-512 to protect against lipid peroxidation induced by sodium nitroprusside

4.7 D-512 prevents temporal increase in phospho-ERK and phospho-JNK signaling molecules induced by 6-OHDA in PC12 cells

We observed an upregulation in phospho-ERK1/2 and phospho-JNK levels in time-dependent manner after exposure of PC12 cells to 6-OHDA (75  $\mu$ M). Therefore, we evaluated the effect of D-512 (10  $\mu$ M) pre-treatment and co-treatment on these signaling molecules in PC12 cells exposed to 75  $\mu$ M 6-OHDA. Surprisingly, we found that D-512 at all three different time points (30 minutes, 2 hours and 4 hours) was able to prevent an upregulation of phospho-ERK1/2 and phospho-JNK induced by 6-OHDA (**figure 4-18 and figure 4-19**). It is possible that the prevention of phospho-ERK and phospho-JNK upregulation by D-512 may be potential molecular mechanism by which it is able to protect against 6-OHDA induced toxicity in PC12

cells. As the time-points assessed preceded the time-point of any other assays, it can be inferred that D-512 may act on these signaling molecules at early time-point which may prevent some downstream signaling events leading to cell death at later time point.

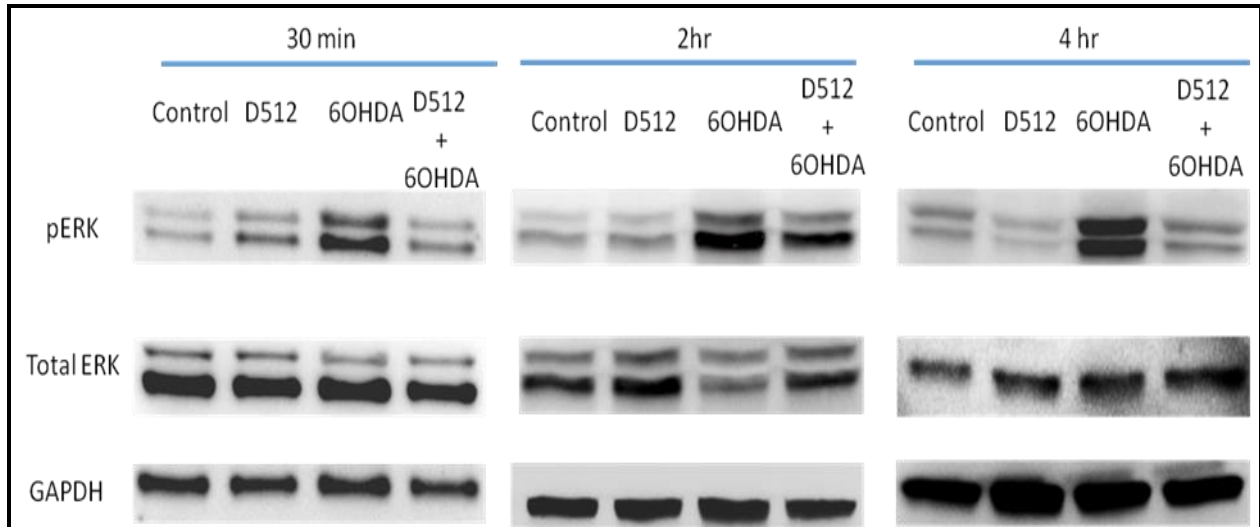


**Figure 4-18.** Effect of D-512 on 6-OHDA induced changes in phospho-ERK

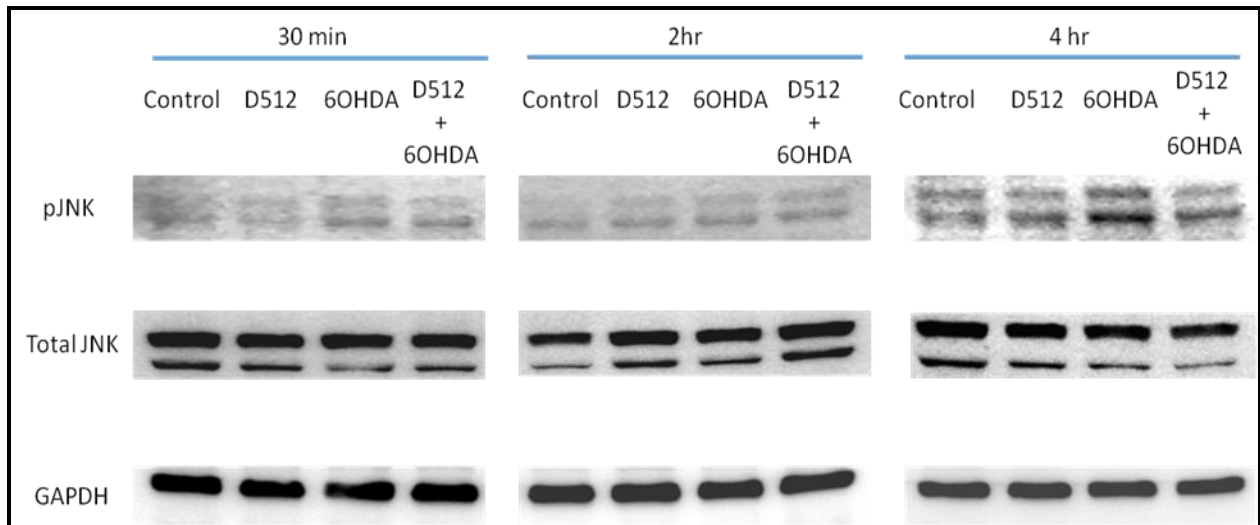


**Figure 4-19.** Effect of D-512 on 6-OHDA induced changes in phospho-JNK

## **DISCUSSION**

Surprisingly, the best available treatment for PD still remains to be L-DOPA, which was discovered immediately following discovery of dopamine as a neurotransmitter (Birkmayer and Hornykiewicz 1961). Approaches to develop a successful therapeutic for PD have failed to achieve disease-modifying therapeutic, possibly because of multi-factorial nature of the disease (Van der Schyf, Mandel et al. 2007, Youdim 2010, Youdim 2013). Although most of the PD cases are sporadic in nature, cardinal clinical features of PD patients remain the same which implies that a common pathological mechanism might be triggered by a variety of etiological factors. Traditional therapeutics for PD are usually designed to act on single pathological target (receptor, enzyme or protein), not considering the complex nature of the disease. However, common PD therapy usually includes polypharmacy i.e. combination of two or more medications (Swanson 1994). Polypharmacy is usually done to improve the effect of prescribed medication or to treat other complications as PD progresses (Swanson 1994, Lemke, Fuchs et al. 2004). Most of the PD medications used clinically are targeted towards restoring the imbalance in neurotransmitter systems and usually provide symptomatic relief rather than addressing the pathological factors involved in PD. Therefore, it is crucial to develop a therapeutic that can not only restore the neurotransmitter system's imbalance in PD patients but which can also act on other common pathological targets of PD. Currently, very limited research has been done towards the development of therapeutics that can target multiple pathological factors associated with PD. Our ultimate goal is to develop a multifunctional therapeutic against PD which can potentially act on multiple pathological targets and can also provide symptomatic relief from PD.

Based on various etiological, epidemiological, and biochemical studies increased oxidative burden can be implicated as a common culprit in all PD patients. DA levels are



substantially depleted in substantia nigra of patients with PD. DA has been shown to undergo auto-oxidation more readily than any other catecholamines, which results in generation of toxic products such as hydrogen peroxide, superoxide, and hydroxyl radicals. DA can also generate quinone species which are transient in nature and can co-valently modify sulfhydryl groups of various biomolecules (enzymes, proteins, and reducing environment). Thus, abnormal DA metabolism may be potentially responsible for selective dopaminergic neuronal loss in PD. Additionally, iron levels in substantia nigra have also been shown to be elevated. Iron catalyzed Fenton's reaction can yield hydroxyl radicals, which can potentially convert dopamine into 6-hydroxydopamine. The generated 6-hydroxydopamine (6-OHDA) and other reactive oxygen species might be responsible for vicious cycle of oxidative stress and the progression of PD. Hence, it is quite convincing to develop therapeutics that can modify oxidative stress in PD. Several clinical trials have been conducted in PD patients that show some convincing data for the use of antioxidants as PD therapy. Interestingly, an open-label clinical trial showed that the rate of PD progression can be decreased by 2.5 years by administration of high-dose  $\alpha$ -tocopherol and ascorbate in early stage PD patients (Fahn 1992). Historical DATATOP trial established deprenyl (a MAO-B inhibitor) as a potent anti-oxidant that can delay the rate of PD progression (Shoulson 1998). Youdim et al. have recently published some ground-breaking work on multifunctional PD therapeutics which combine MAO-B inhibitory and iron-chelator activities based on modification of Rasagiline (Youdim 2013). However, a potential drawback of their drug design may be targeting the inhibition of dopamine metabolism, which still doesn't address the toxicity generated by dopamine auto-oxidation and may not be completely effective as a disease-modifying therapy. We followed a similar approach as Youdim et al., but we designed molecules that can act as dopamine agonist and anti-oxidant. We avoided designing molecules

which can elevate dopamine levels or prevent dopamine metabolism possibly leading to oxidative stress conditions in long-term therapy. We published work on some of our hybrid templates that have iron-chelator, anti-oxidant, and neuroprotective activities in addition to their dopamine D2/D3 receptor agonist activity (Gogoi, Antonio et al. 2011, Johnson, Antonio et al. 2012). We also established recently that 2 of our lead compounds possess multi-functional activities which included dopamine receptor agonist, anti-oxidant, and anti-apoptotic properties using murine mesencephalic dopaminergic cell-line (Santra, Xu et al. 2013).

Current experimental data reflects our efforts to further evaluate the mechanisms of action of one of the lead compounds, D-512 from our hybrid template library. Specifically, we evaluated the anti-oxidant activity of D-512 in PC12 cells against oxidative stress caused by 6-OHDA and similar oxidants (or toxicants) after determining the ability of D-512 to prevent cell death in PC12 cells. PC12 cells are rat adrenal medulla pheochromocytoma cell line. PC12 express tyrosine hydroxylase and possess higher levels of DA than any other catecholamines (Greene and Tischler 1976). PC12 cells have also been shown to express dopamine D1 receptors, D2 receptors, and DAT (Courtney, Howlett et al. 1991, Zhu, Conforti et al. 1997, Pothos, Przedborski et al. 1998, Zachor, Moore et al. 2000). Thus, PC12 cells recapitulate dopaminergic neurons and have been employed routinely in evaluation of PD therapeutics (Tatton, Ju et al. 1994, Abu-Raya, Blaugrund et al. 1999, Fujita, Izawa et al. 2006). 6-OHDA has been considered to be a toxin which might be generated by abnormal metabolism of DA and has been implicated as one of the factors that may cause PD (Linert and Jameson 2000). 6-OHDA is shown to be increased significantly in patients with PD who administer L-DOPA (Linert and Jameson 2000). It is well established that 6-OHDA causes its toxicity in PC12 cells by generation of ROS (Blum, Torch et al. 2000, Hanrott, Gudmunsen et al. 2006). It has been also shown that extracellular

oxidation of 6-OHDA is necessary to induce toxicity in PC12 cells and the toxicity is independent of DA uptake blockade (Abad, Maroto et al. 1995, Yamada, Umegaki et al. 1997, Blum, Torch et al. 2000, Hanrott, Gudmunsen et al. 2006). Non-enzymatic degradation of 6-OHDA results in the generation of p-quinones and hydrogen peroxide extracellularly, which enter PC12 cells and induce their apoptosis. Previously, we established that D-512 is a non-selective D2/D3 receptor agonist and two times potent compared to ascorbic acid as an antioxidant using DPPH (2,2-diphenyl-1-picrylhydrazyl) radical quenching assay (Johnson, Antonio et al. 2012). We also found D-512 to be neuroprotective in a dopaminergic cell-line (MN9D) which doesn't express dopamine receptors (Santra, Xu et al. 2013). Here, we employed versatility of PC12 cells to partially recapitulate dopaminergic neurons and tested multifunctional effects of D-512 using ROS generating toxin 6-OHDA.

Initially, we determined to assess the effect of various treatments on cell viability before evaluating potential mechanisms of neuroprotection conferred by D-512. Our experiments to optimize doses of 6-OHDA and D-512 for neuroprotection studies led us to use 75  $\mu\text{M}$  6-OHDA for neuroprotection experiments, whereas, experiments with D-512 helped us conclude that D-512 was toxic to PC12 cells at 20  $\mu\text{M}$  and 30  $\mu\text{M}$  concentrations. From our neuroprotection experiments, we could conclude that D-512 treatment may not be necessary when cells are exposed to 6-OHDA, and pre-treatment with D-512 alone is sufficient to confer similar extent of protection against 6-OHDA induced cell death. This assay also provided us an insight that D-512 is a potential neuroprotective agent as it is able to rescue PC12 cells from 6-OHDA induced cell death, which can be the effect of its dopamine agonist and/or anti-oxidant activity. Previously, we observed similar neuroprotective effects of D-512 in MN9D cell line treated with 6-OHDA (Santra, Xu et al. 2013).

We aimed our other experiments to determine potential mechanisms of action of D-512 by which it can act as an anti-oxidant. D-512 can be effective in preventing oxidative stress induced by 6-OHDA in two different ways,

- I. It may be able to prevent or decrease the generation of ROS;
- II. It may be able to act via anti-oxidant defenses of PC12 cells to help them resist severe oxidative stress conditions.

As ROS are usually unstable and transient, they are not easily detectable and may not reflect the oxidative burden of cells effectively. However, ROS induced stress can be easily detected by assessing oxidative status of various biomolecules. A potential mechanism of cell survival may also include the alteration in its anti-oxidant defense systems such as glutathione system, superoxide dismutase enzyme, and catalase enzyme. We carried out experiments to evaluate neuroprotective ability of D-512 by estimating oxidized and total glutathione levels, nuclear condensation, DNA fragmentation, and lipid peroxidation.

To evaluate the ability of D-512 to restore glutathione levels altered by 6-OHDA treatment in PC12 cells, we determined the levels of free glutathione and total glutathione in PC12 cells treated with 6-OHDA and D-512. Glutathione is a thiol tripeptide (glutamyl-cysteinyl-glycine), which is abundantly present in healthy cells and responsible for maintaining reduced environment. Free glutathione is responsible for neutralizing any ROS generated as a consequence of cellular metabolism. Initially, we carried out experiments to optimize the concentration of 6-OHDA to carry out further experiments involving D-512. Surprisingly, we observed an opposite trend in total glutathione levels following 6 hour and 24 hour treatment with 6-OHDA in PC12 cells. 6 hour treatment caused a dose-dependent decrease in total

glutathione levels. However, in case of 24 hour treatment of PC12 cells with 6-OHDA, we observed significant increase in total glutathione levels for 25  $\mu\text{M}$  and 50  $\mu\text{M}$  concentrations, whereas, total glutathione levels were significantly depleted after treatment with 100  $\mu\text{M}$  6-OHDA compared to untreated control cells. These results corroborate with previous studies that showed similar effects of relevant PD toxins on total glutathione levels in PC12 cells, other similar cell lines, and primary neuronal cultures (Seyfried, Soldner et al. 2000, Shimizu, Hashimoto et al. 2002, Takata, Yamaguchi et al. 2005, Zhang, Hu et al. 2005). For 6 hour experiment, it can be concluded that before 6-OHDA exposed PC12 cells undergo cell death, they are depleted of total glutathione either by corresponding increase in oxidized glutathione (Seyfried, Soldner et al. 2000) or by efflux of glutathione out of the cells (Di Monte, Sandy et al. 1987). For 24 hour experiment, it can be inferred that lower doses of 6-OHDA (25  $\mu\text{M}$  and 50  $\mu\text{M}$ ) may induce apoptosis in most of the cells and induce cell death in small percentage of cells after 24 hours. After depletion of pre-existing glutathione, the remaining surviving cells may increase glutathione levels as a protective mechanism before undergoing cell death at a later time. Contrary to this, at higher doses of 6-OHDA (75  $\mu\text{M}$  and 100  $\mu\text{M}$ ), most PC12 cells are dead (as shown in MTT assay data) and very few surviving cells may decrease or lose their ability to increase glutathione levels.

We utilized 25  $\mu\text{M}$  6-OHDA to evaluate effect of D-512 on free glutathione and total glutathione levels in PC12 cells treated with 6-OHDA for 6 hours and 24 hours. Our experiments suggested that there was no significant increase in oxidized glutathione at either time-point. This suggests that glutathione levels in PC12 cells may decrease by efflux mechanism under apoptotic condition rather than its oxidation under 6-OHDA treatment. We observed similar trend in the levels of total glutathione and free glutathione at both time-points. In case of 6 hour experiment,

we observed a dose-dependent restoration in free and total glutathione levels by D-512 in 6-OHDA treated PC12 cells, which can be correlated to higher number of cells in healthy condition and possibly less efflux of glutathione out of these cells. Surprisingly, in case of 24 hour exposure to 6-OHDA, we didn't see restoration effects of D-512 on free and total glutathione levels in PC12 cells. Instead, we found the glutathione levels to be very similar to that observed with 6-OHDA alone treated cells. This may possibly be due to inability of D-512 to protect against 6-OHDA induced glutathione changes at a higher time point. An alternative explanation can be a mild oxidative stress induced by D-512, which may result in increase in glutathione content as has been observed with L-DOPA (Han, Mytilineou et al. 1996). Exposure to mild oxidative stress may prevent PC12 cells from stronger oxidative burden induced by ROS formed after 6-OHDA exposure.

As the mechanism by which 6-OHDA alters glutathione levels in PC12 cells is not fully elucidated, we wanted to further verify the ability of D-512 to restore total glutathione levels in PC12 cells using a toxicant with known mechanism of action on glutathione system. We employed buthionine sulfoximine (BSO) which inhibits enzyme  $\gamma$ -glutamylcysteine synthetase, which is involved in first step of glutathione synthesis. In case of BSO dose optimization experiments, we observed a dose-dependent depletion of total glutathione levels in both 6 hour and 24 hour time points. Our experiments involving D-512 and BSO led us to conclude that D-512 has an ability to restore BSO-induced changes in total glutathione levels in a dose-dependent manner at both the time points. Thus, we were able to verify that D-512 has a potential to restore glutathione levels in PC12 cells treated with 6-OHDA or BSO. Therefore, D-512 must possess broad mechanism of action by which it is able to protect against glutathione alteration induced by toxins acting by different mechanisms of action.

We intended to verify the ability of D-512 to protect against lipid peroxidation induced by 6-OHDA in PC12 cells. However, we didn't observe significant changes in lipid peroxidation at different time points with different doses of 6-OHDA (data not shown). However, it is important to assess the ability of D-512 to prevent lipid peroxidation as PD patient's substantia nigra show significant increase in lipid peroxidation. We were able to induce significant increase in lipid peroxidation with 200  $\mu$ M sodium nitroprusside (SNP). SNP is an ideal toxicant to induce lipid peroxidation as it possesses iron as well as nitric oxide in its chemical structure, which can generate lipid peroxides and simulate PD pathological condition. We found D-512 to be dose-dependently effective in preventing lipid peroxidation induced by SNP. Thus, D-512 also possesses an ability to prevent damage to lipids induced by oxidative insult and excessive iron accumulation. We observed similar results of toxins as well as D-512 in our previous study using MN9D cell line (Santra, Xu et al. 2013).

Apoptotic cell death can cause nuclear condensation and DNA fragmentation. We evaluated D-512's ability to protect against apoptosis induced by 6-OHDA by Hoescht staining. We found D-512 to be partially protective against 6-OHDA induced nuclear condensation. However, nuclear condensation is a qualitative technique and we wanted to evaluate effect of D-512 in dose-dependent manner using semi-quantitative technique. Therefore, we assessed D-512's ability to protect against DNA fragmentation, which is also the hallmark of apoptotic cell death. We observed DNA laddering in case of 6-OHDA treatment, whereas, D-512 dose-dependently prevented fragmentation of DNA induced by 6-OHDA. Thus, D-512 has an ability to protect against apoptotic cell death and DNA as well as nuclear damage induced by 6-OHDA in PC12 cells. Similar effect of D-512 to prevent apoptotic change has been reported by us previously (Santra, Xu et al. 2013).

We also wanted to understand the possible molecular mechanisms by which D-512 may be able to protect PC12 cells against oxidative stress caused by 6-OHDA. Therefore, we evaluated the ability of D-512 to alter 6-OHDA-induced changes in mitogen activated protein kinases (MAPKs). As anticipated, we observed a time-dependent, sustained increase in expression of phospho-ERK1/2 and phospho-JNK signaling molecules in presence of 6-OHDA (Kim, Kim et al. 2011, Zhang, Xue et al. 2012). In case of D-512 alone, we observed a transient increase in phospho-ERK1/2 at 30 minutes, whereas, at 2 hours and 4 hours time point we didn't observe significant differences compared to control PC12 cells. Interestingly, we observed a significant down regulation of phospho-ERK at all the time-points compared to 6-OHDA treated alone when D-512 pre-treated PC12 cells were exposed to 6-OHDA. Transient versus sustained phosphorylation of ERK1/2 has been shown to be a determining step for cell signaling decisions (Marshall 1995, Xia, Dickens et al. 1995). Abnormal activation pattern of ERK1/2 has been shown to be responsible for 6-OHDA induced toxicity in various dopaminergic cell lines (Kulich, Horbinski et al. 2007, Lin, Cavanaugh et al. 2008, Kim, Kim et al. 2011). Sustained activation of ERK1/2 can cause the phospho-ERK1/2 to translocate into nucleus to modify other transcription factors and may be responsible for cell death in case of 6-OHDA exposure (Marshall 1995), whereas, in case of D-512 treatment, transient activation may not be sufficient for phospho-ERK1/2 to translocate to nucleus and cause transcriptional changes. JNK is a stress-activated protein kinase (SAPK), which has been shown to be activated in response to stress (serum withdrawal, growth factor withdrawal, hypoxia, 6-OHDA, H<sub>2</sub>O<sub>2</sub>) in various dopaminergic cell lines (Xia, Dickens et al. 1995, Kang, Jang et al. 1998, Hou, Huang et al. 2003, Fujita, Izawa et al. 2006, Zhang, Xue et al. 2012). 6-OHDA induces the generation of H<sub>2</sub>O<sub>2</sub>, hydroxyl radical, and other ROS which may induce stress signals and activation of JNK. 6-



OHDA has also been shown to cause mitochondrial activation of ERK1/2 (Kulich, Horbinski et al. 2007) and inhibition of complex-I and complex-IV in isolated mitochondria (Glinka and Youdim 1995), which may cause generation of more free radicals and result in increased stress to the cells. D-512 also exhibited an ability to prevent phospho-JNK increase induced by 6-OHDA, which further proves its ability to prevent development of stress signaling related pathways following 6-OHDA exposure. 6-OHDA induced toxicity has been shown to be significantly associated with the generation of H<sub>2</sub>O<sub>2</sub> by auto-oxidation of 6-OHDA in PC12 cells (Kostrzewa and Jacobowitz 1974, Saito, Nishio et al. 2007). Interestingly, Fujita et al. also observed very similar results using hydrogen peroxide as a toxin in PC12 cells with Pramipexole (Fujita, Izawa et al. 2006). Various studies have shown similar results using potent anti-oxidants (Kang, Jang et al. 1998, Hou, Huang et al. 2003, Saito, Nishio et al. 2007). Previously, we also observed similar effect of D-512 on signaling pathways using cell line devoid of dopamine receptors (Santra et al., 2013).

Although not fully elucidated, significant features observed in PD pathology were able to be recapitulated using 6-OHDA as a toxin for PC12 cells. From our current experimental data we conclude that D-512 prevents the cell death induced by 6-OHDA in our two different experimental paradigms as assessed by MTT assay. Detailed investigation into experiments relevant to oxidative stress proves that D-512 is able to restore glutathione levels altered by toxins acting by different mechanisms, prevents DNA fragmentation, inhibits significant changes in nuclear morphology, and decreases lipid peroxidation to some extent. Further investigation into molecular mechanism showed that D-512 prevents temporal changes in pERK1/2 and pJNK induced by 6-OHDA, which might be some of the molecular mechanisms by which D-512 is able to protect against ROS induced damage by 6-OHDA. As D-512 showed significant ability

to restore cellular viability, various biochemical functions, and signaling pathways, it warrants further study as a potential Parkinson's disease therapeutic with multifunctional activity.

## CHAPTER 5

### RESULTS

#### 5.1 Dopamine induces SDS-resistant, ThT-negative, and morphologically distinct oligomers of $\alpha$ -synuclein

Dopamine auto-oxidation has been shown to be involved in the formation of SDS-resistant, soluble  $\alpha$ -synuclein oligomers, which may be one of the culprits responsible for dopaminergic neuronal death in PD. We developed a cell-free system to generate co-valently modified aggregates of  $\alpha$ -synuclein by dopamine. Our shaking experiments, which included  $\alpha$ -synuclein (17.5  $\mu$ M) and dopamine (200  $\mu$ M) yielded  $\alpha$ -synuclein aggregates that were resistant to SDS, as determined by SDS-PAGE separation of various time-point samples from 0 day to 10 days. As shown in **figure 5-1**, dopamine induced formation of  $\alpha$ -synuclein oligomers in time-dependent manner and higher time-points resulted in SDS-resistant, high molecular weight oligomers.

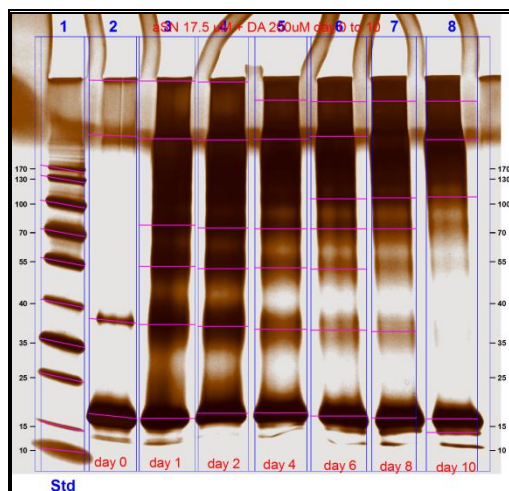


**Figure 5-1.** Silver staining of dopamine induced changes in  $\alpha$ -synuclein

We also determined the protein structure of aggregates formed at various time-points of experiment. Thioflavin-T (ThT) is a dye which selectively binds to protein structures that have  $\beta$ -sheet confirmation.  $\alpha$ -synuclein aggregates known as fibrils (strongly ThT positive,  $\beta$ -sheet structures) have been shown to be present in the brain of post-mortem PD patients. Our experimental samples showed very less increase in ThT fluorescence. As shown in **figure 5-2**, we observed ~4-fold increase in ThT signal in our experiment involving dopamine and  $\alpha$ -synuclein.

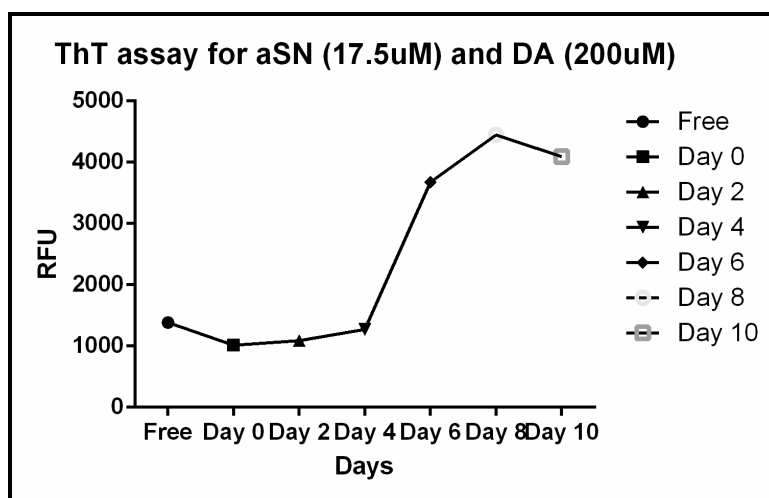


**Figure 5-2.** ThT assay for  $\alpha$ -synuclein and dopamine experiment

We also analyzed physical characteristics of the oligomers formed by shaking  $\alpha$ -synuclein and dopamine for 4 days. We developed a transmission electron microscopy protocol to determine morphology of aggregates formed after various experiments. As shown in **figure 5-3**, we observed heterogenous protofibrillar structures in case of  $\alpha$ -synuclein and dopamine experiment, whereas, we found  $\alpha$ -synuclein monomer sample to be of homogenous spherical structures.

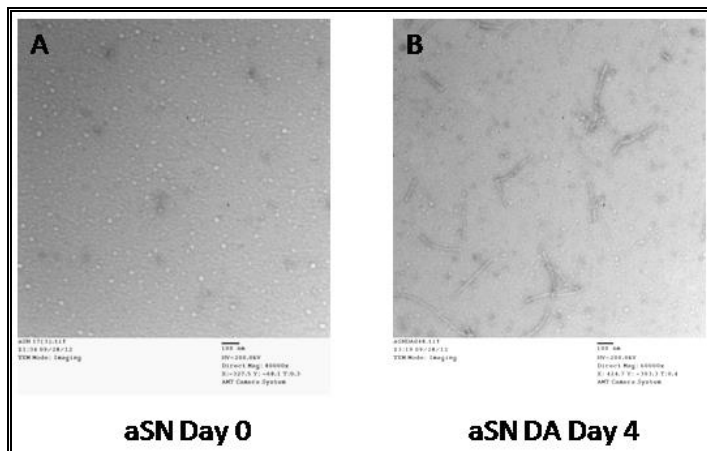


**Figure 5-3.** TEM images of  $\alpha$ -synuclein and  $\alpha$ -synuclein with dopamine experiments

5.2  $\alpha$ -synuclein at higher concentration (50 $\mu$ M) generates SDS-resistant, ThT positive, and morphologically “fiber shaped” fibrils of the protein

$\alpha$ -synuclein locus duplication and triplication have been shown to be related to genetic forms of PD. Therefore,  $\alpha$ -synuclein concentration may play an important role in its aggregation process. We have developed a cell-free system to assess the characteristics of  $\alpha$ -synuclein aggregates by shaking  $\alpha$ -synuclein at higher concentration (50  $\mu$ M). Our shaking experiments yielded  $\alpha$ -synuclein aggregates, which were resistant to SDS as determined by fractionation using SDS-PAGE. We observed a time-dependent decrease in  $\alpha$ -synuclein monomer and corresponding increase in higher molecular weight aggregates of  $\alpha$ -synuclein (**figure 5-4**). Surprisingly, after 10 days of shaking we observed disappearance of higher molecular weight structure and significant decrease in monomer (**figure 5-4**). This may be due to formation of insoluble fibrils of  $\alpha$ -synuclein, which do not enter the polyacrylamide gel.

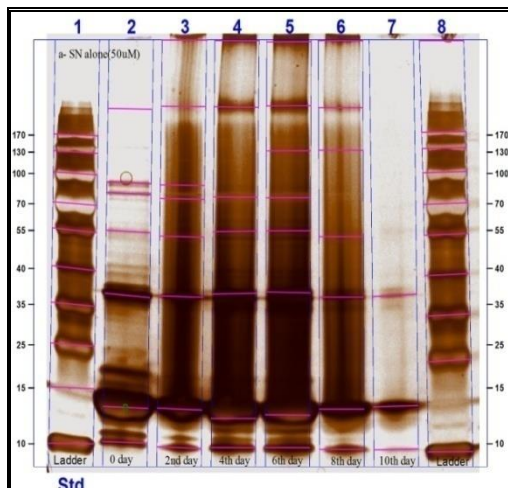


**Figure 5-4.** Silver staining of  $\alpha$ -synuclein shaken at higher concentration

We analyzed samples collected at various time-points for determination of  $\beta$ -sheet positive fibrillar structure of  $\alpha$ -synuclein using ThT assay. ThT assay showed a significant increase in fluorescence in time-dependent manner. As shown in **figure 5-5**, at day 10, we observed ~110-fold increase in ThT signal compared to day 0.

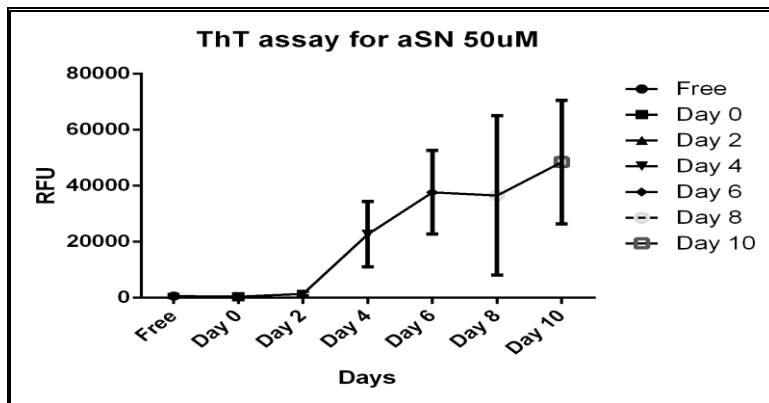


**Figure 5-5.** ThT assay of  $\alpha$ -synuclein (50 $\mu$ M) experiment

We also analyzed morphology of aggregates formed by  $\alpha$ -synuclein after 10 days of shaking. We utilized transmission electron microscopy to observe the physical structure of

aggregates formed after shaking  $\alpha$ -synuclein at higher concentration (50  $\mu$ M). As shown in **figure 5-6 (C)**, we found the aggregates of fibrillar morphology and significantly different than aggregates formed by dopamine and  $\alpha$ -synuclein experiment (**figure 5-6 (B)**).

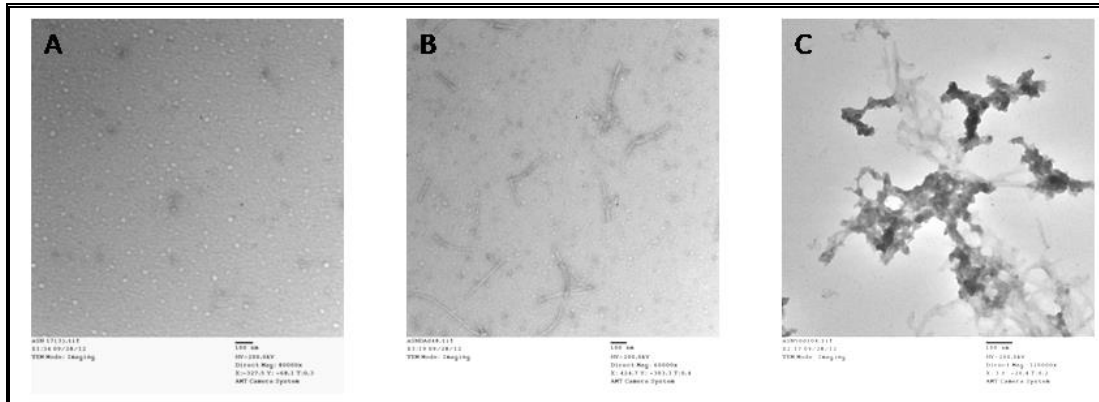


**Figure 5-6. TEM images of various  $\alpha$ -synuclein experiments**

**(A)  $\alpha$ -synuclein monomer; (B)  $\alpha$ -synuclein (17.5  $\mu$ M and dopamine 200  $\mu$ M 10 days sample); (C).  $\alpha$ -synuclein (50  $\mu$ M) 10 day sample.**

### 5.3 Iron(III) induces SDS-sensitive and ThT positive fibrils of $\alpha$ -synuclein

Iron(III) concentration has been shown to be significantly increased in the substantia nigra of patients with PD. Iron is also present in the Lewy bodies found in PD brain. We developed a cell-free system to determine ability of iron to modify  $\alpha$ -synuclein and induce its aggregation. We performed shaking experiment with equimolar concentrations (17.5  $\mu$ M) of  $\alpha$ -synuclein and iron(III) for 6 days. We observed formation of SDS-sensitive  $\alpha$ -synuclein aggregates as determined by fractionation of samples using SDS-PAGE (**figure 5-7**). Iron(III) has been shown to generate non-covalent aggregates of  $\alpha$ -synuclein, which are sensitive to detergent and fall apart into smaller forms of aggregates or monomers. We also determined the structure of aggregates formed by ThT assay. We observed an increase in ThT fluorescence in

time-dependent manner (**figure 5-8**). 6 days of shaking resulted in ~20 fold increase in ThT signal compared to 0 day sample.

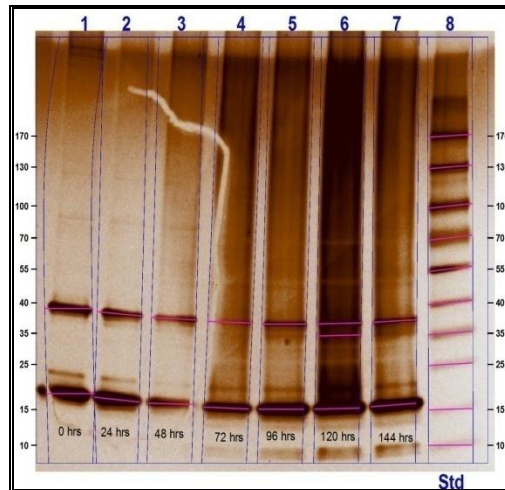


**Figure 5-7.** Silver staining of  $\alpha$ -synuclein and iron experiment

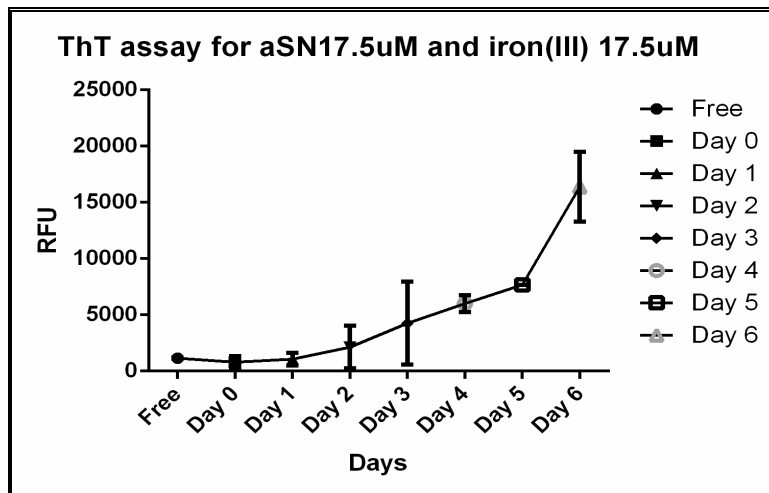


**Figure 5-8.** ThT assay of  $\alpha$ -synuclein and iron experiment

5.4 D-520 has an ability to modify  $\alpha$ -synuclein aggregation in presence of dopamine relative to ascorbic acid, rifampicin, and D-436

Various studies have shown that polyphenolic compounds have an ability to prevent/modify aggregation of  $\alpha$ -synuclein. Some studies have implicated oxidation of dopamine leads to



generation of dopamine quinones and neuromelanin, which have strong tendency to co-valently modify  $\alpha$ -synuclein and bind to iron(III) respectively. Rifampicin was shown to decrease the incidence of Lewy body related diseases in an epidemiological study.

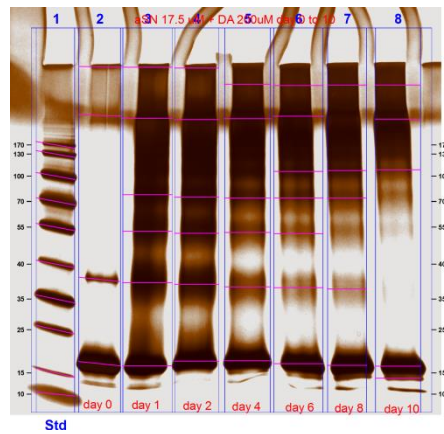


Figure 5-9 (a)

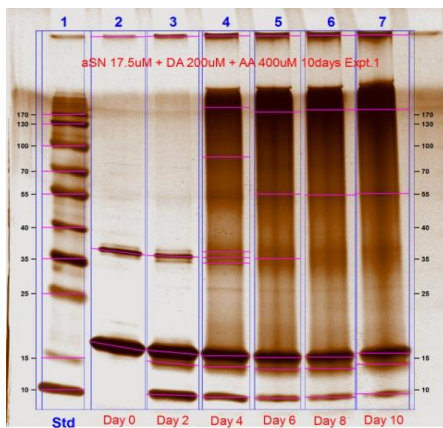


Figure 5-9 (b)

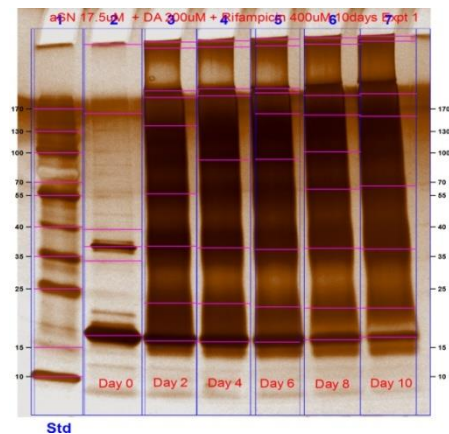


Figure 5-9 (c)

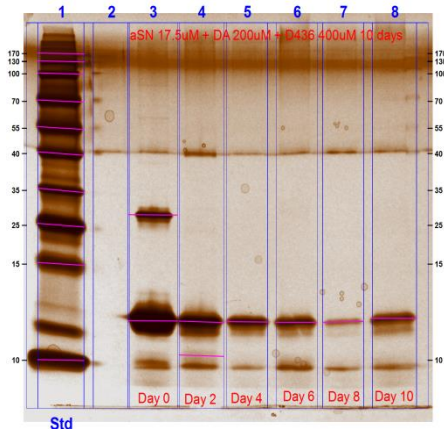


Figure 5-9 (d)

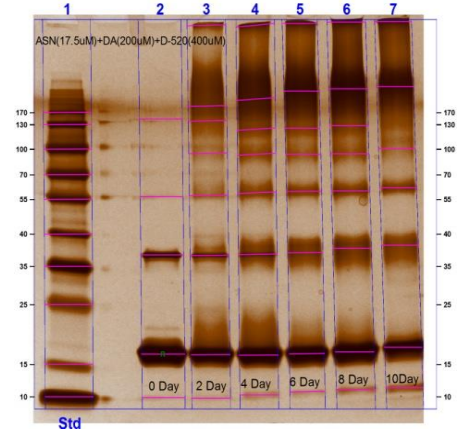


Figure 5-9 (e)

**Figure 5-9. Silver staining images of effect of various compounds on dopamine induced  $\alpha$ -synuclein aggregation**

**5-9 (a)  $\alpha$ -synuclein (17.5  $\mu$ M) and dopamine (200  $\mu$ M); 5-9 (b)  $\alpha$ -synuclein(17.5  $\mu$ M), dopamine (200  $\mu$ M) and ascorbic acid (400  $\mu$ M); 5-9 (c)  $\alpha$ -synuclein (17.5  $\mu$ M), dopamine (200  $\mu$ M) and rifampicin (400  $\mu$ M); 5-9 (d)  $\alpha$ -synuclein (17.5  $\mu$ M), dopamine (200  $\mu$ M), and D-436 (400  $\mu$ M); 5-9 (e)  $\alpha$ -synuclein (17.5  $\mu$ M), dopamine (200  $\mu$ M), and D-520 (400 $\mu$ M).**

Therefore, we developed a cell-free system including  $\alpha$ -synuclein and dopamine with the compounds of interest to compare our lead compounds' ability to prevent/modify the aggregation of  $\alpha$ -synuclein. We used rifampicin as a polyphenolic drug and ascorbic acid as an anti-oxidant of dopamine to evaluate the potential mechanism(s) of action of our lead compounds. We conducted five different shaking experiments using cell-free system. Our experiments included,

- i.  $\alpha$ -synuclein (17.5  $\mu$ M) and dopamine (200  $\mu$ M)
- ii.  $\alpha$ -synuclein (17.5  $\mu$ M), dopamine (200  $\mu$ M), and ascorbic acid (400  $\mu$ M) [anti-oxidant]
- iii.  $\alpha$ -synuclein (17.5  $\mu$ M), dopamine (200  $\mu$ M), and rifampicin (400  $\mu$ M) [polyphenolic standard drug]
- iv.  $\alpha$ -synuclein (17.5  $\mu$ M), dopamine (200  $\mu$ M), and D-436 (400  $\mu$ M) [lead compound]

v.  $\alpha$ -synuclein (17.5  $\mu$ M), dopamine (200  $\mu$ M), and D-520 (400  $\mu$ M) [lead compound]

We evaluated samples from different time points and different experiments using silver-staining, TEM, and size-exclusion chromatography (SEC). As shown in **figure 5-9 (a)**, we observed time-dependent increase in formation of dopamine-induced co-valently modified oligomers of  $\alpha$ -synuclein. Surprisingly, we found ascorbic acid to be preventing the generation of higher molecular weight oligomers of  $\alpha$ -synuclein and dopamine (**figure 5-9 (b)**). We found rifampicin to be partially effective in preventing generation of high molecular weight oligomers induced by co-valent modification of  $\alpha$ -synuclein by dopamine (**figure 5-9 (c)**). However, when compared to ascorbic acid, rifampicin wasn't very effective in preventing  $\alpha$ -synuclein aggregation, as it generated dimers, trimers and corresponding high molecular weight structures of  $\alpha$ -synuclein while decreasing the amount of monomer in time-dependent manner. Interestingly, we found D-436 to be very distinct in modifying  $\alpha$ -synuclein aggregation. D-436 caused a decrease in  $\alpha$ -synuclein monomer in time-dependent manner (**figure 5-9 (d)**). However, we didn't observe any higher molecular weight structures formed by D-436. This may be due to the generation of insoluble protein aggregates, which weren't able to be fractionated by gel electrophoresis. Surprisingly, D-520 showed an ability to prevent dopamine induced  $\alpha$ -synuclein aggregation partially (**figure 5-9 (e)**). We observed generation of well-structured aggregates in presence of D-520. This suggests that, D-520 may be able to stabilize  $\alpha$ -synuclein aggregates such that it may prevent seeding phenomenon, by which dimers, trimers and corresponding structures combine to form higher molecular weight fibrillar or oligomeric structures.

We further evaluated the experimental samples by transmission electron microscopy to determine physical difference between samples from various experiments. We used samples from 4<sup>th</sup> day of experiment to evaluate physical characteristics of aggregates. As shown in **figure**

**5-10 (A)**,  $\alpha$ -synuclein monomers appeared as a small spherical homogeneous structures, whereas, dopamine incubated  $\alpha$ -synuclein appeared as a protofibrillar heterogeneous structure (**figure 5-10 (B)**). Experiment involving ascorbic acid prevented generation of protofibrillar structure (**figure 5-10 (C)**), but it generated homogenous spherical structures, which were of increased radius compared to monomers (**figure 5-10 (A) vs. figure 5-10 (C)**). Rifampicin also prevented the generation of protofibrillar structure (**figure 5-10 (D)**), but it formed somewhat distinct shaped aggregates of  $\alpha$ -synuclein, which were morphologically different compared to  $\alpha$ -synuclein monomer. Our results of TEM corroborated with silver-staining results for D-436, as we found D-436 to be forming  $\alpha$ -synuclein aggregates of significantly higher dimensions in presence of dopamine (**figure 5-10 (E)**). Interestingly, D-520 prevented the generation of protofibrils and gave rise to heterogeneous aggregates of  $\alpha$ -synuclein ranging from apparent monomers to aggregates of higher dimensions but smaller than protofibrils (**figure 5-10 (F)**).

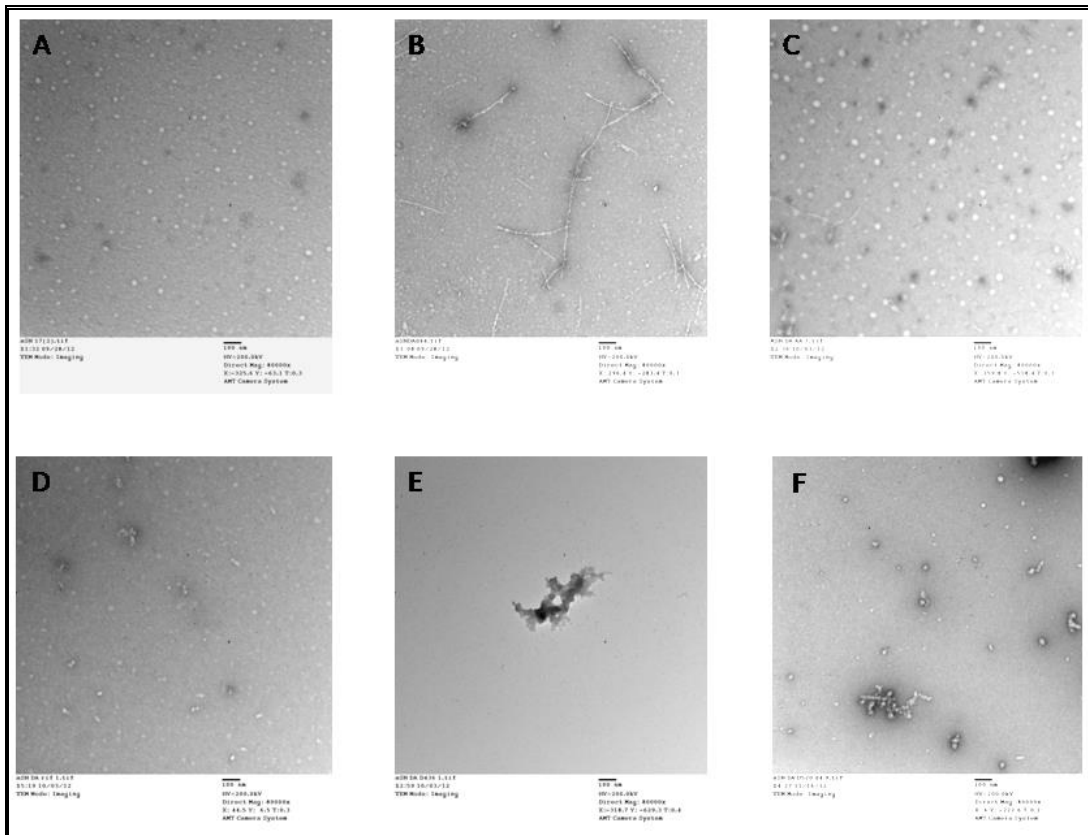


**Figure 5-10.** TEM images of various experiments conducted to evaluate effect of various compounds on dopamine induced aggregation of  $\alpha$ -synuclein

**5-10 (a)**  $\alpha$ -synuclein day 0; **5-10 (b)**  $\alpha$ -synuclein, dopamine and ascorbic acid day 4; **5-10 (c)**  $\alpha$ -synuclein, dopamine, and ascorbic acid day 4; **5-10 (d)**  $\alpha$ -synuclein, dopamine, and rifampicin day 4; **5-10 (e)**  $\alpha$ -synuclein, dopamine, and D-436 day 4; **5-10 (f)**  $\alpha$ -synuclein, dopamine, and D-520 day 4.

In our lab, we also have developed a size-exclusion chromatography (SEC) method to determine the hydrodynamic radius of aggregates formed at various time-points of our experiments. SEC is also alternatively called gel filtration chromatography when used to separate macromolecules of different size. SEC separates macromolecules on the basis of the volume that they see while passing through the analytical column. As small molecules can pass through small pores as well as larger pores of the gel filtration column, they elute at a later time when compared to molecules of relatively bigger size.

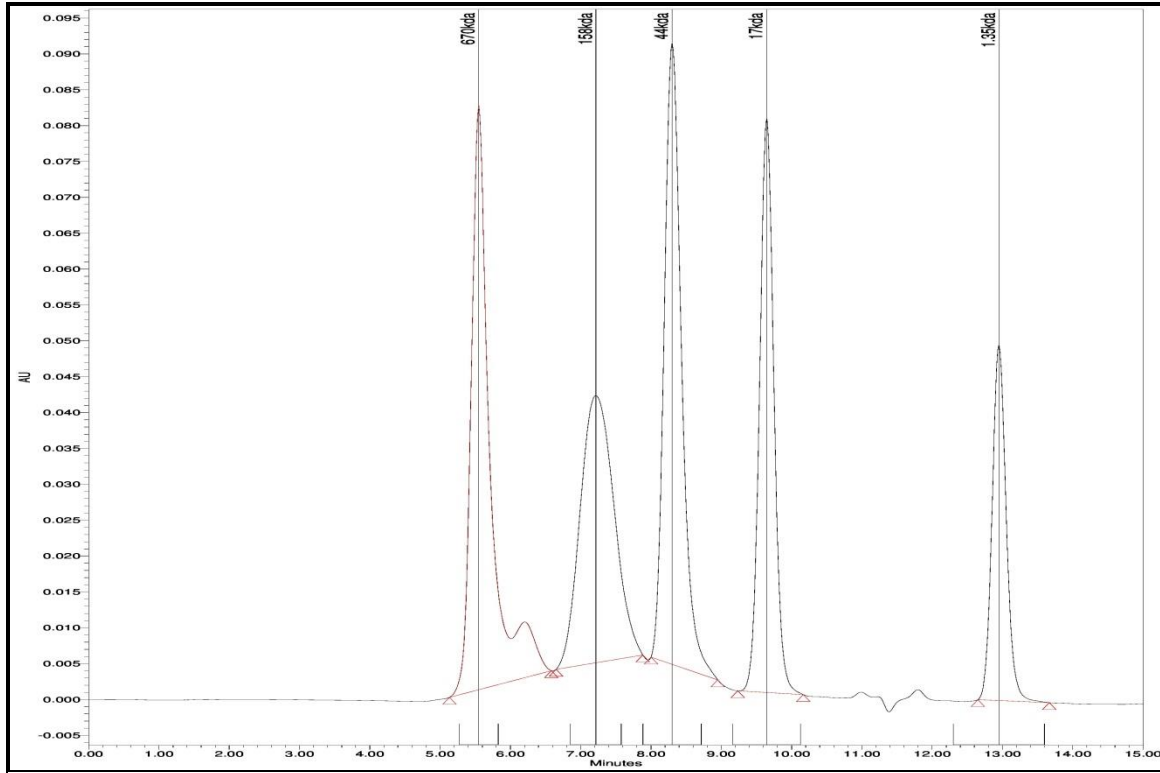


**Figure 5-11.** SEC profile of biorad globular protein standards

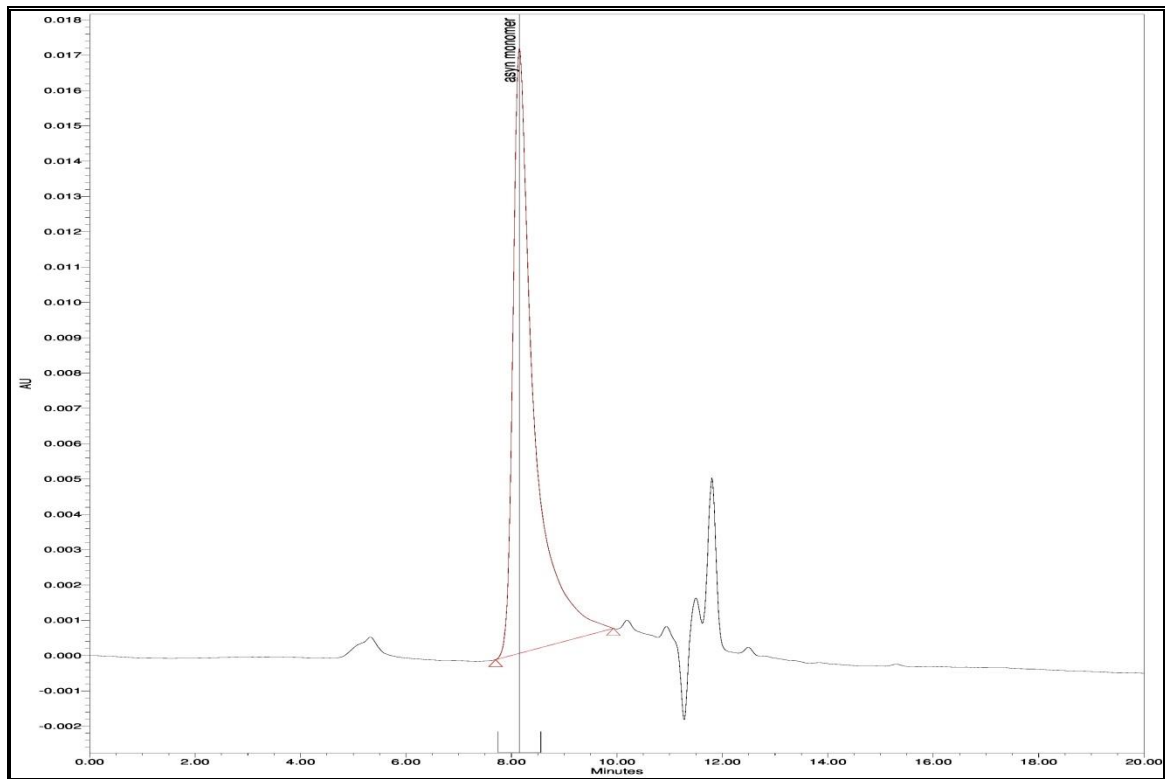


**Figure 5-12.** SEC profile of industrial grade  $\alpha$ -synuclein monomer

As shown in **figure 5-11**, we initially ran bio-rad globular protein standard to determine the elution pattern of protein mixture of known molecular weight. Afterwards, we ran fresh  $\alpha$ -synuclein sample, which eluted at ~8 minutes (**figure 5-12**). Accordingly, we could determine that the apparent molecular weight of  $\alpha$ -synuclein is around ~44kda, which has been reported previously. Afterwards, we ran samples from various experiments and various time-points to determine the fraction of monomer left and the fraction of higher molecular weight (oligomer or probably fibril) aggregates formed. As shown in **figure 5-13**, we observed almost complete conversion of monomer into oligomeric form after 10 days of shaking in case of  $\alpha$ -synuclein and dopamine experiment, whereas, in case of experiment involving ascorbic acid and dopamine (**figure 5-14**), we found that large amount of monomer was spared even after 10 days of experiment. However, in the experiment involving rifampicin and dopamine (**figure 5-15**), we found that the monomer was completely depleted after 10 days of shaking and corresponding increase in oligomeric species was apparent. In case of D-436 and dopamine experiment, we observed a significant decrease in monomeric fraction and corresponding increase in oligomeric fraction (**figure 5-16**), whereas, in case of D-520 and dopamine experiment, we observed that significant fraction of monomer was spared even after shaking for 10 days (**figure 5-17**). **Figure 5-18** represents analysis of all experimental samples from different time-points. As shown in **figure 5-18**, in experiments involving dopamine and dopamine and rifampicin, monomer was significantly depleted (~88% and ~86%) after 2 days of shaking. However, experiment involving ascorbic acid and dopamine showed significant fraction of monomer form (~24%) even after 10 days of experiment. Interestingly, in experiment involving D-520 and dopamine we observed that after 10 days of shaking significant amount of protein was still retained in its monomeric form (~40%), whereas, in case of D-436 and dopamine experiment fraction of monomer retained

wasn't significantly different after 10 days of shaking (~8%). Thus, from our experiments using size-exclusion chromatography, we concluded that D-520 has a potential to retain  $\alpha$ -synuclein in its monomeric form even after long period of incubation with dopamine, which is very similar to results obtained with ascorbic acid and dopamine experiment. Therefore, D-520 might be potentially preventing the oxidation of dopamine, which can generate quinones to cause covalent modification of  $\alpha$ -synuclein resulting in its oligomeric forms.

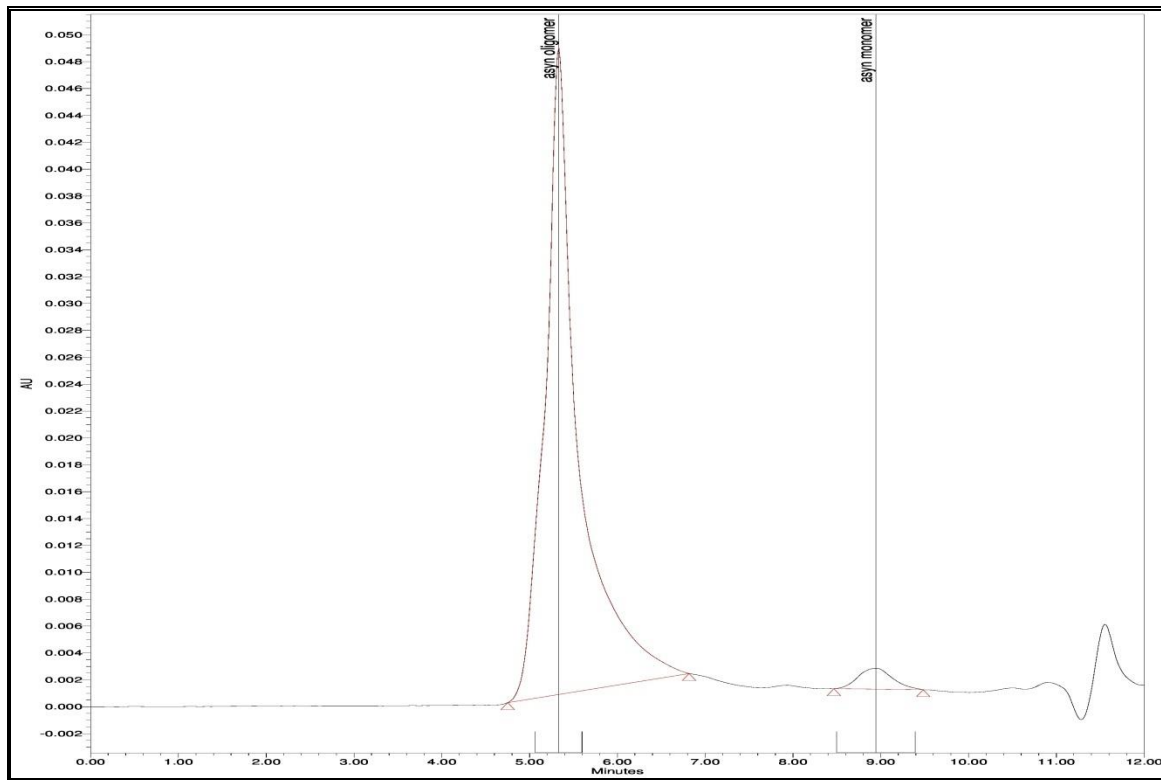


**Figure 5-13.** SEC profile of  $\alpha$ -synuclein after 10 days shaking with dopamine



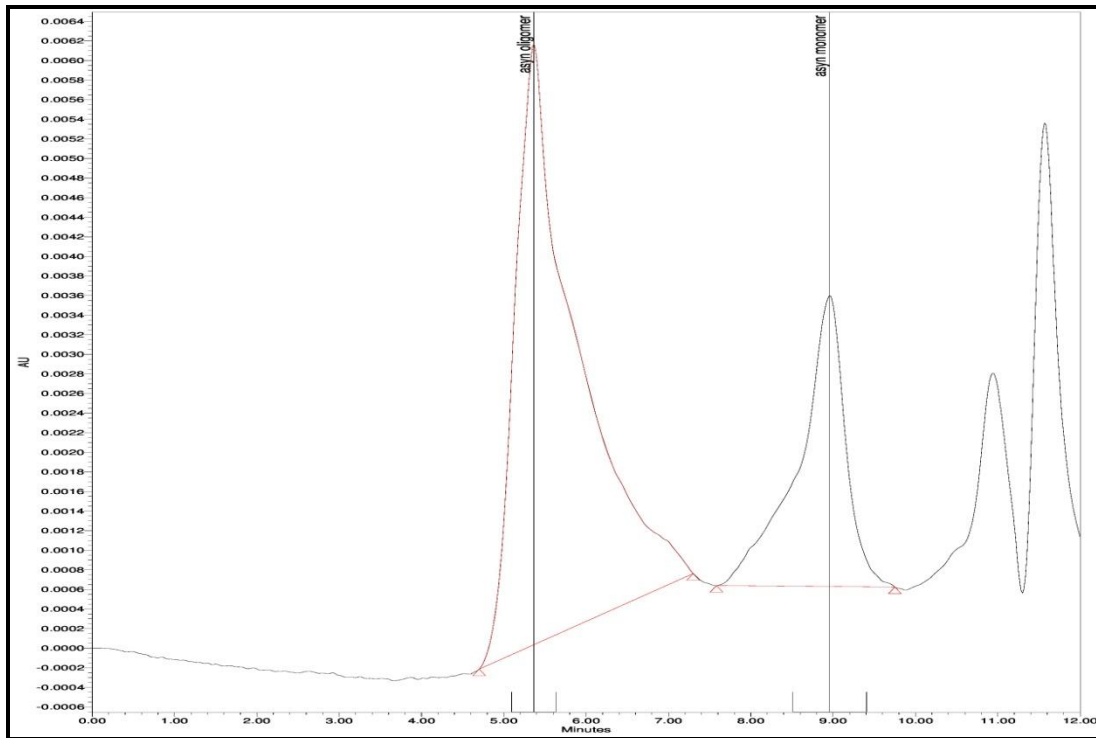


**Figure 5-14.** SEC profile of  $\alpha$ -synuclein after 10 days shaking with dopamine and ascorbic acid

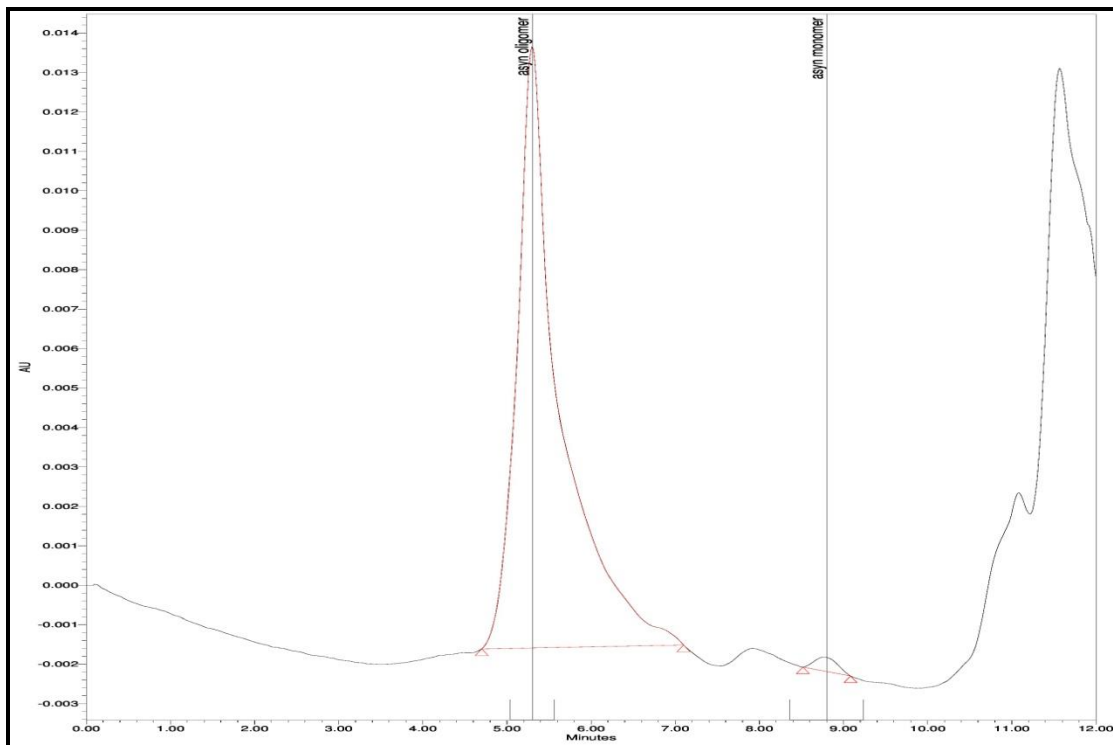


**Figure 5-15.** SEC profile of  $\alpha$ -synuclein after 10 days shaking with dopamine and rifampicin

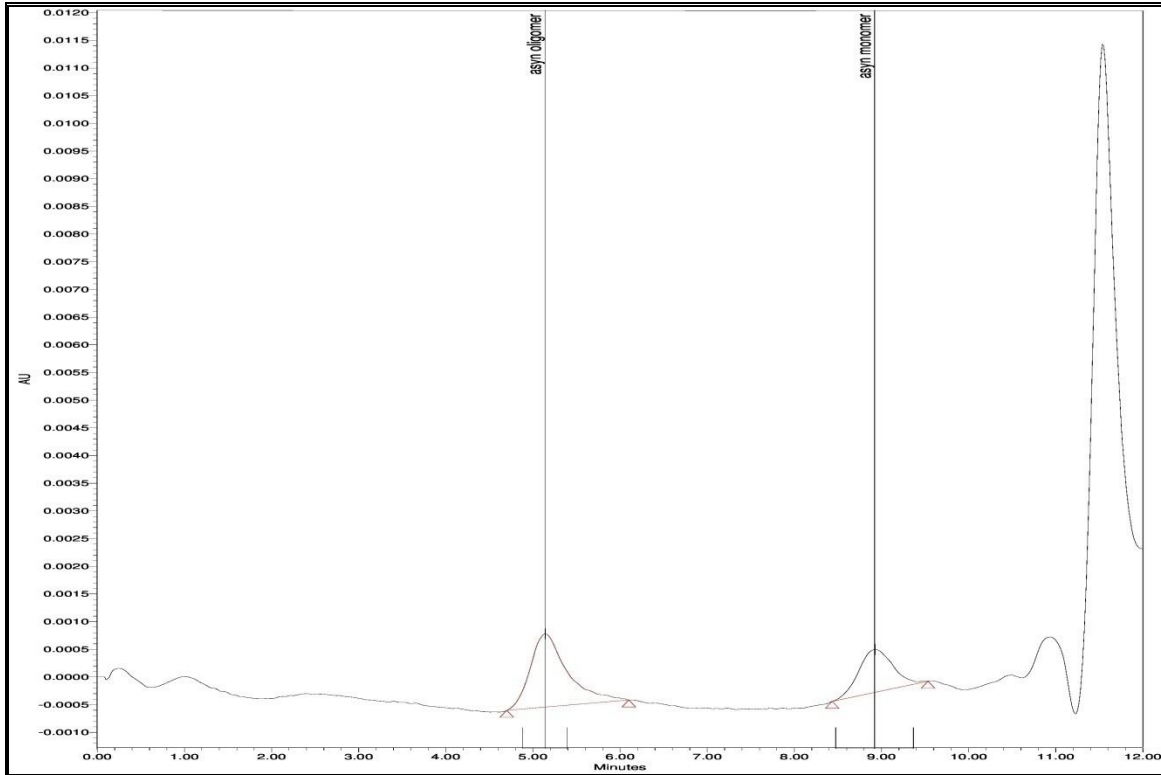


**Figure 5-16.** SEC profile of  $\alpha$ -synuclein after 10 days shaking with dopamine and D-436

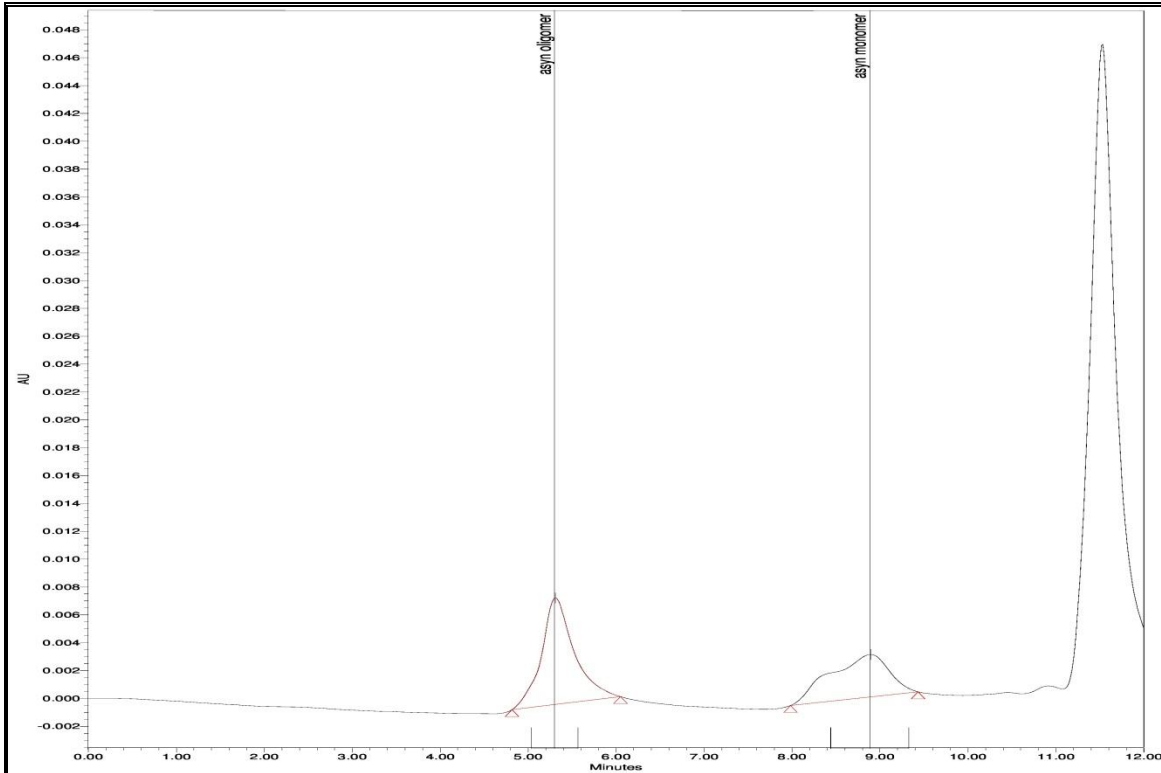


**Figure 5-17.** SEC profile of  $\alpha$ -synuclein after 10 days shaking with dopamine and D-520

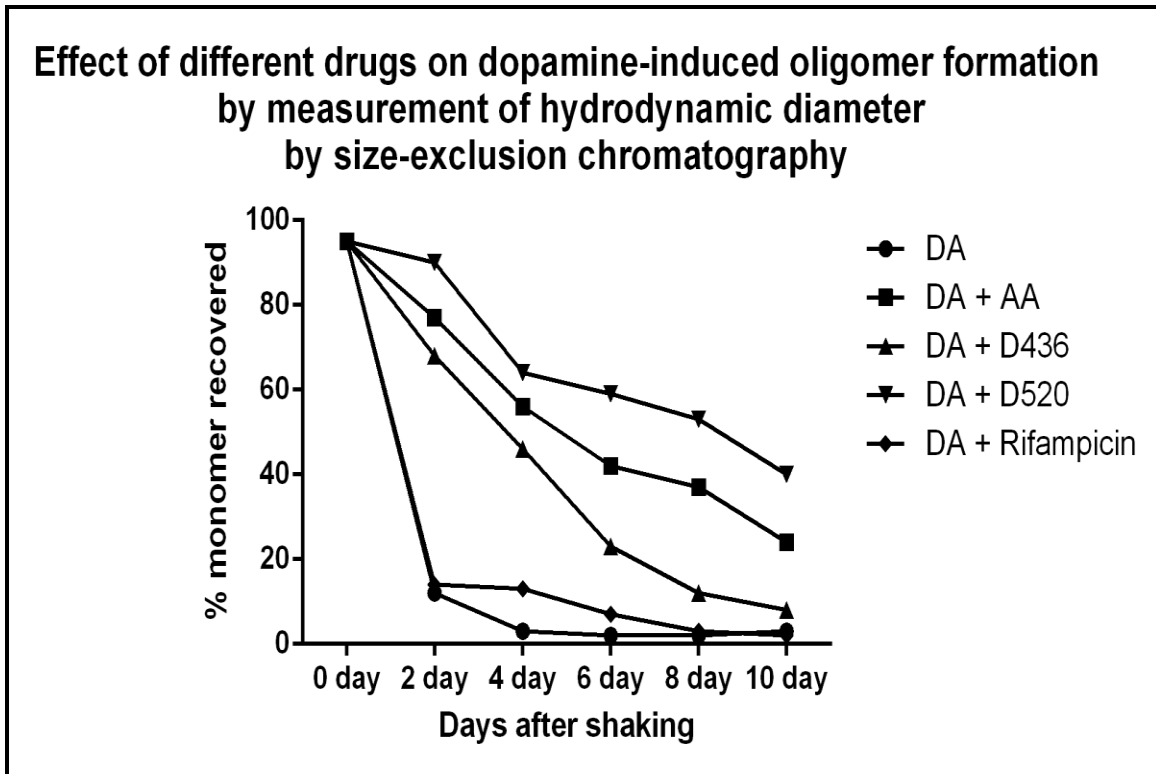


**Figure 5-18. SEC profiles of various experiments**

5.5 Extracellular fibrils of  $\alpha$ -synuclein (60  $\mu$ M) are more toxic to PC12 cells compared to extracellular oligomers of  $\alpha$ -synuclein (60  $\mu$ M) and dopamine (90  $\mu$ M)

We wanted to determine the cellular toxicity profile of  $\alpha$ -synuclein aggregates by incubating them extracellularly with PC12 cells. We generated aggregates of  $\alpha$ -synuclein by two different methods,

- i. Shaking  $\alpha$ -synuclein (60  $\mu$ M) for 10 days and collecting an aliquot at 2 days interval,
- ii. Shaking  $\alpha$ -synuclein (60  $\mu$ M) and dopamine (90  $\mu$ M) for 10 days and collecting an aliquot every 2 days.

Afterwards, we carried out cellular viability assay (MTT assay) by incubating aliquots obtained from various time-points at a final concentration of 10  $\mu$ M  $\alpha$ -synuclein with PC12 cells. As

shown in **figure 5-19**, we observed that in both cases, extracellular  $\alpha$ -synuclein incubation resulted in cell-death of PC12 cells. In case of  $\alpha$ -synuclein alone (60  $\mu$ M), we observed statistically significant decrease in cell viability from day 2 to day 10 samples ( $P < 0.0001$ ). It was interesting to see that  $\alpha$ -synuclein (60  $\mu$ M) samples shaken for 8 days and 10 days were less toxic to PC12 cells when compared to sample shaken for 6 days. We also observed statistically significant decrease in cell viability in the experiment involving  $\alpha$ -synuclein (60  $\mu$ M) and dopamine (90  $\mu$ M) from samples shaken for 2 days to 10 days (**figure 5-19**). We observed maximum cell death in PC12 cells incubated with  $\alpha$ -synuclein (60  $\mu$ M) shaken for 6 days (~35%).

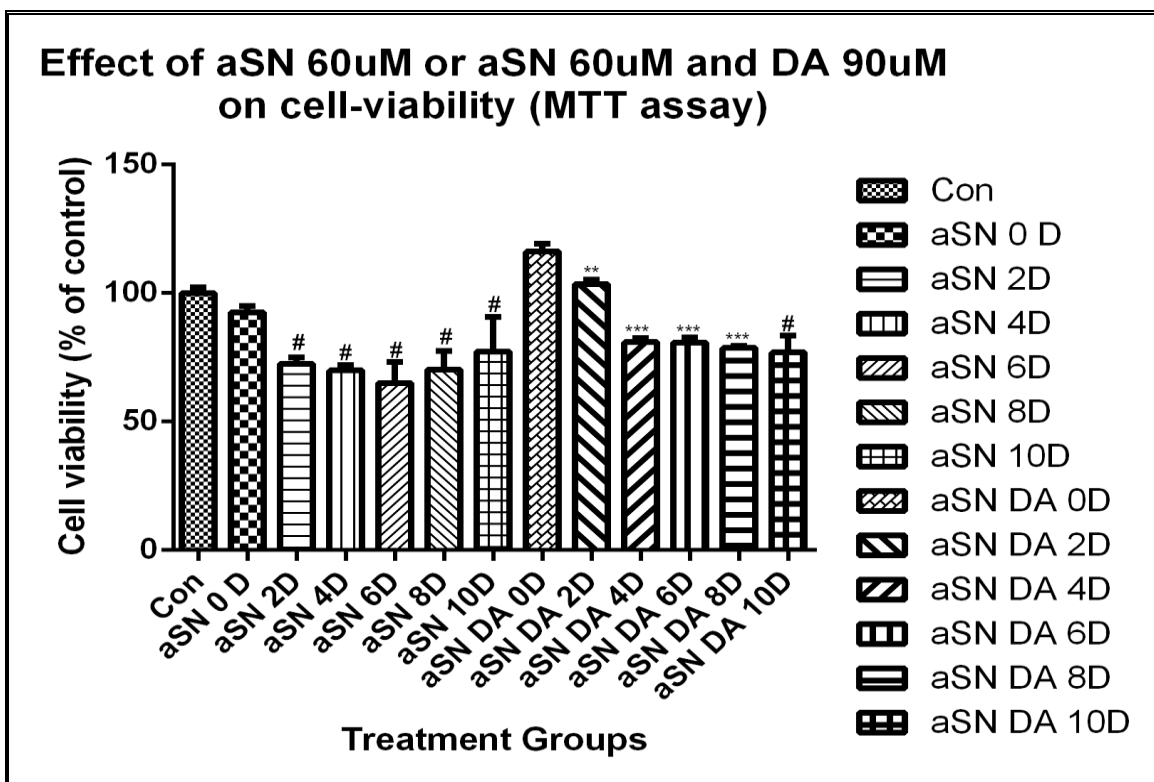


**Figure 5-19.** MTT assay to evaluate effect of extracellular  $\alpha$ -synuclein on PC12 cell viability

We also assessed the presence of  $\beta$ -sheet structure in our experimental samples by ThT assay. As shown in **figure 5-20**, we observed significant increase in ThT signal in case of  $\alpha$ -synuclein (60  $\mu$ M), whereas, dopamine (90  $\mu$ M) and  $\alpha$ -synuclein (60  $\mu$ M) experiment samples didn't show ThT signal. Interestingly, we observed  $\sim$ 350-fold in ThT signal in sample of  $\alpha$ -synuclein (60  $\mu$ M) after 4 days shaking. Surprisingly, the signal diminished at higher time-points.

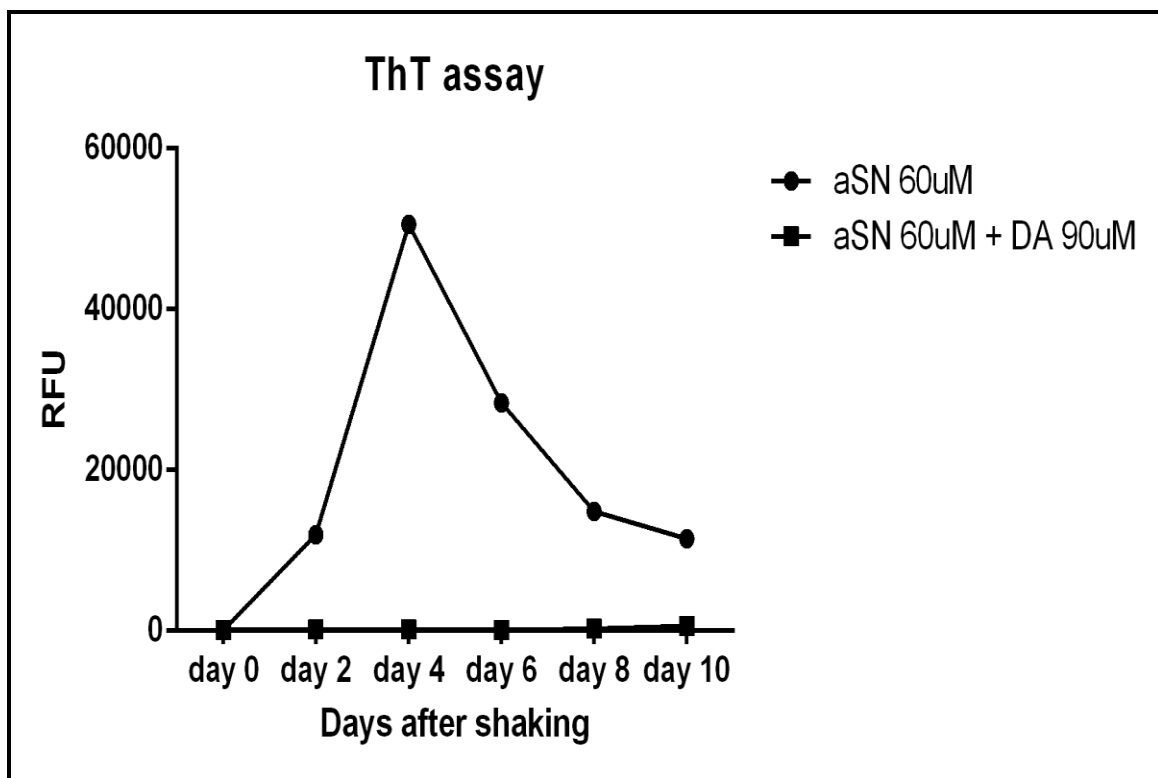


**Figure 5-20.** ThT assay results of  $\alpha$ -synuclein (60  $\mu$ M) and  $\alpha$ -synuclein (60  $\mu$ M) and dopamine (90  $\mu$ M) experiments

We also evaluated the physical appearance of aggregates formed after the experiment. We utilized samples shaken for 6 days for TEM imaging. As shown in **figure 5-21**, we observed

that  $\alpha$ -synuclein (60  $\mu$ M) shaken for 6 days formed aggregates with compact and branched morphology [ThT-positive] (**figure 5-21 (B)**), whereas, dopamine (90  $\mu$ M) and  $\alpha$ -synuclein (60  $\mu$ M) shaken for 6 days formed elongated protofibrillar structures [ThT-negative] (**figure 5-21 (C)**). **Figure 5-21 (A)** depicts  $\alpha$ -synuclein in its monomer form.

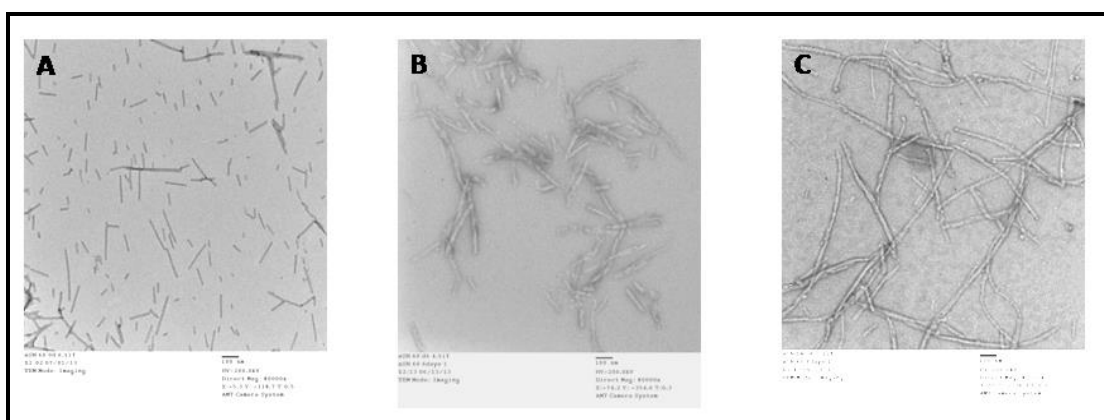


**Figure 5-21.** TEM images of various  $\alpha$ -synuclein experiments

**5-21 (A)**  $\alpha$ -synuclein (60  $\mu$ M) monomer day 0; **5-21 (B)**  $\alpha$ -synuclein (60  $\mu$ M) and dopamine (90  $\mu$ M) day 6; **5-21 (C)**  $\alpha$ -synuclein (60 $\mu$ M) alone day 6.

5.6 D-240 and D-520 possess an ability to protect against cell-death induced by extracellular  $\alpha$ -synuclein in PC12 cells, whereas, D-436 doesn't protect against the toxicity of extracellular  $\alpha$ -synuclein

As per our experiments in **5.5**, we determined to assess the ability of our lead compounds to protect against extracellular  $\alpha$ -synuclein toxicity by shaking them with 60  $\mu$ M  $\alpha$ -synuclein for 6 days. We carried out 5 different experiments,

- i.  $\alpha$ -synuclein (60  $\mu$ M) alone shaken for 6 days (positive control experiment);
- ii.  $\alpha$ -synuclein (60  $\mu$ M) and rifampicin (120  $\mu$ M) shaken for 6 days (standard drug);

- iii.  $\alpha$ -synuclein (60  $\mu$ M) and D-240 (120  $\mu$ M) shaken for 6 days (lead compound);
- iv.  $\alpha$ -synuclein (60  $\mu$ M) and D-436 (120  $\mu$ M) shaken for 6 days (lead compound);
- v.  $\alpha$ -synuclein (60  $\mu$ M) and D-520 (120  $\mu$ M) shaken for 6 days (lead compound).

Samples obtained from these experiments were used to assess the cellular viability by MTT assay. Samples were incubated at a final concentration of 10  $\mu$ M with PC12 cells for 24 hours. As shown in **figure 5-22**,  $\alpha$ -synuclein (60  $\mu$ M) after 6 days of shaking caused ~45% decrease in cell viability, whereas,  $\alpha$ -synuclein (60  $\mu$ M) at 0 days didn't alter cellular viability. Surprisingly, rifampicin wasn't able to rescue PC12 cells from  $\alpha$ -synuclein (60  $\mu$ M) induced cell-death in case of 6 days experiment. Interestingly, D-240 and D-520 completely prevented cell-death induced by  $\alpha$ -synuclein (60  $\mu$ M) after shaking for 6 days ( $P < 0.0001$ ). We didn't observe any protection in case of D-436. It was interesting to observe that D-520 caused ~35% decrease in cell viability when incubated with  $\alpha$ -synuclein at 0 day time-point.

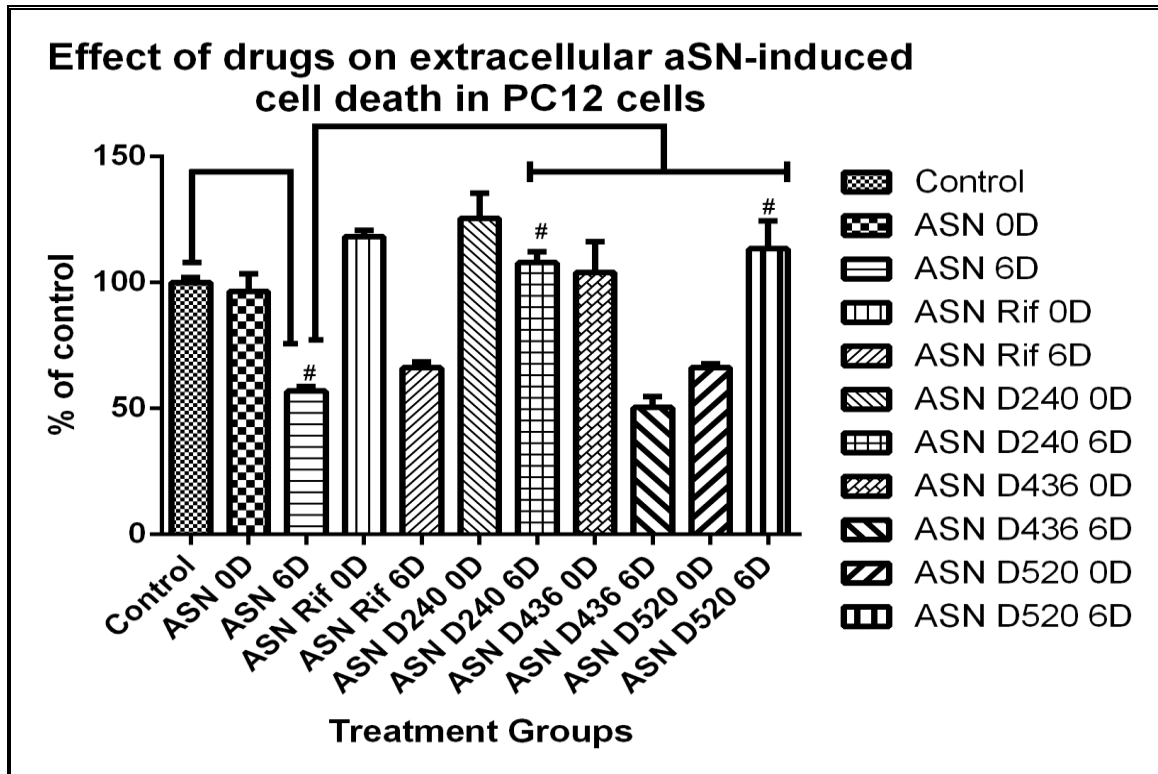


**Figure 5-22. MTT assay to evaluate the effect of various compounds on cell death induced by extracellular  $\alpha$ -synuclein**

We also determined the structure of aggregates formed in various experiments by ThT assay. As shown in **figure 5-23**, we observed a significant increase in ThT signal in case of  $\alpha$ -synuclein shaken for 6 days. D-240 and D-520 incubation prevented the formation of ThT positive  $\beta$ -sheet structure of  $\alpha$ -synuclein aggregates. Surprisingly, D-436 seemed to enhance generation of  $\beta$ -sheet structure of  $\alpha$ -synuclein, as incubation of  $\alpha$ -synuclein with D-436 showed stronger ThT signal than  $\alpha$ -synuclein (60  $\mu$ M) alone (statistically non-significant) (**figure 5-23**).



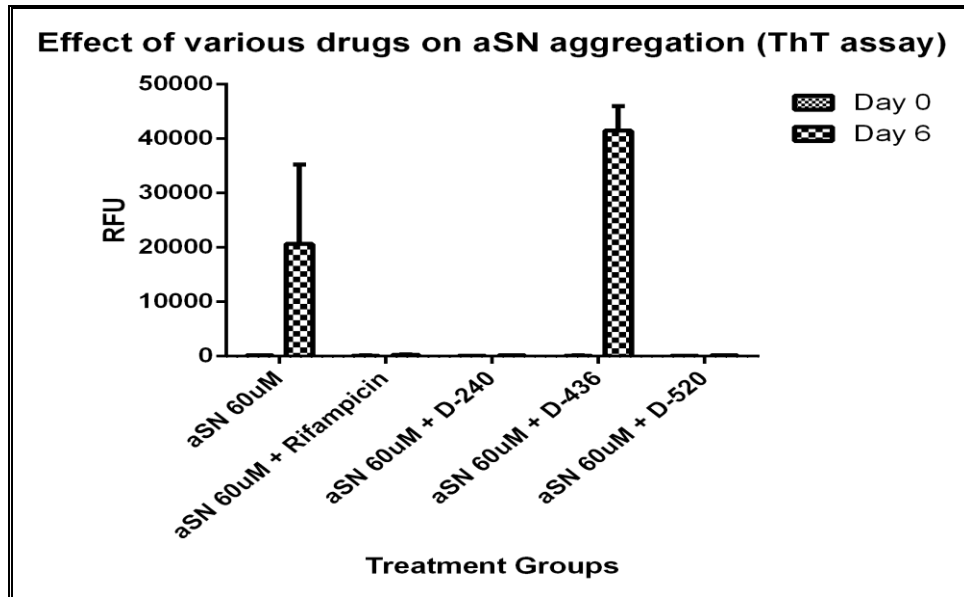


**Figure 5-23.** ThT assay of various experiments

We also evaluated the physical characteristics of  $\alpha$ -synuclein aggregates formed in various experiments that we carried out. As shown in **figure 5-24 (B)**,  $\alpha$ -synuclein (60  $\mu$ M) which was shaken for 6 days generated compact and branched fibrillar structures. Rifampicin prevented the formation of fibrillar structure partially but it formed distinct branched aggregates of  $\alpha$ -synuclein (**figure 5-24 (C)**). D-240 and D-520 almost completely prevented the protofibril formation induced by  $\alpha$ -synuclein and formed heterogenous population of aggregates (**figure 5-24 (D)**, **5-25 (F)**). As expected, D-436 showed formation of aggregates with strikingly different morphology, which consisted of huge amount of monomers and higher molecular weight structures combined together (**figure 5-24(E)**). This may explain a strong ThT signal generated by samples from D-436 experiment.

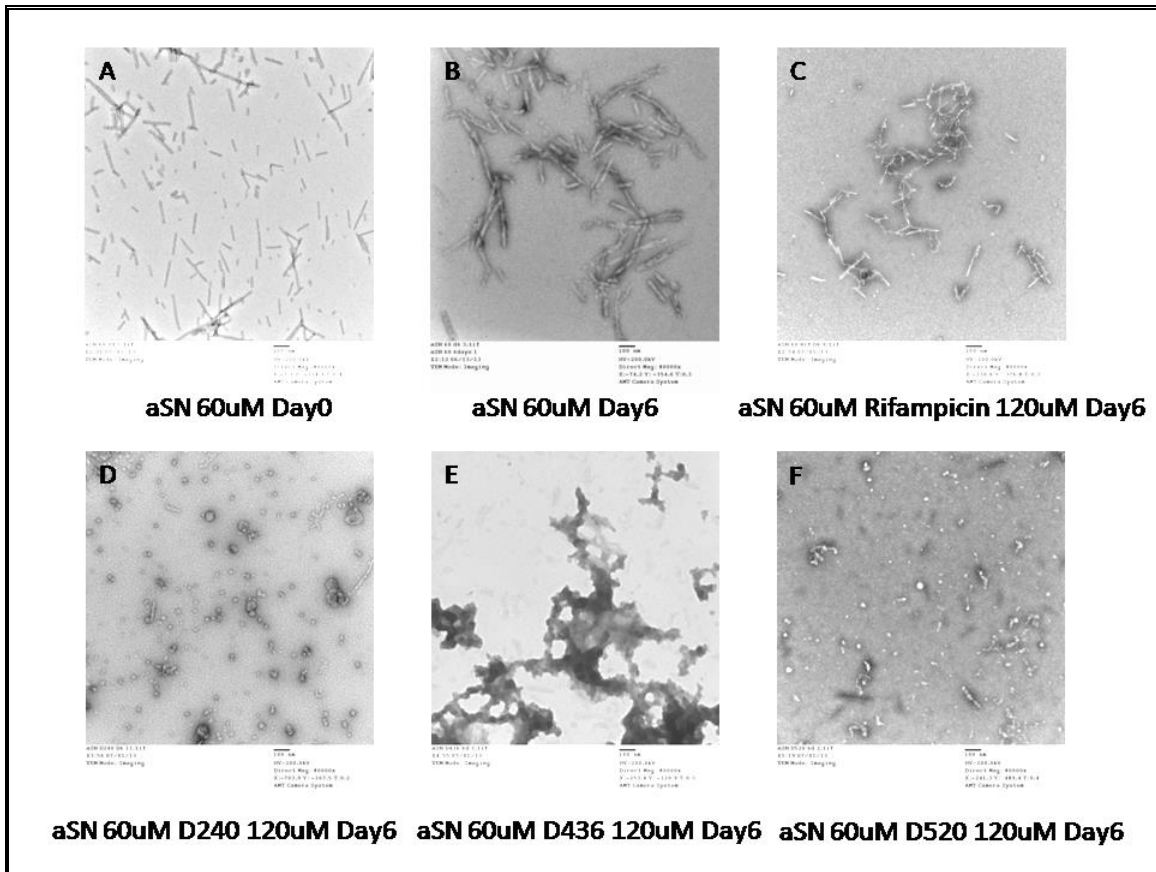


**Figure 5-24. TEM images of various experiments**

## DISCUSSION

Lewy bodies and Lewy neurites have been found to be accumulated in post-mortem brains of PD patients. Various findings have established that  $\alpha$ -synuclein aggregates constitute significant filamentous portion of Lewy bodies and Lewy neurites. In addition, various genetic mutations (point mutations and duplication or triplication of SNCA gene loci) have been also shown to be responsible for genetic form of PD (usually juvenile PD). This has resulted in significant amount of research to investigate the role of  $\alpha$ -synuclein aggregation in the pathology of PD. Various studies have shown that  $\alpha$ -synuclein aggregates in a concentration dependent manner and the aggregation process has been shown to be significantly enhanced in the presence

of dopamine or iron, which have been also strongly implicated in the pathology of PD.  $\alpha$ -synuclein aggregation has been shown to proceed in two steps. Initially, several  $\alpha$ -synuclein molecules form smaller aggregates (“protofibrils”) either in presence of dopamine or above a critical concentration or due to presence of mutations that lower the critical concentration to produce aggregates. Afterwards, these “protofibrils” act as seeds to generate higher molecular weight aggregates known as “fibrils” (Goldberg and Lansbury 2000). These fibrillar structures may coalesce together to generate Lewy bodies in PD. It is not unanimously concluded that which  $\alpha$ -synuclein species may play an important role in selective toxicity of dopaminergic neurons but protofibrils have been shown to be more toxic compared to fibrillar structure of  $\alpha$ -synuclein.

Some studies have shown that dopamine, under oxidizing conditions, prevents the conversion of  $\alpha$ -synuclein protofibrils to fibrils by generating co-valent adduct with  $\alpha$ -synuclein (Conway, Rochet et al. 2001, Cappai, Leck et al. 2005, Li, Lin et al. 2005, Illes-Toth, Dalton et al. 2013). Amino acid residues 125-129 are shown to be essential for dopamine-induced inhibition of fibril formation of  $\alpha$ -synuclein (Norris, Giasson et al. 2005). Selective accumulation of  $\alpha$ -synuclein protofibrils in dopaminergic neurons might be responsible for selective vulnerability of dopaminergic neurons in PD. A30P mutation of  $\alpha$ -synuclein gene has been also shown to prevent the conversion of protofibrils to fibrils and it may be responsible for development of PD.  $\alpha$ -synuclein induces apoptosis in dopaminergic neurons (but not in non-dopaminergic cell line) without generation of detectable inclusion bodies, which further corroborates the hypothesis that protofibrils may be the responsible species for dopaminergic neuronal death (Xu, Kao et al. 2002). Addition of anti-oxidants in cell culture system or prevention of dopamine synthesis prevents  $\alpha$ -synuclein induced apoptosis of dopaminergic

neurons, which implies that dopamine oxidation is necessary to generate toxic  $\alpha$ -synuclein protofibrils (Xu, Kao et al. 2002). Thus, dopamine may be directly involved in  $\alpha$ -synuclein induced apoptosis. Protofibrils have been shown to have ability to form pores in biological membranes and cause leakage of small molecular weight biomolecules such as calcium and dopamine, whereas, large molecular weight molecules such as cytochrome C are spared (Volles, Lee et al. 2001, Volles and Lansbury 2002). In addition, as discussed in introduction, fetal dopaminergic neurons grafted in PD patients also develop Lewy bodies, which further corroborates prion-like phenomenon of  $\alpha$ -synuclein. Some studies have shown that the structure of protofibrils resemble some evolved pore-forming cytotoxins (Volles, Lee et al. 2001). Therefore, not only intracellular protofibrillar forms of  $\alpha$ -synuclein, but also the extracellular species of protofibrillar  $\alpha$ -synuclein may be involved in dopaminergic neuronal toxicity. Some studies have shown that aggregation of  $\alpha$ -synuclein into fibrils might be protective in nature based on the observation that substantia nigra dopaminergic neurons containing Lewy bodies appear healthier than their neighboring neurons. The protective role of fibrils can be further supported by the fact that in many deceased elderly patients, incidental Lewy bodies are detected without any relevant clinical symptoms of PD (Goldberg and Lansbury 2000).

As protofibrils are believed to be the culprits for  $\alpha$ -synuclein induced toxicity, various factors which can thermodynamically (stabilize) or kinetically (decrease the rate) favor the generation of protofibrils and prevent (or decrease) the formation of fibrils may result in toxicity. Dopamine has been shown to prevent the generation of fibrils of  $\alpha$ -synuclein and stabilize  $\alpha$ -synuclein in its protofibrillar form, whereas, structural analogs of dopamine such as catechol and p-benzoquinone have been shown to stabilize  $\alpha$ -synuclein in its monomer or dimer form and prevent the generation of fibrils (Li, Lin et al. 2005). Ideal therapeutic agent,

- i. Should be able to prevent the formation of protofibrillar as well as fibrillar forms of  $\alpha$ -synuclein;
- ii. Should be able to disaggregate the existing fibrillar forms of  $\alpha$ -synuclein into its monomeric or lower molecular weight form;
- iii. Should have an ability to prevent against the cytotoxicity induced by extracellular or intracellular form of aggregated  $\alpha$ -synuclein species.

A study evaluated polyphenols, benzothiazoles, phenothiazines, polyene antibiotics, rifamycin antibiotic, steroids, Congo red and its derivatives, and terpenoids to assess their ability to prevent fibril formation and it was concluded that the most potent inhibitory compounds were from polyphenolic class of compounds (Masuda, Suzuki et al. 2006). The study also showed that the inhibitory compounds generated soluble oligomeric form of  $\alpha$ -synuclein, which wasn't toxic to dopaminergic neuronal cultures when incubated extracellularly with neurons. Another study showed potent anti-fibrillogenic and fibril-destabilizing effects of various antioxidant compounds such as polyphenols, curcumin, rifampicin, and tetracycline (Ono and Yamada 2006). Very low concentration of baicalein, an anti-oxidant flavanoid, has been shown to inhibit the formation of  $\alpha$ -synuclein fibrils. It also has an ability to disaggregate preformed  $\alpha$ -synuclein fibrils (Zhu, Rajamani et al. 2004). In addition, baicalein has been also shown to possess ability to prevent oligomer formation in living cells (Lu, Ardah et al. 2011). Rifampicin has been shown to prevent generation of fibrils of  $\alpha$ -synuclein by stabilizing monomeric and oligomeric form of  $\alpha$ -synuclein. Rifampicin also has an ability to disaggregate preformed  $\alpha$ -synuclein fibrils (Li, Zhu et al. 2004). Rifampicin has been also shown to decrease the expression of higher molecular weight form of  $\alpha$ -synuclein in PC12 cells treated with rotenone (Xu, Wei et al. 2007). In fact,

epidemiological studies have shown that there is less incidence of Lewy body diseases in population consuming rifampicin (leprosy patients) (Li, Zhu et al. 2004). Interestingly, most of the compounds (including dopamine) which prevent the generation of fibrils, require oxidizing conditions and their corresponding quinone forms exhibit more potent ability to prevent fibril formation (Conway, Rochet et al. 2001, Li, Zhu et al. 2004, Zhu, Rajamani et al. 2004). Based on literature evidence, two approaches can be taken to prevent  $\alpha$ -synuclein toxicity. Toxicity can be prevented by inhibiting the oxidation of dopamine (antioxidant compounds), which can prevent the generation of protofibrillar form of  $\alpha$ -synuclein by dopamine quinones. Another approach is to develop compounds, which have similar functionality like dopamine (ability to generate quinone and modify  $\alpha$ -synuclein co-valently), which can stabilize various  $\alpha$ -synuclein species such that the resulting product is rendered non-toxic to the neurons.

In current experiments, we determined our ability to generate various species of  $\alpha$ -synuclein under different conditions relevant to PD. Afterwards we evaluated the ability of some of our potent anti-oxidant lead compounds to alter the aggregation of  $\alpha$ -synuclein in presence of dopamine. We also evaluated the capability of  $\alpha$ -synuclein aggregates generated using higher concentration of  $\alpha$ -synuclein or aggregates generated using dopamine and  $\alpha$ -synuclein to alter cellular viability. In the end, we evaluated the ability of some of our lead compounds to alter the aggregation of  $\alpha$ -synuclein at higher concentration and also their ability to prevent cell death induced by  $\alpha$ -synuclein aggregates.

Our initial attempts in lab were to develop cell-free system assays to generate various types of  $\alpha$ -synuclein aggregates. Our efforts were to develop,

- i. Oligomers (protofibrils) of  $\alpha$ -synuclein in presence of dopamine;

- ii. Fibrillar structures in presence of higher concentration of  $\alpha$ -synuclein;
- iii. Fibrillar structures of  $\alpha$ -synuclein in presence of iron.

We were successfully able to develop dopamine-induced, SDS-resistant, co-valent oligomers of  $\alpha$ -synuclein. Characteristics of the oligomers were confirmed using silver-staining, ThT assay, and TEM imaging. It was quite important to generate the oligomeric structures of  $\alpha$ -synuclein as they have been hypothesized to be the major factor responsible for cytotoxicity of dopaminergic neurons. Therefore, this assay would be highly relevant to assess the ability of potential lead compounds to prevent or alter  $\alpha$ -synuclein aggregation process. We observed that  $\alpha$ -synuclein alone shaken at lower concentration (17.5  $\mu$ M) for longer time periods did not generate ThT positive and SDS-resistant aggregates (data not shown). However, we observed that  $\alpha$ -synuclein, shaken at higher concentration (50  $\mu$ M), was able to generate SDS-resistant, ThT positive fibrillar structures (**figure 5-4**). Characteristics of these structures were determined by silver-staining, ThT assay, and TEM imaging. Generation of fibrils using higher concentrations of  $\alpha$ -synuclein was quite interesting experiment as it would simulate genetic form of PD in which SNCA gene duplication or triplication results in physiological increase in  $\alpha$ -synuclein concentration resulting in early onset PD. Thus, this assay would be quite appropriate to evaluate the ability of some of our lead compounds to prevent or alter  $\alpha$ -synuclein aggregation at higher concentration. Potential candidates from this experiment may possess ability to prevent aggregation of  $\alpha$ -synuclein in genetic forms of PD. We were also able to generate iron-induced, SDS-sensitive and ThT positive fibrils of  $\alpha$ -synuclein (**figure 5-7, 5-8**). Characteristics of the aggregates were evaluated using silver-staining and ThT assay. Iron-induced a rapid formation of  $\beta$ -sheet positive fibrils and did not require higher concentrations of  $\alpha$ -synuclein to induce fibrilization. This assay was important to understand the ability of excess iron (observed in PD

substantia nigra) to give rise to  $\alpha$ -synuclein aggregates. This assay would also be quite relevant to evaluate the ability of our iron-chelator lead compounds to alter  $\alpha$ -synuclein aggregation process.

We also evaluated the ability of our lead compounds to prevent  $\alpha$ -synuclein protofibrils generated by dopamine using cell-free system assay. We used ascorbic acid as a standard anti-oxidant and rifampicin as a model  $\alpha$ -synuclein aggregation inhibitor to relatively compare our lead compounds. We employed silver-staining, TEM imaging, and SEC methods to evaluate the characteristics of aggregates. Interestingly, we observed that ascorbic acid was able to decrease the kinetics of oligomer formation by dopamine, whereas, rifampicin did not seem to have significant impact on oligomer formation by dopamine. Silver staining images clearly revealed that ascorbic acid has an ability to alter the kinetics of  $\alpha$ -synuclein aggregation (**figure 5-9(a) vs. figure 5-9(b)**), whereas, rifampicin has an ability to stabilize various polymerized forms of  $\alpha$ -synuclein (**figure 5-9(a) vs. figure 5-9(c)**). TEM images further corroborate that rifampicin generated aggregates are morphologically different than aggregates generated in presence of ascorbic acid (**figure 5-10(d) vs. figure 5-10(c)**). In addition, our evaluation by SEC profiling of aggregates also proved that the monomer form of  $\alpha$ -synuclein is quickly depleted in case of rifampicin experiment, whereas, significant monomer fraction is retained in case of ascorbic acid experiment (**figure 5-18**). Ideal compound should have an ability to prevent or alter the kinetics of  $\alpha$ -synuclein aggregation. It should be able to retain  $\alpha$ -synuclein in its native monomeric form and shouldn't cause significant morphological changes in  $\alpha$ -synuclein. We observed quite similar results with ascorbic acid, most probably because of its potent anti-oxidant activity, which might have prevented the formation of dopamine-quinones and corresponding modifications of  $\alpha$ -synuclein. Out of the 2 lead compounds tested in this experiment, we observed that D-436 did



not significantly affect dopamine induced  $\alpha$ -synuclein oligomerization. Interestingly, in silver-staining experiments, we observed the disappearance of monomer without corresponding increase in higher molecular weight aggregates of  $\alpha$ -synuclein (**figure 5-9(d)**). Therefore, it might be possible that D-436 may generate SDS-resistant insoluble fibrils of  $\alpha$ -synuclein, which do not enter the SDS-PAGE gel. Similar results were seen with TEM, which showed significant increase in the size of  $\alpha$ -synuclein aggregates in case of D-436 (**figure 5-10(e)**). Furthermore, D-436 also exhibited very similar SEC profile, which helped us conclude that D-436 doesn't possess ability to prevent dopamine induced  $\alpha$ -synuclein aggregation (**figure 5-18**). In fact, it may be possible that D-436 might accelerate the formation of  $\alpha$ -synuclein oligomers. In case of D-520, we observed very interesting results in silver-staining experiments. Surprisingly, incubation of  $\alpha$ -synuclein and dopamine with D-520 generated well-structured and SDS-resistant lower molecular weight aggregates as resolved by SDS-PAGE (**figure 5-9(e)**). TEM imaging also corroborated with the interpretation from silver-staining (**figure 5-10(f)**), where we observed smaller aggregates with heterogeneous morphology in case of D-520 experiment. In addition, SEC profile of samples from the same experiments showed that the monomer fractions retained in various samples were quite comparable to those observed with ascorbic acid experiment (**figure 5-18**). Therefore, it can be concluded that D-520 should be able to significantly alter dopamine induced  $\alpha$ -synuclein aggregation and it holds a potential to prevent cytotoxicity induced by oligomeric  $\alpha$ -synuclein.

We aimed to evaluate the extracellular toxicity of  $\alpha$ -synuclein aggregates (generated using cell-free system) in dopaminergic neuronal culture. We generated  $\beta$ -sheet positive fibrils (60 $\mu$ M  $\alpha$ -synuclein alone) and  $\beta$ -sheet negative protofibrils (60  $\mu$ M  $\alpha$ -synuclein and 90  $\mu$ M dopamine) of  $\alpha$ -synuclein using cell-free system assay. The characteristics of the aggregates

were evaluated by use of ThT assay and TEM imaging (**figures 5-20, 5-21**). TEM imaging revealed that dopamine generated elongated protofibrillar structures, whereas,  $\alpha$ -synuclein alone generated compact and branched fibrillar structures. MTT assay was carried out using PC12 cells, which were incubated with 10  $\mu$ M final concentration of  $\alpha$ -synuclein aggregates from both the experiments (**figure 5-19**). Surprisingly, in case of  $\alpha$ -synuclein (60  $\mu$ M) alone, we observed that from day 0 to day 6, there was a decrease in cellular viability. For day 8 and day 10, we observed somewhat restoration in cellular viability. This may be potentially due to the conversion of protofibrillar species (toxic) into fibrillar (relatively less toxic) structure of  $\alpha$ -synuclein. In an experiment involving  $\alpha$ -synuclein (60  $\mu$ M) and dopamine (90  $\mu$ M), we observed a decrease in cellular viability from day 0 to day 4. However, the cellular toxicity of aggregates from day 6 to day 10 remained similar. This might imply that the chemical interaction of dopamine with  $\alpha$ -synuclein is completed by day 4 leaving no dopamine molecules to interact with ASN further. Thus, further incubation doesn't alter the structural features of the aggregates significantly when compared to aggregates produced after 4 days. Thus, we achieved the maximum amount of cytotoxicity from aggregates generated using  $\alpha$ -synuclein alone (60  $\mu$ M) shaken for 6 days.

Our ultimate goal was to evaluate the ability of some of our lead compounds to prevent the cytotoxicity induced by  $\alpha$ -synuclein (60  $\mu$ M) alone shaken for 6 days. We tested rifampicin as a standard compound and D-240, D-436, and D-520 (lead compounds) to evaluate their ability to alter  $\alpha$ -synuclein aggregation in cell-free system. We characterized the aggregates of  $\alpha$ -synuclein from various experiments using ThT assay and TEM imaging (**figure 5-23, 5-24**). We observed that rifampicin altered the morphology of aggregates significantly, when compared to aggregates generated by  $\alpha$ -synuclein alone. Interestingly, D-240 and D-520, significantly

reduced the size of aggregates and the morphology of aggregates appeared to be comparable to small molecular weight polymeric forms of  $\alpha$ -synuclein. Surprisingly, D-436 again generated aggregates with significantly increased size and distinct morphology. ThT assay revealed that rifampicin, D-240 and D-520 inhibited  $\beta$ -sheet formation, whereas, D-436 significantly enhanced the formation of  $\beta$ -sheet structure. Thus, D-436 failed to alter the aggregation of  $\alpha$ -synuclein fibrils. MTT assay using the samples generated from these experiments provided insightful results (**figure 5-22**). We observed that extracellular incubation of  $\alpha$ -synuclein shaken for 6 days significantly decreased cellular viability. Incubation of protein with rifampicin altered the characteristics of aggregates but the toxicity was not altered. Incubation of protein with D-240 as well as D-520 resulted in prevention of cell-death. As expected, incubation of protein with D-436 resulted in further decrease in cellular viability. From MTT assay results, it can be interpreted that as D-240 and D-520 are able to protect against extracellular toxicity induced by  $\alpha$ -synuclein (60  $\mu$ M), they hold potential to prevent  $\alpha$ -synuclein induced toxicity in genetic form of PD where increased physiological concentrations of  $\alpha$ -synuclein is a major concern. As D-436 accelerated the fibril formation process and caused a further decrease in cellular viability, it may not be an ideal candidate of choice to prevent extracellular toxicity of  $\alpha$ -synuclein. From the study of chemical structure of compounds investigated in this experiment, it can be concluded that di-hydroxyl aromatic groups are essential for a compound to alter the aggregation of  $\alpha$ -synuclein (rifampicin, D-240, D-520 vs. D-436). Adjacent hydroxyl groups may generate structures that have ability to prevent cytotoxicity induced by dopamine induced oligomers (D-240 and D-520). Further investigation into the structural-activity relationship may help generate some potential therapeutic molecule.

**CHAPTER 6**  
**INTRODUCTION**

**6 Amphetamine**

Amphetamine (AMPH) is derived from  $\alpha$ -methyl-phenylethyl-amine structure (**figure 6-1**). AMPHs naturally occur in ephedra and khat plants (Sulzer, Sonders et al. 2005). Ephedra (*Ephedra sinica*) contains natural AMPHs called ephedrine and pseudoephedrine. Khat (*Catha edulis*) contains natural AMPHs called cathine and cathinone (Sulzer, Sonders et al. 2005). The first synthetic amphetamine was synthesized in 1887 by Lazar Edeleanu. However, its sympathomimetic activities were not realized until concept of sympathomimetics developed. AMPH was independently synthesized by Gordon Alles in 1927 in an effort to develop synthetic sympathomimetics. **Figure 6-1** shows the structural similarities of various AMPHs.

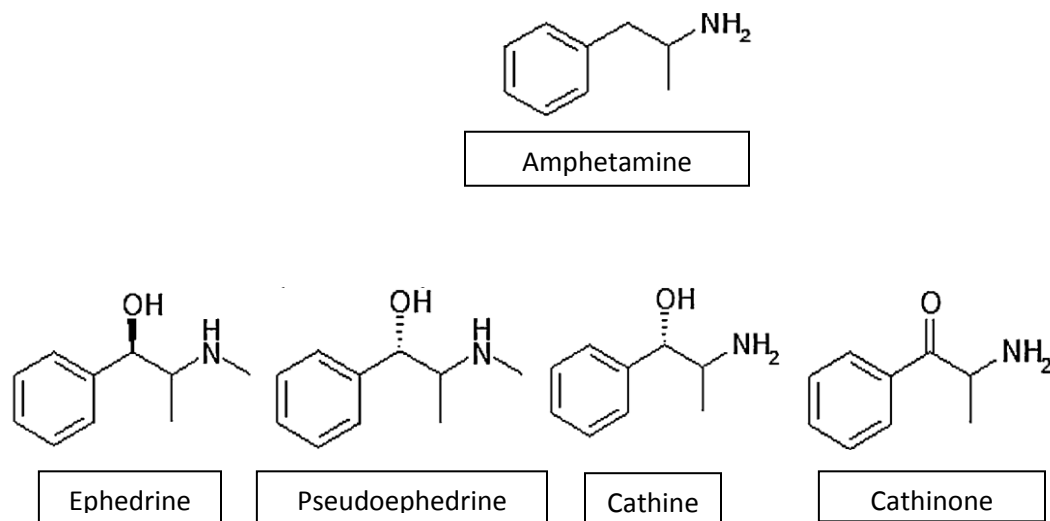


**Figure 6-1. Chemical structures of amphetamines**

AMPH was introduced commercially by Smith, Kline and French as Bensedrine, which was a free base administered in inhaler form to treat nasal congestion (Sulzer 2011, Vearrier, Greenberg et al. 2012). Myron Prinzmetal is credited for the first clinical use of AMPH in the treatment of narcolepsy. AMPH was made available by prescription only in 1939. By 1945, the

drug industry promoted 30 different uses of AMPH including the treatment of schizophrenia, opiate addiction, infantile cerebral palsy, etc. During World War II, AMPH was highly promoted by the militaries of Japan, Germany and Britain to increase alertness in soldiers. AMPH's addictive potential and neurotoxic effects were not widely accepted until the mid-1960s.

Various synthetic AMPHs have been developed as potential therapeutics including fenfluramine (appetite suppressant) and deprenyl (anti-Parkinson's drug). Some of the most widely abused AMPHs are methamphetamine (METH) and methylene dioxymethamphetamine (MDMA) (Sulzer, Sonders et al. 2005) (**figure 6-2**).

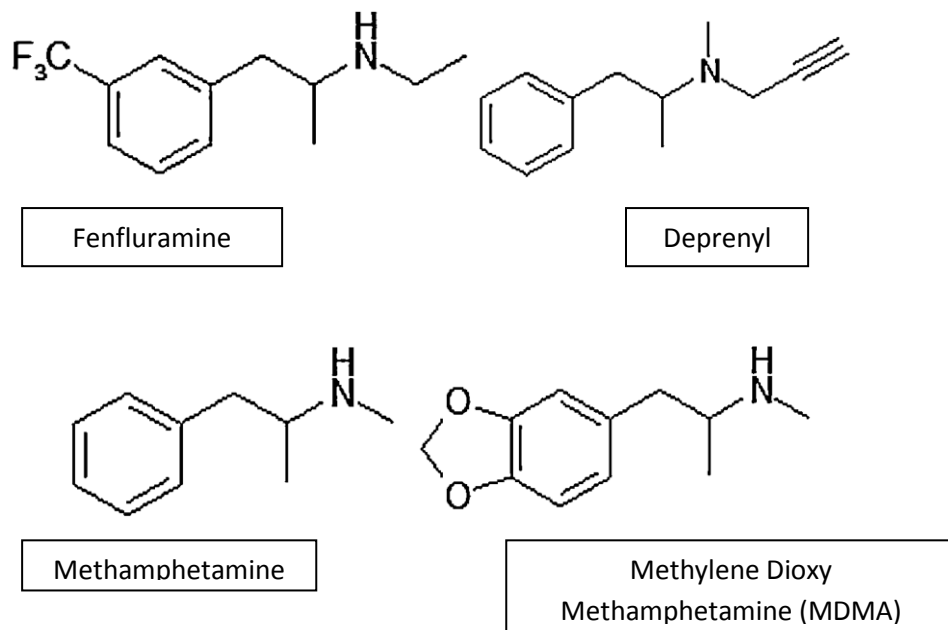


**Figure 6-2. Chemical structures of synthetic amphetamines**

### 6.1 Legal status of amphetamine

Amphetamine is classified by the U.S. Drug Enforcement Agency (DEA) as a schedule II controlled substance, characterizing it as having limited therapeutic value but high abuse potential. Several prescription AMPHs are currently available including Ritalin or Ritalin SR (methylphenidate), Adderall (amphetamine and dextroamphetamine), and Dexedrine

(dextroamphetamine). All of these prescription drugs are non-refillable. Interestingly, it has been demonstrated that therapeutic doses used in the treatment of Attention Deficit Hyperactivity disorder (ADHD) can cause significant neurotoxicity (Ricaurte, Mechan et al. 2005).

## **6.2 Methamphetamine (METH)**

METH is an amphetamine derivative which has a very high abuse potential and has been proven highly neurotoxic in various rodent, non-human primate, and human studies (Woolverton, Ricaurte et al. 1989, Thomas, Walker et al. 2004, Berman, O'Neill et al. 2008). METH acts as a stimulant in the central nervous system (CNS). METH is highly abused, in part, due to its ease of synthesis - including easy access to its precursors: ephedrine and pseudoephedrine. METH is usually consumed by smoking, resulting in an initial rush that lasts for several minutes followed by a prolonged high that includes an extended period of euphoria. METH's half-life is 10-30 hrs based on the amount administered, pH of urine, and purity of the drug (Russell, Dryden et al. 2008). As METH is easily accessible, relatively cheap, and has reinforcing properties, its chronic use can pose significant dangers. METH is also known as Chalk, Crank, Crystal, Glass, Go-Fast, Ice, Methlies Quick, Speed, etc. As of 2000, the U.S. DEA stated that METH is the most prevalent illicitly manufactured controlled substance. The single largest METH seizure to date was 208 pounds of METH confiscated in Las Vegas in July, 2011 near the U.S.-Mexico border. Therefore, it is very important to maintain vigilance in preventing METH trafficking from other countries.

## **6.3 METH statistics**

METH is highly abused by the teenage population. Initially METH abuse was limited to Hawaii and western states of the U.S., but has become more widespread including all rural and urban areas. In 2000, 6394 clandestine METH labs were seized. Illicit METH production operations have been uncovered in all 50 states of U.S. Approximately 13 million people aged 12

years or older, have abused METH in their lifetimes. In 2010, approximately 353,000 people were current users (NIDA report, November, 2011). The 2009 World Drug Report suggested that the global prevalence of METH use is second only to cannabis, with estimates suggesting that up to 51 million individuals (1.2% of the global population aged 15–64 years) have used METH at least once in the past 12 months (World Drug Report, 2009).

#### **6.4 Legal status of METH**

METH is classified by DEA as Schedule II drug, which means that it has limited therapeutic use but high abusive potential. METH is available by prescription under the trade name Desoxyn. Desoxyn is used in the treatment of morbid obesity and ADHD. METH prescriptions can't be refilled.

#### **6.5 Risk factors for METH abuse in youth**

According to the 2004 national survey on drug use and health, 0.6% of the U.S. population had used METH in the previous 12 months. In 2002, street youth aged 14-30 years were surveyed and 71% of respondents reported using amphetamine-type stimulants. Therefore, identification of risk factors for METH abuse can help to prevent or at least decrease METH abuse. An excellent review article by Russel et al. examined risk factors of METH abuse in youth with low risk (youth who did not use illicit drugs) and youth with high risk (youth who had abused illicit drugs other than METH or were recruited from juvenile detention center) (Russell, Dryden et al. 2008).

##### **6.5.1 Risk factors in low risk youth**

###### **6.5.1.1 Gender**

Two cross-sectional studies examined sex as a risk factor. Both have shown that males are more likely to use METH than females (Oetting, Deffenbacher et al. 2000, Sattah, Supawitkul et al. 2002).

#### **6.5.1.2 Ethnicity**

One cross-sectional study examined ethnicity as a risk factor. The study concluded that Caucasian youth are more likely to abuse METH than African American or Asian youth. However, Caucasian youth are significantly less likely to use METH than Hispanic or Native American youth (Oetting, Deffenbacher et al. 2000).

#### **6.5.1.3 Years of education**

Three different studies concluded that METH users had significantly less years of education than non-METH users (Sattah, Supawitkul et al. 2002, Yen 2004, Yen, Yang et al. 2006).

#### **6.5.1.4 Sexual behavior**

Two different studies examined associations between previously engaging in risky sexual behaviors and METH use (Green and Halkitis 2006). It concluded that people who had engaged in unprotected sex, engaged in unplanned sex under the influence of alcohol, or engaged in sexual intercourse with an alcohol-intoxicated-partner were more likely to abuse METH.

#### **6.5.1.5 Alcohol, cigarette and opiate use**

Two studies independently found significant association with alcohol use, cigarette smoking, and heroin/opiate use (Yen, Yang et al. 2006).

#### **6.5.1.6 Psychiatric disorders**

The presence of any psychiatric disorder, adjustment disorder, conduct disorder, or attention deficit hyperactivity disorder (ADHD) significantly increased the risk of METH abuse.



### **6.5.1.7 Other factors**

Other factors including homosexuality or bisexuality, having experienced disruptive parenting, having peers who use or provide METH, and having a family history of drug use all increase the likelihood of METH abuse in low risk youth.

## **6.5.2 Risk factors in high risk youth**

### **6.5.2.1 Gender**

Three studies concluded that female gender was significantly associated with METH abuse than male gender (Kim and Fendrich 2002, Rawson, Gonzales et al. 2005, Miura, Fujiki et al. 2006).

### **6.5.2.2 Ethnicity**

Caucasian youth were significantly more likely to use METH than African-American or Asian youth. However, there was no difference between Caucasian, Hispanic, and Native American youth.

### **6.5.2.3 Family history**

One cross-sectional study reported that a family history of crime or drug use was significantly associated with METH use (Miura, Fujiki et al. 2006).

### **6.5.2.4 Other factors**

Youth receiving psychiatric treatment, youth with greater than two admissions to a juvenile home, and youth with a history of violence were all more prone to METH abuse.

Thus, a history of engaging in various risky behaviors was significantly associated with METH abuse in low risk youth. Being homosexual or bisexual is another risk factor as METH is known to enhance sexual pleasure. In high risk youth, females are more prone to METH abuse, as are youth who have grown up in unstable family environments. Youth who have received

psychiatric treatment were more likely to abuse METH. However, strict parental monitoring was found to decrease the risk of METH abuse.

## **6.6 Consequences of METH abuse**

METH is abused primarily by younger individuals. As it is neurotoxic, it is extremely important to understand the associated mental and physical disorders that develop because of METH addiction. It is particularly important to understand the neurotoxic effects of METH in the younger population as the CNS is still undergoing development during exposure (Marshall and Werb 2010, Vearrier, Greenberg et al. 2012).

### **6.6.1 Mental and behavioral disorders**

Suicidal ideation and eating disorders are more likely in youth abusing METH. Chronic METH users experience paranoia and hallucinations. Hallucinations have been found to be a common problem among METH abusers. METH-induced psychosis has also been well documented. Individuals that undergo treatment for METH abuse are very likely to have major depressive disorders and it is specifically diagnosed in youth who have abused METH by the age of 15.

### **6.6.2 Dermatological disorders**

METH abuse predisposes one to repetitive, stereotypical skin picking, resulting in excoriations on the face and extremities. METH related skin infections may take the form of cellulitis or cutaneous abscess.

### **6.6.3 Hematological disorders**

METH use may increase the risk of contracting Human Immunodeficiency Virus (HIV) because of sharing non-sterile needles for injecting METH. METH users also engage in unsafe sexual practices and usually report more sex partners than non-users. METH users are more likely to participate in sexual activities that may increase the risk of HIV transmission, such as anal sex, unprotected sex, and sex with known injection drug users. METH abuse is also associated with necrotizing angitis. Macroscopically, affected arteries can display segmental narrowing with aneurysm formation.

### **6.6.4 Gastrointestinal disorders**

METH use is known to increase Hepatitis C infection in needle and non-needle users. Even in the absence of hepatitis, METH use has been known to cause hepatic necrosis and centrilobular degeneration.

### **6.6.5 Genitourinary disorders**

METH users are more likely to have Sexually Transmitted Diseases (STDs) because they are more likely to engage in risky sexual behaviors. Prolonged sex while on METH can cause soft tissue injury which can further increase the risk of STDs.

### **6.6.6 Musculoskeletal disorders and “METH mouth”**

METH induces dental decay through multiple mechanisms. It causes xerostomia by sympathetic overstimulation. It also causes bruxism, resulting in multiple dental caries. Dental decay can also occur from an addict's poor hygiene and malnutrition. METH abusers also report rhabdomyolysis. Pott's puffy tumor (osteomyelitis of the frontal bone) has been associated with intranasal METH use.

### **6.6.7 Neurological disorders**

Intracranial hemorrhage is a devastating side-effect of METH abuse. It may occur due to METH-induced hypertension and tachycardia. METH induced necrotizing angiitis may also cause intracerebral hemorrhage. Intraparenchymal bleeds in various brain regions have been reported in METH addicts which may be due to prolonged cardiovascular effects of METH. Fatal intraventricular hemorrhage has been also reported with METH use. METH abuse has been also known to cause ischemic stroke, seizure, and cognitive impairment. METH abstinence in chronic users shows persistent improvement in various cognitive tests.

HIV-positive and hepatitis C patients show more cognitive impairment due to METH abuse. Comorbid patients show additional glial activation and neuronal injury in the frontal cortex and basal ganglia compared to non-disease METH abusers.

### **6.6.8 Prenatal METH exposure**

METH is increasingly a drug of choice in substance dependent women. Prenatal METH use has been associated with fetal growth restriction and premature delivery. Animal studies have shown that prenatal METH exposure may affect the myelination process. Prenatal METH exposure in humans has been shown to decrease inhibitory control in children. Prenatal METH exposure may cause structural damage to frontal-subcortical circuits which may be changing behavior among affected children (LaGasse, Derauf et al. 2012). Heavy METH exposure is known to be associated with lower arousal and excitability in children. Prenatal exposure also results in poor quality of movement and increased stress signs when METH is taken in first trimester, whereas third trimester exposure can be associated with increased lethargy and hypotonicity (LaGasse, Wouldes et al. 2011). A study carried out to understand the outcome of prenatal METH exposure has shown that in 3 and 5 year old children, METH exposure is

associated with increased emotional reactivity and anxiety/depression. Heavy METH exposure was associated with attention problems and withdrawn behavior. In 5 year old children, there is decreased externalizing behavior and ADHD problems (LaGasse, Derauf et al. 2012).

#### **6.6.9 Adverse effects of METH on Brain**

METH is known to cause significant toxicity in the brain. Acute METH intoxication has been shown to cause significant hyperthermia, which is potentiated by associated physiological activation - especially in warm environments which prevent proper heat dissipation (Kiyatkin and Sharma 2009). METH induces structure-specific leakage in the blood-brain barrier (BBB) which can cause water, ions, and various potentially neurotoxic substances contained in plasma to enter the brain (Zlokovic 2008). METH induced BBB leakage is attributed to the hyperthermia induced by it. METH is also known to cause metabolic activation which results in more oxidative species being produced than the body can tolerate. Thus, it induces abnormal levels of oxidative and nitrosative stress in the brain and elsewhere. As METH causes BBB leakage, it can result in brain edema. METH toxicity is also related to the ambient temperature at which it is administered. Higher ambient temperatures can enhance METH toxicity, whereas, lower ambient temperatures can protect from METH-induced toxicity.

Various brain regions show significant overexpression of GFAP in astrocytes after METH intoxication (Thomas, Dowgiert et al. 2004). METH causes morphological changes in neuronal structure in hippocampus, thalamus, hypothalamus, and cortex. The METH “high” is induced by the massive dopamine (DA) released following its administration. As discussed later, METH significantly affects the nigrostriatal pathway, particularly in the striatum, where the DA nerve terminals lie. METH administration results in significant DA depletion and decreased tyrosine hydroxylase (TH) activity in the striatum. METH administration also results in striatal-

specific activation of microglia cells, which are equivalent to the systemic macrophages of the immune system. Surprisingly, the vast majority of microglial activation following METH exposure occurs only in the striatum and not other parts of brain (Thomas, Walker et al. 2004).

## **6.7 Possible mechanisms of actions responsible for neurotoxicity of METH**

METH structurally resembles dopamine. It has been well-established that METH acts on the nigrostriatal pathway to release massive amount of DA. METH-induced DA release is critical for inducing its addiction potential. To understand the mechanisms of actions of METH, it is essential to understand dopaminergic pathways in brain (**figure 6-3**).

### **6.7.1 Dopaminergic pathways in brain**

There are four dopaminergic pathways in brain,

- i. Nigrostriatal pathway
- ii. Mesolimbic pathway
- iii. Mesocortical pathway
- iv. Tuberoinfundibular pathway

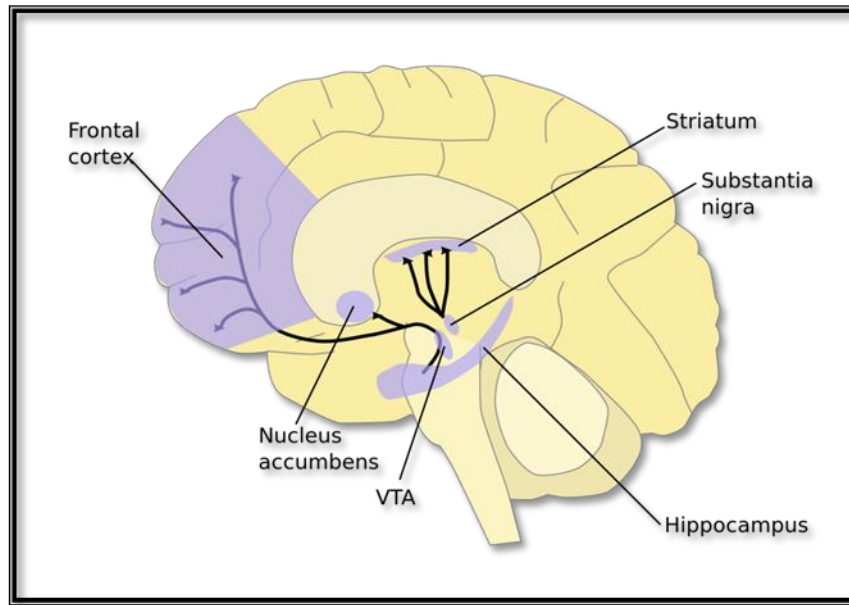


**Figure 6-3. Dopaminergic pathways in brain**

(Adapted from: [http://en.wikipedia.org/wiki/File:Dopamine\\_pathways.svg](http://en.wikipedia.org/wiki/File:Dopamine_pathways.svg))

Dopaminergic neurons originate in the substantia nigra pars compacta (SNPc), ventral tegmental area (VTA) and hypothalamus. They project their axons to other brain areas and constitute the dopamine neurotransmitter system.

1. The nigrostriatal pathway is formed by neurons which project from substantia nigra to neostriatum. The terminals end in caudate nucleus and putamen which form striatum. Nigrostriatal pathway is involved in movement and motor control. PD is caused by destruction of neurons in nigrostriatal pathway.
2. The mesolimbic pathway is formed by neurons projecting from the VTA to the nucleus accumbens, and is mainly involved in the “reward system.” Food, sex, and pleasure of any kind (including METH administration) involve activation of this pathway, resulting in reward.

3. The mesocortical pathway is formed by neurons projecting from the VTA to the prefrontal cortex, hippocampus and amygdala. This pathway is involved in motivation, emotion, memory and cognition. Dysfunction of this pathway is sometimes associated with schizophrenia.
4. The tuberoinfundibular pathway is formed by neurons projecting from the hypothalamus to the pituitary gland. It is mainly involved in prolactin release and is associated with maternal behavior, hormonal regulation, and pregnancy.

### **6.7.2 Components of the Dopaminergic neuronal system**

METH-induced toxicity can easily be detected in the striatum of METH addicts. Understanding the components of the dopaminergic system can help explain the possible mechanisms of METH action (**figure 6-4**).

DA is synthesized from tyrosine by tyrosine hydroxylase, which converts tyrosine to 3,4-dihydroxy phenylalanine (L-DOPA). L-DOPA is converted to DA through decarboxylation by dopa decarboxylase. Once synthesized, DA is transported from the cytosol into synaptic vesicles by VMAT-2. Upon appropriate stimulus, these vesicles fuse to the presynaptic membrane and release DA. Post-synaptically, DA binds to D1 and D2 receptors. DA also binds to presynaptic DA receptors which are auto-inhibitory and prevent further DA release. Once DA has elicited the appropriate response, it dissociates from its receptors and can be recycled back into the pre-synaptic neuron by the dopamine transporter (DAT). Some of the cytoplasmic DA is then transported back into synaptic vesicle by VMAT-2.



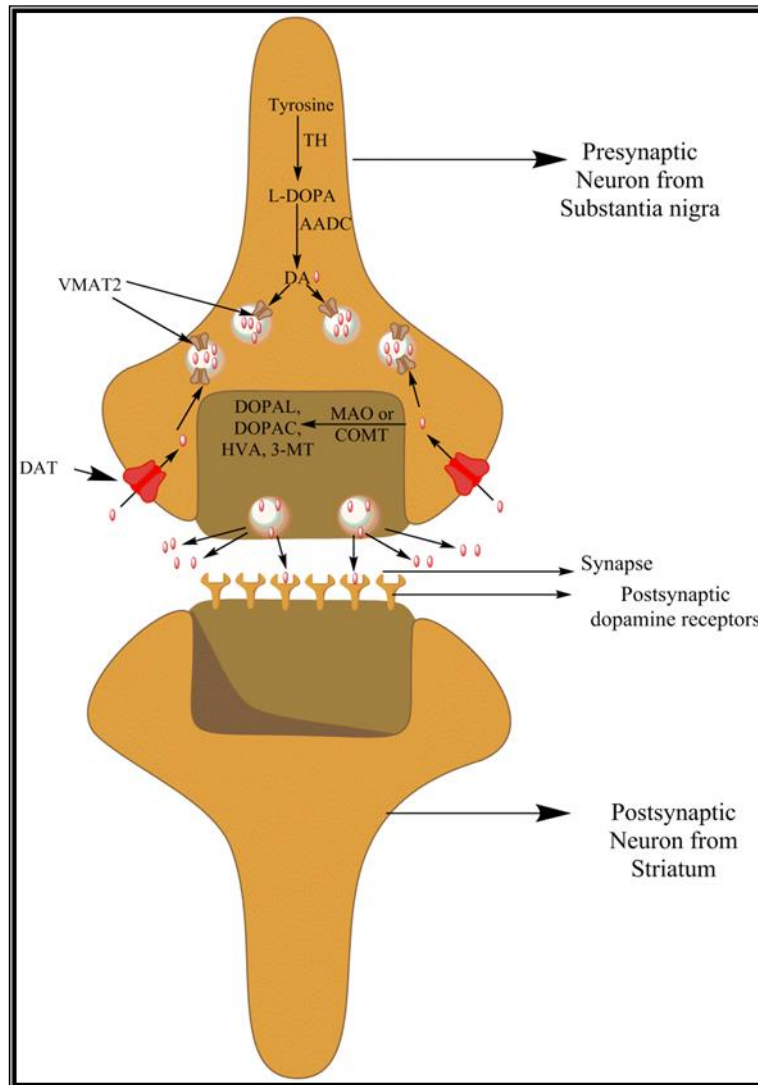


**Figure 6-4. Components of Dopaminergic neuronal system**

Another fraction of cytoplasmic DA is metabolized by MAO and COMT enzymes. Different metabolites of DA include dihydroxyphenyl acetaldehyde (DOPAL), dihydroxyphenyl acetic acid (DOPAC), 3-methoxytyramine (3-MT), and homovanillic acid (HVA).

### 6.7.3 Proposed Mechanisms of action of METH

Several studies have shown that METH is a strong substrate for DAT. Other studies support that other components of the dopaminergic neuronal system may be responsible for

METH-induced neurotoxicity (Fleckenstein and Hanson 2003, Yamamoto, Moszczynska et al. 2010).

#### **6.7.3.1 Dopamine transporter blocker and dopamine transporter reverse transport facilitator**

METH has been shown to be a strong substrate for the DAT. METH and similar weak bases not only block the reuptake of DA by DAT but it also facilitates the reverse transport of DA (Sulzer, Chen et al. 1995). This results in excessive DA accumulation in the synaptic cleft. Thus, excessive DA in the synapse continuously binds to post-synaptic DA receptors, resulting in its euphoric effect. DAT expression has been shown to be persistently depleted in METH addicts, even after long term abstinence. However, the DAT alone doesn't cause massive DA release following METH administration. The VMATs also appear to play an important role in METH action.

#### **6.7.3.2 Vesicular monoamine transporter-2 blocker**

METH is a substrate for VMAT-1 and VMAT-2. METH has 10 times more affinity for VMAT-2 than VMAT-1 (Peter, Jimenez et al. 1994). VMAT-2 knock-out animals do not survive. However, VMAT-2 knock-out animal derived cell-culture data has shown that, in the absence of VMAT-2, the METH-induced release of DA is significantly decreased. METH is also known to block VMAT-2 once inside the neurons, which results in high cytoplasmic concentrations of DA. METH has been shown to deplete two different types of dopaminergic vesicles. At low doses, METH depletes vesicles that are large in size; whereas, at high doses, METH depletes small size vesicles (Anderson, Chen et al. 1998).

### **6.7.3.3 Tyrosine hydroxylase inhibitor**

METH at lower concentrations enhances DA synthesis and TH activity. This requires extracellular calcium. At higher concentrations, METH inhibits TH activity (Sulzer, Sonders et al. 2005). Inhibition of TH activity results in lower DA levels in the striatum following METH administration.

### **6.7.3.4 Monoamine oxidase inhibitor**

METH prevents deamination of DA most potently by acting at the DAT to block reuptake and by facilitating the efflux of DA from the cytoplasm. In addition, METH is also a direct inhibitor of MAO, which results in more DA available for release into the synaptic space.

### **6.7.3.5 Dopamine transporter and vesicular monoamine transporter trafficking alteration**

METH has been shown to promote DAT redistribution. METH administration results in a decrease in the expression of cell surface DAT and increased redistribution of DAT on cellular endosomes (Saunders, Ferrer et al. 2000). Western blot analysis has shown that neurotoxic METH regimen causes decreases in DAT monomers and a corresponding increase in higher weight DAT complexes.

METH has been shown to decrease vesicular DA transport by promoting the redistribution of VMAT-2. METH also accumulates in synaptic vesicles because of its structural similarity to DA and its ability to collapse the pH gradient across synaptic vesicle membranes. METH-induced VMAT-2 dysfunction causes high concentration of DA in cytoplasm, which can cause increases in reactive species generated by DA metabolism.

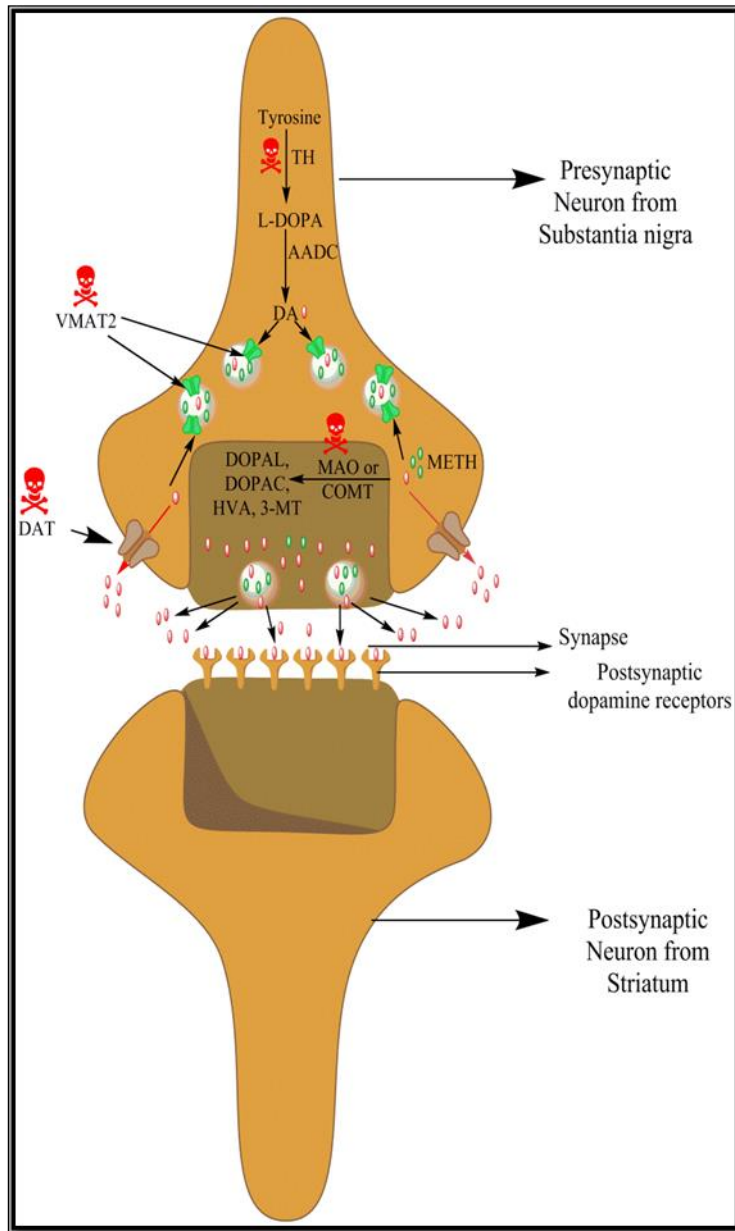


**Figure 6-5. Adverse consequences of METH administration**

### **6.7.3.6 Significant increase in reactive oxygen species and inflammation**

METH treatment results in striatal microglia activation, which in turn can produce ROS. In addition to microglia, METH treatment can increase ROS in several ways (Riddle, Fleckenstein, and Hanson 2006). METH treatment can:

- i) significantly increase cytoplasmic DA which can then undergo auto-oxidation
- ii) cause glutamate release, subsequent mitochondrial dysfunction, and glutamate-induced NO production
- iii) activate D1 dopaminergic receptors, which increases nNOS expression
- iv) induce inhibition of mitochondrial function which increases mitochondria-mediated reactive species generation.

Using various approaches, our lab has shown that METH-induced striatal microglial activation *precedes* dopaminergic neuronal damage. Microglia forms key immune system of central nervous system (CNS) and their persistent activation has been widely accepted to represent CNS pathology.

## 6.8 Microglia cells

CNS is separated from peripheral parts of body by BBB. BBB prevents the entry of various potentially pathological substances into CNS. Thus, brain is immunologically privileged organ. Microglia cells are considered resident macrophages of brain and are known to be most effective sensors of brain pathology. The exact function of microglia is unknown. However, massive amount of activated microglia are shown to be present in various brain regions of patients with neurodegenerative diseases such as Parkinson's disease (PD), Alzheimer's disease (AD), Kreutzfeldt-Jacob disease, multiple sclerosis (MS), etc. As dysfunction of microglia results in mostly all pathologies of CNS, they must be playing an important role in maintenance of homeostasis in CNS. Microglia were first introduced as a cellular element of CNS by Pio del Rio-Hortega in 1932. He used a modified silver carbonate impregnation to label the microglia

cells. Most of the description that was given by Rio-Hortega about microglia still holds true. He advocated that,

- i) Microglia enter the brain during early development;
- ii) These cells have amoeboid morphology and are mesodermal in origin;
- iii) They transform into a branched, ramified morphological phenotype in matured brain;
- iv) In mature brain, they are found almost evenly dispersed throughout the CNS and display little variation;
- v) After a pathological event, these cells undergo a transformation;
- vi) Transformed cells acquire amoeboid morphology similar to that observed early in development;
- vii) These cells have the capacity to migrate, proliferate, and phagocytose.



**Figure 6-6. Microglia morphology as depicted by Rio-Hortega**

### **6.8.1 Microglia cells- Morphology and response to native environment**

Elegant in-vivo 2-photon imaging studies show that microglia continuously monitor their native environment using their cellular processes (Davalos, Grutzendler et al. 2005, Nimmerjahn, Kirchhoff et al. 2005, Raivich 2005). Previously, when it was not known that microglia actively survey their surrounding environment, native state of microglia was termed as “resting” state. However, because of their active search for and reading of signals from neighboring environment, microglia’s native state is termed “surveying” state. In healthy CNS, “surveying” microglia have ramified morphology i.e. small soma with fine processes. Because of wide diversity of receptors for various molecules, microglia can immediately sense signs of change in homeostasis. Various insults such as infection, trauma, ischemia, neurodegenerative disease, neurotoxin exposure or altered neuronal activity i.e. disturbance or loss of homeostasis in brain can induce rapid changes in microglia cell shape, gene expression, and the functional behavior which can be termed “activated” microglia. Phenotypically, “activated” microglia have ramified morphology and the complexity of its processes is reduced. Microglia can engulf foreign molecules (activated state), but they also remove dead or dying cells (surveying state). Activated microglia release inflammatory molecules upon bacterial invasion, whereas, in response to dead or dying cells microglia release anti-inflammatory molecules (“surveying” microglia). Hence, it is very important to understand the role of microglia under “surveying” state versus under “activated” state and also understand how they transform from one state to another.

Microglia should have some function in healthy brain. They can act to maintain homeostasis in CNS as they form immune system of CNS. In healthy state, minor damages in CNS can happen such as ischemic event, minor capillary rupture, or small damage to BBB which can cause entry of plasma components into brain. Microglia respond to these types of damages

and react to prevent further damage in CNS because of them. They are also known to remove dead cells or debris by phagocytosis. However, very few functions of “surveying” microglia have been reported in literature. Interestingly, there is plethora of literature showing “activated” microglia in various chronic neurodegenerative diseases.

There is increasing evidence that microglial activation is not an “all-or- none” process, neither is it a linear path with a fixed uniform outcome (**figure 6-7**). To the contrary, activated microglia can acquire distinct functional states. Transformation of microglia to reactive state in response to pathology is very diverse and dynamic process. Chronic pathology in CNS can lead to persistently activated state of microglia which can harm their neighbor environment.

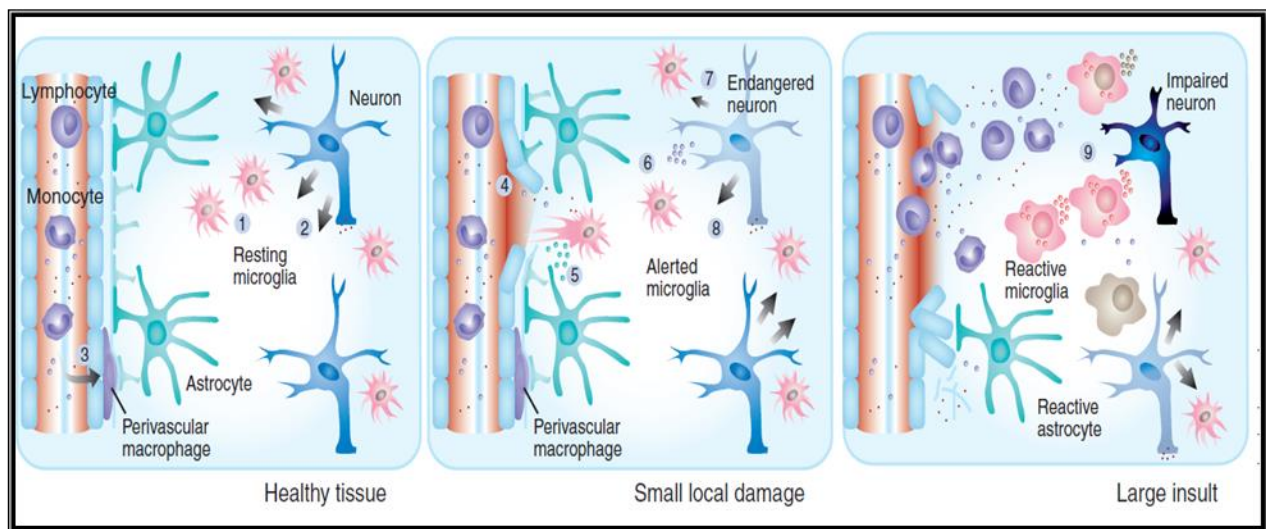


**Figure 6-7. Activation States of Microglia**

As shown in **figure 6-7** (Hanisch and Kettenmann 2007), in healthy tissue, microglia are in a surveying state. In this state, neurons may be continuously emitting signals which keep them in that state. However, upon minor changes in the state of the CNS, microglia respond by reorganizing their processes toward the site of insult. Neighboring astrocytes can support



microglia by releasing appropriate ligands such as purinoceptor ligands. During minor injuries, microglia release anti-inflammatory and neurotrophic molecules which can protect endangered neurons from insult. Neurons can cause microglial transformations by preventing or altering the release of “calming signals” that are present under normal conditions. Small local damages usually go unnoticed as it is very difficult to distinguish transformed microglia from surveying microglia after some period following injury. Significant infections, neurotoxic challenges or significant tissue injury can cause a large insult to the CNS. These drastic changes can alter the functional phenotype of microglia. These types of chronic or disruptive insults significantly damage the normal functions of microglia and neurons. Under these circumstances, microglia adopt an “activated” state which can result in damage to neighboring neurons and induce chronic pathology.

### **6.8.2 Microglia cells-Role in various neurodegenerative disorders**

Activated microglia have been found in various chronic neurodegenerative disorders such as Parkinson’s disease (PD), Alzheimer’s disease (AD), Amyotrophic lateral sclerosis (ALS), multiple sclerosis (MS), Kreutzfeldt-Jacob disease, etc. It is important to note there is no specific single activated state of microglia. Activated microglia can have diverse profiles of chemokines, cytokines, or cell-surface receptor expression patterns based on their exposure to native chemical or cell-based environmental cues. A positive feedback loop has been hypothesized in which microglia become activated by neuronal degeneration, then secrete neurotoxic molecules which, in turn, promote further neurodegeneration. Neurodegenerative diseases progress slowly and the morphology of activated microglia under these conditions is not well defined. A variety of receptors known as “Damage Associated Molecular Patterns” (DAMP) have been shown to be present on the microglial membranes.

Microglial morphology may be different in neurodegenerative disease such as AD in which misfolded proteins accumulate extracellularly, whereas in diseases such as PD, ALS, and Huntington's disease, accumulations of misfolded proteins occur inside microglia, neurons, and astrocytes. The morphology of activated microglia may vary widely in the latter diseases compared to AD. Peripheral benzodiazepine receptors have been shown to upregulate in activated microglia. A benzodiazepine ligand, C-R-PK11195 has been developed to image activated microglia in living brain. PET-imaging using C-R-PK11195 has shown that cognitive function in AD patients is inversely proportional to C-R-PK11195 signal.

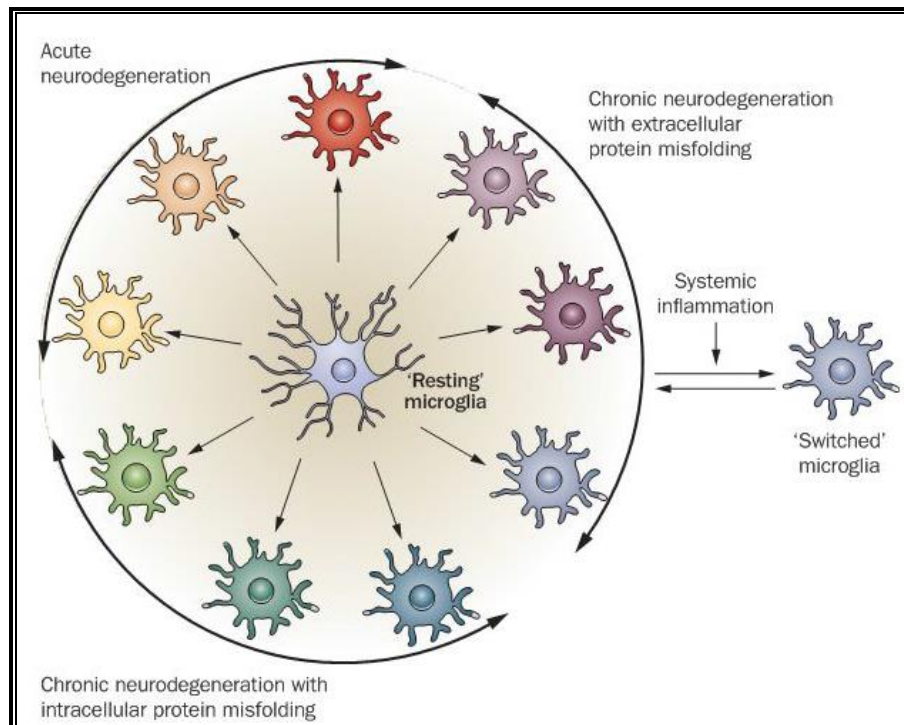


**Figure 6-8.** Possible cues that can activate (or “switch”) microglia

### 6.8.3 Microglia cells- Effect of acute injury

Acute exposure to endotoxins or neurotoxins (including METH) can also activate microglia. Acute injury can expose microglia to serum proteins such as albumin. It can also

cause increased local concentrations of glutamate, ATP, and ADP. These types of signals are sensed by microglia as dangerous. In response, they transform into an activated state. The response of microglia is not a linear process; rather, it is highly dependent on the nature of stimulus, the receptors involved, and the prior state of the microglia.

There is some evidence showing that the number of microglia in mouse substantia nigra is highest followed by striatum. Various acute neurodegeneration models involving dopaminergic toxins have been widely studied. 6-OHDA, MPTP, rotenone, and METH have been shown to cause dopaminergic neurodegeneration and microglial activation. The inflammatory agent lipopolysaccharide (LPS) has been shown to cause selective death of dopaminergic neurons when injected into the substantia nigra. LPS also causes microglial activation in brain. However, dopaminergic neurons may be undergoing selective degeneration because of a distinct local population of microglia and astrocytes present in substantia nigra.

Using 2-photon imaging technique, two independent studies have shown that acute tissue injury causes neighboring microglia to re-orient their processes toward the site of injury and increases their capability to phagocytose the foreign material being introduced into the CNS. Minor acute injuries can trigger the transformation of microglia such that they would protect the neighboring environment from toxic insult and shield the injured site. Massive injury can release overwhelming amounts of foreign material into the CNS, causing microglia to overreact and resulting in their persistent activation - a potentially harmful state.

### **6.9 Microglia activation- Possible molecular mechanisms**

To understand how microglia transform from a surveying to an activated state, it is of utmost importance to understand the molecular mechanisms involved in this process. To

understand the molecular mechanisms, it is essential to know which type of surface receptors, chemokines, cytokines, and other secretory molecules are released from microglia under normal and pathological states.

### **6.9.1 Microglia molecular expression under healthy and “pathological” states**

As discussed previously, microglia continuously survey their environments using their fine processes and quickly respond to potential harm. This implies that microglia must have a complex communication network of molecules through which they can continuously integrate environmental inputs and respond appropriately. As such, microglia should have molecular machinery by which they can interact with the surrounding neurons and astrocytes. Microglia signaling can be distinguished as an “ON” or “OFF” process. The "OFF" signal may be inferred as a “healthy” environment, where the neighboring environment is under homeostatic conditions. Detection of foreign molecules can trigger the “ON” signal, causing expression of distinct molecules instructing the microglia to neutralize the foreign molecule, protecting the susceptible cell population.

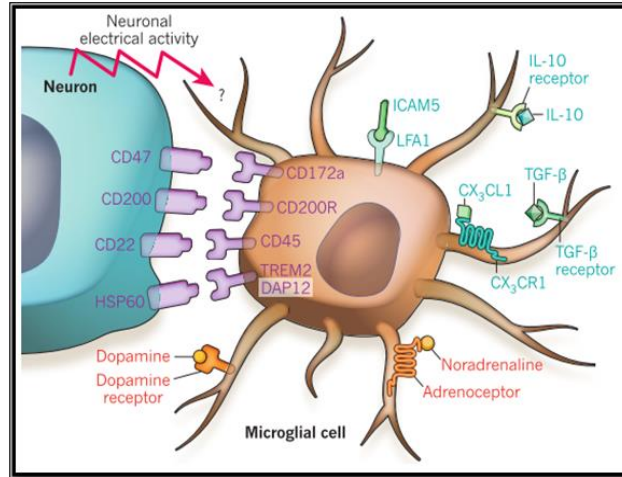


**Figure 6-9. Neuronal inhibitory influences on parenchymal microglia**

(Ransohoff and Cardona 2010)

One particular hypothesis is based on the “OFF” signal. It assumes that if the “OFF” signal has been terminated, it causes microglia to transform into the activated state. This hypothesis is important to understand as microglia which are very similar cells to mononuclear phagocytes, express ion channels, neurotransmitter receptors, and have very high expression of purinergic receptors.

Microglia continuously receive “OFF” signals from neurons via a contact-dependent receptor interaction as well as soluble factor/cytokine based signals, which under normal conditions keep microglia in the surveying state. Contact-dependent inhibition occurs by CD200-CD200R, HSP60-TREM2-DAP12, CD22-CD45, and CD47-CD172A, whereas, ICAM5 (Intracellular Adhesion Molecule-5) and LFA-1 (Lymphocyte Function Associated antigen-1), CX3CL1-CX3CR1, IL-10- IL-10 receptor, and TGF- $\beta$ -TGF- $\beta$  receptor signals are soluble factor/cytokine mediated signals.

Microglia also possess neurotransmitter receptors on their surface and thus may react to abrupt changes in concentration of the respective neurotransmitters. Various neurotransmitter receptors such as GABA receptors, glutamate receptors, adrenergic receptors and DA receptors have been shown to be present on the microglial cell surface. Purinergic receptors are also present in high abundance. The activation of microglial receptors has been shown to alter the immunological functioning of microglia. Therefore, extra-synaptic neurotransmitter receptors may play important roles in various regulatory functions.

### **6.9.2 Microglial pattern recognition receptors for sensing neighbor environment**

Microglia can enter an activated state in response to environmental toxins and endogenous proteins. Diverse toxin signals are thought to be translated into microglial ROS production through pattern recognition receptors (PRR). A variety of PRRs have been shown to be present on the microglial surface, which can identify diverse arrays of molecular determinants. Therefore, a wide range of foreign or toxic molecules can also be readily recognized, and microglia can respond to protect the native environment - when the insult is small and controllable. Various molecules such as estrogen, glucocorticoids, neuropeptides, and anti-inflammatory cytokines such as IL-10 and TGF- $\beta$  can inhibit microglial activation under small insult condition. However, massive insult by foreign molecules or toxic components can cause over-activation of microglia. This over-activation can result in the over-expression of iNOS and COX-II which cause ROS generation. In addition, microglia can also release pro-inflammatory cytokines such as IL-1 $\beta$  and TNF $\alpha$ . Over-activation of microglia can also cause overexpression of NADPH oxidase, generating massive amounts of ROS inside microglia cells

as well as in their immediate environment. Chronic over-activation of microglia can even result in neuronal death, which is observed in various neurodegenerative diseases.

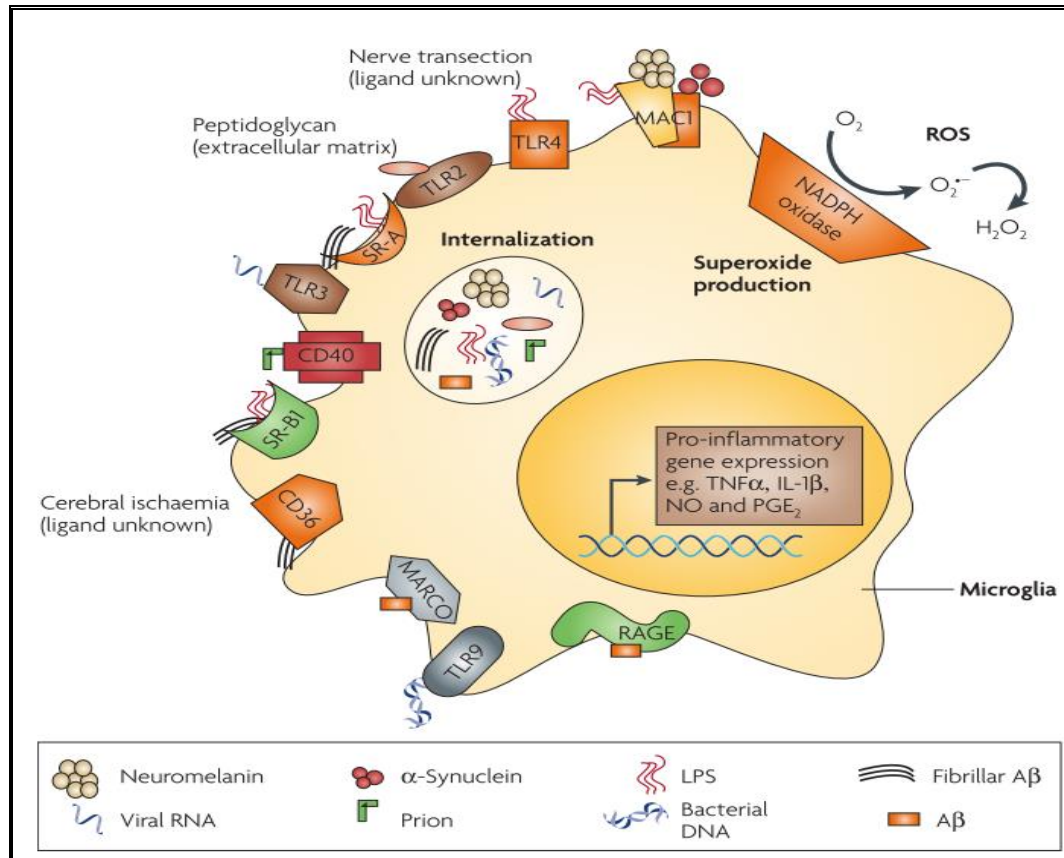


**Figure 6-10. Microglial PRRs identify neurotoxic and pro-inflammatory ligands**

(Block, Zecca et al. 2007)

Microglial PRRs identify and bind pathogen associated molecular patterns by PRRs. Toll-like receptors (TLRs) are one of the widely studied PRRs. Microglia have been shown to express 9 different types of TLRs. TLR4 is primarily responsible for LPS-induced neurotoxicity. Various TLRs have been shown to be responsible for microglia-induced immune responses. Activation of TLRs mainly induce microglial response resulting in the production of NO.

Another class of PRRs are scavenger receptors, which recognize various modified lipoproteins and polyanionic ligands. The activation of scavenger receptors has been shown to result in ligand internalization and/or the production of extracellular superoxide by microglia. Macrophage antigen complex-1 (MAC-1) functions as an adhesion molecule and PRR that recognizes a variety of ligands. MAC-1 receptors are located on microglia and have been shown to be part of a primary mechanism by which toxins activate microglia to produce extracellular superoxide, inducing subsequent neurotoxicity. It has also been demonstrated that multiple PRRs can identify a single neurotoxin, implying that combinations of receptors may be involved in the recognition of some neurotoxic ligands. NADPH oxidase is known to be responsible for the generation of ROS following microglia activation. MAC-1 receptors may be crucial for microglial NADPH oxidase activation in response to neurotoxic insult. NADPH oxidase has also been shown to generate extremely high levels of ROS under neurotoxic stimuli, which can cause microglia to generate various proinflammatory molecules, causing inflammation in surrounding areas.



## CHAPTER 7

### HYPOTHESES

Our lab initially carried out a microarray analysis on striatum of METH-treated animals and observed significant changes in genes related to inflammatory or immune responses, receptor/signal transduction components and ion channel/transport proteins. Subsequently, we established that microglial activation is induced specifically in striatum following a neurotoxic METH regimen (Thomas, Dowgiert et al. 2004). We were also able to verify that other brain areas displayed a normal microglial phenotype (Thomas, Walker et al. 2004). We also demonstrated that NMDA receptor antagonists such as MK-801 and dextromethorphan were able to attenuate METH-induced microglial activation in striatum (Thomas and Kuhn 2005), suggesting excitotoxicity must be involved. Furthermore, striatal gene expression studies and knockout mouse studies indicated that cyclooxygenase-2 (COX-2) is essential for METH-induced dopaminergic neurotoxicity. From the same study we concluded that the peroxidase activity of COX-2, which leads to the formation of ROS including dopamine quinones, is responsible for METH-induced neurotoxicity in striatum (Thomas and Kuhn 2005). Microarray analysis of cultured microglia treated with DA quinones demonstrated that various genes associated with microglial protective and phagocytic functions decreased in expression, whereas, genes associated with inflammatory and cytokine functions increased in expression (Kuhn, Francescutti-Verbeem et al. 2006). Thus, increased oxidative stress may play an important role in microglial activation, especially by increasing DA's oxidation to DA quinones. Our additional findings using LPS and HIV-tat protein to activate microglia also showed similar genetic expression changes in cultured microglia cells (Thomas, Francescutti-Verbeem et al. 2006).

From our previous studies, we hypothesized that, as METH causes striatal-specific activation of microglia, METH should induce significant alterations in protein expression of striatal microglia, and understanding these changes will elucidate the mechanisms of neurotoxicity induced by METH. In addition, we also hypothesized that either the unique striatal environment or the differential protein expression by microglia in other brain regions may be responsible for striatal specific microglial activation. Quite possibly, the elucidation of protein expression profiles might assist in the understanding of METH addiction and its treatment.

### **RATIONALE AND STUDY DESIGN**

The main objective of the first part of this project was to develop a cell-culture model for METH-induced neurotoxicity using cultured microglia cells. We focused on determining the proteomic expression changes in BV2 murine microglial cells after their treatment with low dose METH, high dose METH, and LPS in presence or absence of MN9D cells. We used the BV2 microglial cell line because it is well-established, widely used, and is derived from murine mesencephalic microglia. BV2 cells retain many of the functions and features of *in vivo* microglia, thus they serve as an ideal cell model system (Henn, Lund et al. 2009). We planned to co-culture MN9D and BV2 cells if unable to observe significant protein expression changes in BV2 cells with METH treatment. We planned to use MN9D cells as they possess tyrosine hydroxylase and DA, and can partially recapitulate dopaminergic neurons to assess the direct effect of METH on microglia as well as indirect effects of METH treated dopaminergic neurons on microglial protein expression. We determined to use two different doses of METH because of the possibility that METH might alter microglial protein expression in different manners at low (50  $\mu$ M) and high doses (500  $\mu$ M). We used LPS, as we successfully carried out microarray

analysis of BV2 microglia following LPS treatment and had possession of their gene expression profile (Thomas, Francescutti-Verbeem et al. 2006). We planned to determine protein expression changes of microglia (as opposed to gene expression changes), as proteins are ultimately responsible for the phenotypic changes under pathological conditions.

To achieve the objectives of this project, I determined cellular viability of BV2 cells following their exposure to low dose METH, high dose METH, and LPS. I also determined the effect of each treatment on dopaminergic levels in MN9D cells. Proteomic expression profiles for each treatment were evaluated to understand the effects of each treatment. To accomplish my objectives, I proposed to:

- ❖ Test the ability of low dose METH, high dose METH or previously used doses of LPS to alter the viability of BV2 cells.

This analysis was crucial to evaluate the data obtained from proteomic study. If METH significantly altered cellular viability, it may manifest as an alteration in protein expression may or may not be important for METH-induced neurotoxic damage and/or its addictive properties. The interpretation of data from the proteomic studies would be more conclusive after understanding each treatment's direct effect on cell viability.

- ❖ Test the ability of different drug treatments to alter DA levels in the dopaminergic cell line MN9D.

This experiment was carried out to determine if METH or LPS have the ability to deplete DA levels from the dopaminergic MN9D cell line. As we previously carried out microarray analysis of cultured microglia cells using DA quinones, it would be highly relevant to understand

the direct effect of DA and probably other molecules released from MN9D cells following their treatment with METH or LPS. Therefore, it is important to understand the effect of each treatment on DA levels in MN9D cells.

- ❖ Test the proteomic expression change of BV2 cells following their treatment with low dose METH, high dose METH, and LPS.

This experiment was important as there are not many findings that have measured the effect of METH on cultured microglia cells. At the very least, our findings would provide us an understanding as to whether or not any significant protein expression changes take place in the cellular proteome following exposure to different doses of METH or LPS.

- ❖ Verify the proteomic expression changes of BV2 cells exposed to low dose METH, high dose METH, and LPS following growth in an environment where they have had access to various secretory molecules (including DA) from the MN9D cell line.

This experiment was carried out to understand the possible influence of secretory factors (including DA) released from MN9D cells upon exposure to low dose METH, high dose METH, and LPS, in addition to the drug's direct influence on protein expression changes induced on cultured microglia cells. This experiment could be highly relevant to an *in vivo* state as it would involve two cell types (dopaminergic neurons and microglia cells), both of which have been shown to be affected by exposure to METH.

The main objective of the second part of this study was to evaluate the proteomic expression changes in microglia isolated from the striatum of animals treated with METH and

compare to the microglial profile from untreated controls. To achieve these objectives, I proposed to:

Compare various methods of microglia isolation and determine the most suitable method for isolation of highly pure microglial fractions from various brain tissues of the transgenic mouse strain B6.129P- Cx3cr1tm1Litt/J.

The rationale behind using the transgenic mouse strain (B6.129P- Cx3cr1tm1Litt/J) was to have the ability to readily isolate microglia from all other brain cells. In this transgenic strain, the fractalkine receptor gene of microglia has been knocked out and a gene encoding enhanced green fluorescent protein (eGFP) knocked-in, resulting in microglia that express eGFP (Thomas, Francescutti-Verbeem et al. 2008). The rationale behind comparing various methods of microglia isolation was to determine the best possible method to isolate microglia. It was of utmost importance to optimize a rapid isolation protocol that could be used downstream of our animal experiments. We compared fluorescence activated cell sorting (FACS), magnetic activated cell sorting (MACS), and density gradient centrifugation procedures. Subsequently, we optimized a density gradient centrifugation protocol to isolate microglia from various brain regions. Flow cytometry and fluorescence microscopy were used to verify microglia purity. These methods were ideal as all microglia expressed eGFP and could be easily distinguished from non-microglia. We also performed microglial isolation on wild-type mice (C57BL6), and labeled them with CD11b (a microglia-specific antigen) antibody to compare their purity with those isolated from the eGFP mice.

- ❖ Isolate microglia from the striatum of non-treated control animals (C57BL6 mice) and animals treated with METH and determine changes in their protein expression.

The purpose of this experiment was to compare the striatal microglia protein expression profiles from METH-treated and untreated animals. Due to the specificity of their activation, only striatal microglia examined. Evaluating the differences in protein expression between striatal microglia isolated from control animals and METH-treated animals might assist us in identifying specific proteins involved in the neurotoxic and/or addictive processes following METH administration.

## CHAPTER 8

### MATERIALS AND METHODS

#### 8.1 Materials

Methamphetamine hydrochloride, methyl thiazolyl blue tetrazolium bromide (MTT), LPS (from *E.coli* serotype 055:B5), dimethyl sulfoxide (DMSO), poly-L-lysine, and dopamine hydrochloride were purchased from Sigma. Methanol, sodium phosphate (monobasic), sodium citrate, ethylene diamino tetraacetic acid (EDTA), sodium hydroxide, tris, glycine, sodium dodecyl sulfate (SDS), fetal clone-III bovine serum, and perchloric acid were purchased from Fisher Scientific. Heptane sulfonic acid was purchased from TCI. BCA protein assay kits were purchased from Pierce. Nano orange protein quantification kits, DPBS, 1X PBS, DMEM media, penicillin/streptomycin, trypsin, and 8-16% tris-glycine gels were purchased from Invitrogen. CD11b microbeads, CD11b-FITC antibody, LS columns, and column adapters were purchased from Miltenyi Biotech. Percoll was purchased from GE Healthcare. 6 well plates with 0.45 $\mu$ M inserts and CD11b-APC antibody were purchased from BD Biosciences.

#### Cell culture and treatments

The hybridoma dopaminergic MN9D cells are derived from the somatic infusion of rostral mesencephalic neurons from embryonic C57BL/6J (E14) mice with N18TG2 mouse cells. MN9D cells were obtained from Dr. Michael Zigmond's laboratory. They were cultured in T-75 flasks (Greiner Bio One, Frickenhausen, Germany) coated with 1 mg/ml poly-L-lysine and maintained in DMEM (high glucose with phenol red) supplemented with 10% fetal Clone III serum, penicillin (50 units/ml) and streptomycin (50  $\mu$ g/ml) at 37°C under 5% CO<sub>2</sub> atmosphere.

Murine microglia BV2 cells were grown in DMEM (high glucose with phenol red) supplemented with 5% fetal calf serum, 1mM sodium pyruvate, and 100 U/ml penicillin/streptomycin in T-75 flask. Cells were maintained at 37°C under 5% CO<sub>2</sub>.

For co-culture experiments, BV2 and MN9D cells were incubated with their corresponding media in 1:1 proportions. Methamphetamine hydrochloride and LPS were dissolved in media as stock solutions. Methamphetamine hydrochloride solutions were prepared fresh every time, whereas LPS aliquots were prepared and stored at -20°C.

### **Animals**

Female C57BL/6 mice (Harlan, Indianapolis, IN, USA) were primarily used for proteomic expression experiments and, in some instances, additional protocols to verify the reproducibility of microglia isolation. For the optimization of microglial isolation protocol, mice in which the CX3CR1 gene was deleted and replaced with a cDNA of eGFP (Jung, Aliberti et al. 2000) were purchased as breeding pairs from The Jackson Laboratory (Bar Harbor, ME; strain B6.129P-Cx3cr1tm1Litt/J). Mice homozygous for the deletion of the CX3CR1 gene were used to establish a colony of male and female offspring for use in these studies. All mice were housed five per cage in large shoebox cages in a light- and temperature-controlled room and were approximately 8-10 weeks old at the time of experimentation. Mice had free access to food and water. The Institutional Animal Care and Use Committee of Wayne State University approved the animal care and experimental procedures. All procedures were also in compliance with the NIH Guide for the Care and Use of Laboratory Animals.

### **8.2 Measurement of BV2 cell viability**



To determine the effect of each treatment on BV2 cell viability, quantitative and colorimetric MTT assays were used. BV2 cells were plated at a density of 10,000 cells/well in 96 well plates and afforded 24 hours of growth to ensure adherence. BV2 cells were treated with the above mentioned treatments for 6 hours, 12 hours or 24 hours. After incubation, MTT was added to each well at final concentration of 0.5 mg/mL and the plate was further incubated at 37°C in 95% air/5% CO<sub>2</sub> atmosphere for 3 hours to produce dark blue formazan crystals. The supernatants were carefully removed and the formazan crystals dissolved by adding 100 µL of a DMSO/methanol (50:50) mixture to each well and shaking the plate gently at room temperature for 30 minutes. The absorbance values were measured using a microplate reader at 570 nm with a background correction done at 690nm. Data from 3 experiments were analyzed using GraphPad software (Version 4, San Diego, USA). Cell viability was defined as a percentage reduction in absorbance compared to untreated controls.

### **8.3 Measurement of dopamine levels in MN9D cells**

Two different protocols were followed to determine DA levels in MN9D cells.

- I. To determine the direct effect of each treatment on dopaminergic neurons, DA levels of MN9D cells were determined using HPLC coupled with electrochemical detection. MN9D cells were plated at  $5 \times 10^5$  cells/well in 6 well plates for 48 hours to allow their attachment. Adherent MN9D cells were treated with 50 µM METH, 500 µM METH or LPS (100 ng/mL) for 12 hours. After incubation, the media was removed and cells washed with 1X PBS. 50 µL 0.16N perchloric acid was added to each well and cells were harvested with a rubber policeman and sonicated 3 times for 5 seconds each. Cell lysates were centrifuged at 14000 rpm

for 10 minutes at 4°C. The resulting supernatant was diluted 1:4 with 0.16N perchloric acid. 50 µL of the resulting mixture was used to determine DA levels using a Shimadzu HPLC system equipped with an electrochemical detector and reverse phase C18 column. The mobile phase consisted of 50 mM sodium citrate, 50 mM sodium phosphate, 200 µM EDTA, 1.5 mM heptane sulphonic acid, and 14% methanol. Concentrations of DA were quantified by interpolating peak areas relative to those generated by a range of DA standards that were run in parallel. DA levels were adjusted by determining protein concentrations of cell pellets by BCA protein assay, which were dissolved by boiling at 95°C for 5 minutes in 50 µL 0.5M sodium hydroxide.

- II. To determine the direct and indirect effects of each treatment on dopaminergic neurons, DA levels of MN9D cells cultured with BV2 cells were determined using HPLC. MN9D cells were plated at a density of  $2 \times 10^5$  cells/well in a 6 well plate insert, and BV2 cells were plated at  $5 \times 10^5$  cells/well density in 6 well plate. The plate was incubated for 48 hours to allow the attachment of both cell lines. Adherent MN9D and BV2 cells were treated with 50 µM METH, 500 µM METH or LPS (100 ng/mL) for 12 hours. After incubation, the media was removed and cells were washed with 1X PBS. MN9D cells were harvested by adding 50 µL 0.16N perchloric acid to each well. Cells were harvested with a rubber policeman and sonicated 3 times for 5 seconds each. Cell lysates were centrifuged at 14000 rpm for 10 minutes at 4°C. The resulting supernatant was diluted 1:4 with 0.16N perchloric acid. 50 µL of the resulting mixture was used to determine DA levels using a Shimadzu HPLC system equipped with an electrochemical detector and

reverse phase C18 column. The mobile phase consisted of 50 mM sodium citrate, 50 mM sodium phosphate, 200  $\mu$ M EDTA, 1.5 mM heptane sulphonic acid, and 14% methanol. Concentrations of DA were quantified by interpolating peak areas relative to those generated by a range of DA standards that were run in parallel. DA levels were adjusted by determining the protein concentrations of cell pellets by BCA protein assay, which were dissolved by boiling at 95°C for 5 minutes in 0.5M sodium hydroxide.

#### **8.4 Determination of changes in protein expression in BV-2 cells**

To determine changes in protein expression, BV-2 cells were plated at  $5 \times 10^5$  cells/well in 6 well plates for 24 hours to allow their attachment. Adherent BV-2 cells were treated with 50  $\mu$ M METH (low dose METH), 500  $\mu$ M METH (high dose METH), or LPS (100 ng/mL) for 12 hours. After incubation, media was aspirated and cells were washed twice with 1X PBS. Washed cells were lysed with 1% SDS and protein concentrations were determined using a BCA protein assay kit. 15 $\mu$ g of protein from each treatment were fractionated on 8-16% tris-glycine gradient gels. Gels were stained with SYPRO-ruby dye. Each lane was cut into 20 pieces, reduced, alkylated and digested. The resulting peptides were separated by reverse phase chromatography (Magic C18 column, Michrom), followed by ionization with ADVANCE ion source (Michrom), and introduced into an LTQ-XL mass spectrometer (Thermo Electron). The data was analyzed using scaffold (Proteome software).

#### **8.5 Determination of changes in protein expression in BV-2 cells in the presence of secretory factors released by MN9D cells**

To determine the effect of various soluble factors (including DA) released from MN9D cells upon exposure to various treatments as well as the direct effects of the treatments, 6 well plates with cell-culture inserts were used. MN9D cells were plated at  $2 \times 10^5$  cells/well on cell culture inserts and BV-2 cells were plated at  $5 \times 10^5$  cells/well in the wells of the same plate. The inserts were made of a  $0.45 \mu\text{M}$  semi-permeable membrane which allowed various soluble factors (including DA) released from MN9D cells to pass the membrane and come into contact with BV-2 cells. 48 hours after plating, the cells were treated with  $50 \mu\text{M}$  METH,  $500 \mu\text{M}$  METH or  $100 \text{ ng/mL}$  LPS for 12 hours. After incubation, the media was aspirated and the inserts containing MN9D cells were removed (they were used for HPLC determination of DA levels) and BV-2 cells were washed twice with 1X PBS. Washed cells were lysed with 1% SDS and protein concentrations determined using a BCA protein assay kit.  $15 \mu\text{g}$  of protein from each treatment were fractionated on 8-16% tris-glycine gradient gels. Gels were stained with SYPRO-ruby dye. Each lane was cut into 20 pieces, reduced, alkylated and digested. The resulting peptides were separated by reverse phase chromatography (Magic C18 column, Michrom), followed by ionization with ADVANCE ion source (Michrom), and introduced into an LTQ-XL mass spectrometer (Thermo Electron). The data was analyzed using Scaffold (Proteome software).

## **8.6 Development of a protocol to isolate purified fractions of microglia from brain tissue**

For this experiment, we used a transgenic mouse strain (B6.129P- Cx3cr1tm1Litt/J) which harbor eGFP labeled microglia. We evaluated 3 different isolation protocols designed to produce highly purified fractions of microglia from various brain regions. The first step is to prepare a single cell suspension of tissue before isolating microglia.

### **8.6.1 Preparation of single cell suspension from mouse brain tissue**

8-10 mice (B6.129P-Cx3cr1tm1Litt/J) were used for this experiment. Mice were sacrificed after briefly anesthetizing them with isoflurane. The brain was immediately isolated and regions of interest (striatum, hippocampus or prefrontal cortex) were pooled together in a petri-dish containing 3 mL 1X DPBS supplemented with 0.02% glucose. Tissues were minced using a sterile surgical blade before transferring to a 7 mL Dounce tissue homogenizer for further dissociation. The tissue homogenate was passed several times through a fire-polished Pasteur pipette before filtering through a 30 micron filter to remove non-dissociated cells. This filtrate represented the heterogeneous single cell suspension. The resulting single cell suspension was subjected to 3 different microglia-isolation methods to evaluate the best method to isolate highly pure fraction of microglia from different brain regions.

### **8.6.2 Evaluation of fluorescence assisted cell sorting to isolate microglia**

As microglia isolated from the mice expressed eGFP, we evaluated fluorescence activated cell sorting (FACS) to separate microglia from other cell types in the single cell suspension. The single cell suspension was subjected to FACS using FACSDiva (BD Biosciences). Microglia cells were sorted based on their green fluorescence because of their eGFP expression.

### **8.6.3 Evaluation of magnetic-activated cell sorting to isolate microglia**

The number of cells in the single cell suspension was determined and the cells were centrifuged at 300g for 10 minutes at 4°C. The cell pellet was resuspended in 180 µL buffer (1X PBS, 0.5% BSA, 2 mM EDTA, pH 7.2) then incubated with 20 µL CD11b microbeads for 15 minutes at 4°C. Cells were washed with 2 mL buffer then centrifuged at 300g for 10 minutes.

The supernatant was removed and cells resuspended in 500  $\mu$ L buffer. The labeled cell suspension was applied to an LS column (Miltenyi Biotech) in the presence of a strong magnetic field. Unlabeled cells were collected as a pass through, and the column was washed three times with 3 mL ice-cold buffer. The column was removed from the magnetic field and 5 mL buffer was used to elute the retained, labeled cells. Microglia were isolated based on their expression of CD11b receptors and the ability of CD11b microbeads to selectively bind to the receptors and be retained in column due to the strong magnetic field.

#### **8.6.4 Evaluation of density gradient centrifugation to isolate microglia**

The single cell suspension was centrifuged at 300g for 10 minutes at 4°C and the supernatant aspirated. The cell pellet was resuspended in 1 mL freshly prepared 70% sterile isotonic percoll (SIP). Resuspended cells were passed through a fire-polished Pasteur pipette several times to make a homogenous cell suspension. 2 mL freshly prepared 50% SIP was gently layered on top of 70% SIP layer using a fire-polished Pasteur pipette (without disturbing the 70% SIP layer). 1 mL 1X DPBS was gently layered on top of 50% SIP (without disturbing the 50% SIP layer). The resulting density gradient tube was centrifuged in a swinging bucket rotor centrifuge at 1200g for 45 minutes. After centrifugation, 2 distinct layers appeared at the interface of 1X PBS and 50% SIP as well as at the interface of 50% SIP and 70% SIP. Both the layers were removed and used for FACS analysis to determine the percentage of eGFP expressing microglia cells. The purity of the isolated fraction was also determined using fluorescence microscopy.

#### **8.7 Identification of protein expression profile of pure microglial fraction isolated from various brain regions following METH treatment**



assay kit. 5 µg proteins from each treatment were fractionated using 8-16% tris-glycine gradient gels. Gels were stained with SYPRO-ruby stain. Each lane was cut into 20 pieces, reduced, alkylated and digested. The resulting peptides were separated by reverse phase chromatography (Magic C18 column, Michrom), followed by ionization with ADVANCE ion source (Michrom), and introduced into an LTQ-XL mass spectrometer (Thermo Electron) The data was analyzed using Scaffold (Proteome software).



## CHAPTER 9

### RESULTS

#### 9.1 Methamphetamine causes time-dependent and dose-dependent decreases in BV2 cell viability

After exposure to various treatments for 6 hours, higher concentration of METH (500  $\mu$ M) significantly altered BV-2 cell viability. However, lower concentrations of METH (50  $\mu$ M) or LPS treatment did not alter BV-2 cell viability significantly as shown in **figure 9-1**. The toxicity profile of various treatments remained quite similar to 6 hours profile after exposure of BV2 cells for 12 hours (**figure 9-2**). We observed dose dependent reductions in cellular viability with METH in the case of the 24 hour treatment of BV-2 cells, whereas LPS treatment did not seem to affect cellular viability even after that longer exposure (**figure 9-3**).

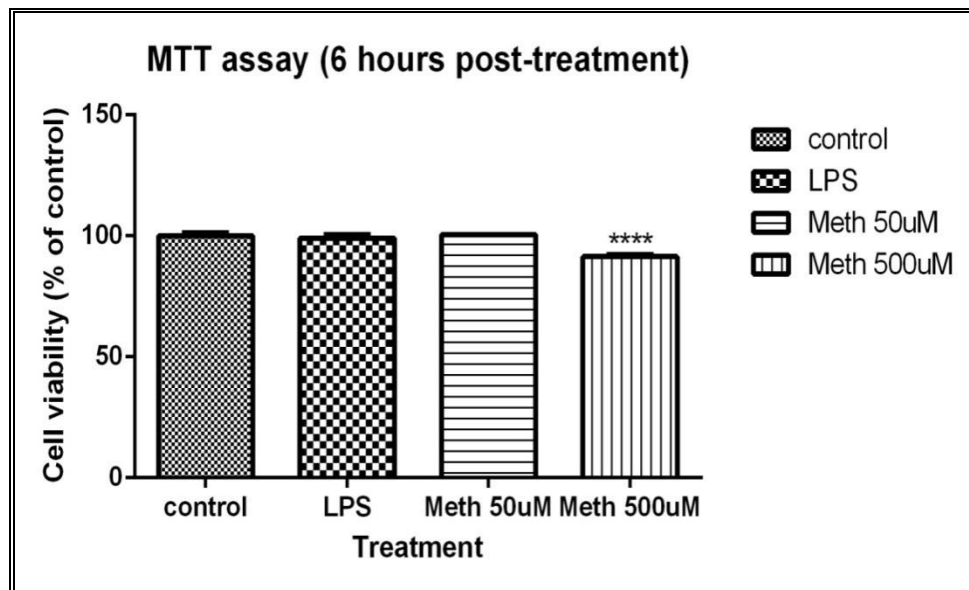


**Figure 9-1.** MTT assay BV2 cells (6 hours post-treatment)

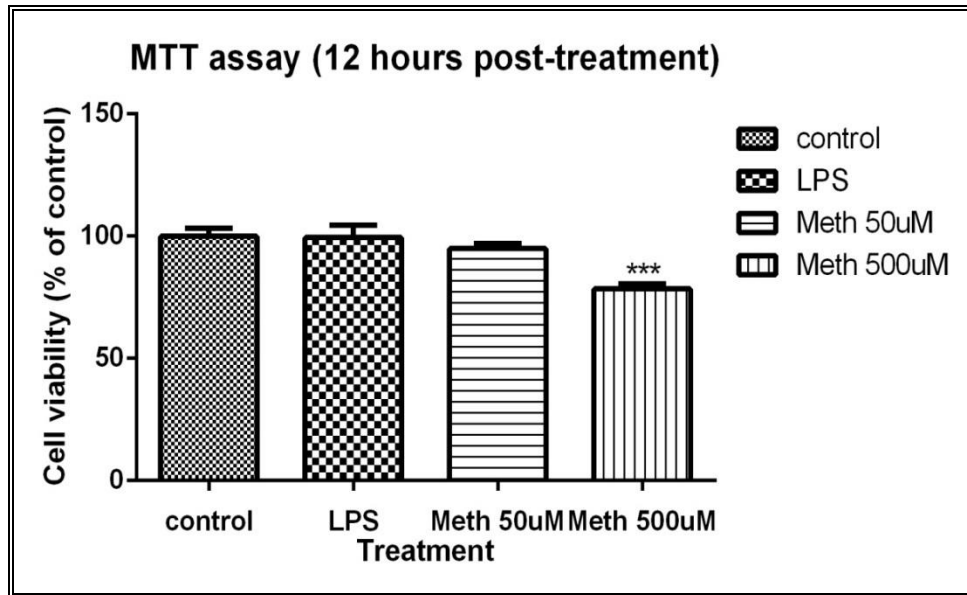


**Figure 9-2.** MTT assay BV2 cells (12 hours post-treatment)

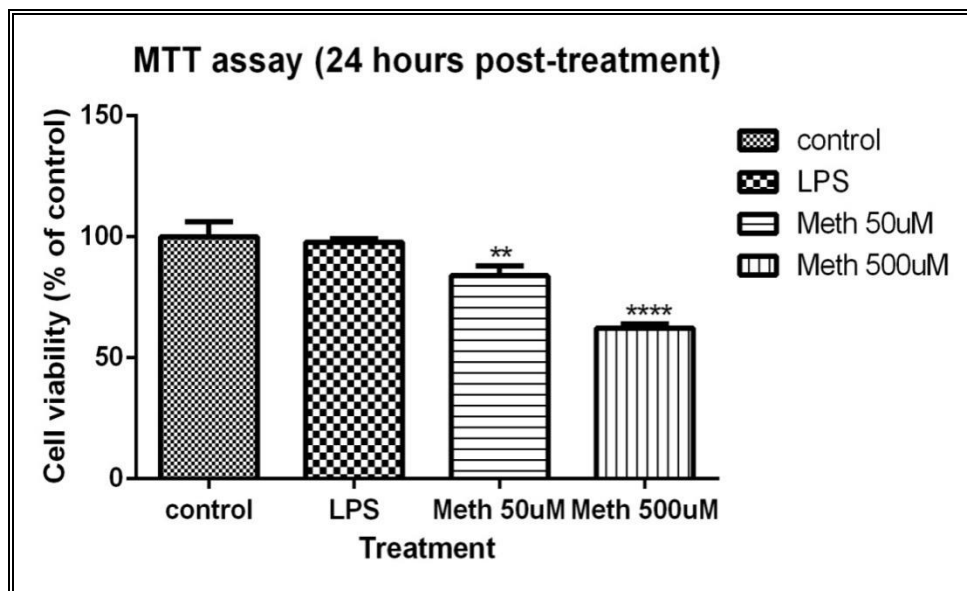


**Figure 9-3.** MTT assay BV2 cells (24 hours post-treatment)

9.2 Methamphetamine treatment causes a decrease in DA levels in MN9D cells

We observed significant reductions in DA levels in the dopaminergic neuronal cell line MN9D following their exposure to 50  $\mu$ M METH and 500  $\mu$ M METH for 12 hours. However, treatment with LPS induced a non-significant increase in DA levels of MN9D cells (**figure 9-4**).

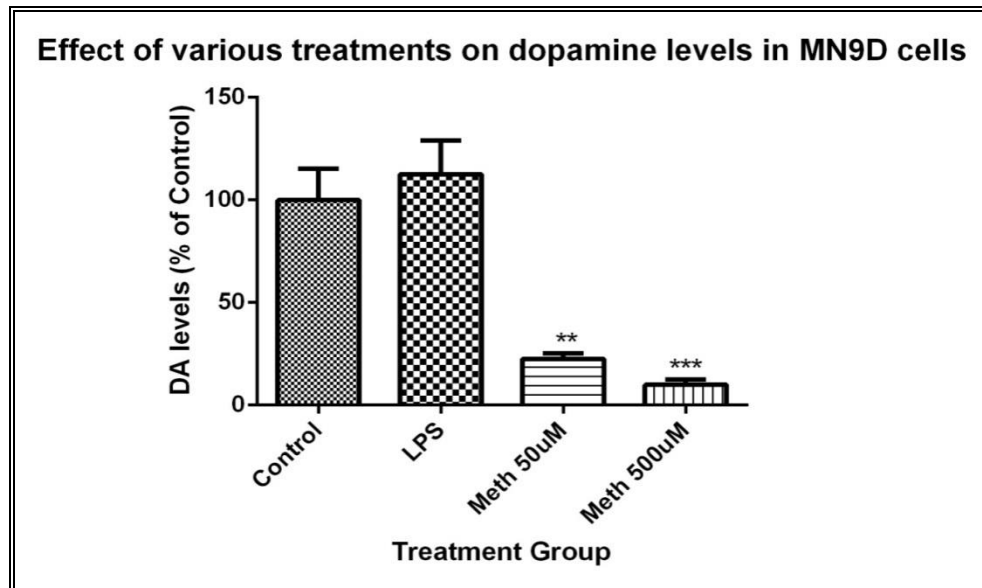


**Figure 9-4. Dopamine levels of MN9D cells (12 hours post-treatment)**

### 9.3 Methamphetamine treatment induces a decrease in DA levels of MN9D cells cultured in the presence of BV2 cells

The experiment utilizing cell-culture inserts to allow MN9D cells to be in indirect contact with BV-2 cells (to simulate tissue microenvironment) showed that both concentrations of METH caused a significant decrease in DA levels of MN9D cells. In the case of LPS treatment, we observed a non-significant reduction in DA levels of MN9D cells (**figure 9-5**).

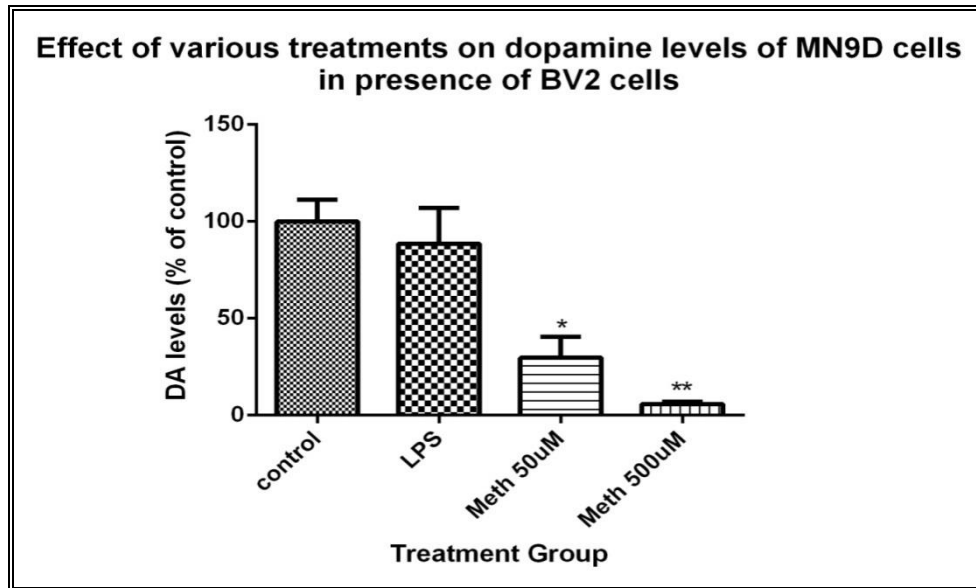


**Figure 9-5.** Effect of various treatments on dopamine levels of MN9D Cells cultured in presence of BV-2 cells

9.4 Treatment of BV-2 cells with different agents results in significant protein expression changes compared to untreated control cells

We observed significant alterations in protein expression following treatment of BV-2 cells with various treatments. Some proteins were induced upon treatment with LPS, METH 50 µM or METH 500 µM treatment, whereas expression of some proteins was completely attenuated following treatment. As shown in **figure 9-6**, we found 3061 proteins were expressed in both control and LPS-treated BV-2 cells, whereas, LPS-treated BV-2 cells expressed 119 proteins that were exclusive, and untreated BV2 cells expressed 90 exclusive proteins.

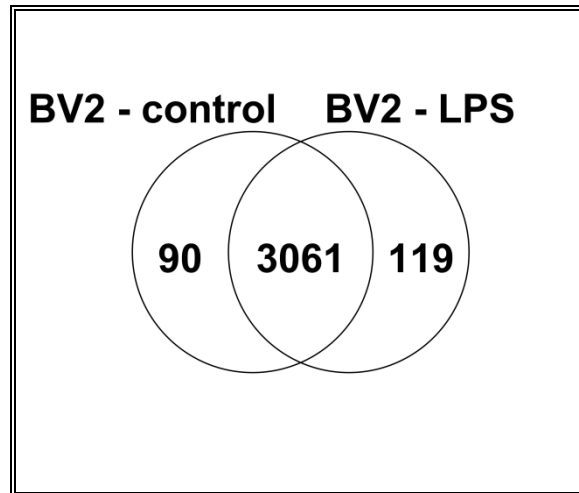


**Figure 9-6. Protein expression changes between control and LPS-treated BV-2 cells**

Statistical analysis ( $p$ -value  $< 0.05$ ) revealed the expression of 161 proteins as significantly altered following LPS treatment of BV-2 cells. Upon further examination, it was observed that significantly altered proteins represented molecules associated with cell survival and cell death, cell function and cell maintenance, cellular compromise, cell morphology, and protein synthesis. The most significantly altered proteins included inducible nitric oxide synthase, poly [ADP-ribose] polymerase 14, immune-responsive gene 1 protein, pyruvate kinase isozymes M1/M2, heme oxygenase 1, macrophage migration inhibitory factor, interferon-induced very large GTPase 1, histone H4, interferon-activatable protein 204, prostaglandin G/H synthase 2, prolow-density lipoprotein receptor-related protein 1, signal transducer and activator of transcription 1, intercellular adhesion molecule 1, profilin-1, integrin alpha-5, heat shock cognate 71 kDa protein ( $p$ -value  $< 0.0001$ ).

With 50  $\mu$ M METH treatment, we observed that 3062 proteins were expressed in untreated and 50  $\mu$ M METH treated BV-2 cells. However, 89 proteins were exclusively present in untreated BV-2 cells and 95 proteins were exclusively expressed in BV-2 cells treated with 50  $\mu$ M METH (**figure 9-7**). Statistical analysis ( $p$ -value  $< 0.05$ ) revealed that expression levels of

36 proteins were significantly altered following the treatment of BV-2 cells with 50  $\mu$ M METH. Significantly altered molecules were associated with dermatological diseases, developmental disorders, neurological disorders and connective tissue disorders. Significantly altered proteins included keratin family proteins, talin-1, talin-2, UDP-N-acetylhexosamine pyrophosphorylase, histone-H2A, serine-threonine protein phosphatase 6, heat-shock related 70 kda protein, pyruvate kinase isozymes M1/M2, mitochondrial 10-formyltetrahydrofolate dehydrogenase, and melanoma inhibitory activity protein ( $p$ -value < 0.01).

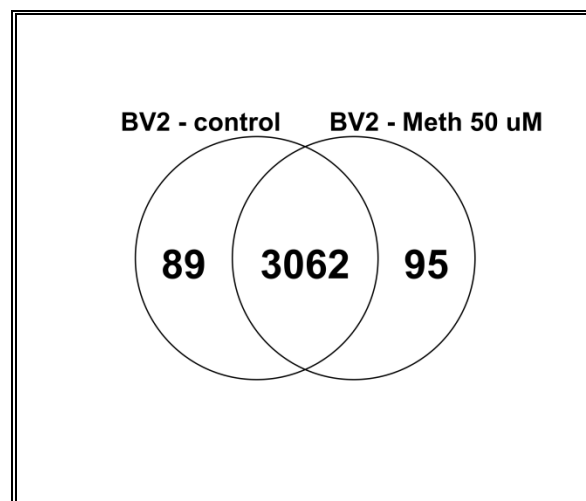


**Figure 9-7. Protein expression changes between control and 50  $\mu$ M METH-treated BV2 cells**

With the 500  $\mu$ M METH treatment, we observed that 3083 proteins were expressed in untreated and 500  $\mu$ M METH treated BV-2 cells. Interestingly, 68 proteins were exclusively present in untreated BV-2 cells and 93 proteins were exclusively expressed in BV-2 cells treated with 500  $\mu$ M METH (**figure 9-8**). Statistical analysis ( $p$ -value < 0.05) revealed that expression levels of 62 proteins were significantly altered following treatment of BV-2 cells with 500  $\mu$ M METH. Significantly altered molecules were associated with cell morphology, cell death, cell

survival, cellular proliferation, nucleic acid metabolism, and small molecule biochemistry. Significantly altered proteins included keratin family proteins, heat-shock related 70kda protein, ATP synthase, E3- ubiquitin protein ligase, serine/arginine repetitive matrix protein, perilipin, endoplasmic reticulum resident protein, bi-functional purine biosynthesis protein, Rab GDP dissociation inhibitor ( $p$ -value < 0.01).

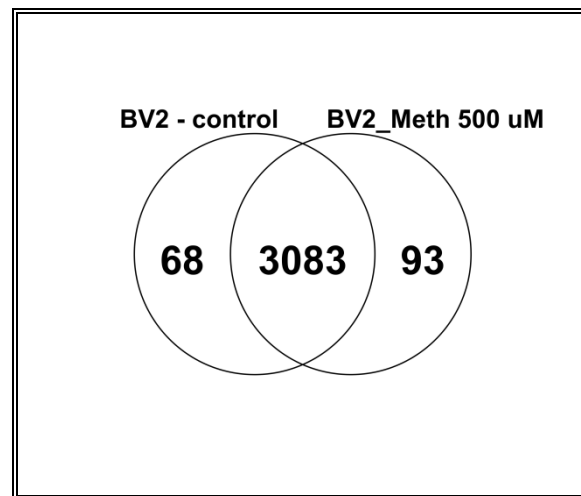


**Figure 9-8. Protein expression changes between control and 500  $\mu$ M METH-treated BV-2 cells**

9.5 Treatment of BV-2 cells (cultured in the presence of MN9D cells) with different agents resulted in significant protein expression changes compared to untreated control cells

We observed significant alterations in protein expression following treatment of BV-2 cells (cultured in the presence of MN9D cells) with various treatments. Some proteins were induced upon treatment with LPS, METH 50  $\mu$ M or METH 500  $\mu$ M treatment, whereas the expression of some proteins was completely attenuated following treatment. As shown in **figure**

**9-9**, we found 2886 proteins were expressed in both control and LPS-treated BV-2 cells, whereas LPS-treated BV-2 cells expressed 126 proteins that were exclusive and untreated BV-2 cells expressed 114 exclusive proteins.

Statistical analysis ( $p$ -value  $< 0.05$ ) revealed that expression of 273 proteins was significantly altered following LPS treatment of co-cultured BV-2 cells. Upon further examination, it was observed that significantly altered proteins represented molecules associated with carbohydrate metabolism, immunological disease, RNA post-transcriptional modification, molecular transport, nucleic acid metabolism, metabolic disease, energy production, neurological disease, cell growth and proliferation, cell survival. The most significantly altered proteins included inducible nitric oxide synthase, cytoplasmic dynein, alpha-enolase, filamin, talin-1, ADP-ribosylation factor 2, elongation factor-2, immune-responsive gene-2, histone H2A type 1-F, interferon-activable protein 204, signal transducer and activator of transcription 1, interferon-induced protein with tetratricopeptide repeats 1, mitochondrial ATP synthase, histone H2Ax, hemoglobin subunit alpha, interferon-induced very large GTPase, histone H2A type-2, E3 ubiquitin-protein ligase, UMP-CMP kinase 2, ubiquitin-like protein, vimentin, and flavin reductase ( $p$ -value  $< 0.0001$ ).



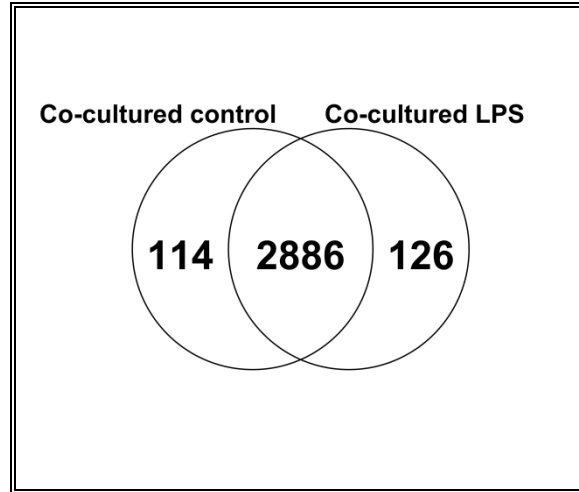


**Figure 9-9. Protein expression changes between control and LPS-treated co-cultured BV-2 cells**

With 50  $\mu$ M METH treatment, we observed that 2911 proteins were expressed in untreated and 50  $\mu$ M METH treated BV-2 cells. However, 89 proteins were exclusively present in untreated BV-2 cells and 119 proteins were exclusively expressed in BV-2 cells treated with 50  $\mu$ M METH (**figure 9-10**). Statistical analysis ( $p$ -value < 0.05) revealed that expression levels of 208 proteins were significantly altered following treatment of co-cultured BV-2 cells with 50  $\mu$ M METH. Significantly altered molecules were associated with RNA post-transcriptional modification, cell-to-cell signaling and interaction, inflammatory response, nucleic acid metabolism, energy production, cellular assembly and organization, cellular function and maintenance, developmental disorder, and neurological disease. Significantly altered proteins included talin-1, elongation factor 2, vimentin, myosin-9, Ras-related protein Rab-11A, keratin (type II cytoskeletal 6A), pyruvate kinase isozymes M1/M2, fatty acid synthase, cytoplasmic dynein 1 heavy chain 1, alpha-enolase, E3 ubiquitin-protein ligase, histone H2A type 1-F, hemoglobin subunit alpha, and hemoglobin subunit beta-2 ( $p$ -value < 0.0001).

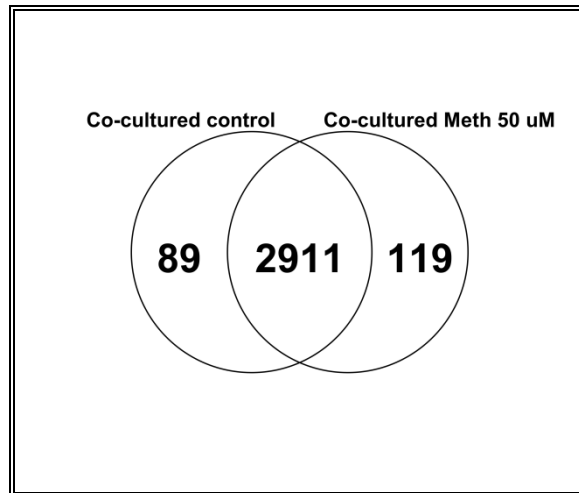


**Figure 9-10. Protein expression changes between control and 50  $\mu$ M METH-treated co-cultured BV-2 cells**

With 500  $\mu$ M METH treatment, we observed that 2926 proteins were expressed in untreated and 500  $\mu$ M METH treated BV-2 cells. Interestingly, 74 proteins were exclusively present in untreated BV-2 cells and 125 proteins were exclusively expressed in BV-2 cells treated with 500  $\mu$ M METH (**figure 9-11**). Statistical analysis ( $p$ -value < 0.05) revealed that expression levels of 264 proteins were significantly altered following treatment of BV-2 cells with 500  $\mu$ M METH. Significantly altered molecules were associated with RNA post-transcriptional modification, cell death and survival, post-translational modification, protein folding, cellular movement, DNA replication, recombination and repair, protein trafficking and developmental disorder. Significantly altered proteins included alpha-enolase, ADP/ATP translocase 2, fatty acid synthase, ATP synthase subunit alpha, beta-enolase, elongation factor 2, talin-1, ADP/ATP translocase 1, pyruvate kinase isozymes M1/M2, ATP synthase subunit beta, myosin-9, phosphoglycerate kinase 1, hemoglobin subunit alpha, hemoglobin subunit beta-2, vimentin, cytoplasmic dynein 1 heavy chain 1, heat shock 70 kDa protein 1A, 78 kDa glucose-regulated protein ( $p$ -value < 0.0001).

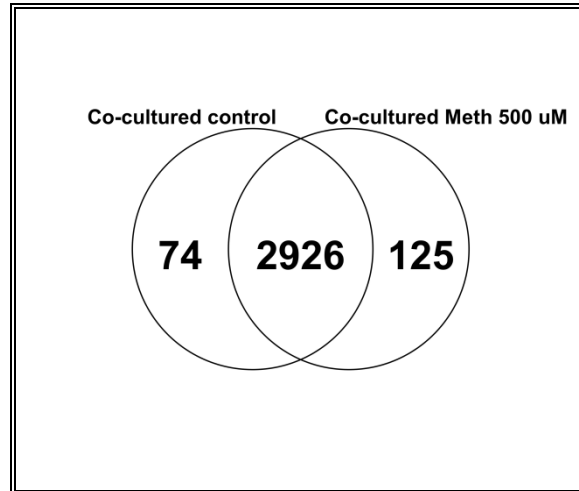


**Figure 9-11. Protein expression changes between control and 500  $\mu$ M METH-treated co-cultured BV-2 cells**

9.6 Density gradient centrifugation yields significantly pure fraction of microglia compared to fluorescence activated cell sorting or magnetic activated cell sorting

Our initial attempts to isolate GFP expressing microglia using FACS did not yield significant number of cells. In addition, as the FACS facility was not available in-house, it took significant amount of time from the time of animal sacrifice to obtaining the pure microglial fraction. As shown in **figure 9-12**, it was very difficult to separate GFP expressing microglia because of the presence of a significantly high number of other cell types as well as cell debris, (which also possessed some auto-fluorescence).

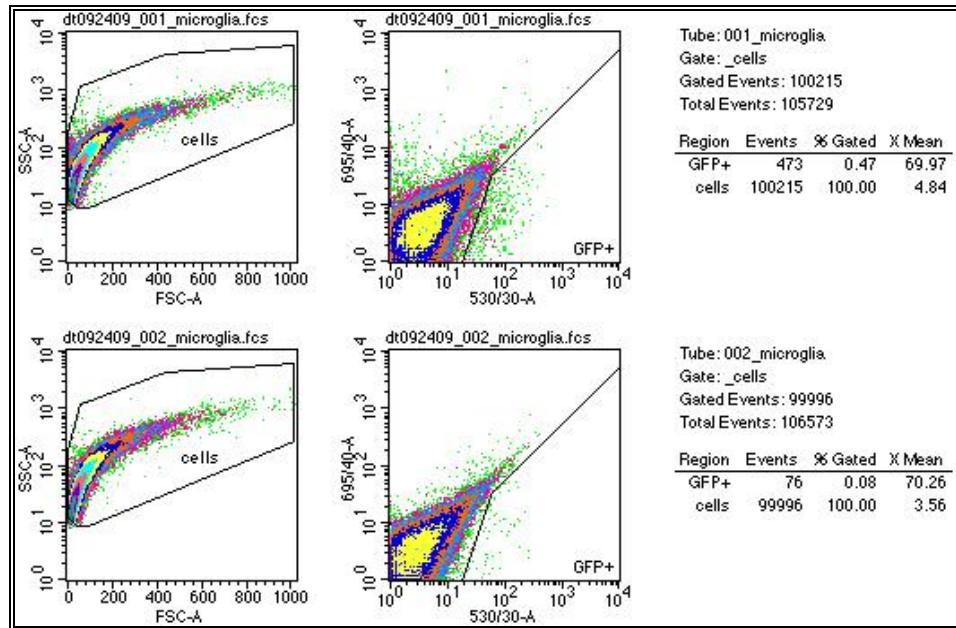


**Figure 9-12.** Microglia isolation using fluorescence activated cell sorting

We also used magnetic activated cell sorting to isolate microglia based on their expression of CD11b receptors by incubating the single cell suspension with anti-CD11b antibody conjugated to iron beads. The labeled cells were passed through a column in the presence of a strong magnetic field which removed all the unlabeled cells. The retained labeled cells were collected by removing the column from the magnetic field. The FACS analysis revealed that the microglia fraction obtained using MACS technique was ~80% pure and the unlabeled fraction did not contain significant numbers of microglia cells.

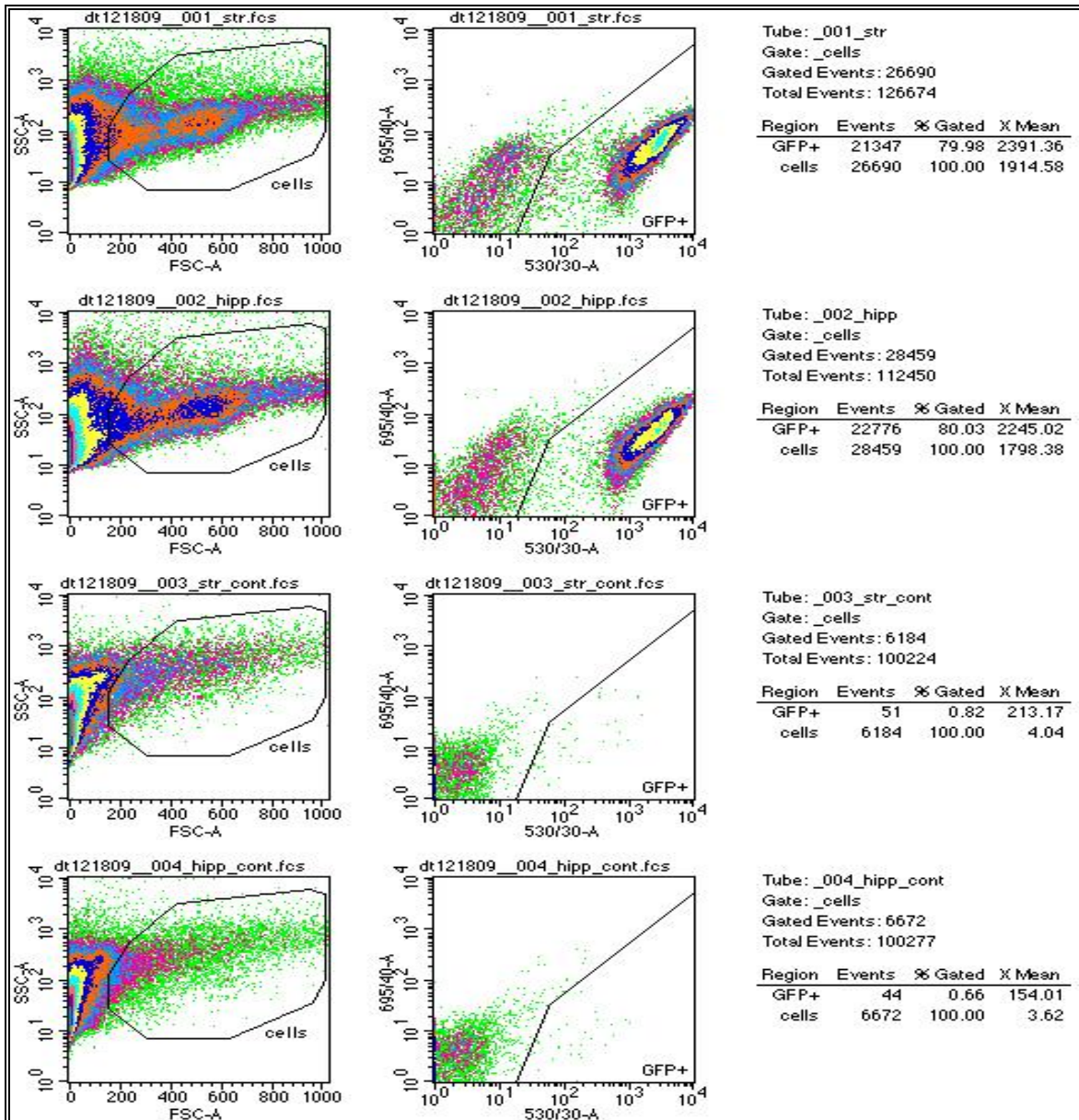


**Figure 9-13.** Evaluation of effectiveness of MACS as a technique to isolate microglia

We also attempted to perform density gradient centrifugation to yield purified fraction of microglia. As different cells vary in their density, appropriate gradients can help in isolating cells of interest from mixture of cells. We evaluated the purified fraction and non-purified remnants for the presence of GFP expressing microglia cells. We observed ~90-95% pure fraction of microglia from striatum, hippocampus, and prefrontal cortex (**figure 9-14, 9-15**). We also

observed the pure microglia fraction via fluorescence microscopy. Interestingly, all the cells from the fractions appeared to be green fluorescent microglia cells (**figure 9-16**).

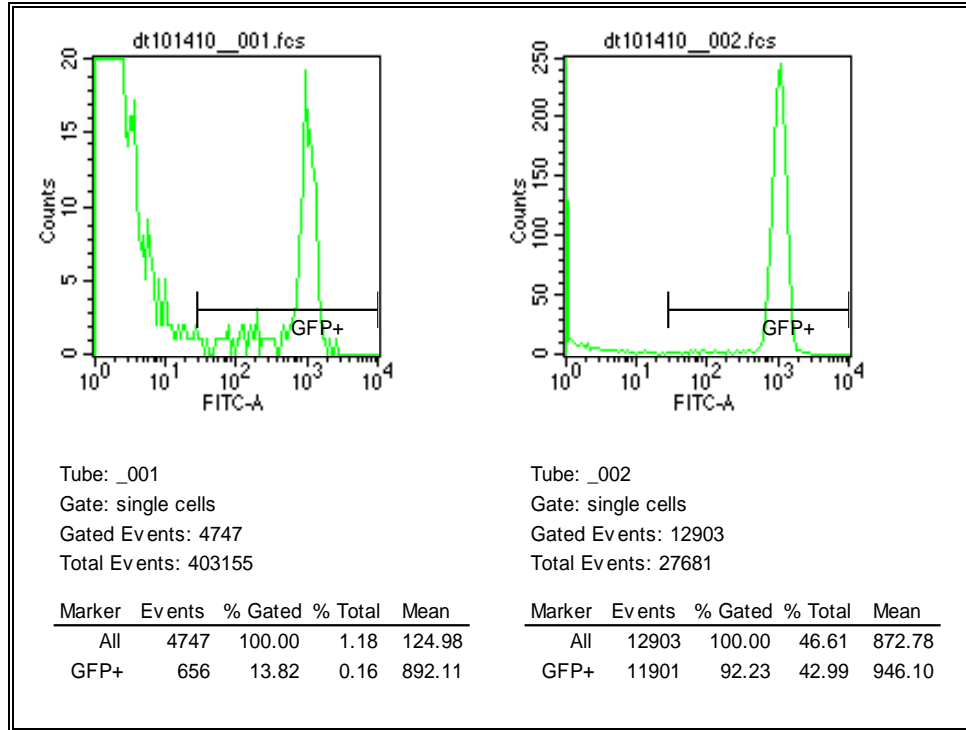


**Figure 9-14. FACS analysis of striatal microglia fraction isolated by density gradient centrifugation**

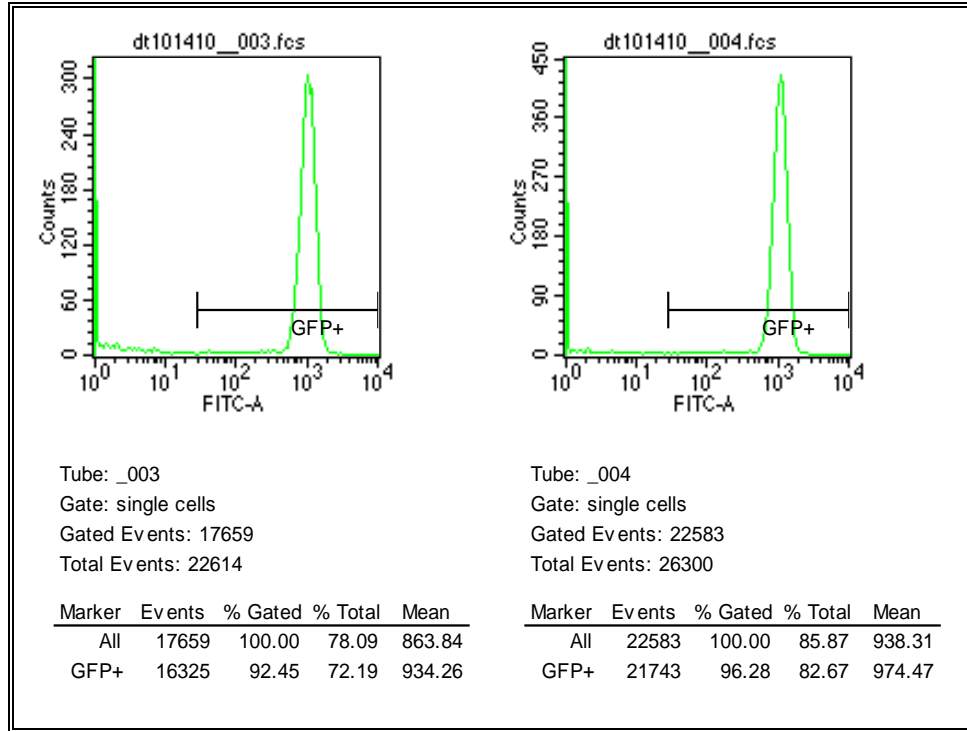


**Figure 9-15. FACS analysis of hippocampal and prefrontal cortical microglia fractions isolated by density gradient centrifugation**

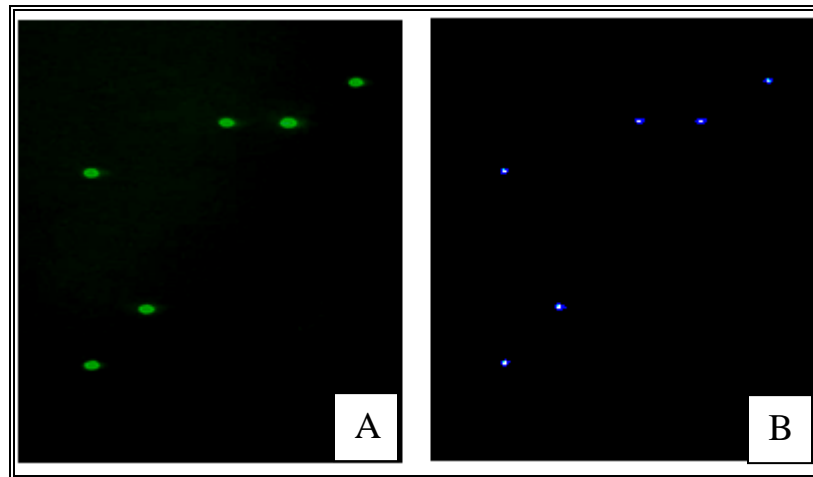


**Figure 9-16. Fluorescence microscope images of eGFP expressing microglia**

**A. GFP microglia under blue filter; B. GFP microglia stained with nuclear stain DAPI.**

We also tried to isolate microglia from wild-type animals (C57BL6 mice) and labeled them with CD11b antibody to specifically recognize microglia cells. We evaluated the purity of microglia cells isolated from various brain regions of wild-type animals by FACS. As shown in **figure 9-17**, we observed > 90% microglia cells in purified fractions.

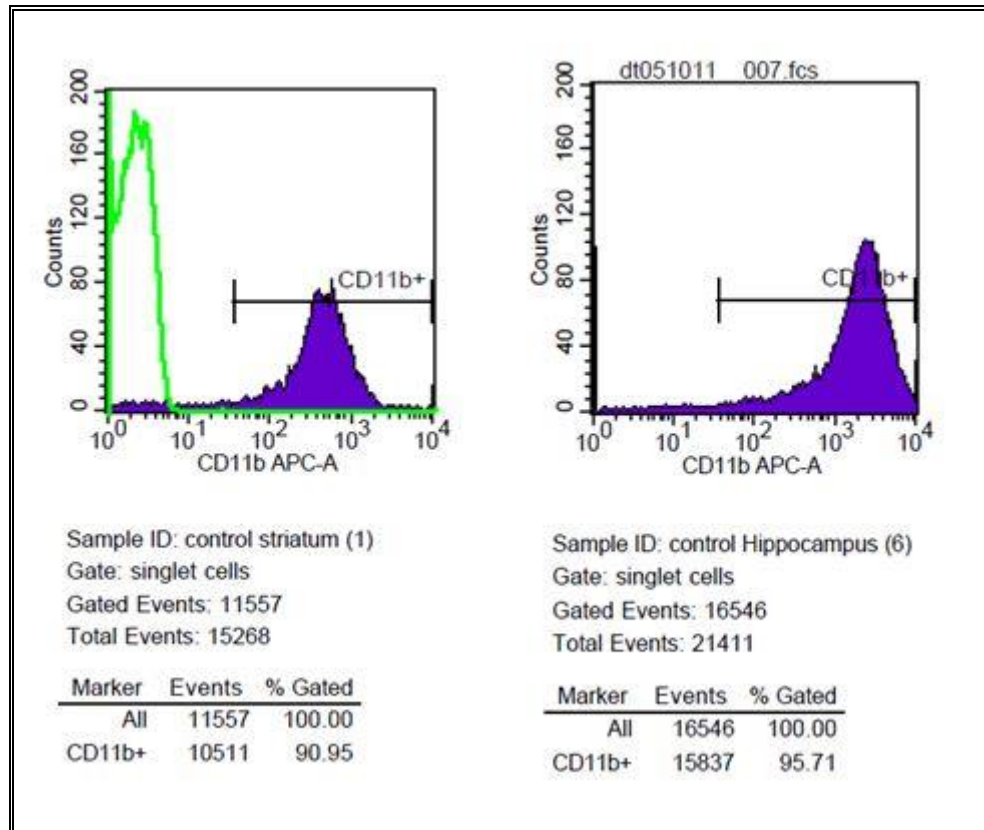


**Figure 9-17. Evaluation of microglial fraction isolated from wild-type animals**

### 9.7 METH significantly alters expression of some essential proteins in microglia isolated from striatum

We observed significant alterations in protein expression in microglia isolated from animals following their treatment with METH compared to microglia isolated from untreated control animals. Some proteins were induced upon treatment METH, whereas, expression of



some proteins was completely attenuated following treatment. As shown in **figure 9-18**, we found 1613 proteins were expressed in both control and LPS-treated BV-2 cells, whereas, microglia from untreated animals expressed 25 proteins that were exclusive and microglia isolated from METH-treated animals expressed 88 exclusive proteins.

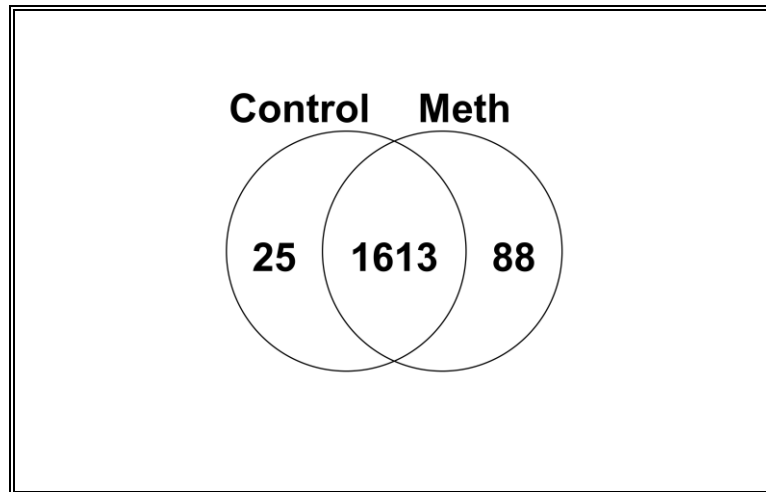


**Figure 9-18. Proteomic expression changes between microglia isolated from striata of METH-treated animals and untreated control animals**

Statistical analysis ( $p$ -value < 0.05) revealed that expression of 141 proteins was significantly altered following treatment of animals with METH. Upon further examination, it was observed that significantly altered proteins represented molecules associated with RNA post-transcriptional modification, cellular growth and proliferation, cellular development, neurological disease, psychological disorders, nucleic acid metabolism, developmental disorders, hematological disease, DNA replication, recombination and repair. The proteins were directly associated with hematological diseases, immunological disease, inflammatory disease, and inflammatory response. Most significantly altered proteins included clathrin heavy chain-1, ATP synthase, malate dehydrogenase, dihydropyrimidinase related protein 2, glyceraldehyde-3-

phosphate dehydrogenase, aconitate hydratase, fructose bisphosphate aldolase A, gamma enolase, microtubule associated protein 1A and 6, elongation factor-1, ADP/ATP translocase, pyruvate kinase isozymes M1/M2, tubulin beta-2A, heat shock protein HSP-90 alpha, and histone H2A type 2-A ( $p$ -value < 0.0001).

## **DISCUSSION**

METH is highly abused drug that is popular among or youth, and requires immediate attention because of its highly addictive properties. As the precursors of METH (e.g. pseudoephedrine, red phosphorus, anhydrous ammonia, etc.) are readily available in the U.S. and many other countries, it is difficult to control the illicit manufacture of METH. Previous attempts to restrict the distribution of METH precursors have resulted in an increase in METH trafficking from neighboring countries. As METH causes severe neurotoxic effects, and most of the addicted people are among the young, it can significantly damage the development of the CNS. Because of METH's ability to cause massive DA release and subsequent euphoric effects, its addictive potential is extremely high. Surprisingly, METH is also used as a medication for ADHD. Thus, the understanding of the mechanisms underlying METH's addictive and neurotoxic properties is very critical. In-depth analyses of factors responsible for addictive and neurotoxic properties of METH may provide important targets to ease METH addiction and the neurotoxicity induced by it.

Various studies have evaluated the ability of anti-inflammatory molecules, radical scavenger molecules, and molecular inhibitors of excitotoxicity that prevent the neurotoxicity induced by METH. Some of these studies also evaluated the ability of potential therapeutics to prevent the self-administration of METH, which simulates addictive behavior. The non-steroidal

anti-inflammatory drug (NSAID) ibuprofen has been shown to prevent neurotoxicity of METH because of its agonistic activity on PPAR $\gamma$  (Tsuji, Asanuma et al. 2009). Another study established the ability of the NSAID indomethacin to prevent METH induced microglia and astrocyte activation (Goncalves, Baptista et al. 2010). This same study implicated significant alterations in the tumor necrosis factor system as a cause of METH-induced neuroinflammation. Ketoprofen is another NSAID that has been shown to attenuate METH-induced neurotoxicity by preventing the loss of DAT and decreasing the accumulation of activated microglia in striatum (Asanuma, Tsuji et al. 2003). Surprisingly, several studies showed that aspirin, also an NSAID, does not prevent neurotoxicity induced by METH (Asanuma, Tsuji et al. 2003, Tsuji, Asanuma et al. 2009). Therefore, the prevention of METH-induced neurotoxicity appears to be independent of its effect on the COX-2 enzyme and may be related to the agonistic potency of NSAIDs as PPAR $\gamma$  agonists (Tsuji, Asanuma et al. 2009). This is further supported by a study showing that endogenous PPAR $\gamma$  might play an essential role in the prevention of METH-induced neurotoxicity *in vivo* (Yu, Airavaara et al. 2012). The sigma-receptor antagonist SN79 has been shown to block METH-induced microglia activation. SN79 has also been shown to attenuate the release of IL-6 family cytokines following METH treatment (Robson, Turner et al. 2013). We observed prevention of striatal microglia activation and prevention of damage to dopaminergic nerve terminals by the NMDA receptor antagonists MK-801 and dextromethorphan, which implicate excitotoxicity as a possible causative factor for METH-induced striatal microglia activation (Thomas and Kuhn 2005). The radical scavenger edaravone has been shown to partially protect against METH-induced neurotoxicity by blocking peroxynitrite production in astrocytes. However, edaravone doesn't prevent microglial activation or METH-induced decreases in striatal DA levels (Kawasaki, Ishihara et al. 2006). This implies

that METH might be activating microglia independent of its ability to generate free radicals. Another study focusing on the mechanism of action of minocycline concluded this antibiotic is able to prevent METH as well as MPTP-induced microglia activation, but doesn't protect dopaminergic neurons from toxicity as it doesn't affect TNF- $\alpha$  signaling. Therefore, TNF- $\alpha$  may not be essential for METH-induced microglial activation, but it is responsible for METH-induced dopaminergic neuronal damage (Sriram, Miller et al. 2006). METH-induced increases in iNOS and the release of inflammatory cytokines in microglia cell lines has been shown to be inhibited by melatonin through the inhibition of NF $\kappa$ B transcription factor (Sriram, Miller et al. 2006).

METH self-administration experiments ideally replicate the behavior-based addictive properties of METH. Therefore, molecules that are able to reverse such behavior can be ideal candidates to prevent METH addiction and the potential neurotoxicity associated with it. Lobelane and lobeline have been shown to prevent METH self-administration because of their ability to block VMAT-2 and DAT (Harrod, Dwoskin et al. 2001, Neugebauer, Harrod et al. 2007). METH self-administration is also decreased by minocycline, ibudilast, and AV1013 (an amino analog of ibudilast) which have the ability to modulate glial cell responses (Snider, Hendrick et al. 2013). Minocycline has been shown to exert its effect by inhibition of various mitogen-activated protein kinase family proteins and IkappaB $\alpha$  degradation in microglia (Nikodemova, Duncan et al. 2006). A study on Ibudilast and AV1013 concluded that, although their ability to modulate glial reactivity to METH plays an important role in decreasing METH self-administration, their phosphodiesterase inhibition activity also plays an important role in decreasing addictive behaviors induced by METH (Snider, Hendrick et al. 2013). Several other studies have shown that various compounds which have an ability to inhibit the

phosphodiesterase-4 enzyme (elevating cAMP levels) prevent METH induced behaviors (Iyo, Bi et al. 1996, Iyo, Bi et al. 1996, Mori, Baba et al. 2000, Yan, Mizuno et al. 2004). Modafinil, bupropion, naltrexone, varenicline, and disulfiram are being tested, or have been tested in clinical trials to prevent METH dependence in addicted individuals. Ibudilast, which prevents the neuroinflammatory effects of glial cells has been fast-tracked in clinical trials to treat METH addiction. In addition, minocycline, which has been shown to prevent glial responses to METH, has also been shown to prevent METH use disorders (Tanibuchi, Shimagami et al. 2010). Thus, some molecules which target particular pathways associated with METH-induced responses in glial cells may help develop potent molecules which can prevent METH addiction or METH associated behavioral changes.

In the aforementioned studies, we attempted to develop an *in vitro* model of METH-induced microglia activation by utilizing the murine BV-2 microglia cell line, which was treated with METH or LPS. Our initial experiments examined the effects of our treatments on cell viability and subsequent proteomic expression studies. However, our experiments showed relatively non-significant alterations in protein expression of BV-2 cells in case of METH treatment, whereas, BV-2 cells treated with LPS exhibited significant alterations in their protein expression. We then evaluated the ability of METH to deplete DA levels in the dopaminergic MN9D cell line. We used a unique approach by employing culture inserts which exposed microglia to various molecules released by the dopaminergic neuronal cells (MN9D) while being exposed to METH. These experiments seemed to partially recapitulate the *in vivo* environment, as permitted some interactions between the different cell types. Furthermore, we optimized a protocol to isolate microglia from the striata of animals and determined their protein expression changes in order to identify key molecules that might be involved in addictive and behavioral

properties associated with METH dependence. Various studies have evaluated the ability of diverse molecules to prevent or decrease METH dependence. We intended to obtain a list of targets which might have been involved in METH addiction and/or neurotoxicity. Appropriate drug design approaches to restore the protein signatures of microglial cells might ameliorate the inflammation and neurotoxicity associated with METH abuse.

We observed time- and dose-dependent toxicity in BV-2 cells when treated with METH. Surprisingly, LPS did not induce a decrease in BV-2 cell viability at any of the examined time-points (**figures 9-1, 9-2, and 9-3**). It is important to note that the dose of LPS used was significantly lower than the concentrations of METH tested. LPS is an endotoxin from gram negative bacteria and has been well-established as a potent agent that can induce microglia activation in different brain regions. METH is an amphetamine class of drug, which is known to cause striatal-specific microglia activation. Therefore, METH-induced microglia activation may require a unique environment and may involve modulators from other cell types which may promote striatal-specific microglia activation. As METH administration evokes massive DA depletion in striatum, we evaluated the ability of METH to deplete DA levels from the MN9D dopaminergic cell-line. We observed a dose-dependent decrease in DA following METH treatment, whereas LPS treatment seemed to induce a non-significant increase in DA levels (**figure 9-4**). As MN9D cells possess DAT and have been shown to be depleted of DA in the presence of MPP<sup>+</sup> in a dose-dependent manner, it is possible that METH may also induce the depletion of DA from MN9D cells in a DAT-dependent manner (Choi, Won et al. 1991). As some studies have investigated the effects of various molecules derived from neurons on microglia upon neurotoxic damage, it seemed appropriate to verify the changes in protein expression of BV-2 cells cultured in an environment where they would be exposed to various

secretory factors of dopaminergic neurons in presence of METH (Glanzer, Enose et al. 2007, Reynolds, Glanzer et al. 2008, Dutta, Barber et al. 2012). To determine how co-culture experiments alter METH-induced depletion of DA in MN9D cells, we determined DA levels in MN9D cells co-cultured with BV-2 cells. We observed a dose-dependent depletion in DA levels in MN9D cells in the presence of METH, which was very similar to the DA depletion observed in the absence of BV-2 cells (**figure 9-5**). Therefore, co-culturing did not seem to affect DA levels in dopaminergic neurons. Interestingly, we observed a non-significant reduction following LPS treatment in co-cultured MN9D cells. This result was the opposite of what we observed with LPS treated MN9D cells cultured alone. This implies that secretory molecules released from LPS-treated BV-2 cells may alter dopaminergic neurons such that it induces a non-significant reduction in DA levels in MN9D cells (**figure 9-5**).

The LPS treatment of BV-2 cells caused significant changes in protein expression (**figure 9-6**). The most significantly altered protein was inducible nitric oxide synthase (iNOS), which was completely absent in untreated BV-2 cells. The significant induction of prostaglandin G/H synthase 2 (PGS2) was also observed in LPS treated BV-2 cells but not expressed in untreated cells. PGS2 produces COX-2 enzyme. Both COX-2 and iNOS have been strongly implicated in the inflammatory response of microglia following LPS treatment (Thomas, Francescutti-Verbeem et al. 2006). We also observed a strong induction of the oxidative stress responsive protein poly (ADP-ribose) polymerase-14. A significant up-regulation of proteins related to inflammatory and cytokine cascades was also observed (TNF-system proteins, IFN-system proteins, macrophage migration inhibitory factor). A strong up-regulation of heme oxygenase-1 was also observed which may play a protective role against the toxicity induced by LPS. The up-regulation of various proteins important for microglial migration was also observed (integrin

alpha-5, intercellular adhesion molecule-5, filamin-B, and cytoplasmic dynein 1 heavy chain 1). Significantly altered signaling molecules included: STAT-1, STAT-2, NFκB, MAPKKK4, and PI3K adapter protein. Thus, most of the significantly altered signaling molecules are the cause or consequence of interferon release induced by LPS treatment. Our experiments involving co-cultured microglia and dopaminergic cell lines also yielded significant protein expression changes in BV-2 cells (**figure 9-9**). In this experiment, we also observed the most significant change in induction: that of inducible nitric oxide synthase. A similar induction of PGS2 was also observed. Therefore, in co-culture conditions, iNOS and COX-2 induced inflammatory signaling seemed to remain unaltered. Poly (ADP-ribose) polymerase-14 was also induced following LPS treatment. Significant expression changes were observed in inflammatory and cytokine cascade related proteins (TNF-system proteins, IFN-system proteins). Significant over-expression of proteins related to the glycolytic pathway was also observed (alpha-enolase, pyruvate kinase, phosphoglycerate kinase, phosphoglyceratemutase, hexokinase). A significant-down regulation was observed in mitochondrial oxidative phosphorylation related proteins (heat-shock protein 75 kDa, glycerol-3-phosphate dehydrogenase, NADH dehydrogenase, mitochondrial Rho GTPase 2, mitochondrial 2-oxoglutarate/malate carrier protein, apoptosis-inducing factor 1, succinate dehydrogenase, NADH ubiquinone oxidoreductase, ATP synthase), whereas, mitochondrial UMP-CMP kinase which is required for pyrimidine biosynthesis by mitochondrial DNA was up-regulated following LPS treatment. These changes can be explained as injury to BV-2 cell mitochondria (affecting mitochondrial complex-I, II, and V), resulting in a switch from oxidative phosphorylation to glycolysis (similar to that observed in cancer cells) and mitochondrial DNA damage requiring the generation of pyrimidine to repair the damage. Proteins related to microglial migration and cell-cell contact were also significantly up-regulated



(cytoplasmic dynein 1 heavy chain, filamin-B, talin-1). Important signaling molecules that were significantly up-regulated included STAT-1, STAT-2, dual-specificity mitogen activated protein kinasekinase 1, protein tyrosine kinase 2-beta, phosphatidylinositol 3,4,5-trisphosphate-dependent Rac exchanger 1 protein. Thus, important signaling molecules altered in co-culture condition involved response to cytokines or inflammation as well as anti-viral responses which may promote cell survival.

50  $\mu$ M METH did not induce significant protein expression changes in BV-2 cells compared to LPS or 500  $\mu$ M METH (**figure 9-7**). However, significant up-regulation was observed in heat-shock related 70kDa protein and serine/threonine protein phosphatase 6 regulatory subunit.. Interestingly, significant alterations in protein expression were observed in BV-2 cells co-cultured with MN9D cells treated with 50  $\mu$ M METH (**figure 9-10**). We observed significant alterations in proteins associated with glycolysis (alpha-enolase, beta-enolase, pyruvate kinase, triosephosphateisomerase, L-lactate dehydrogenase A chain, fructose bisphosphate aldolase, glyceraldehyde-3-phosphate dehydrogenase). Vimentin, which is implicated in glial cell differentiation was significantly down-regulated by 50  $\mu$ M, which may cause decreased glial reactivity to infectious or injurious stimuli. Various proteins related to intracellular protein trafficking were altered such that it would result in inefficient membrane trafficking of proteins (ras-related protein rab-11A, ras-related protein rab-35, rab GDP dissociation inhibitor beta). Mitochondrial dysfunction was observed as alterations of key proteins required for oxidative phosphorylation (ADP/ATP translocase, ATP synthase, succinate dehydrogenase iron-sulphur subunit, NADH ubiquinone oxidoreductase, trifunctional enzyme subunit alpha, apoptosis-inducing factor-1, succinate dehydrogenase). Heat-shock protein HSP-90 alpha was significantly up-regulated, which may help in chaperone functions to generate

protein assemblies. E3 ubiquitin-protein ligase was also up-regulated which may assist in the degradation of dysfunctional proteins. Significantly altered cell signaling molecules include STE-20 like serine/threonine protein kinase, serine/threonine protein kinase, 1-phosphatidylinositol-4,5-bisphosphate phosphodiesterase beta-3, c-JUN amino-terminal kinase interacting protein 4, serine/threonine protein kinase N1. Thus, significant protein expression changes were observed related to apoptosis and cellular stress signaling.

500  $\mu$ M METH significantly altered protein expression in BV-2 cells (**figure 9-8**). The most significantly altered protein was heat-shock related 70kDa protein 2. Its up-regulation may be a cellular response to stress, stabilizing various protein against aggregation to maintain their appropriate function. We observed down-regulation of mitochondrial enzymes following 500  $\mu$ M METH treatment (ATP synthase and NADH dehydrogenase). Serine/arginine-repetitive matrix (SRRM) and E3 ubiquitin-protein ligase were significantly down-regulated which may explain the toxic effects of 500  $\mu$ M METH as SRRM is involved in the generation of appropriate functional proteins and E3 ubiquitin-protein ligase is responsible for the destruction of dysfunctional proteins. Interestingly, when BV-2 cells were co-cultured in the presence of MN9D cells, the protein expression was significantly changed, involving many other proteins that were not changed when BV-2 cells were exposed to 500  $\mu$ M METH in monoculture (**figure 9-11**). A significant up-regulation of glycolytic enzymes was observed (alpha enolase, beta enolase, pyruvate kinase, phosphoglycerate kinase, fructose bisphosphate aldolase, glyceraldehyde-3-phosphate dehydrogenase). As observed in the case of 50  $\mu$ M METH, mitochondrial dysfunction was also observed for higher concentrations of METH as the expression of many mitochondrial proteins was altered (ADP/ATP translocase, ATP synthase, apoptosis-inducing factor 1, NADH dehydrogenase, cytochrome C1, succinate dehydrogenase).

500  $\mu$ M METH may induce the reduction in oxidative phosphorylation and subsequent increases in glycolysis to generate ATP. Significantly altered signaling molecules included serine-threonine protein kinase mTOR, 1-phosphatidylinositol-4,5-bisphosphate phosphodiesterase beta-3, phosphoinositide 3-kinase regulatory subunit, STE20-like serine/threonine-protein kinase, serine/threonine protein kinase, 1-phosphatidylinositol-3-phosphate 5-kinase. In addition, many members of ras-related protein rab family were down regulated. Thus, METH may be altering proteins critical for membrane trafficking, vesicular trafficking and neurotransmitter release.

We explored several different techniques to isolate microglia from various brain regions. A significant amount of work has been published using primary microglia cultures, but there is limited evidence in which microglia are used for experimental purposes immediately following their isolation (Parvathenani, Tertyshnikova et al. 2003, Moussaud and Draheim 2010, Ohtaki, Tsumuraya et al. 2013). Our objective was to determine the effect of METH on striatal microglia. Hence, it was essential to follow a protocol that could yield microglia that could be used for proteomic experiments without extended culturing, which would alter microglial protein expressions extensively. In our effort to yield purified microglia fraction, we avoided the use of enzymes such as trypsin which are known to disturb microglial homeostasis (Park, Jeon et al. 2010). We optimized a protocol to generate single-cell suspension using a mechanical dissociation method to verify the ability of 3 different methods to yield pure microglia fractions from various brain regions. We found the density gradient centrifugation protocol to be the most efficient in yielding purified microglia fractions from single-cell suspensions, regardless of the brain region examined. Our verification of isolated microglia fractions confirmed the purity of isolated microglia (**figures 9-14, 9-15, and 9-16**). Density gradient centrifugation has been

previously used to isolate pure microglia fraction from a variety of brain regions and seemed compatible with our downstream experiments (Frank, Wieseler-Frank et al. 2006, Hussain, Yang et al. 2006, Frank, Barrientos et al. 2010, Olah, Raj et al. 2012).

Microglia isolated from the striatum of METH-treated animals also exhibited significant alterations in protein expression compared to striatal microglia isolated from untreated control animals (**figure 9-18**). The most significantly altered protein was junction plakoglobin, which was almost completely absent in microglia isolated from the striatum of METH-treated animals. It is shown to be essential for cell migration and cell-cell adhesion. Heat shock 70 kDa protein 1A was significantly up-regulated in microglia isolated from the striatum of METH-treated animals and corroborates that there is significant protein aggregation or dysfunction induced by METH in striatal microglia. Interestingly, mitochondrial stress-70 protein and heat shock protein 75 kDa were also up-regulated in METH-treated microglia, which implies the presence of dysfunctional proteins in mitochondria. Several essential proteins involved in protein transport were significantly up-regulated (clathrin heavy chain 1 and spectrin beta chain), which implies increased protein transport due to increased transcription and translation in response to stress induced by METH. Subsequent increases in clathrin-coated pits associated protein required for endocytosis was also observed (epidermal growth factor receptor substrate 15-like 1). Mitochondrial proteins were significantly up-regulated in microglia isolated from METH-treated animals (ATP synthase subunit alpha, NADH dehydrogenase, mitochondrial inner membrane protein, ADP/ATP translocase 1 and ADP/ATP translocase 2). Many mitochondrial enzymes associated with tricarboxylic acid cycle were also up-regulated in microglia isolated from METH-treated animals. Significant increases in endoplasmic reticulum quality control protein UDP-glucose:glycoprotein glucosyltransferase 1 and 78 kDa glucose-regulated protein were also

observed, which implies protein misfolding or dysfunction following METH exposure. Significant over-expression of DNA damage binding protein and proliferating cell nuclear antigen in striatal microglia isolated from METH implies significant DNA damage following METH exposure. There was a down-regulation of 1-phosphatidylinositol-4,5-bisphosphate phosphodiesterase beta-1 and subsequent up regulation of diacyl glycerol kinase beta. Therefore, the intracellular signal transduction machinery might alter based on METH induced protein alterations. Surprisingly, no significant alterations in any inflammatory or cytokine related proteins were observed. Except for the heat-shock protein family and some mitochondrial proteins, no similarity was observed when comparing proteomic data obtained from BV-2 cells (in monoculture or co-culture systems). Therefore, the native environment of the striatum, in which many different types of neurons, astrocytes, etc. exist, certainly plays a critical role in the striatal-specific activation of microglia following METH exposure.

## REFERENCES

1. Abad, F., R. Maroto, M. G. Lopez, P. Sanchez-Garcia and A. G. Garcia (1995). "Pharmacological protection against the cytotoxicity induced by 6-hydroxydopamine and H<sub>2</sub>O<sub>2</sub> in chromaffin cells." Eur J Pharmacol **293**(1): 55-64.
2. Abou-Sleiman, P. M., M. M. Muqit and N. W. Wood (2006). "Expanding insights of mitochondrial dysfunction in Parkinson's disease." Nat Rev Neurosci **7**(3): 207-219.
3. Abu-Raya, S., E. Blaugrund, V. Trembovler, E. Shilderman-Bloch, E. Shohami and P. Lazarovici (1999). "Rasagiline, a monoamine oxidase-B inhibitor, protects NGF-differentiated PC12 cells against oxygen-glucose deprivation." J Neurosci Res **58**(3): 456-463.
4. Alam, Z. I., S. E. Daniel, A. J. Lees, D. C. Marsden, P. Jenner and B. Halliwell (1997). "A generalised increase in protein carbonyls in the brain in Parkinson's but not incidental Lewy body disease." J Neurochem **69**(3): 1326-1329.
5. Alam, Z. I., A. Jenner, S. E. Daniel, A. J. Lees, N. Cairns, C. D. Marsden, P. Jenner and B. Halliwell (1997). "Oxidative DNA damage in the parkinsonian brain: an apparent selective increase in 8-hydroxyguanine levels in substantia nigra." J Neurochem **69**(3): 1196-1203.
6. Anderson, B. B., G. Chen, D. A. Gutman and A. G. Ewing (1998). "Dopamine levels of two classes of vesicles are differentially depleted by amphetamine." Brain Res **788**(1-2): 294-301.
7. Asanuma, M., T. Tsuji, I. Miyazaki, K. Miyoshi and N. Ogawa (2003). "Methamphetamine-induced neurotoxicity in mouse brain is attenuated by ketoprofen, a non-steroidal anti-inflammatory drug." Neurosci Lett **352**(1): 13-16.

8. Barbeau, A. (1962). "The pathogenesis of Parkinson's disease: a new hypothesis." Can Med Assoc J **87**: 802-807.
9. Basma, A. N., E. J. Morris, W. J. Nicklas and H. M. Geller (1995). "L-dopa cytotoxicity to PC12 cells in culture is via its autoxidation." J Neurochem **64**(2): 825-832.
10. Berman, S., J. O'Neill, S. Fears, G. Bartzokis and E. D. London (2008). "Abuse of amphetamines and structural abnormalities in the brain." Ann N Y Acad Sci **1141**: 195-220.
11. Betarbet, R., T. B. Sherer, G. MacKenzie, M. Garcia-Osuna, A. V. Panov and J. T. Greenamyre (2000). "Chronic systemic pesticide exposure reproduces features of Parkinson's disease." Nat Neurosci **3**(12): 1301-1306.
12. Bharath, S., M. Hsu, D. Kaur, S. Rajagopalan and J. K. Andersen (2002). "Glutathione, iron and Parkinson's disease." Biochem Pharmacol **64**(5-6): 1037-1048.
13. Birkmayer, W. and O. Hornykiewicz (1961). "[The L-3,4-dioxyphenylalanine (DOPA)-effect in Parkinson-akinesia]." Wien Klin Wochenschr **73**: 787-788.
14. Birkmayer, W. and O. Hornykiewicz (1998). "The effect of l-3,4-dihydroxyphenylalanine (=DOPA) on akinesia in parkinsonism." Parkinsonism Relat Disord **4**(2): 59-60.
15. Biswas, S., S. Hazeldine, B. Ghosh, I. Parrington, E. Kuzhikandathil, M. E. Reith and A. K. Dutta (2008). "Bioisosteric heterocyclic versions of 7-{{2-(4-phenyl-piperazin-1-yl)ethyl}propylamino}-5,6,7,8-tetrahydronaphthalen-2-ol: identification of highly potent and selective agonists for dopamine D3 receptor with potent in vivo activity." J Med Chem **51**(10): 3005-3019.
16. Block, M. L., L. Zecca and J. S. Hong (2007). "Microglia-mediated neurotoxicity: uncovering the molecular mechanisms." Nat Rev Neurosci **8**(1): 57-69.

17. Blum, D., S. Torch, M. F. Nissou, A. L. Benabid and J. M. Verna (2000). "Extracellular toxicity of 6-hydroxydopamine on PC12 cells." Neurosci Lett **283**(3): 193-196.
18. Braak, H., K. Del Tredici, U. Rub, R. A. de Vos, E. N. Jansen Steur and E. Braak (2003). "Staging of brain pathology related to sporadic Parkinson's disease." Neurobiol Aging **24**(2): 197-211.
19. Bucciantini, M., E. Giannoni, F. Chiti, F. Baroni, L. Formigli, J. Zurdo, N. Taddei, G. Ramponi, C. M. Dobson and M. Stefani (2002). "Inherent toxicity of aggregates implies a common mechanism for protein misfolding diseases." Nature **416**(6880): 507-511.
20. Cappai, R., S. L. Leck, D. J. Tew, N. A. Williamson, D. P. Smith, D. Galatis, R. A. Sharples, C. C. Curtain, F. E. Ali, R. A. Cherny, J. G. Culvenor, S. P. Bottomley, C. L. Masters, K. J. Barnham and A. F. Hill (2005). "Dopamine promotes alpha-synuclein aggregation into SDS-resistant soluble oligomers via a distinct folding pathway." FASEB J **19**(10): 1377-1379.
21. Carlsson, A. (1959). "The occurrence, distribution and physiological role of catecholamines in the nervous system." Pharmacol Rev **11**(2, Part 2): 490-493.
22. Carlsson, A., M. Lindqvist and T. Magnusson (1957). "3,4-Dihydroxyphenylalanine and 5-hydroxytryptophan as reserpine antagonists." Nature **180**(4596): 1200.
23. Carlsson, A., M. Lindqvist, T. Magnusson and B. Waldeck (1958). "On the presence of 3-hydroxytyramine in brain." Science **127**(3296): 471.
24. Chartier-Harlin, M. C., J. Kachergus, C. Roumier, V. Mouroux, X. Douay, S. Lincoln, C. Levecque, L. Larvor, J. Andrieux, M. Hulihan, N. Waucquier, L. Defebvre, P. Amouyel, M. Farrer and A. Destee (2004). "Alpha-synuclein locus duplication as a cause of familial Parkinson's disease." Lancet **364**(9440): 1167-1169.



25. Choi, H. K., L. A. Won, P. J. Kontur, D. N. Hammond, A. P. Fox, B. H. Wainer, P. C. Hoffmann and A. Heller (1991). "Immortalization of embryonic mesencephalic dopaminergic neurons by somatic cell fusion." Brain Res **552**(1): 67-76.
26. Conway, K. A., J. D. Harper and P. T. Lansbury, Jr. (2000). "Fibrils formed in vitro from alpha-synuclein and two mutant forms linked to Parkinson's disease are typical amyloid." Biochemistry **39**(10): 2552-2563.
27. Conway, K. A., J. C. Rochet, R. M. Bieganski and P. T. Lansbury, Jr. (2001). "Kinetic stabilization of the alpha-synuclein protofibril by a dopamine-alpha-synuclein adduct." Science **294**(5545): 1346-1349.
28. Courtney, N. D., A. C. Howlett and T. C. Westfall (1991). "Dopaminergic regulation of dopamine release from PC12 cells via a pertussis toxin-sensitive G protein." Neurosci Lett **122**(2): 261-264.
29. Dauer, W. and S. Przedborski (2003). "Parkinson's disease: mechanisms and models." Neuron **39**(6): 889-909.
30. Davalos, D., J. Grutzendler, G. Yang, J. V. Kim, Y. Zuo, S. Jung, D. R. Littman, M. L. Dustin and W. B. Gan (2005). "ATP mediates rapid microglial response to local brain injury in vivo." Nat Neurosci **8**(6): 752-758.
31. de Lau, L. M. and M. M. Breteler (2006). "Epidemiology of Parkinson's disease." Lancet Neurol **5**(6): 525-535.
32. Dexter, D. T., C. J. Carter, F. R. Wells, F. Javoy-Agid, Y. Agid, A. Lees, P. Jenner and C. D. Marsden (1989). "Basal lipid peroxidation in substantia nigra is increased in Parkinson's disease." J Neurochem **52**(2): 381-389.

33. Di Monte, D., M. S. Sandy and M. T. Smith (1987). "Increased efflux rather than oxidation is the mechanism of glutathione depletion by 1-methyl-4-phenyl-1,2,3,6-tetrahydropyridine (MPTP)." Biochem Biophys Res Commun **148**(1): 153-160.
34. Dooley, M. and A. Markham (1998). "Pramipexole. A review of its use in the management of early and advanced Parkinson's disease." Drugs Aging **12**(6): 495-514.
35. Dutta, G., D. S. Barber, P. Zhang, N. J. Doperalski and B. Liu (2012). "Involvement of dopaminergic neuronal cystatin C in neuronal injury-induced microglial activation and neurotoxicity." J Neurochem **122**(4): 752-763.
36. Exner, N., A. K. Lutz, C. Haass and K. F. Winklhofer (2012). "Mitochondrial dysfunction in Parkinson's disease: molecular mechanisms and pathophysiological consequences." EMBO J **31**(14): 3038-3062.
37. Fahn, S. (1992). "A pilot trial of high-dose alpha-tocopherol and ascorbate in early Parkinson's disease." Ann Neurol **32 Suppl**: S128-132.
38. Fahn, S. (1996). "Is levodopa toxic?" Neurology **47**(6 Suppl 3): S184-195.
39. Fleckenstein, A. E. and G. R. Hanson (2003). "Impact of psychostimulants on vesicular monoamine transporter function." Eur J Pharmacol **479**(1-3): 283-289.
40. Floor, E. and M. G. Wetzel (1998). "Increased protein oxidation in human substantia nigra pars compacta in comparison with basal ganglia and prefrontal cortex measured with an improved dinitrophenylhydrazine assay." J Neurochem **70**(1): 268-275.
41. Frank, M. G., R. M. Barrientos, L. R. Watkins and S. F. Maier (2010). "Aging sensitizes rapidly isolated hippocampal microglia to LPS ex vivo." J Neuroimmunol **226**(1-2): 181-184.

42. Frank, M. G., J. L. Wieseler-Frank, L. R. Watkins and S. F. Maier (2006). "Rapid isolation of highly enriched and quiescent microglia from adult rat hippocampus: immunophenotypic and functional characteristics." J Neurosci Methods **151**(2): 121-130.
43. Fujita, Y., Y. Izawa, N. Ali, Y. Kanematsu, K. Tsuchiya, S. Hamano, T. Tamaki and M. Yoshizumi (2006). "Pramipexole protects against H<sub>2</sub>O<sub>2</sub>-induced PC12 cell death." Naunyn Schmiedebergs Arch Pharmacol **372**(4): 257-266.
44. Ghosh, B., T. Antonio, M. E. Reith and A. K. Dutta (2010). "Discovery of 4-(4-(2-((5-Hydroxy-1,2,3,4-tetrahydronaphthalen-2-yl)(propyl)amino)ethyl)piperazin-1-yl)quinolin-8-ol and its analogues as highly potent dopamine D<sub>2</sub>/D<sub>3</sub> agonists and as iron chelator: in vivo activity indicates potential application in symptomatic and neuroprotective therapy for Parkinson's disease." J Med Chem **53**(5): 2114-2125.
45. Glanzer, J. G., Y. Enose, T. Wang, I. Kadiu, N. Gong, W. Rozek, J. Liu, J. D. Schlautman, P. S. Ciborowski, M. P. Thomas and H. E. Gendelman (2007). "Genomic and proteomic microglial profiling: pathways for neuroprotective inflammatory responses following nerve fragment clearance and activation." J Neurochem **102**(3): 627-645.
46. Glinka, Y. Y. and M. B. Youdim (1995). "Inhibition of mitochondrial complexes I and IV by 6-hydroxydopamine." Eur J Pharmacol **292**(3-4): 329-332.
47. Goedert, M., F. Clavaguera and M. Tolnay (2010). "The propagation of prion-like protein inclusions in neurodegenerative diseases." Trends Neurosci **33**(7): 317-325.
48. Goedert, M., M. G. Spillantini, K. Del Tredici and H. Braak (2013). "100 years of Lewy pathology." Nat Rev Neurol **9**(1): 13-24.
49. Gogoi, S., T. Antonio, S. Rajagopalan, M. Reith, J. Andersen and A. K. Dutta (2011). "Dopamine D<sub>2</sub>/D<sub>3</sub> agonists with potent iron chelation, antioxidant and

- neuroprotective properties: potential implication in symptomatic and neuroprotective treatment of Parkinson's disease." ChemMedChem **6**(6): 991-995.
50. Goldberg, M. S. and P. T. Lansbury, Jr. (2000). "Is there a cause-and-effect relationship between alpha-synuclein fibrillization and Parkinson's disease?" Nat Cell Biol **2**(7): E115-119.
51. Goncalves, J., S. Baptista, T. Martins, N. Milhazes, F. Borges, C. F. Ribeiro, J. O. Malva and A. P. Silva (2010). "Methamphetamine-induced neuroinflammation and neuronal dysfunction in the mice hippocampus: preventive effect of indomethacin." Eur J Neurosci **31**(2): 315-326.
52. Green, A. I. and P. N. Halkitis (2006). "Crystal methamphetamine and sexual sociality in an urban gay subculture: an elective affinity." Cult Health Sex **8**(4): 317-333.
53. Greene, L. A. and A. S. Tischler (1976). "Establishment of a noradrenergic clonal line of rat adrenal pheochromocytoma cells which respond to nerve growth factor." Proc Natl Acad Sci U S A **73**(7): 2424-2428.
54. Hall, E. D., P. K. Andrus, J. A. Oostveen, J. S. Althaus and P. F. VonVoigtlander (1996). "Neuroprotective effects of the dopamine D2/D3 agonist pramipexole against postischemic or methamphetamine-induced degeneration of nigrostriatal neurons." Brain Res **742**(1-2): 80-88.
55. Han, S. K., C. Mytilineou and G. Cohen (1996). "L-DOPA up-regulates glutathione and protects mesencephalic cultures against oxidative stress." J Neurochem **66**(2): 501-510.
56. Hanisch, U. K. and H. Kettenmann (2007). "Microglia: active sensor and versatile effector cells in the normal and pathologic brain." Nat Neurosci **10**(11): 1387-1394.

57. Hanrott, K., L. Gudmunsen, M. J. O'Neill and S. Wonnacott (2006). "6-hydroxydopamine-induced apoptosis is mediated via extracellular auto-oxidation and caspase 3-dependent activation of protein kinase Cdelta." J Biol Chem **281**(9): 5373-5382.
58. Hansen, C. and J. Y. Li (2012). "Beyond alpha-synuclein transfer: pathology propagation in Parkinson's disease." Trends Mol Med **18**(5): 248-255.
59. Harrod, S. B., L. P. Dwoskin, P. A. Crooks, J. E. Klebaur and M. T. Bardo (2001). "Lobeline attenuates d-methamphetamine self-administration in rats." J Pharmacol Exp Ther **298**(1): 172-179.
60. Hawkes, C. H. (2008). "The prodromal phase of sporadic Parkinson's disease: does it exist and if so how long is it?" Mov Disord **23**(13): 1799-1807.
61. Henn, A., S. Lund, M. Hedtjarn, A. Schrattenholz, P. Porzgen and M. Leist (2009). "The suitability of BV2 cells as alternative model system for primary microglia cultures or for animal experiments examining brain inflammation." ALTEX **26**(2): 83-94.
62. Hornykiewicz, O. and S. J. Kish (1987). "Biochemical pathophysiology of Parkinson's disease." Adv Neurol **45**: 19-34.
63. Hou, R. C., H. M. Huang, J. T. Tzen and K. C. Jeng (2003). "Protective effects of sesamin and sesamol on hypoxic neuronal and PC12 cells." J Neurosci Res **74**(1): 123-133.
64. Hussain, S. F., D. Yang, D. Suki, E. Grimm and A. B. Heimberger (2006). "Innate immune functions of microglia isolated from human glioma patients." J Transl Med **4**: 15.

65. Illes-Toth, E., C. F. Dalton and D. P. Smith (2013). "Binding of Dopamine to Alpha-Synuclein is Mediated by Specific Conformational States." J Am Soc Mass Spectrom **24**(9): 1346-1354.
66. Iyo, M., Y. Bi, K. Hashimoto, T. Inada and S. Fukui (1996). "Prevention of methamphetamine-induced behavioral sensitization in rats by a cyclic AMP phosphodiesterase inhibitor, rolipram." Eur J Pharmacol **312**(2): 163-170.
67. Iyo, M., Y. Bi, K. Hashimoto, S. I. Tomitaka, T. Inada and S. Fukui (1996). "Does an increase of cyclic AMP prevent methamphetamine-induced behavioral sensitization in rats?" Ann N Y Acad Sci **801**: 377-383.
68. Jellinger, K., E. Kienzl, G. Rumpelmair, P. Riederer, H. Stachelberger, D. Ben-Shachar and M. B. Youdim (1992). "Iron-melanin complex in substantia nigra of parkinsonian brains: an x-ray microanalysis." J Neurochem **59**(3): 1168-1171.
69. Jellinger, K., W. Paulus, I. Grundke-Iqbal, P. Riederer and M. B. Youdim (1990). "Brain iron and ferritin in Parkinson's and Alzheimer's diseases." J Neural Transm Park Dis Dement Sect **2**(4): 327-340.
70. Jenner, P. (2003). "Oxidative stress in Parkinson's disease." Ann Neurol **53 Suppl 3**: S26-36; discussion S36-28.
71. Jenner, P., D. T. Dexter, J. Sian, A. H. Schapira and C. D. Marsden (1992). "Oxidative stress as a cause of nigral cell death in Parkinson's disease and incidental Lewy body disease. The Royal Kings and Queens Parkinson's Disease Research Group." Ann Neurol **32 Suppl**: S82-87.
72. Jenner, P. and C. W. Olanow (1996). "Oxidative stress and the pathogenesis of Parkinson's disease." Neurology **47**(6 Suppl 3): S161-170.

73. Johnson, M., T. Antonio, M. E. Reith and A. K. Dutta (2012). "Structure-activity relationship study of N(6)-(2-(4-(1H-Indol-5-yl)piperazin-1-yl)ethyl)-N(6)-propyl-4,5,6,7-tetrahydrobenzo[d]thiazole-2,6-diamine analogues: development of highly selective D3 dopamine receptor agonists along with a highly potent D2/D3 agonist and their pharmacological characterization." J Med Chem **55**(12): 5826-5840.
74. Jung, S., J. Aliberti, P. Graemmel, M. J. Sunshine, G. W. Kreutzberg, A. Sher and D. R. Littman (2000). "Analysis of fractalkine receptor CX(3)CR1 function by targeted deletion and green fluorescent protein reporter gene insertion." Mol Cell Biol **20**(11): 4106-4114.
75. Kang, C. D., J. H. Jang, K. W. Kim, H. J. Lee, C. S. Jeong, C. M. Kim, S. H. Kim and B. S. Chung (1998). "Activation of c-jun N-terminal kinase/stress-activated protein kinase and the decreased ratio of Bcl-2 to Bax are associated with the auto-oxidized dopamine-induced apoptosis in PC12 cells." Neurosci Lett **256**(1): 37-40.
76. Kawasaki, T., K. Ishihara, Y. Ago, S. Nakamura, S. Itoh, A. Baba and T. Matsuda (2006). "Protective effect of the radical scavenger edaravone against methamphetamine-induced dopaminergic neurotoxicity in mouse striatum." Eur J Pharmacol **542**(1-3): 92-99.
77. Kim, J. Y. and M. Fendrich (2002). "Gender differences in juvenile arrestees' drug use, self-reported dependence, and perceived need for treatment." Psychiatr Serv **53**(1): 70-75.
78. Kim, M. K., S. C. Kim, J. I. Kang, J. H. Hyun, H. J. Boo, S. Y. Eun, D. B. Park, E. S. Yoo, H. K. Kang and J. H. Kang (2011). "6-Hydroxydopamine-induced PC12 cell death is mediated by MEF2D down-regulation." Neurochem Res **36**(2): 223-231.

79. Kiyatkin, E. A. and H. S. Sharma (2009). "Acute methamphetamine intoxication: brain hyperthermia, blood-brain barrier, brain edema, and morphological cell abnormalities." Int Rev Neurobiol **88**: 65-100.
80. Kostrzewa, R. M. and D. M. Jacobowitz (1974). "Pharmacological actions of 6-hydroxydopamine." Pharmacol Rev **26**(3): 199-288.
81. Kuhn, D. M., D. M. Francescutti-Verbeem and D. M. Thomas (2006). "Dopamine quinones activate microglia and induce a neurotoxic gene expression profile: relationship to methamphetamine-induced nerve ending damage." Ann N Y Acad Sci **1074**: 31-41.
82. Kulich, S. M., C. Horbinski, M. Patel and C. T. Chu (2007). "6-Hydroxydopamine induces mitochondrial ERK activation." Free Radic Biol Med **43**(3): 372-383.
83. LaGasse, L. L., C. Derauf, L. M. Smith, E. Newman, R. Shah, C. Neal, A. Arria, M. A. Huestis, S. DellaGrotta, H. Lin, L. M. Dansereau and B. M. Lester (2012). "Prenatal methamphetamine exposure and childhood behavior problems at 3 and 5 years of age." Pediatrics **129**(4): 681-688.
84. LaGasse, L. L., T. Wouldes, E. Newman, L. M. Smith, R. Z. Shah, C. Derauf, M. A. Huestis, A. M. Arria, S. Della Grotta, T. Wilcox and B. M. Lester (2011). "Prenatal methamphetamine exposure and neonatal neurobehavioral outcome in the USA and New Zealand." Neurotoxicol Teratol **33**(1): 166-175.
85. Langston, J. W., P. Ballard, J. W. Tetrud and I. Irwin (1983). "Chronic Parkinsonism in humans due to a product of meperidine-analog synthesis." Science **219**(4587): 979-980.
86. Lemke, M. R., G. Fuchs, I. Gemende, B. Herting, C. Oehlwein, H. Reichmann, J. Rieke and J. Volkmann (2004). "Depression and Parkinson's disease." J Neurol **251 Suppl 6**: VI/24-27.



87. Lesage, S. and A. Brice (2009). "Parkinson's disease: from monogenic forms to genetic susceptibility factors." Hum Mol Genet **18**(R1): R48-59.
88. Li, C., S. Biswas, X. Li, A. K. Dutta and W. Le (2010). "Novel D3 dopamine receptor-preferring agonist D-264: Evidence of neuroprotective property in Parkinson's disease animal models induced by 1-methyl-4-phenyl-1,2,3,6-tetrahydropyridine and lactacystin." J Neurosci Res **88**(11): 2513-2523.
89. Li, H. T., D. H. Lin, X. Y. Luo, F. Zhang, L. N. Ji, H. N. Du, G. Q. Song, J. Hu, J. W. Zhou and H. Y. Hu (2005). "Inhibition of alpha-synuclein fibrillization by dopamine analogs via reaction with the amino groups of alpha-synuclein. Implication for dopaminergic neurodegeneration." FEBS J **272**(14): 3661-3672.
90. Li, J., M. Zhu, S. Rajamani, V. N. Uversky and A. L. Fink (2004). "Rifampicin inhibits alpha-synuclein fibrillation and disaggregates fibrils." Chem Biol **11**(11): 1513-1521.
91. Li, J. Y., E. Englund, J. L. Holton, D. Soulet, P. Hagell, A. J. Lees, T. Lashley, N. P. Quinn, S. Rehnrcrona, A. Bjorklund, H. Widner, T. Revesz, O. Lindvall and P. Brundin (2008). "Lewy bodies in grafted neurons in subjects with Parkinson's disease suggest host-to-graft disease propagation." Nat Med **14**(5): 501-503.
92. Lin, E., J. E. Cavanaugh, R. K. Leak, R. G. Perez and M. J. Zigmond (2008). "Rapid activation of ERK by 6-hydroxydopamine promotes survival of dopaminergic cells." J Neurosci Res **86**(1): 108-117.
93. Lin, M. T. and M. F. Beal (2006). "Mitochondrial dysfunction and oxidative stress in neurodegenerative diseases." Nature **443**(7113): 787-795.
94. Linert, W. and G. N. Jameson (2000). "Redox reactions of neurotransmitters possibly involved in the progression of Parkinson's Disease." J Inorg Biochem **79**(1-4): 319-326.

95. Liou, H. H., M. C. Tsai, C. J. Chen, J. S. Jeng, Y. C. Chang, S. Y. Chen and R. C. Chen (1997). "Environmental risk factors and Parkinson's disease: a case-control study in Taiwan." Neurology **48**(6): 1583-1588.
96. Lotharius, J. and P. Brundin (2002). "Pathogenesis of Parkinson's disease: dopamine, vesicles and alpha-synuclein." Nat Rev Neurosci **3**(12): 932-942.
97. Lu, J. H., M. T. Ardah, S. S. Durairajan, L. F. Liu, L. X. Xie, W. F. Fong, M. Y. Hasan, J. D. Huang, O. M. El-Agnaf and M. Li (2011). "Baicalein inhibits formation of alpha-synuclein oligomers within living cells and prevents Abeta peptide fibrillation and oligomerisation." Chembiochem **12**(4): 615-624.
98. Markey, S. P., J. N. Johannessen, C. C. Chiueh, R. S. Burns and M. A. Herkenham (1984). "Intraneuronal generation of a pyridinium metabolite may cause drug-induced parkinsonism." Nature **311**(5985): 464-467.
99. Marsden, C. D. and J. D. Parkes (1976). "'On-off' effects in patients with Parkinson's disease on chronic levodopa therapy." Lancet **1**(7954): 292-296.
100. Marshall, B. D. and D. Werb (2010). "Health outcomes associated with methamphetamine use among young people: a systematic review." Addiction **105**(6): 991-1002.
101. Marshall, C. J. (1995). "Specificity of receptor tyrosine kinase signaling: transient versus sustained extracellular signal-regulated kinase activation." Cell **80**(2): 179-185.
102. Martin, H. L. and P. Teismann (2009). "Glutathione--a review on its role and significance in Parkinson's disease." FASEB J **23**(10): 3263-3272.

103. Masuda, M., N. Suzuki, S. Taniguchi, T. Oikawa, T. Nonaka, T. Iwatsubo, S. Hisanaga, M. Goedert and M. Hasegawa (2006). "Small molecule inhibitors of alpha-synuclein filament assembly." Biochemistry **45**(19): 6085-6094.
104. McCormack, A. L., M. Thiruchelvam, A. B. Manning-Bog, C. Thiffault, J. W. Langston, D. A. Cory-Slechta and D. A. Di Monte (2002). "Environmental risk factors and Parkinson's disease: selective degeneration of nigral dopaminergic neurons caused by the herbicide paraquat." Neurobiol Dis **10**(2): 119-127.
105. Mecocci, P., U. MacGarvey, A. E. Kaufman, D. Koontz, J. M. Shoffner, D. C. Wallace and M. F. Beal (1993). "Oxidative damage to mitochondrial DNA shows marked age-dependent increases in human brain." Ann Neurol **34**(4): 609-616.
106. Miura, H., M. Fujiki, A. Shibata and K. Ishikawa (2006). "Prevalence and profile of methamphetamine users in adolescents at a juvenile classification home." Psychiatry Clin Neurosci **60**(3): 352-357.
107. Mori, T., J. Baba, Y. Ichimaru and T. Suzuki (2000). "Effects of rolipram, a selective inhibitor of phosphodiesterase 4, on hyperlocomotion induced by several abused drugs in mice." Jpn J Pharmacol **83**(2): 113-118.
108. Moussaud, S. and H. J. Draheim (2010). "A new method to isolate microglia from adult mice and culture them for an extended period of time." J Neurosci Methods **187**(2): 243-253.
109. Neugebauer, N. M., S. B. Harrod, D. J. Stairs, P. A. Crooks, L. P. Dwoskin and M. T. Bardo (2007). "Lobeline decreases methamphetamine self-administration in rats." Eur J Pharmacol **571**(1): 33-38.

110. Nikodemova, M., I. D. Duncan and J. J. Watters (2006). "Minocycline exerts inhibitory effects on multiple mitogen-activated protein kinases and IkappaBalpha degradation in a stimulus-specific manner in microglia." J Neurochem **96**(2): 314-323.
111. Nimmerjahn, A., F. Kirchhoff and F. Helmchen (2005). "Resting microglial cells are highly dynamic surveillants of brain parenchyma in vivo." Science **308**(5726): 1314-1318.
112. Norris, E. H., B. I. Giasson, R. Hodara, S. Xu, J. Q. Trojanowski, H. Ischiropoulos and V. M. Lee (2005). "Reversible inhibition of alpha-synuclein fibrillization by dopaminochrome-mediated conformational alterations." J Biol Chem **280**(22): 21212-21219.
113. Ochu, E. E., N. J. Rothwell and C. M. Waters (1998). "Caspases mediate 6-hydroxydopamine-induced apoptosis but not necrosis in PC12 cells." J Neurochem **70**(6): 2637-2640.
114. Oetting, E. R., J. L. Deffenbacher, M. J. Taylor, N. Luther, F. Beauvais and R. W. Edwards (2000). "Methamphetamine Use by High School Students: Recent Trends, Gender and Ethnicity Differences, and Use of Other Drugs." Journal of Child & Adolescent Substance Abuse **10**(1): 33-50.
115. Ohtaki, H., T. Tsumuraya, D. Song, A. Sato, K. Ohara, K. Miyamoto, H. Nakano, K. Kiriya, K. Dohi, Y. Hiraizumi, M. Matsunaga and S. Shioda (2013). "Establishment and characterization of primary adult microglial culture in mice." Acta Neurochir Suppl **118**: 49-54.

116. Olah, M., D. Raj, N. Brouwer, A. H. De Haas, B. J. Eggen, W. F. Den Dunnen, K. P. Biber and H. W. Boddeke (2012). "An optimized protocol for the acute isolation of human microglia from autopsy brain samples." *Glia* **60**(1): 96-111.
117. Olanow, C. W. (1990). "Oxidation reactions in Parkinson's disease." *Neurology* **40**(10 Suppl 3): suppl 32-37; discussion 37-39.
118. Olanow, C. W., O. Rascol, R. Hauser, P. D. Feigin, J. Jankovic, A. Lang, W. Langston, E. Melamed, W. Poewe, F. Stocchi and E. Tolosa (2009). "A double-blind, delayed-start trial of rasagiline in Parkinson's disease." *N Engl J Med* **361**(13): 1268-1278.
119. Ono, K. and M. Yamada (2006). "Antioxidant compounds have potent anti-fibrillogenic and fibril-destabilizing effects for alpha-synuclein fibrils in vitro." *J Neurochem* **97**(1): 105-115.
120. Park, G. H., S. J. Jeon, H. M. Ko, J. R. Ryu, J. M. Lee, H. Y. Kim, S. H. Han, Y. S. Kang, S. H. Park, C. Y. Shin and K. H. Ko (2010). "Activation of microglial cells via protease-activated receptor 2 mediates neuronal cell death in cultured rat primary neuron." *Nitric Oxide* **22**(1): 18-29.
121. Parkinson, J. (2002). "An essay on the shaking palsy. 1817." *J Neuropsychiatry Clin Neurosci* **14**(2): 223-236; discussion 222.
122. Parvathenani, L. K., S. Tertyshnikova, C. R. Greco, S. B. Roberts, B. Robertson and R. Posmantur (2003). "P2X7 mediates superoxide production in primary microglia and is up-regulated in a transgenic mouse model of Alzheimer's disease." *J Biol Chem* **278**(15): 13309-13317.
123. Perry, T. L., D. V. Godin and S. Hansen (1982). "Parkinson's disease: a disorder due to nigral glutathione deficiency?" *Neurosci Lett* **33**(3): 305-310.

124. Peter, D., J. Jimenez, Y. Liu, J. Kim and R. H. Edwards (1994). "The chromaffin granule and synaptic vesicle amine transporters differ in substrate recognition and sensitivity to inhibitors." J Biol Chem **269**(10): 7231-7237.
125. Polymeropoulos, M. H., C. Lavedan, E. Leroy, S. E. Ide, A. Dehejia, A. Dutra, B. Pike, H. Root, J. Rubenstein, R. Boyer, E. S. Stenroos, S. Chandrasekharappa, A. Athanassiadou, T. Papapetropoulos, W. G. Johnson, A. M. Lazzarini, R. C. Duvoisin, G. Di Iorio, L. I. Golbe and R. L. Nussbaum (1997). "Mutation in the alpha-synuclein gene identified in families with Parkinson's disease." Science **276**(5321): 2045-2047.
126. Pothos, E. N., S. Przedborski, V. Davila, Y. Schmitz and D. Sulzer (1998). "D2-Like dopamine autoreceptor activation reduces quantal size in PC12 cells." J Neurosci **18**(15): 5575-5585.
127. Prusiner, S. B. (2012). "Cell biology. A unifying role for prions in neurodegenerative diseases." Science **336**(6088): 1511-1513.
128. Raivich, G. (2005). "Like cops on the beat: the active role of resting microglia." Trends Neurosci **28**(11): 571-573.
129. Ramirez, A., A. Heimbach, J. Grundemann, B. Stiller, D. Hampshire, L. P. Cid, I. Goebel, A. F. Mubaidin, A. L. Wriekat, J. Roeper, A. Al-Din, A. M. Hillmer, M. Karsak, B. Liss, C. G. Woods, M. I. Behrens and C. Kubisch (2006). "Hereditary parkinsonism with dementia is caused by mutations in ATP13A2, encoding a lysosomal type 5 P-type ATPase." Nat Genet **38**(10): 1184-1191.
130. Ramirez, A. D., S. K. Wong and F. S. Menniti (2003). "Pramipexole inhibits MPTP toxicity in mice by dopamine D3 receptor dependent and independent mechanisms." Eur J Pharmacol **475**(1-3): 29-35.

131. Ransohoff, R. M. and A. E. Cardona (2010). "The myeloid cells of the central nervous system parenchyma." Nature **468**(7321): 253-262.
132. Rawson, R. A., R. Gonzales, J. L. Obert, M. J. McCann and P. Brethen (2005). "Methamphetamine use among treatment-seeking adolescents in Southern California: participant characteristics and treatment response." J Subst Abuse Treat **29**(2): 67-74.
133. Reynolds, A. D., J. G. Glanzer, I. Kadiu, M. Ricardo-Dukelow, A. Chaudhuri, P. Ciborowski, R. Cerny, B. Gelman, M. P. Thomas, R. L. Mosley and H. E. Gendelman (2008). "Nitrated alpha-synuclein-activated microglial profiling for Parkinson's disease." J Neurochem **104**(6): 1504-1525.
134. Ricaurte, G. A., A. O. Mehan, J. Yuan, G. Hatzidimitriou, T. Xie, A. H. Mayne and U. D. McCann (2005). "Amphetamine treatment similar to that used in the treatment of adult attention-deficit/hyperactivity disorder damages dopaminergic nerve endings in the striatum of adult nonhuman primates." J Pharmacol Exp Ther **315**(1): 91-98.
135. Riederer, P., E. Sofic, W. D. Rausch, B. Schmidt, G. P. Reynolds, K. Jellinger and M. B. Youdim (1989). "Transition metals, ferritin, glutathione, and ascorbic acid in parkinsonian brains." J Neurochem **52**(2): 515-520.
136. Robson, M. J., R. C. Turner, Z. J. Naser, C. R. McCurdy, J. D. Huber and R. R. Matsumoto (2013). "SN79, a sigma receptor ligand, blocks methamphetamine-induced microglial activation and cytokine upregulation." Exp Neurol **247**: 134-142.
137. Rochet, J. C., T. F. Outeiro, K. A. Conway, T. T. Ding, M. J. Volles, H. A. Lashuel, R. M. Bieganski, S. L. Lindquist and P. T. Lansbury (2004). "Interactions among alpha-synuclein, dopamine, and biomembranes: some clues for understanding neurodegeneration in Parkinson's disease." J Mol Neurosci **23**(1-2): 23-34.

138. Ross, O. A., A. T. Braithwaite, L. M. Skipper, J. Kachergus, M. M. Hulihan, F. A. Middleton, K. Nishioka, J. Fuchs, T. Gasser, D. M. Maraganore, C. H. Adler, L. Larvor, M. C. Chartier-Harlin, C. Nilsson, J. W. Langston, K. Gwinn, N. Hattori and M. J. Farrer (2008). "Genomic investigation of alpha-synuclein multiplication and parkinsonism." Ann Neurol **63**(6): 743-750.
139. Russell, K., D. M. Dryden, Y. Liang, C. Friesen, K. O'Gorman, T. Durec, T. C. Wild and T. P. Klassen (2008). "Risk factors for methamphetamine use in youth: a systematic review." BMC Pediatr **8**: 48.
140. Sagi, Y., S. Mandel, T. Amit and M. B. Youdim (2007). "Activation of tyrosine kinase receptor signaling pathway by rasagiline facilitates neurorescue and restoration of nigrostriatal dopamine neurons in post-MPTP-induced parkinsonism." Neurobiol Dis **25**(1): 35-44.
141. Saito, Y., K. Nishio, Y. Ogawa, T. Kinumi, Y. Yoshida, Y. Masuo and E. Niki (2007). "Molecular mechanisms of 6-hydroxydopamine-induced cytotoxicity in PC12 cells: involvement of hydrogen peroxide-dependent and -independent action." Free Radic Biol Med **42**(5): 675-685.
142. Santra, S., L. Xu, M. Shah, M. Johnson and A. Dutta (2013). "D-512 and D-440 as Novel Multifunctional Dopamine Agonists: Characterization of Neuroprotection Properties and Evaluation of In Vivo Efficacy in a Parkinson's Disease Animal Model." ACS Chem Neurosci.
143. Sattah, M. V., S. Supawitkul, T. J. Dondero, P. H. Kilmarx, N. L. Young, T. D. Mastro, S. Chaikummao, C. Manopaiboon and F. Griensven (2002). "Prevalence of and risk



- factors for methamphetamine use in northern Thai youth: results of an audio-computer-assisted self-interviewing survey with urine testing." *Addiction* **97**(7): 801-808.
144. Saunders, C., J. V. Ferrer, L. Shi, J. Chen, G. Merrill, M. E. Lamb, L. M. Leeb-Lundberg, L. Carvelli, J. A. Javitch and A. Galli (2000). "Amphetamine-induced loss of human dopamine transporter activity: an internalization-dependent and cocaine-sensitive mechanism." *Proc Natl Acad Sci U S A* **97**(12): 6850-6855.
145. Schapira, A. H. and E. Tolosa (2010). "Molecular and clinical prodrome of Parkinson disease: implications for treatment." *Nat Rev Neurol* **6**(6): 309-317.
146. Seyfried, J., F. Soldner, W. S. Kunz, J. B. Schulz, T. Klockgether, K. A. Kovar and U. Wullner (2000). "Effect of 1-methyl-4-phenylpyridinium on glutathione in rat pheochromocytoma PC 12 cells." *Neurochem Int* **36**(6): 489-497.
147. Shen, X. M. and G. Dryhurst (1996). "Further insights into the influence of L-cysteine on the oxidation chemistry of dopamine: reaction pathways of potential relevance to Parkinson's disease." *Chem Res Toxicol* **9**(4): 751-763.
148. Shigenaga, M. K., E. N. Aboujaoude, Q. Chen and B. N. Ames (1994). "Assays of oxidative DNA damage biomarkers 8-oxo-2'-deoxyguanosine and 8-oxoguanine in nuclear DNA and biological fluids by high-performance liquid chromatography with electrochemical detection." *Methods Enzymol* **234**: 16-33.
149. Shimizu, E., K. Hashimoto, N. Komatsu and M. Iyo (2002). "Roles of endogenous glutathione levels on 6-hydroxydopamine-induced apoptotic neuronal cell death in human neuroblastoma SK-N-SH cells." *Neuropharmacology* **43**(3): 434-443.
150. Shimizu, K., K. Ohtaki, K. Matsubara, K. Aoyama, T. Uezono, O. Saito, M. Suno, K. Ogawa, N. Hayase, K. Kimura and H. Shiono (2001). "Carrier-mediated processes in

- blood--brain barrier penetration and neural uptake of paraquat." Brain Res **906**(1-2): 135-142.
151. Shoulson, I. (1998). "DATATOP: a decade of neuroprotective inquiry. Parkinson Study Group. Deprenyl And Tocopherol Antioxidative Therapy Of Parkinsonism." Ann Neurol **44**(3 Suppl 1): S160-166.
152. Shulman, J. M., P. L. De Jager and M. B. Feany (2011). "Parkinson's disease: genetics and pathogenesis." Annu Rev Pathol **6**: 193-222.
153. Sian, J., D. T. Dexter, A. J. Lees, S. Daniel, P. Jenner and C. D. Marsden (1994). "Glutathione-related enzymes in brain in Parkinson's disease." Ann Neurol **36**(3): 356-361.
154. Singleton, A. B., M. Farrer, J. Johnson, A. Singleton, S. Hague, J. Kachergus, M. Hulihan, T. Peuralinna, A. Dutra, R. Nussbaum, S. Lincoln, A. Crawley, M. Hanson, D. Maraganore, C. Adler, M. R. Cookson, M. Muentner, M. Baptista, D. Miller, J. Blancato, J. Hardy and K. Gwinn-Hardy (2003). "alpha-Synuclein locus triplication causes Parkinson's disease." Science **302**(5646): 841.
155. Snider, S. E., E. S. Hendrick and P. M. Beardsley (2013). "Glial cell modulators attenuate methamphetamine self-administration in the rat." Eur J Pharmacol **701**(1-3): 124-130.
156. Sofic, E., K. W. Lange, K. Jellinger and P. Riederer (1992). "Reduced and oxidized glutathione in the substantia nigra of patients with Parkinson's disease." Neurosci Lett **142**(2): 128-130.
157. Spencer, J. P., P. Jenner, S. E. Daniel, A. J. Lees, D. C. Marsden and B. Halliwell (1998). "Conjugates of catecholamines with cysteine and GSH in Parkinson's disease: possible

- mechanisms of formation involving reactive oxygen species." J Neurochem **71**(5): 2112-2122.
158. Spillantini, M. G., R. A. Crowther, R. Jakes, M. Hasegawa and M. Goedert (1998). "alpha-Synuclein in filamentous inclusions of Lewy bodies from Parkinson's disease and dementia with lewy bodies." Proc Natl Acad Sci U S A **95**(11): 6469-6473.
159. Spillantini, M. G., M. L. Schmidt, V. M. Lee, J. Q. Trojanowski, R. Jakes and M. Goedert (1997). "Alpha-synuclein in Lewy bodies." Nature **388**(6645): 839-840.
160. Spira, P. J., D. M. Sharpe, G. Halliday, J. Cavanagh and G. A. Nicholson (2001). "Clinical and pathological features of a Parkinsonian syndrome in a family with an Ala53Thr alpha-synuclein mutation." Ann Neurol **49**(3): 313-319.
161. Sriram, K., D. B. Miller and J. P. O'Callaghan (2006). "Minocycline attenuates microglial activation but fails to mitigate striatal dopaminergic neurotoxicity: role of tumor necrosis factor-alpha." J Neurochem **96**(3): 706-718.
162. Sulzer, D. (2011). "How addictive drugs disrupt presynaptic dopamine neurotransmission." Neuron **69**(4): 628-649.
163. Sulzer, D., T. K. Chen, Y. Y. Lau, H. Kristensen, S. Rayport and A. Ewing (1995). "Amphetamine redistributes dopamine from synaptic vesicles to the cytosol and promotes reverse transport." J Neurosci **15**(5 Pt 2): 4102-4108.
164. Sulzer, D., M. S. Sonders, N. W. Poulsen and A. Galli (2005). "Mechanisms of neurotransmitter release by amphetamines: a review." Prog Neurobiol **75**(6): 406-433.
165. Swanson, P. D. (1994). "Drug treatment of Parkinson's disease: is "polypharmacy" best?" J Neurol Neurosurg Psychiatry **57**(4): 401-403.

166. Takata, M. K., F. Yamaguchi, K. Nakanose, Y. Watanabe, N. Hatano, I. Tsukamoto, M. Nagata, K. Izumori and M. Tokuda (2005). "Neuroprotective effect of D-psicose on 6-hydroxydopamine-induced apoptosis in rat pheochromocytoma (PC12) cells." J Biosci Bioeng **100**(5): 511-516.
167. Tanibuchi, Y., M. Shimagami, G. Fukami, Y. Sekine, M. Iyo and K. Hashimoto (2010). "A case of methamphetamine use disorder treated with the antibiotic drug minocycline." Gen Hosp Psychiatry **32**(5): 559 e551-553.
168. Tatton, W. G., W. Y. Ju, D. P. Holland, C. Tai and M. Kwan (1994). "(-)-Deprenyl reduces PC12 cell apoptosis by inducing new protein synthesis." J Neurochem **63**(4): 1572-1575.
169. Thomas, D. M., J. Dowgiert, T. J. Geddes, D. Francescutti-Verbeem, X. Liu and D. M. Kuhn (2004). "Microglial activation is a pharmacologically specific marker for the neurotoxic amphetamines." Neurosci Lett **367**(3): 349-354.
170. Thomas, D. M., D. M. Francescutti-Verbeem and D. M. Kuhn (2006). "Gene expression profile of activated microglia under conditions associated with dopamine neuronal damage." FASEB J **20**(3): 515-517.
171. Thomas, D. M., D. M. Francescutti-Verbeem and D. M. Kuhn (2008). "Methamphetamine-induced neurotoxicity and microglial activation are not mediated by fractalkine receptor signaling." J Neurochem **106**(2): 696-705.
172. Thomas, D. M. and D. M. Kuhn (2005). "Cyclooxygenase-2 is an obligatory factor in methamphetamine-induced neurotoxicity." J Pharmacol Exp Ther **313**(2): 870-876.

173. Thomas, D. M. and D. M. Kuhn (2005). "MK-801 and dextromethorphan block microglial activation and protect against methamphetamine-induced neurotoxicity." Brain Res **1050**(1-2): 190-198.
174. Thomas, D. M., P. D. Walker, J. A. Benjamins, T. J. Geddes and D. M. Kuhn (2004). "Methamphetamine neurotoxicity in dopamine nerve endings of the striatum is associated with microglial activation." J Pharmacol Exp Ther **311**(1): 1-7.
175. Tietze, F. (1969). "Enzymic method for quantitative determination of nanogram amounts of total and oxidized glutathione: applications to mammalian blood and other tissues." Anal Biochem **27**(3): 502-522.
176. Tsuji, T., M. Asanuma, I. Miyazaki, K. Miyoshi and N. Ogawa (2009). "Reduction of nuclear peroxisome proliferator-activated receptor gamma expression in methamphetamine-induced neurotoxicity and neuroprotective effects of ibuprofen." Neurochem Res **34**(4): 764-774.
177. Van Den Eeden, S. K., C. M. Tanner, A. L. Bernstein, R. D. Fross, A. Leimpeter, D. A. Bloch and L. M. Nelson (2003). "Incidence of Parkinson's disease: variation by age, gender, and race/ethnicity." Am J Epidemiol **157**(11): 1015-1022.
178. Van der Schyf, C. J., S. Mandel, W. J. Geldenhuys, T. Amit, Y. Avramovich, H. Zheng, M. Fridkin, S. Gal, O. Weinreb, O. Bar Am, Y. Sagi and M. B. Youdim (2007). "Novel multifunctional anti-Alzheimer drugs with various CNS neurotransmitter targets and neuroprotective moieties." Curr Alzheimer Res **4**(5): 522-536.
179. VanderJagt, D. J., J. M. Harrison, D. M. Ratliff, L. A. Hunsaker and D. L. Vander Jagt (2001). "Oxidative stress indices in IDDM subjects with and without long-term diabetic complications." Clin Biochem **34**(4): 265-270.

180. Vearrier, D., M. I. Greenberg, S. N. Miller, J. T. Okaneku and D. A. Haggerty (2012). "Methamphetamine: history, pathophysiology, adverse health effects, current trends, and hazards associated with the clandestine manufacture of methamphetamine." Dis Mon **58**(2): 38-89.
181. Volles, M. J. and P. T. Lansbury, Jr. (2002). "Vesicle permeabilization by protofibrillar alpha-synuclein is sensitive to Parkinson's disease-linked mutations and occurs by a pore-like mechanism." Biochemistry **41**(14): 4595-4602.
182. Volles, M. J., S. J. Lee, J. C. Rochet, M. D. Shtilerman, T. T. Ding, J. C. Kessler and P. T. Lansbury, Jr. (2001). "Vesicle permeabilization by protofibrillar alpha-synuclein: implications for the pathogenesis and treatment of Parkinson's disease." Biochemistry **40**(26): 7812-7819.
183. Woolverton, W. L., G. A. Ricaurte, L. S. Forno and L. S. Seiden (1989). "Long-term effects of chronic methamphetamine administration in rhesus monkeys." Brain Res **486**(1): 73-78.
184. Xia, Z., M. Dickens, J. Raingeaud, R. J. Davis and M. E. Greenberg (1995). "Opposing effects of ERK and JNK-p38 MAP kinases on apoptosis." Science **270**(5240): 1326-1331.
185. Xu, J., S. Y. Kao, F. J. Lee, W. Song, L. W. Jin and B. A. Yankner (2002). "Dopamine-dependent neurotoxicity of alpha-synuclein: a mechanism for selective neurodegeneration in Parkinson disease." Nat Med **8**(6): 600-606.
186. Xu, J., C. Wei, C. Xu, M. C. Bennett, G. Zhang, F. Li and E. Tao (2007). "Rifampicin protects PC12 cells against MPP<sup>+</sup>-induced apoptosis and inhibits the expression of an alpha-Synuclein multimer." Brain Res **1139**: 220-225.

187. Yamada, K., H. Umegaki, I. Maezawa, A. Iguchi, T. Kameyama and T. Nabeshima (1997). "Possible involvement of catalase in the protective effect of interleukin-6 against 6-hydroxydopamine toxicity in PC12 cells." Brain Res Bull **43**(6): 573-577.
188. Yamamoto, B. K., A. Moszczynska and G. A. Gudelsky (2010). "Amphetamine toxicities: classical and emerging mechanisms." Ann N Y Acad Sci **1187**: 101-121.
189. Yan, Y., T. Mizuno, A. Nitta, K. Yamada and T. Nabeshima (2004). "Nefiracetam attenuates methamphetamine-induced discriminative stimulus effects in rats." Ann N Y Acad Sci **1025**: 274-278.
190. Yen, C. F. (2004). "Relationship between methamphetamine use and risky sexual behavior in adolescents." Kaohsiung J Med Sci **20**(4): 160-165.
191. Yen, C. F., Y. H. Yang and M. Y. Chong (2006). "Correlates of methamphetamine use for Taiwanese adolescents." Psychiatry Clin Neurosci **60**(2): 160-167.
192. Youdim, M. B. (2010). "Why do we need multifunctional neuroprotective and neurorestorative drugs for Parkinson's and Alzheimer's disorders?" Rambam Maimonides Med J **1**(2): e0011.
193. Youdim, M. B. (2013). "Multi target neuroprotective and neurorestorative anti-Parkinson and anti-Alzheimer drugs ladostigil and m30 derived from rasagiline." Exp Neurobiol **22**(1): 1-10.
194. Yu, S. J., M. Airavaara, H. Shen, J. Chou, B. K. Harvey and Y. Wang (2012). "Suppression of endogenous PPARgamma increases vulnerability to methamphetamine-induced injury in mouse nigrostriatal dopaminergic pathway." Psychopharmacology (Berl) **221**(3): 479-492.

195. Zachor, D. A., J. F. Moore, C. Brezaussek, A. Theibert and A. K. Percy (2000). "Cocaine inhibits NGF-induced PC12 cells differentiation through D(1)-type dopamine receptors." Brain Res **869**(1-2): 85-97.
196. Zarranz, J. J., J. Alegre, J. C. Gomez-Esteban, E. Lezcano, R. Ros, I. Ampuero, L. Vidal, J. Hoenicka, O. Rodriguez, B. Atares, V. Llorens, E. Gomez Tortosa, T. del Ser, D. G. Munoz and J. G. de Yebenes (2004). "The new mutation, E46K, of alpha-synuclein causes Parkinson and Lewy body dementia." Ann Neurol **55**(2): 164-173.
197. Zecca, L., M. B. Youdim, P. Riederer, J. R. Connor and R. R. Crichton (2004). "Iron, brain ageing and neurodegenerative disorders." Nat Rev Neurosci **5**(11): 863-873.
198. Zhang, J., J. Hu, J. H. Ding, H. H. Yao and G. Hu (2005). "6-Hydroxydopamine-induced glutathione alteration occurs via glutathione enzyme system in primary cultured astrocytes." Acta Pharmacol Sin **26**(7): 799-805.
199. Zhang, L. J., Y. Q. Xue, C. Yang, W. H. Yang, L. Chen, Q. J. Zhang, T. Y. Qu, S. Huang, L. R. Zhao, X. M. Wang and W. M. Duan (2012). "Human albumin prevents 6-hydroxydopamine-induced loss of tyrosine hydroxylase in in vitro and in vivo." PLoS One **7**(7): e41226.
200. Zhu, M., S. Rajamani, J. Kaylor, S. Han, F. Zhou and A. L. Fink (2004). "The flavonoid baicalein inhibits fibrillation of alpha-synuclein and disaggregates existing fibrils." J Biol Chem **279**(26): 26846-26857.
201. Zhu, W., W. Xie, T. Pan, J. Jankovic, J. Li, M. B. Youdim and W. Le (2008). "Comparison of neuroprotective and neurorestorative capabilities of rasagiline and selegiline against lactacystin-induced nigrostriatal dopaminergic degeneration." J Neurochem **105**(5): 1970-1978.



202. Zhu, W., W. Xie, T. Pan, P. Xu, M. Fridkin, H. Zheng, J. Jankovic, M. B. Youdim and W. Le (2007). "Prevention and restoration of lactacystin-induced nigrostriatal dopamine neuron degeneration by novel brain-permeable iron chelators." FASEB J **21**(14): 3835-3844.
203. Zhu, W. H., L. Conforti and D. E. Millhorn (1997). "Expression of dopamine D2 receptor in PC-12 cells and regulation of membrane conductances by dopamine." Am J Physiol **273**(4 Pt 1): C1143-1150.
204. Zlokovic, B. V. (2008). "The blood-brain barrier in health and chronic neurodegenerative disorders." Neuron **57**(2): 178-201.

**ABSTRACT****PROGRESS TOWARDS UNDERSTANDING OF MECHANISMS OF ACTION OF  
POTENT MULTIFUNCTIONAL DISEASE MODIFYING  
THERAPEUTICS FOR PARKINSON'S DISEASE**

by

**MRUDANG MANOJKUMAR SHAH****May 2014****Advisor:** Dr. Alope Dutta**Major:** Pharmaceutical Sciences**Degree:** Doctor of Philosophy

Our *long term goal* is to design and develop potent multifunctional disease modifying therapeutics for Parkinson's disease. The *objective* of my dissertation was to understand the mechanisms of action of some potent small molecules (synthesized in our lab) as a disease modifying Parkinson's disease therapeutic. The objective was achieved by pursuing the following *two specific aims*:

1. Investigating anti-oxidant and neuroprotective effects of a lead molecule (D-512) generated in our lab.
2. Assessing the ability of some of our potential lead compounds (D-240, D-436, and D-520) to prevent the aggregation of  $\alpha$ -synuclein.

Oxidative stress is one of the major factors implicated in the pathogenesis and progression of Parkinson's disease. To investigate the neuroprotective effects of D-512 in Parkinson's disease, we determined the ability of D-512 to rescue against 6-hydroxydopamine induced cell death in dopaminergic cell line PC12 under two different protocols. Once it was established that D-512 is able to prevent/rescue the cell death induced by 6-hydroxydopamine in

PC12 cells, various other assays to determine its ability to confer neuroprotection were performed.

As Parkinson's disease patients have elevated levels of oxidative stress and subsequent damage of their glutathione system, excessive lipid peroxidation, and DNA damage, we evaluated D-512's ability to protect against 6-hydroxydopamine induced changes in glutathione levels and DNA damage. We also evaluated the ability of D-512 to protect against the lipid peroxidation induced by sodium nitroprusside. In addition, we also evaluated the possible molecular mechanism by which D-512 may be able to confer neuroprotection against 6-hydroxydopamine induced cell death.

$\alpha$ -synuclein aggregation has been shown to be present in post-mortem brains of Parkinson's disease patients and SNCA gene mutations as well as gene duplication and triplication results in familial form of Parkinson's disease. To assess the ability of some of our lead compounds against  $\alpha$ -synuclein aggregation, we developed a cell-free system assay. We simulated different Parkinson's disease associated factors to generate different types of  $\alpha$ -synuclein aggregates. We also developed various assays to determine the type of aggregates formed following our experiments. After optimizing assays to generate  $\alpha$ -synuclein oligomers and fibrils, we evaluated the ability of some standard compounds (ascorbic acid and rifampicin) and some of our lead compounds (D-436 and D-520) to prevent  $\alpha$ -synuclein aggregation in presence of dopamine. We employed numerous assays to verify the morphology and structural characteristics of the aggregates formed under various conditions.

$\alpha$ -synuclein aggregates have been known to transfer from one neuron to another by their ability to form pores in biological membranes. Therefore, we developed an in-vitro assay to determine the extracellular toxicity of  $\alpha$ -synuclein aggregates generated under high concentration

of  $\alpha$ -synuclein and  $\alpha$ -synuclein in presence of dopamine by cell-free system assay. Afterwards, we evaluated the ability of a standard compound (rifampicin) and our lead compounds (D-240, D-436, and D-520) to prevent  $\alpha$ -synuclein aggregation and subsequent cytotoxicity of extracellular  $\alpha$ -synuclein aggregates. We also evaluated the ability of our compounds to prevent  $\alpha$ -synuclein aggregation and the morphological changes induced in presence of our lead compounds.

## INVESTIGATING THE METHAMPHETAMINE-INDUCED STRIATAL MICROGLIA ACTIVATION

by

**MRUDANG MANOJKUMAR SHAH**

**May 2014**

**Advisor:** Dr. David Thomas

**Major:** Pharmaceutical Sciences

**Degree:** Doctor of Philosophy

Methamphetamine is a highly abused, addictive and neurotoxic drug which causes striatal-specific activation of microglia cells. Our *long term goal* is to identify the potential molecular targets of methamphetamine induced neurotoxicity and addiction. The *objective* of my dissertation was to develop a cell-culture model of methamphetamine neurotoxicity and determine proteomic expression changes in microglia isolated from striatum of methamphetamine treated animals. I achieved my objective by pursuing following *two specific aims*:

1. Identifying the proteomic expression changes of cultured microglia cells after exposure to methamphetamine or similar insult.

2. Optimization of a protocol to isolate highly purified fraction of microglia from various regions of brain and identification of protein expression changes in striatal microglia isolated from control and methamphetamine treated animals.

The addictive property of methamphetamine is because of its ability to cause release of dopamine from striatum, which cause euphoria. Dopamine quinones have been shown to cause significant changes in gene expression profile of culture microglia cells (BV2 cells). We determined to evaluate the effect of different concentrations of methamphetamine and lipopolysaccharide (gram negative endotoxin which causes strong immune response) on cultured microglia cells alone and cultured microglia cells which have access to various soluble factors secreted by cultured dopaminergic cell line (MN9D cells). We also verified the differences in protein expression profile of BV2 cells alone or BV2 cells co-cultured with dopaminergic neuronal cell line to determine if either of the cell-culture systems can be used as a model to determine methamphetamine-induced neurotoxicity in striatal microglia.

As striatum is a region where all dopaminergic nerve terminals of nigrostriatal tract end and methamphetamine has been shown to cause significant alterations in dopaminergic neuronal system, we determined to isolate microglia from striatum. We compared and optimized various protocols for microglial isolation to achieve method to isolate highly pure fraction of microglia cells. Afterwards, we also isolated microglia from striatum of untreated animals and animals treated with methamphetamine to determine protein expression changes between them. We analyzed the differences in protein expression between isolated microglia to understand the molecular mechanisms or pathways which are altered or affected by methamphetamine which might be responsible for addictive and neurotoxic properties of methamphetamine.

## AUTOBIOGRAPHICAL STATEMENT

### EDUCATION

- 2003-2007 Bachelor of Pharmacy; Sardar Patel University, Anand, India
- 2008-2013 Doctor of Philosophy; Wayne State University, Detroit, Michigan

### AWARDS

- 2011 Travel award from college of Pharmacy for 42<sup>nd</sup> Society for Neuroscience conference
- 2012 Rumble fellowship from Wayne State University
- 2013 George C. Fuller endowed scholarship, Department of Pharmaceutical Sciences
- 2013 Frank O. Taylor scholarship, Department of Pharmaceutical Sciences

### PUBLICATIONS

1. Santra S, Xu L, Shah M, Johnson M, Dutta A. (2013) D-512 and D-440 as Novel Multi-functional Dopamine Agonists: Characterization of Neuroprotection Properties and Evaluation of In Vivo Efficacy in a Parkinson's Disease Animal Model. ACS Chem Neuroscience.
2. Bhoopalan V, Han SG, Shah MM, Thomas DM, Bhalla DK. (2013) Tobacco smoke modulates ozone-induced toxicity in rat lungs and central nervous system. Inhalation Toxicology, Jan;25(1):21-8.
3. Pérez MA, Kane MJ, Briggs DI, Francescutti DM, Sykes CE, Shah MM, Thomas DM, Kuhn DM. (2013) Mephedrone does not damage dopamine nerve endings of the striatum, but enhances the neurotoxicity of methamphetamine, amphetamine, and MDMA. Journal of Neurochemistry, 125(1):102-10.
4. Pérez MA, Kane MJ, Briggs DI, Sykes CE, Shah MM, Francescutti DM, Rosenberg DR, Thomas DM, Kuhn DM. (2012) Genetic depletion of brain 5HT reveals a common molecular pathway mediating compulsivity and impulsivity. Journal of Neurochemistry, 121:974-84.
5. Pérez MA, Kane MJ, Francescutti DM, Sykes KE, Shah MM, Mohammed AM, Thomas DM, and Kuhn DM. (2011) Mephedrone, an Abused Psychoactive Component of "Bath Salts" and Methamphetamine Congener, Does not Cause Neurotoxicity to Dopamine Nerve endings of the Striatum. Journal of Neurochemistry, 120: 1097-107.
6. Thomas DM, Pérez MA, Francescutti-Verbeem DM, Shah MM, Kuhn DM. (2010), The role of endogenous serotonin in methamphetamine-induced neurotoxicity to dopamine nerve endings of the striatum. Journal of Neurochemistry, 115: 595–605.